RESTRAINED COMPOSITE COLUMNS

by

IAN MELVILLE MAY

A Thesis submitted to the Department of Engineering

of The University of Warwick

for the Degree of Doctor of Philosophy

October 1976.

TO MY FAMILY

SUMMARY

This Thesis describes the development of an analysis for inelastic columns, with cross-sections composed of one or more materials, loaded with axial load and biaxial moments. The column can have both rotational and directional restraints at its ends. The analysis has been programmed for a computer and subsequently tested against published results for steel columns, reinforced concrete columns, and concrete-encased steel composite columns and shown to give good agreement.

A test rig with an axial load capacity of 2MN and capable of testing full-scale columns of any practical length has been designed and built. Columns with elastic and elastic-plastic rotational restraints or pin-ends or any combination can be tested and column end-moments of up to 50 kNm can be applied through the beams. One important feature of the test rig is sets of crossed knife-edges, which give both major and minor axis rotational freedom and thus allow accurate positioning of the axial load.

Eight elastically restrained concrete-encased steel composite no-sway columns have been tested, three with biaxial restraints and loadings, using the rig. The results from the tests have been compared with predictions using the computer program and agreement between the observed and predicted results for ultimate loads, deflections, and end-moments is good.

The behaviour of column lengths within rigid-jointed no-sway frames with both plastically and elastically designed beams has been studied. For the case of a column with elastic restraints design proposals have been checked and shown to be conservative. When the beams are designed plastically it is recommended that a conservative approach should be adopted until further research has been carried out into this topic.

CONTENTS

LIST OF TABLES

LIST OF FIGURES

ACKNOWLEDGEMENTS

I would like to thank both my supervisor Professor R.P. Johnson and also Dr. R.H. Wood of the Building Research Establishment, for their guidance and helpful criticisms throughout the duration of the research.

I am very grateful for the assistance given by Mr. A. Redhead, Senior Technician, and other members of the staff of the Engineering Department in the design and building of the test rig and in carrying out the tests.

The Building Research Establishment is to be thanked for financial support of the research work.

Thanks are due to Mrs. J. Carrington for the careful typing of the manuscript.

NOTATION

A	Cross-sectional area
A_c	Area of concrete
A_{ij}	Area of (ij)th element
A_r	Cross-sectional area of longitudinal reinforcement
A_s	Cross-sectional area of joist
B	Breadth of section
b	Flange width
C_m	Equivalent moment factor
$C_1, \ldots . C_4$	Coefficients in concrete stress-strain curve
c	Stability function
D	Depth of section
d	Distance from centroid to extreme fibre
	Clear depth of web
E	Young's modulus
	Error matrix
E_c	Young's modulus of concrete
E_s	Young's modulus of steel
E_x, E_y	Elastic beams about x and y axes respectively
e	Eccentricity of load
G_o, H_o	Constants in extrapolated Liebemann Method
I	Second moment of area
I_y	Second moment of area about minor axis
i	Number of element along x axis
	Node number
j	Number of element along y axis

K, K_1, K_2, K_3	Stiffness of member
	Concrete strength conversion factor
	Parameters to describe axial-load-moment interaction curve
K_b	Stiffness of beam
K_c	Stiffness of column
k	Factor proportional to stiffness of beam
L	Length of a member
L_c	Critical length of a member
ℓ	Elemental length
ℓ_s	Stub-stanchion length
M	Moment
M_{cen}	Moment at centre of column
M_{col}	Moment acting on column
M_d	Moment due to dead load
M_F	Fixed end moment
M_p	Plastic moment of section
M_{ULT}	Ultimate moment with N = 0
M_{ux}	Ultimate moment, about x axis, with axial load N.
M_{uy}	Ultimate moment, about y axis, with axial N
$M_x, M_{x1}, \ldots M_{x4}$	Major axis moment
$M_y, M_{y1}, \ldots M_{y4}$	Minor axis moment
$\bar{M}, \overline{M1}, \ldots \overline{M4}$	Miscloses
m	Number of elements along x axis
	Modular ratio
$(m_x)_{ij}$	Major axis moment on (ij)th element
$(m_y)ij$	Minor axis moment on (ij)th element
N	Axial load

N_A Axial load

N_a Ultimate axial load

N_{ax} Ultimate axial load when constrained to fail about the x axis.

N_{cr} Critical axial load

N_E Euler load

N_{EX} Euler load about x axis

N_{EY} Euler load about y axis

N_f Failure load

N_{sq} Squash load

N_{TH} Theoretical failure load

N_u Required axial load capacity

N_x Uniaxial failure load with major axis bending

N_{xy} Biaxial failure load

N_y Uniaxial failure load with minor axis bending

$N_1, \ldots N_4$ Axial load

n Node number

Number of elements along y axis

N_{ij} Axial load on (ij)th element

O_x, O_y Pin-joints about x and y axes, respectively

p Number of analysis

P_x, P_y Plastic hinges, adjacent to column, in beams about x and y axes, respectively.

R Reduction factor

r radius of gyration

S_i Shear force at node i

S_x Shear about x axis

S_y Shear about y axis

s	Stability function
$\bar{s}_i$	Directional restraint at node i.
t	Thickness of flange
U_n	Required deflection at node n.
u	Displacement
u_i	Displacement at node i
u_{ij}	x co-ordinate of (ij)th element
V_n	Required deflection at node n
v	Displacement
v_i	Displacement at node i
v_{ij}	y co-ordinate of (ij)th element
v_{req}	Required deflection
W	Width of steel section
w	Thickness of web
w_i	Displacement of node i
	Load on beam i
x	Distance along column
	Linear axis
y	Deflection
	Linear axis
y_m	Deflection at mid-height
z	Linear axis
z_{ij}	Distance of centroid of (ij)th element to neutral axis
z_n	Depth of neutral axis
α	Constant
	Concrete contribution factor

α_n	Factor in biaxial interaction formula
β	Ratio of end-moments
	Constant
γ, γ_2	Constants in concrete stress-strain curve
δ	Sway deflection of column
	Deflection at end of beam
ε	Strain
ε_f	Maximum concrete strain
ε_{ij}	Strain on (ij)th element
ε_u	Strain at maximum concrete stress
ε_y	Yield strain of steel
ε_η	Measure of initial out-of-straightness
ε_θ	Rotation
	Orientation of neutral axis
θ_A	Rotation
θ_{bx}	End-rotation about x axis at bottom of column
θ_{by}	End-rotation about y axis at bottom of column
θ_c	End-rotation of column
$\theta_{n1},....\theta_{n4}$	Hinge rotations
θ_m, θ_m, θ_p, θ'_p	- Rotations used to describe hinge characteristics
θ_{sh}	Rotation of hinge at commencement of strain-hardening
θ_{tx}	End-rotation about x axis at top of column
θ_{ty}	End-rotation about y axis at top of column
θ_x, θ_y, θ_z	Rotation about x, y, and z axes respectively
σ	Stress
σ_a	Axial compressive stress
σ_{bc}	Bending compressive stress
σ_{bx}	Bending stress about major axis
σ_{by}	Bending stress about minor axis

σ_{ic}	Initial curvature stress
σ_{ij}	Stress on (ij)th element
σ_{pc}	Permissible axial stress
σ_{pbc}	Permissible bending stress
σ_{u}	Maximum concrete stress
σ_{us}	Ultimate tensile strength of steel
σ_{y}	Yield stress of steel
σ_{yr}	Yield stress of reinforcement
Φ	Curvature
	Ratio $A_{r\ yr}/A_{s\ y}$
Φ_{o}	Curvature due to initial imperfections
ϕ	Curvature
ϕ_{x}	Curvature about x axis
ϕ_{y}	Curvature about y axis

CHAPTER 1. REVIEW OF RELEVANT RESEARCH AND DESIGN METHODS

1.1 Introduction

Analysis, testing and design methods for columns have involved much research over the last 200 years. The object of this chapter is to report the major developments over this period under three major headings,

1.2 General column behaviour

1.3 Composite column behaviour

1.4 Current design methods.

Sections 1.2 and 1.3 include the major theoretical contributions and also deal with tests carried out and their influence on the then current design rules. Section 1.4 covers the most recent proposals for design in both the United Kingdom and abroad, and any tests used to verify these methods.

1.2 General column behaviour

The analysis of members under compression loading has developed a long way since Euler[1][2] first proposed his analysis for the strength of elastic columns in the 18th century. However, Euler's formula was found to over-estimate the strength of short columns, the error increasing as columns became shorter. Lamarle established that the elastic limit was the limit of validity of Euler's formula. Considére[3] and Engesser[4], independently of each other, solved the problem of errors in the load by generalizing the Euler formula. Kármán[5] performed a series of tests to show that Engesser's assumptions in his double modulus formula were correct.

Kármán[5][6] was the first to consider the buckling of eccentrically loaded columns as a stability problem and in 1908 gave a complete and exact analysis for the problem. Westergaard and Osgood[7], in 1928, used Kármán's analysis with the assumption of a part cosine deflected shape to analyse a series of eccentrically loaded columns. This assumption simplified Kármán's analysis without impairing the accuracy too much. They also investigated the effect of initial out-of-straightness on the behaviour of columns.

Chwalla[8] used Kármán's analysis to investigate the stability of eccentrically loaded columns with various cross-sections, slenderness ratios and eccentricity. Jezek[9] showed that the use of a simplified bi-linear stress-strain curve for steel had little effect on the results of the analysis. Because of the immense amount of labour required to produce each solution for the inelastic behaviour of a column results existed only for a few special cases.

Baker and Holder[10] carried out a series of theoretical studies for the Steel Structures Research Committee, (S.S.R.C.), on the behaviour of restrained elastic stanchions. They were particularly interested in the distribution of moments at the stanchion-beam connection and so compared the moments obtained using linear elastic theory with those obtained from an elastic analysis including loss of stiffness due to axial load. Because they were producing working load methods and maximum permissible stresses were low, they found that values of N/N_E, where N is the axial load in the column and N_E is the Euler load of the column, were very low and hence the effect of reduced stiffness due to axial load on the

moments was very small. They therefore produced design charts, which also included the effects of initial curvature, based on moments and stresses determined using linear elastic theory.

Following the theoretical work for the S.S.R.C. Baker and Roderick[11] carried out two series of tests of model columns with elastic restraint and loading about the minor axis. The first series was on columns bent in uniform single curvature. The results showed that the choice of initial yield as a failure criterion by the S.S.R.C. was grossly conservative, that moment reversal could occur in slender columns, and that redistribution of moments occurred more rapidly with the spread of plasticity in the column. They also showed that in uniform single curvature bending the load producing collapse is not determined by the condition of the column at mid-height alone. Before collapse can occur the end sections must also be incapable of resisting further moment.

In 1948[11] tests on columns in symmetric double-curvature were carried out on similar model columns. In these tests failure always occurred with "unwrapping" from double curvature into single curvature. As in the single curvature tests the results showed the failure criterion of the attainment of first yield to be grossly conservative.

Both series of tests showed how little effect the beam loading had on the collapse axial load of the column.

Horne, Roderick, and Heyman[11] developed the theory of restrained elastic-plastic columns including the effects of unloading and analysed some of the columns tested and concluded that the effect of ignoring unloading was not significant and lead to conservative results.

Roderick[11] developed an approximate analysis based on the assumption of the development of plastic hinges in the column, Fig. 1.1. A discontinuity due to hinge rotation existed at the centre hinge but the other two hinges were assumed to have just formed and thus the column end rotation was equal to the beam rotation. The column lengths between hinges was assumed to remain elastic. The test results were analysed using this simplified theoretical method and good agreement was obtained.

In 1956 Horne[12] produced his classification chart for biaxially loaded columns, Fig. 1.2, in which P indicates that the adjoining beams have plastic hinges at the beam-column joint, O indicates pinned joints, and E indicates elastic restraint from the beams. He recognised that the P_xE_y case would give higher failure loads, even with small y axis beams, than the P_xP_y case but stated that, at that time, the problem was intractable.

He proposed a P_xP_y design method which took account of the possibility of flexural torsional buckling due to moments about the major axis.

He later proposed[13][14] a P_xO_y method which allowed the development of plastic hinges at the end of the column. As in his P_xP_y method account was taken of lateral instability.

In 1960 research at Lehigh commenced with Galambos and Ketter[15] producing an analysis based on the numerical integration of the equilibrium equation using Newmark's[16] method. They analysed two cases, $\beta = +1$ and $\beta = 0$, where β is the ratio of end moments and is equal to $+1$ for single curvature. Ketter[17] later

analysed $\beta = +0.5$, and -1.0 but found some difficulty with the $\beta = -1.0$ case since the calculation predicted a neutrally stable symmetrically deflected shape since these analyses did not allow for initial curvature although residual stresses were included.

Rossow, Barney and Lee[18], 1967, investigated the effects of initial curvature on the buckling loads of columns again using a Newmark type integration method.

The methods discussed up to this point had been used for the analysis of columns with simple stress-strain curves. The axial load, moment and curvature relationships had been expressed algebraically with recognition of three distinct phases in the spread of plasticity, Fig. 1.3. If more complex non-linear stress-strain relationships, strain-hardening and cross-sections of irregular shape or more than one material were to be analysed, then numerical methods would have to be used.

Cranston[19], 1966, proposed a method to obtain axial load, moment and curvature relationships which he subsequently used in his analysis for reinforced concrete columns. To obtain the relationship he made the following assumptions:-

(a) moment is applied about an axis at right angles to an axis of symmetry,

(b) plane sections remain plane

(c) longitudinal stress at a point is a function only of longitudinal strain

(d) stress-strain relationships are known for the materials in the cross-section

and (e) strain reversal does not occur.

The cross-section was divided into a number of elements in the plane normal to the applied bending moment. The stress on these elements was then assumed to be uniform over an element. A strain profile was assumed across the cross-section and hence the axial load and moment were calculated. If the axial load was close to the specified value then the proposed strain profile was correct; if not the profile was modified and the method repeated. Cranston produced results for a reinforced concrete tee section and gave proposals for extension of the method for the analysis of prestressed sections and biaxial bending.

Cranston[20] used this routine within an analysis for uniaxially bent and restrained columns. The analysis estimated an initial deflected shape and then calculated moments, curvatures and deflections and checked equilibrium and compatability. If convergence was not achieved a new deflected shape was estimated and the analysis repeated. Elastic unloading was considered and special idealizations to speed up the analysis of symmetrical cases were used. The method was also applicable to the analysis of sway columns.

Cranston[21], 1972, used this analysis to help in the development of the clauses for column design in the Code of Practice for Reinforced Concrete, CP110[22].

Harstead, Birnstiel and Leu[23], 1968, studied the behaviour of inelastic H columns under biaxial loading and produced a solution

based on a trial and correction method, using a second order method similar to the Newton-Raphson technique.

They used a computer program to analyse a series of columns. The analysis was also used to check the results of tests carried out on pin-ended biaxially loaded columns.

Vinnakota and Aoshima[24], 1974, have presented a method of analysis for the inelastic behaviour of rotationally restrained columns under biaxial loading. Account of residual strains in the cross-section and warping strains that result from the twisting of the section is included in the analysis.

The deflected shape of the column was estimated and section properties and torsional loads calculated. Using these section properties and considering equilibrium, a new set of deflections were calculated. These were compared with the estimated deflections. If the required degree of convergence had not been achieved the routine is repeated using the new deflections.

The analysis has been used to check experimental results of columns tested by Birnstiel[25] and Gent and Milner[26].

Young[27][28], 1971, used a method based on the correction of an initially estimated deflected shape by block relaxation for the analysis of axially loaded columns. For beam-columns, because of the lack of symmetry in the deflected shape, point relaxation was tried but found to converge only slowly. Therefore, to speed up the rate of convergence, the extrapolated Liebemann over-relaxation procedure was used.

Young[29] also examined the moment-curvature relationships for hot rolled, doubly symmetric, I section column and beam shapes containing realistic residual stress patterns. He examined both major and minor axis uniaxial bending.

In the column analysis Young considered two load paths, Fig. 1.4, and took account of elastic unloading of plastic sections when using load path 2. It was shown that choice of load path 2 only had any effect if yield had taken place under the application of axial load only and that even then the effects were small.

Young examined the effect of imperfections, both initial curvatures and residual stresses, on the failure loads of columns. He pointed out the importance of stocky columns in design and produced beam-column design charts. That charts, Fig. 1.5, which he called "beta" charts used the three parameters $\frac{M}{M_p}$, $\frac{L}{L_c}$ and β

where M is the applied moment at the top of the column

M_p is the reduced plastic moment under axial load

L is the length of the column

L_c is the critical length of an axially loaded column

and β is the ratio of the moments at the top and the bottom of the column, single curvature being +ve.

The slenderness ratio and axial load have been absorbed into the single parameter L/L_c. Thus each point on a line of given β represents an instability failure of a column for a given applied moment and axial load. He compared these charts with test results from Lehigh[30][31] and Liège[32] and showed that when lateral failure

was not allowed to occur, In the case of major axis applied moments, the charts gave good results. However If out of plane failure was allowed to occur then the charts were of little use. Because of this problem a design method was proposed[33] for the pin-ended biaxially loaded column. Young did not produce an analysis to check this design method but did check it against available experimental results.

Young also proposed a method[34] for the design of elastically restrained columns using his "beta" charts with moment rotation curves. The method was based on the assumption that the deflected shape of the column can be represented by a part sine curve. For out-of-plane buckling Young used the criterion suggested by Gent[35] i.e. that a lower bound to the buckling load for I section columns will be given by the consideration of the minor axis stability of one flange.

The effects of restraint have been studied by Gent[35] who tested models representing a typical heavily loaded no-sway universal column subjected to single curvature bending about its major axis and with elastic beams. The loading path chosen was to apply high end moments, equal at top and bottom, and then to apply axial load to failure. Gent showed that failure occurred either near the squash load or as a snap-through failure about the minor axis. Torsional buckling was shown to be of secondary importance in his tests of elastic-plastic columns restrained by elastic beams. He proposed that minor axis stability could be considered as a deterioration of stiffness and that a lower bound on the minor axis buckling load should be provided by the

elastic critical load of the tension flange alone. He showed this to be true with further model tests.

Gent and Milner[26] extended the work to cover the case of biaxially loaded, elastically restrained columns. They showed the importance of the critical load of one flange for the biaxially loaded columns. They concluded that there is no combination of bending and axial load under which the ultimate axial load capacity would be directly reduced by bending in accordance with the combined stress concept. They produced axial load slenderness curves for minor axis buckling of elastic-plastic columns with imperfections when the stability is controlled by one flange.

1.3 Composite columns

The problem of the analysis of concrete and steel composite columns has not received as much attention as that of bare steel columns.

Bondale[36] carried out an extensive survey of work on composite columns prior to 1959 and therefore this review will only briefly mention work up to 1959.

In 1912 Talbot and Lord[37] attempted to evaluate the effect of the various parameters in a series of 32 tests on axially loaded columns with a built up steel section, Fig. 1.6. 10 bare steel columns were tested, 12 columns were tested with a concrete core inside, 3 were tested with concrete cover as well and the remainder were encased columns with $\frac{1}{4}$" diameter wire spirals at either 2" or $1\frac{1}{2}$" spacing. From the tests on the bare steel section a rule of the form

$$\frac{N}{A} = \alpha - \beta\frac{L}{r} \qquad (1.1)$$

where A is the cross-sectional area of the column

r is the radius of gyration of the steel core

and α and β are constants

was proposed. They suggested that for the cored columns and the spirally reinforced columns the effect of the concrete could be included by adding to the strength of the bare steel column an additional strength equal to 2/3 of the 6" cube strength multiplied by the area of concrete. For the unreinforced encased sections the concrete was found to only carry a stress equal to about 1/3 of the 6" cube strength, due to premature spalling, and it was suggested that no allowance should be taken for the concrete in design.

These tests together with further tests, carried out between 1912 and 1936, by Mensch[38], Emperger[39], Burr[40], Faber[41] and Stang Whittemore and Parson[42] all indicated an increase of strength of up to six times for encased columns over the bare columns.

As a result of the above tests BS449: 1948[43] permitted partial account of the concrete encasement to be taken in design calculations. The permissible load, however, was not to exceed 150 per cent of the bare steel stanchion load.

In 1956 Faber[44] proposed design formulae from the results of tests carried out by him.

Rizk[45], 1957, tested a series of axially loaded columns,

8 were encased and 3 were bare steel. The results compared well with the "law of addition".

Rizk also studied eccentrically loaded columns in uniaxial and biaxial bending and proposed an iterative method for predicting failure.

Stevens[46], 1959, carried out a series of 35 tests on encased stanchions, in which the variables were slenderness ratio, reinforcement area and concrete strength. He used the "law of addition" to predict the strengths and concluded that this was safe. As a result of Stevens' work BS449: 1959[47] allowed the value of axial load to be increased to twice the value permitted on the bare steel section.

Bondale[36] applied Westergaard and Osgood's[7] method to the analysis of composite columns. He used algebraic expressions for the calculation of moment - curvature-axial load relationships and assumed the deflected shape to be part of a cosine curve. He also tested eight encased columns with in-plane bending.

Basu[48] extended Bondale's analysis for use on digital computers by replacing his algebraic moment curvature relationships with the iterative method as used by Cranston.[19]

From Fig. 1.7 it can be shown that if the deflected shape of the column is given by

$$y = y_m \cos[(2x/L)\cos^{-1}(e/y_m)] \qquad (1.2)$$

where y is the deflection measured from the line of action of the load

e is the eccentricity of the load

y_m is the deflection of the centre of the column

x is the position of a point along the column measured from the centre of the column

L is the length of the column,

then the curvature, at the centre due to bending is

$$\Phi = [(2/L) \cos^{-1} (e/y_m)]^2 y_m - \Phi_o \qquad (1.3)$$

where Φ_o is the curvature due to initial out of straightness.

The moment at the central section is

$$M = Ny_m \qquad (1.4)$$

where N is the axial load.

From the moment curvature relationships the value of curvature corresponding to the moment can be obtained

$$M = Ny_m = F(\phi) \qquad (1.5)$$

and thus

$$y_m = f(\phi) \qquad (1.6)$$

The analysis involves the solution of equations (1.3) and (1.6) to give values of y_m and Φ for a particular load N.

Basu compared his analysis with exact solutions for universal columns, unreinforced elastic concrete (brittle) columns and with test results for composite columns. He concluded that this analysis gave good agreement with exact analyses and test results but that more tests were required.

Basu and Hill[49] produced a more exact method of analysis based on the true equilibrium shape. This method had the advantage over the previous method of being able to handle all ratios of end eccentricity more accurately. A number of comparisons

with exact solutions were made. The previous part cosine curve solution was also checked and found to compare well.

They concluded that the use of the straight line interaction formula as used in steel design for columns with equal end eccentricities:

$$\frac{N}{N_a} + \frac{N.e}{M_{ULT}} = 1 \qquad (1.7)$$

Where N_a is the ultimate load under pure axial load

and M_{ULT} is the ultimate moment when $N = 0$,

is not generally applicable to the failure load of composite columns. They showed it to be safe for medium and short columns; but it could be unsafe for slender columns.

Basu and Somerville[50] used these analyses to develop a design method for pin-ended composite columns; this method is mentioned in more detail in Section 1.4.

Roderick and Rogers[51] proposed an analysis for columns in single curvature uniaxial bending. The main steps in the method are:-

(1) Estimate deflections.

(2) Calculate moments.

(3) Calculate curvatures using moment-curvature relationships.

(4) Calculate rotations, θ.

(5) Calculate deflections, y.

(6) Compare calculated and estimated deflections; if not within required degree of accuracy then use calculated deflections and repeat steps 2 to 6.

The moment-curvature relationships were obtained from a set of algebraic expressions. A bi-linear stress strain curve was used for steel and a tri-linear curve for concrete.

Three small scale composite columns were tested and experimental and theoretical results compared. The results of the columns tested at the Building Research Station by Stevens[46] were also compared with the theory. Reasonable agreement between theory and test was noted.

Shaples[52] proposed an analysis for uniaxial bending of composite columns in which an initial estimation of end rotation, θ, was made. Equilibrium was then established at each node using an iterative process:

(1) Calculate the moment, M_n, at the node ignoring secondary moments due to deflection of the node.

(2) Obtain the curvature, Φ_n, at the node from the moment-curvature relationships.

(3) Knowing Φ_{n-1}, θ_{n-1}, y_{n-1} and Φ_n, θ_n and y_n can be obtained.

(4) Calculate the moment M_n at the node including secondary effects (Ny_n).

(5) Repeat steps 2, 3 and 4 until consecutive values of y_n are within a stated tolerance.

This process is carried out at each node until the last node is reached, at which overall convergence is also checked, In a no-sway case the deflection should be zero. If convergence is not obtained a new estimation of the initial rotation is made.

The analysis was extended to biaxial columns but an approximate failure criterion was used to determine the failure load due to lateral instability.

Sharples tested a series of model composite columns to obtain moment rotation curves which he compared with his analysis. Reasonable agreement was found. His tests and theory also pointed out the possibility of lateral instability.

Virdi and Dowling[53] tested nine columns in biaxial single curvature bending and proposed a method of analysis for biaxial bending of composite columns. The deflected shape of the column about each axis was assumed to be represented by a part osine curve. The test results were compared with the analysis and found to give reasonable agreement. The interaction formula proposed by Basu and Somerville was also checked and found to give good results for short columns and conservative results for more slender columns.

The effects of residual stresses in the steel section in an encased section were also investigated and found to give a variation of ± 3 per cent in the failure load compared to the failure load of stress-free sections. The use of initial out of straightness to represent all imperfections was investigated and it was found that an all-inclusive lack of straightness of $0.0006L^2/D$, where D is the depth of the section, or residual stresses plus a lack of straightness of L/1000 gave results closest to the test results.

Virdi[54] later proposed a more exact method for biaxial bending

based on the Newton-Raphson procedure. An initial estimation of the deflected shape was made. Internal moments, calculated from curvatures, and external moments, calculated considering equilibrium, were compared. If the convergence criterion was not satisfied then the deflected shape was modified. Results from the analysis were compared with results from the part cosine deflected shape analysis and with the test results and reasonable agreement was shown to exist.

Virdi and Dowling[55] extended this method to analyse restrained columns. They showed that the analysis gave reasonable agreement with tests carried out by Milner[56] on restrained bare steel columns. No restrained composite columns or columns loaded to give conditions other than symmetrical single curvature were analysed.

1.4 Current design methods.

1.4.1 Steel columns

Most column design methods are based on strut curves of the form shown in Fig. 1.8 which relate the failure load, N, of an axially loaded pin-ended strut of given slenderness ratio, L/r, to the squash load, N_{sq}, of that cross-section.

The strut curve used in BS449 : 1959[47] is based on the Perry Robertson Formula. The non-dimensional quantity, n, which is a measure of the initial out-of-straightness, y_m, at midheight, is defined as

$$\eta = \frac{y_m d}{r^2} \qquad (1.8)$$

where d is the distance from centroid to the extreme fibre and r is the radius of gyration. The value of η used in BS449 : 1959 is $0.3(L/100r)^2$, which corresponds to a y_m of about $L/660$ for the minor axis of a typical universal column section, and was found by fitting curves to experimental results. This factor thus also allows for residual stresses.

The revised BS449 is likely to have a series of strut curves to allow for different steels and cross-sections. These are based on both theoretical work and experimental results.

The present BS449 : 1959 uses an elastic interaction formula to check column designs:-

$$\frac{\sigma_a}{\sigma_{pc}} + \frac{\sigma_{bc}}{\sigma_{pbc}} \leq 1 . \qquad (1.9)$$

where σ_a = calculated average axial compressive stress;

σ_{pc} = allowable compressive stress in axially loaded struts;

σ_{bc} = resultant compressive stress due to bending about both rectangular axes;

σ_{pbc} = allowable compressive stress in bending.

To obtain the moments and axial loads acting on a column the code has three classes of design:-

1) Simple design - for nominally pin-jointed frames in which beam loads are applied at an eccentricity of 100 mm from the face of the section or at the centre of the bearing, whichever is the greater.

2) Semi-rigid design - which permits a reduction of the maximum bending moment in beams suitably connected to their supports so as to provide a degree of direction fixity.

3) Rigid design - which states that design should be carried out in accordance with accurate methods of elastic analysis.

Since the last revision of BS449 in 1959 a number of design methods have been proposed. Two important ones are the JCR2[57] method and Wood's vanishing stiffness[58] method.

The JCR2 method is basically a design method for rigid jointed frames which allows plasticity in the beams but not in the columns. For braced frames a limited substitute frame is used, loaded as shown in Fig. 1.9, plastic hinges being assumed to occur in those beams which have both dead and live load. The ratio of elastic critical load to Euler load of the column is then found from charts, using the elastic stiffness of the non-plastic beams. The magnification of bending moment due to axial load is then found from Fig. 1.10.

The criterion for collapse of the column is first yield of the extreme fibres. The total stress is found from

$$\sigma_a + \sigma_{bx} + m\sigma_{by} + \sigma_{ic} \nmid \sigma_y \qquad (1.10)$$

where σ_a = direct stress due to axial load;

σ_{bx} = bending stress about major axis neglecting instability effects;

σ_{by} = bending stress about minor axis neglecting instability effects;

σ_{ic} = initial curvature stress;

and m = magnification factor;

The initial curvature stress is to allow for initial imperfections in the column.

This method was tested[59],[60], and found to be conservative, in two full scale three storey frames.

Following these tests Wood[58] proposed a method based on the deterioration of stiffness due to plasticity for the design of columns in no-sway frames. The method is based on the estimation of the remaining elastic core after application of moments and, hence, the calculation of the reduced critical load.

If we have a column bent in single curvature about the major axis, Fig. 1.11, failure is likely to occur about the minor axis. Initially, assuming no plasticity, the failure load, N_f, is given by

$$N_f = N_E = \frac{\pi^2 E I_Y}{L^2} \qquad (1.11)$$

If the moment is increased, compression yielding occurs and the inertia, I_Y, about the minor axis is reduced to say, RI_Y. The failure load is now

$$N_F = RN_E = \frac{\pi^2 E R I_Y}{L^2} \qquad (1.12)$$

Wood has established formulae for R which include effects of initial imperfections and variation of the ratio of end moments. The effects of end restraints, in-plane failure and torsional instability are also included in the method.

1.4.2 Reinforced concrete columns

CP114 : 1957[61], in common with other codes for the design of reinforced concrete members, divides columns into short and slender

members. Short columns are defined as those in which instability effects can be ignored, and these columns are designed using elastic theory or the load factor method.

Long columns are designed using elastic theory but with a reduction factor applied to the permissible stresses. The reduction factor is dependent on the effective length of the column. The code also gives approximate values for the estimation of this effective length.

CP110 : 1972[22] also considers columns as being either short or slender. Short columns are designed by use of a reduced squash load. Slender columns are designed using the additional moment concept. The additional moments are those caused by the lateral deformations of the column. The code gives formulae, derived by Cranston[21], for both major axis and minor axis additional moments which are to be added to the end moment. These formulae also include an allowance for long-term loading effects. Expressions are given in the code for the calculation of effective lengths. These are necessarily conservative because of the approximate nature of the calculation of relative stiffnesses of beams and columns.

Having calculated the axial load and moments on the cross-section design is carried out using ultimate load theory. Biaxial bending is dealt with by the use of an interaction formula proposed by Bresler[62]

$$\left(\frac{M_x}{M_{ux}}\right)^{\alpha_n} + \left(\frac{M_y}{M_{uy}}\right)^{\alpha_n} \leq 1.0 \qquad (1.13)$$

where M_x and M_y are moments about the major and minor axis respectively;

M_{ux} is the maximum moment capacity assuming axial load N and bending about the major axis only;

M_{uy} is the maximum moment capacity assuming axial load N and bending about the minor axis only;

N is the axial load;

α_n is a factor dependent on the value of N/N_{sq};

and N_{sq} is the axial load capacity of the cross-section.

If the method is used to design columns subjected to unequal end moments it will be unconservative to use the maximum of these as the end moment, especially when they are of opposite sign. This is because the method assumes maximum moment to occur at the centre of the column. The code therefore gives a formula which converts these unequal moments to an equivalent set of uniform single-curvature moments.

The American Concrete Building Code[63] until 1971 used a reduction factor method similar to CP114:1957. In this method, loads and moments from an elastic analysis are divided by a factor R to give design moments and axial load, Fig. 1.12.

The 1971 ACI code suggests that for the design of slender columns a second order analysis should be carried out. If this is not used then the moment magnifier method is used. This method, which is similar to the CP110 method, estimates the maximum moment on the column, Fig. 1.13 , by multiplying the end moment by an magnification factor F.

The magnification factor is based on elastic stability theory and is given by

$$F = \frac{C_m}{1-N_u/N_{cr}} \geq 1 \qquad (1.14)$$

where F is a magnification factor;

C_m is the equivalent moment factor;

N_u is the required axial load capacity;

and N_{cr} is the elastic critical load.

The code gives recommendations for the value of flexural rigidity, EI, to be taken in the calculation of N_{cr}.

The method is based on elastic theory but has been extensively checked[64] against inelastic theory and experimental results.

1.4.3 Composite columns

The present BS449 : 1959[47] includes a method for the design of concrete encased steel columns known as the cased strut method. The method allows an increase of up to 100 per cent of the capacity of the steel column alone but restricts the amount of useful cover on the steel and the slenderness of the columns. The method uses the elastic interaction formula similar to that used for steel columns but replaces the axial stress term with axial loads. Bending is assumed to be taken on the steel section alone.

Taylor[65] has made many improvements to the cased strut method for inclusion in the revised BS449. He has eased some of the limitations and has made the method more suitable for ultimate load design.

Basu and Somerville[56] proposed a method of design for composite columns in 1969. The method was based on data from computer analyses.

The interaction curve for a composite column is shown in Fig. 1.14. The method entails the approximate description of this curve by the parameters K_1, K_2 and K_3. The value of K_1 is obtained from a strut curve, and values for K_2 and K_3 have been formulated for various concrete contributions, α, ratios of ends moments and slenderness ratios. The concrete contribution α is given by

$$\alpha = \frac{A_c \sigma_u}{N_{sq}} \qquad (1.15)$$

where A_c is the area of concrete in the cross-section;

and σ_u is the maximum concrete stress.

A modification for the effects of long term loading is also given. For biaxial bending a modified version of the Bresler[62] formula is used,

$$\frac{1}{N_{xy}} = \frac{1}{N_x} + \frac{1}{N_y} - \frac{1}{N_{ax}} \qquad (1.16)$$

where N_{xy} is the biaxial failure load;

N_x is the uniaxial failure load with bending about major axis;

N_y is the uniaxial failure load with bending about minr axis;

and N_{ax} is the failure load under axial loading constrained to fail about major axis.

Virdi[53] has checked this formula against theoretical results for composite columns in biaxial bending and found it to be conservative.

1.5 Conclusions

1.5.1 Analyses

The main short-coming of most of the methods of analysis proposed are that they are only applicable to columns loaded and constrained to fail about one axis. The biaxial methods proposed are limited, in general, to no-sway pin-ended columns loaded with biaxial end-moments and axial load. Of the analyses that include rotational restraints, that due to Virdi and Dowling[55] has large error matrices and cannot analyse columns with sway. That due to Vinnakota and Aoshima[24] was for columns composed of one material and, because the method used for correction of the deflections is first order, could be expected to converge only slowly for composite columns.

1.5.2 Tests

Most recent work on composite columns has been on the development of suitable analysis and design methods for pin-ended columns and the tests that have been carried out have been to confirm this work. No tests on columns with unequal end-moments or tests on restrained composite columns have been reported.

1.5.3 Design methods.

Design methods for columns generally recognise two classes of columns, sway and no-sway. Most methods then further divide these

into short and slender. The design of short columns is usually simple often being based on a proportion of the squash load and neglecting stability effects.

In a survey[64] carried out in the United States of America it was found that 90 per cent of reinforced concrete columns in no-sway frames and 40 per cent of columns in sway frames could be classified as short, that is L/D less than about 10 where L is the effective length, and D the breadth of the section in the plane of buckling. If a similar study of concrete encased steel sections in frames were made it is reasonable to expect similar results. For steel columns however a smaller proportion would fall into the short category.

Any design method for columns should therefore be capable of treating short columns in a simple yet economic way.

For slender columns stability effects must be included, either by the use of additional moments or some form of stiffness reduction which can be related to the elastic critical load.

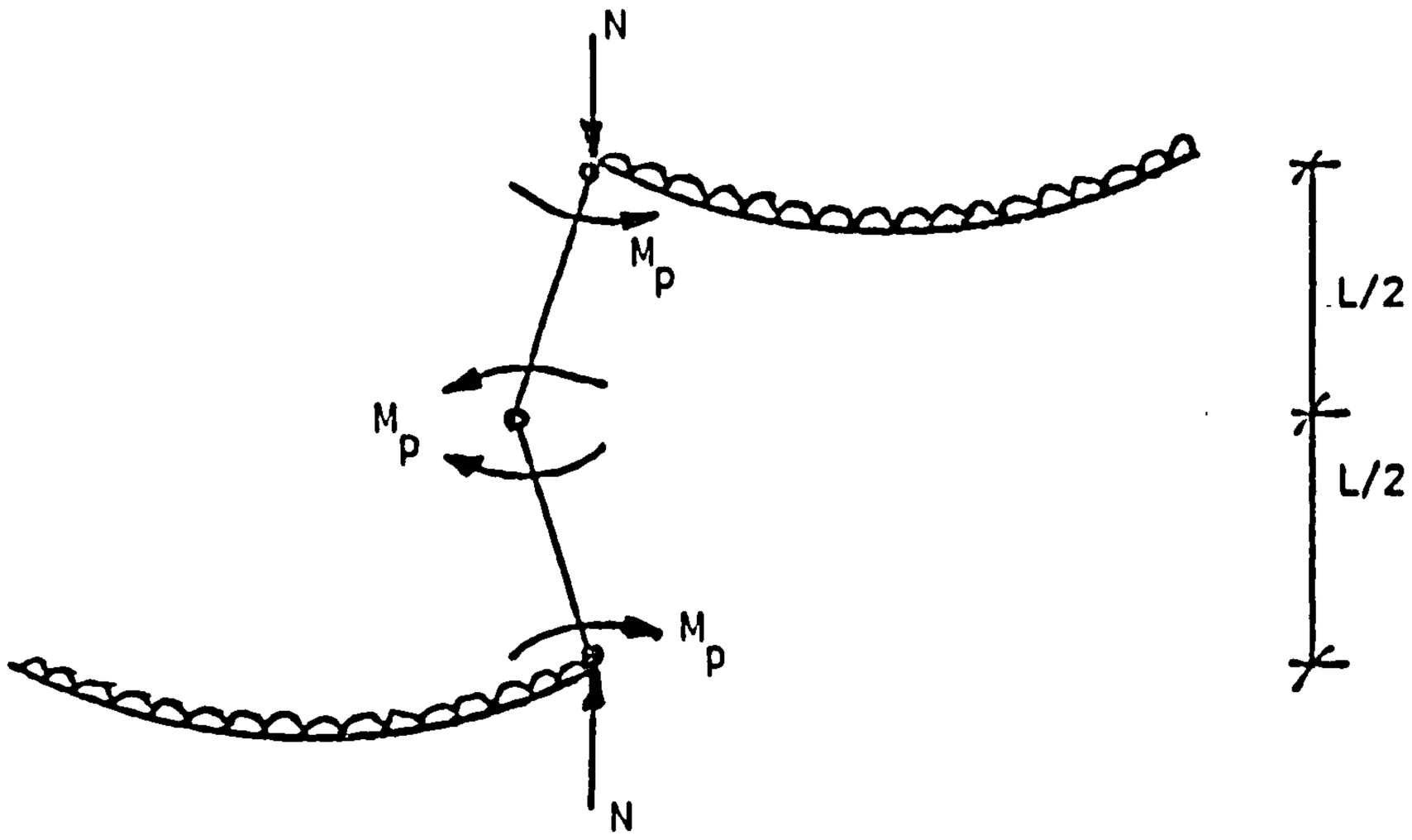

FIG.1.1 ASSUMPTIONS FOR THE SIMPLIFIED ANALYSIS USED BY RODERICK[11]

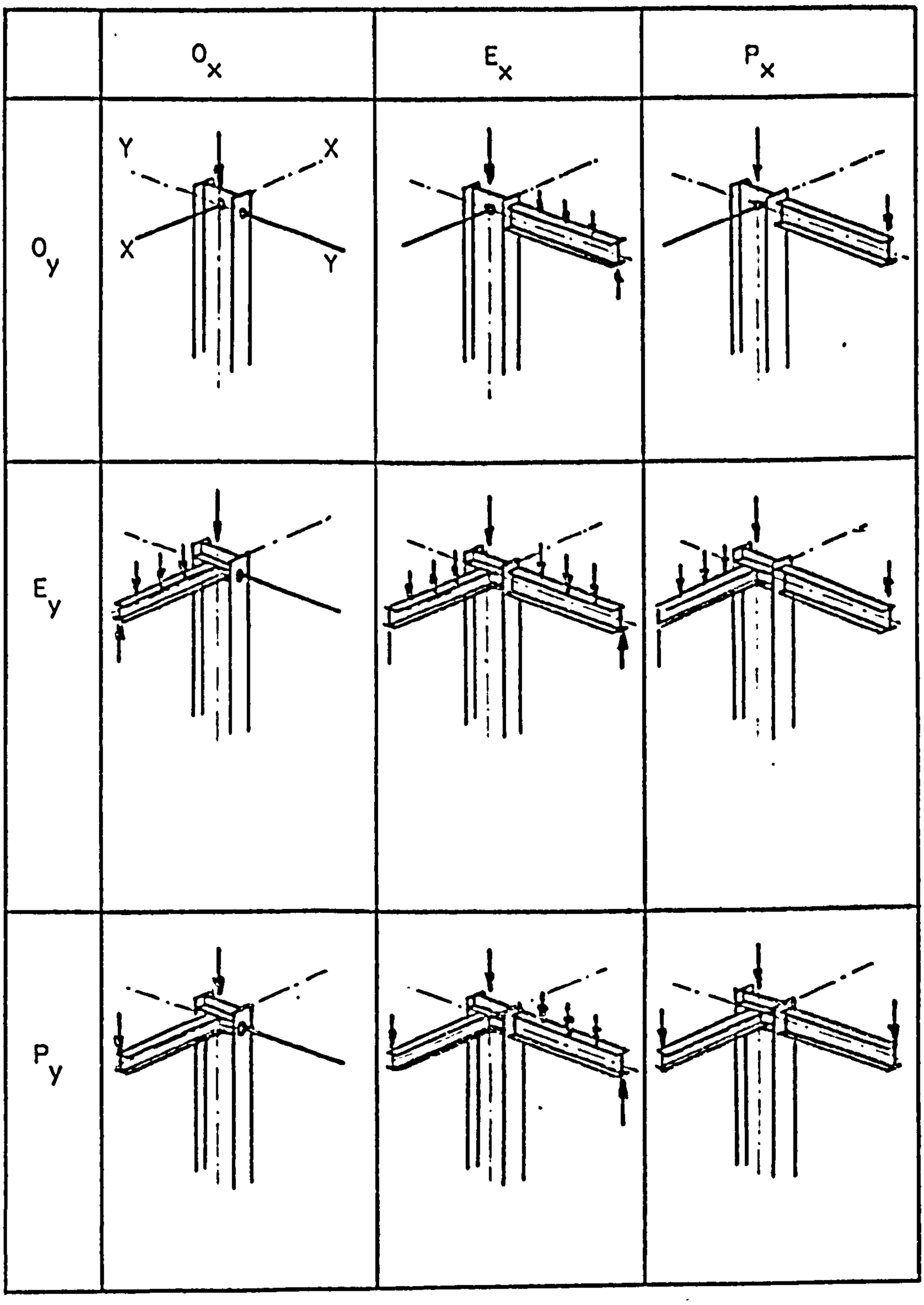

FIG. 1.2 HORNES[12] CLASSIFICATION OF THE STANCHION PROBLEM

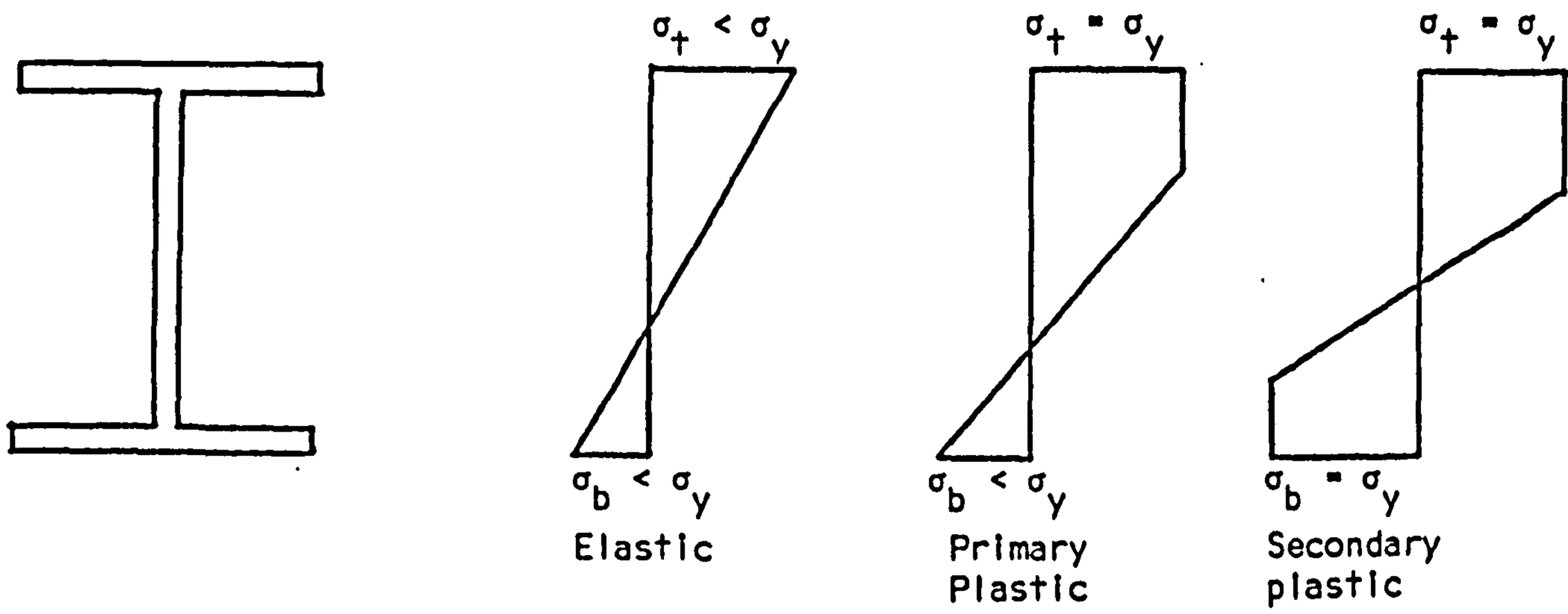

FIG. 1.3 SPREAD OF PLASTICITY IN A CROSS-SECTION

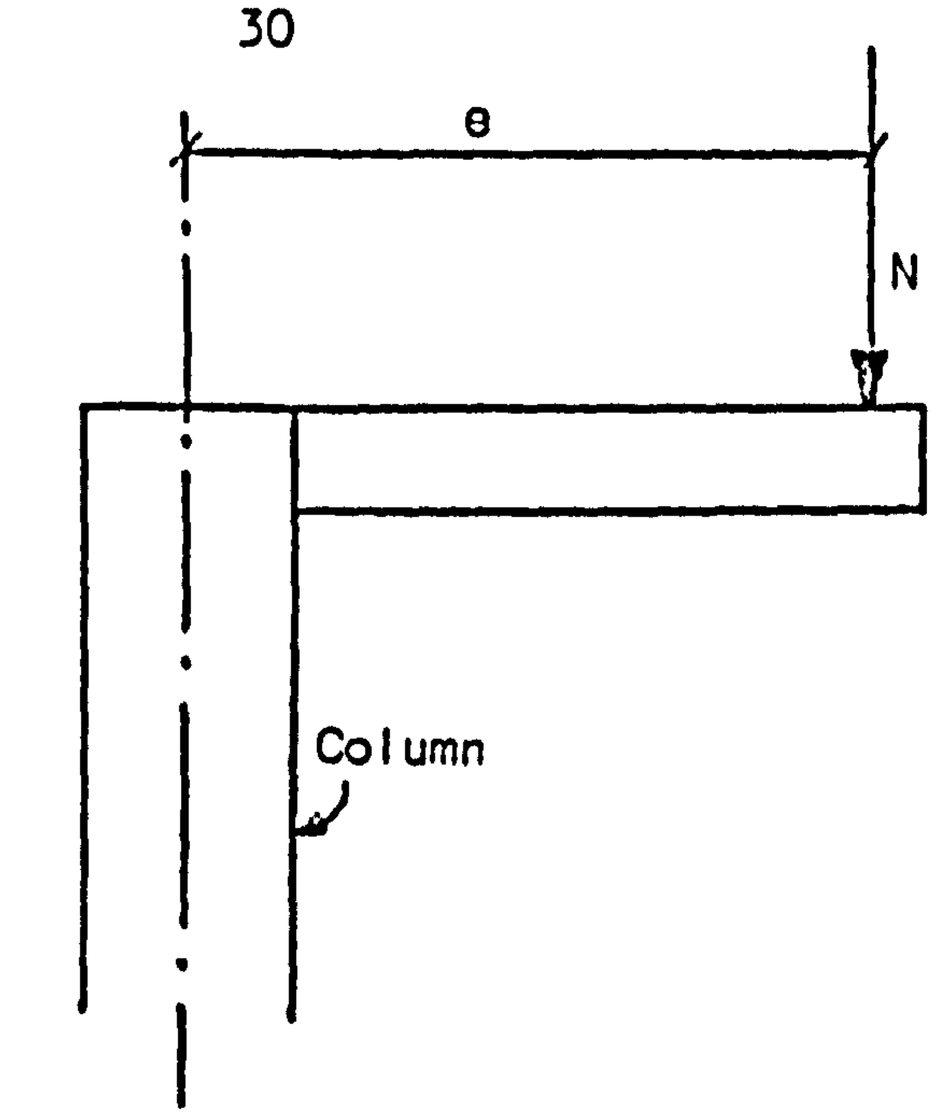

Load path 1 e fixed N varied

Load path 2 e varied N fixed

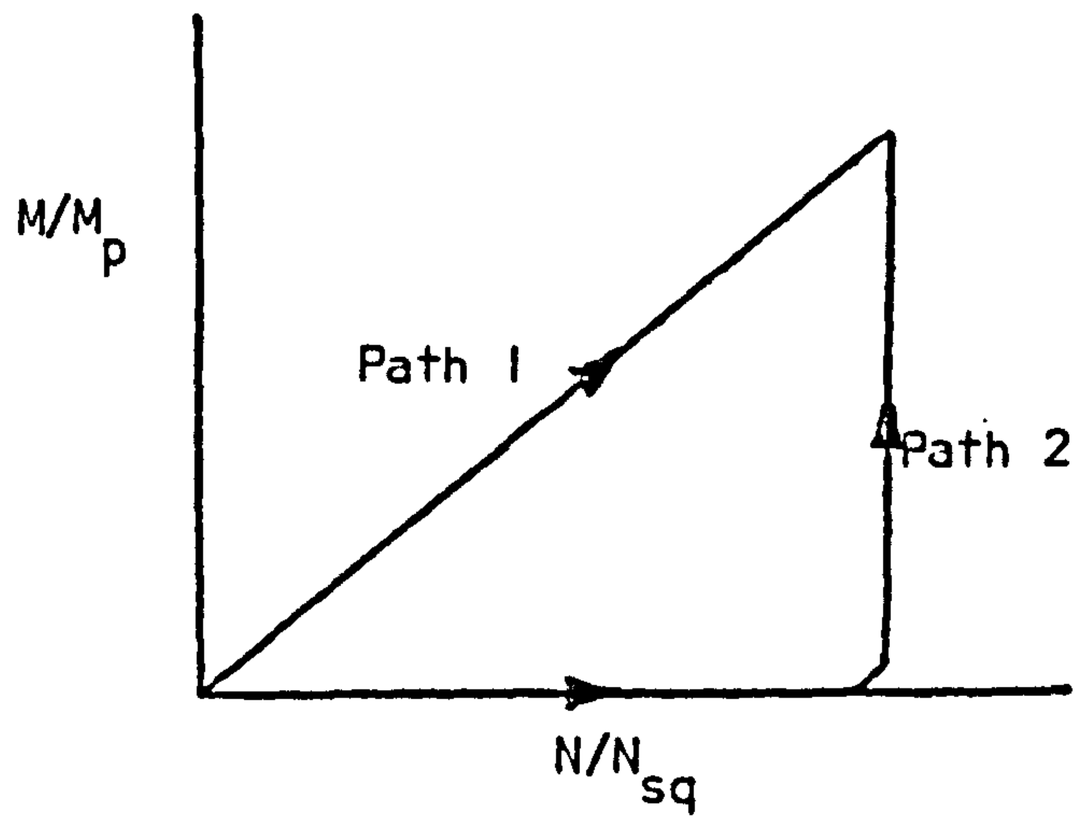

FIG. 1.4 LOAD PATHS USED BY YOUNG[27]

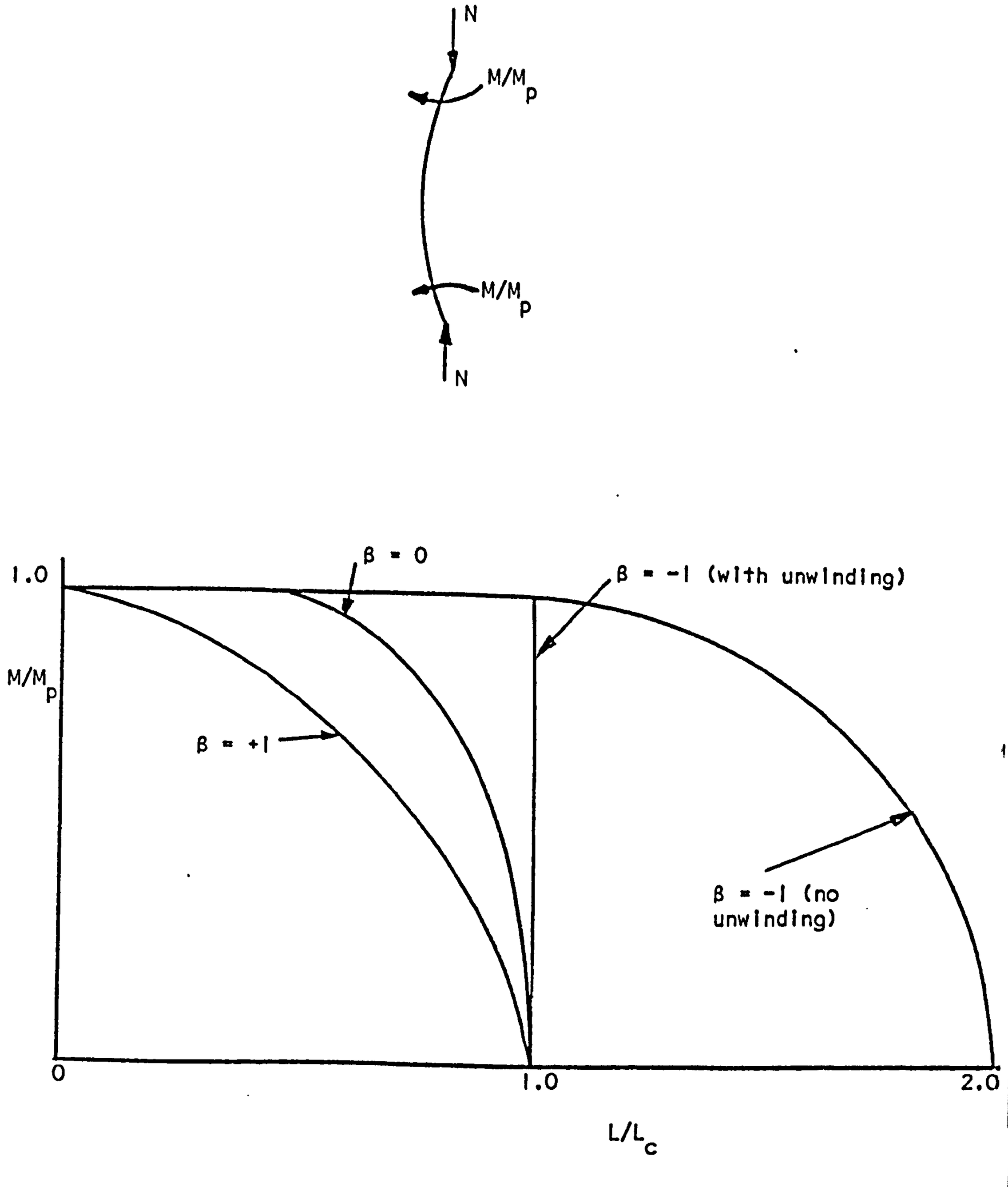

FIG. 1.5 IDEAL "BETA" CHART.

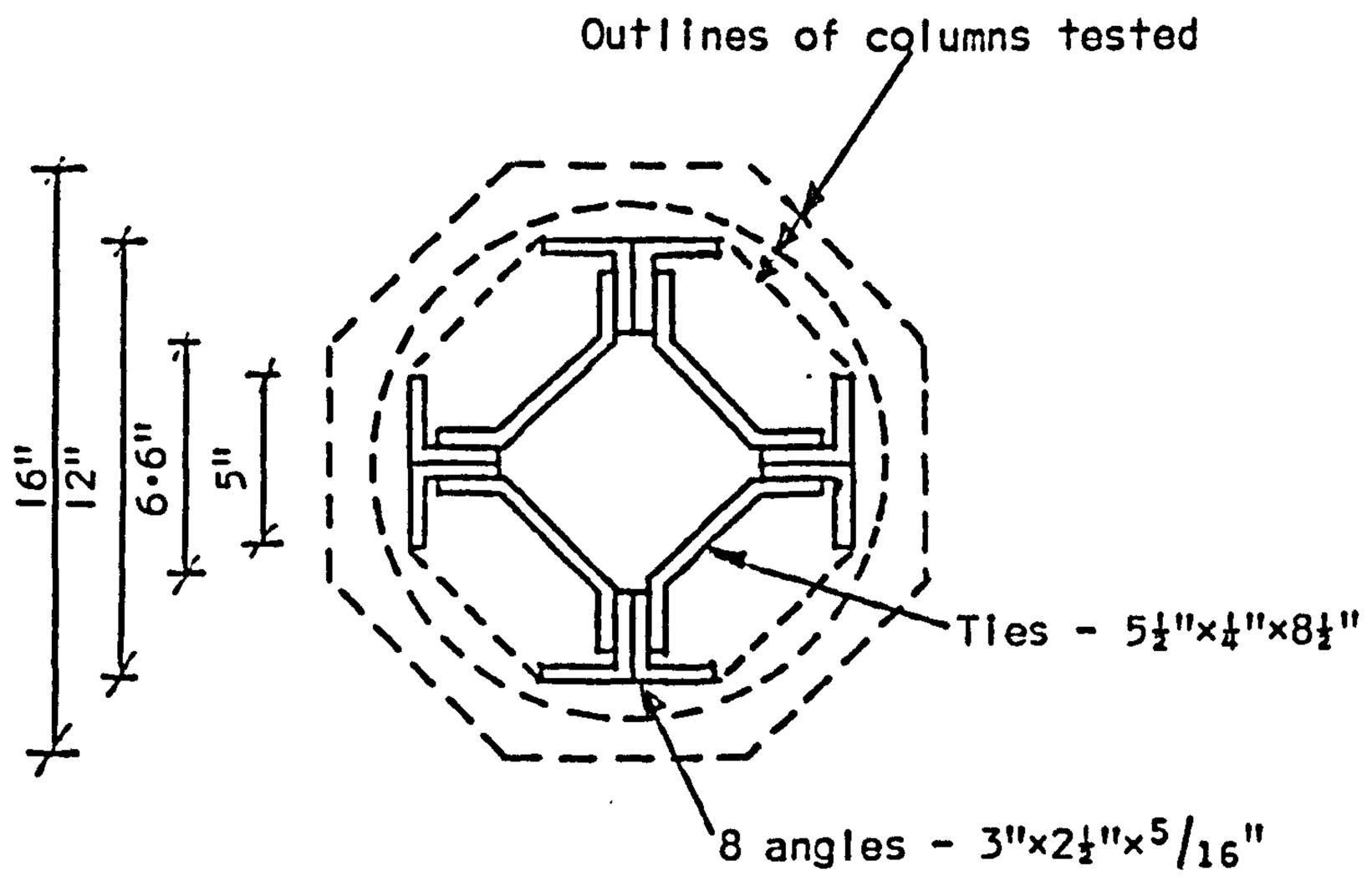

FIG. 1.6 CROSS-SECTIONS OF COLUMNS TESTED BY TALBOT AND LORD[37]

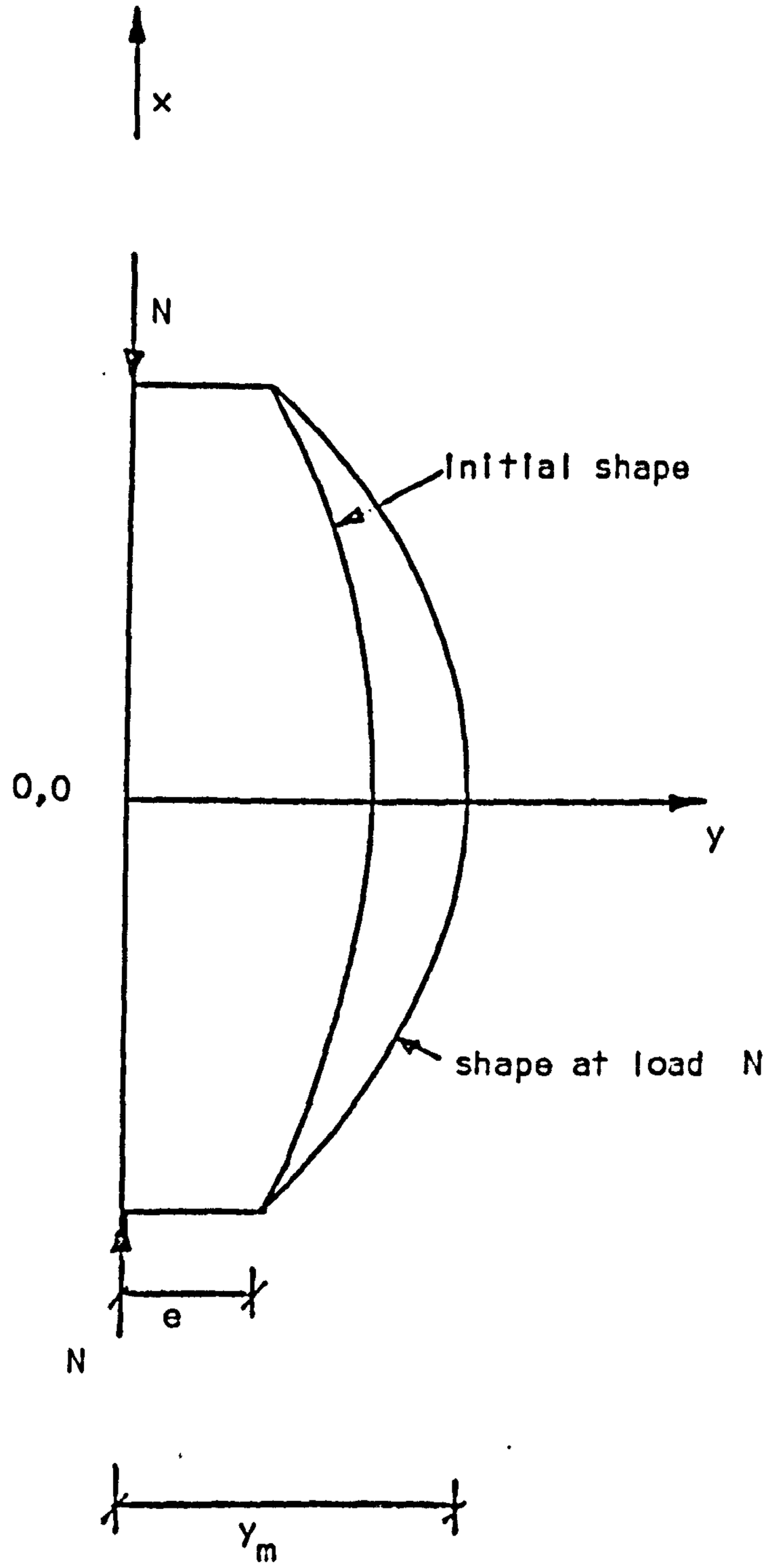

FIG. 1.7 ASSUMED DEFLECTED SHAPE OF COLUMN.

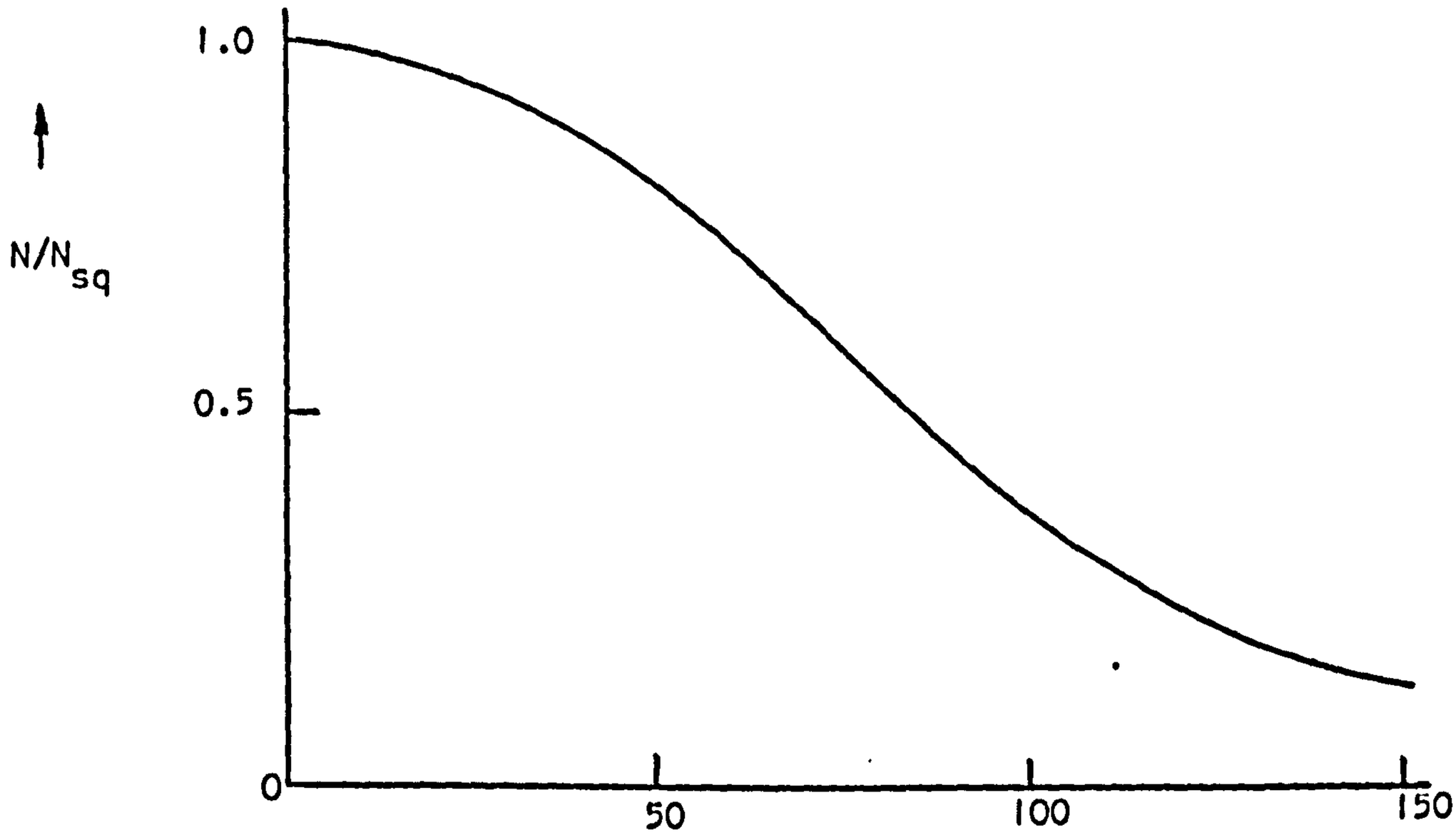

FIG.1.8 FORM OF STRUT CURVE

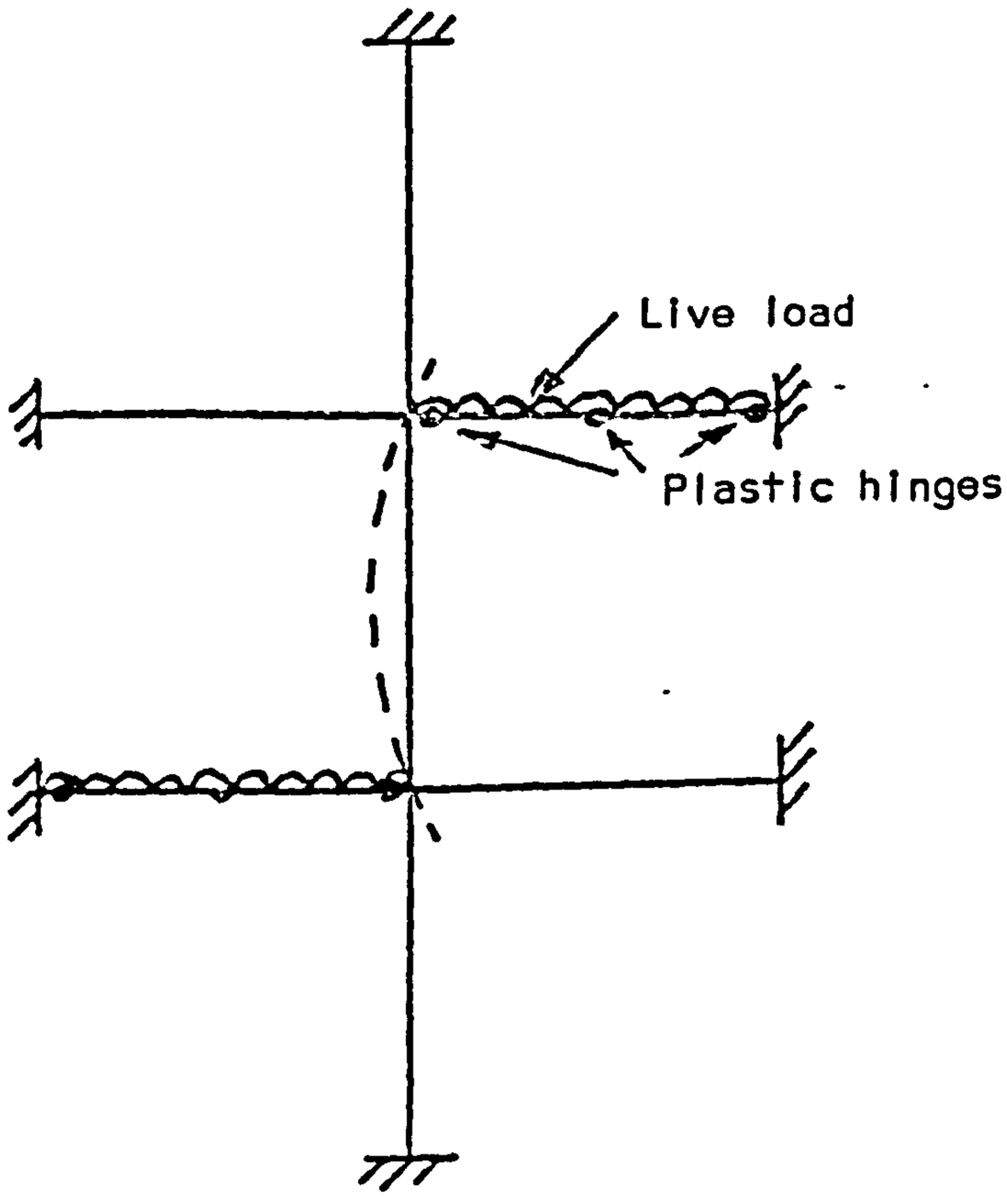

FIG. 1.9 LIMITED FRAME FOR COLUMN DESIGN

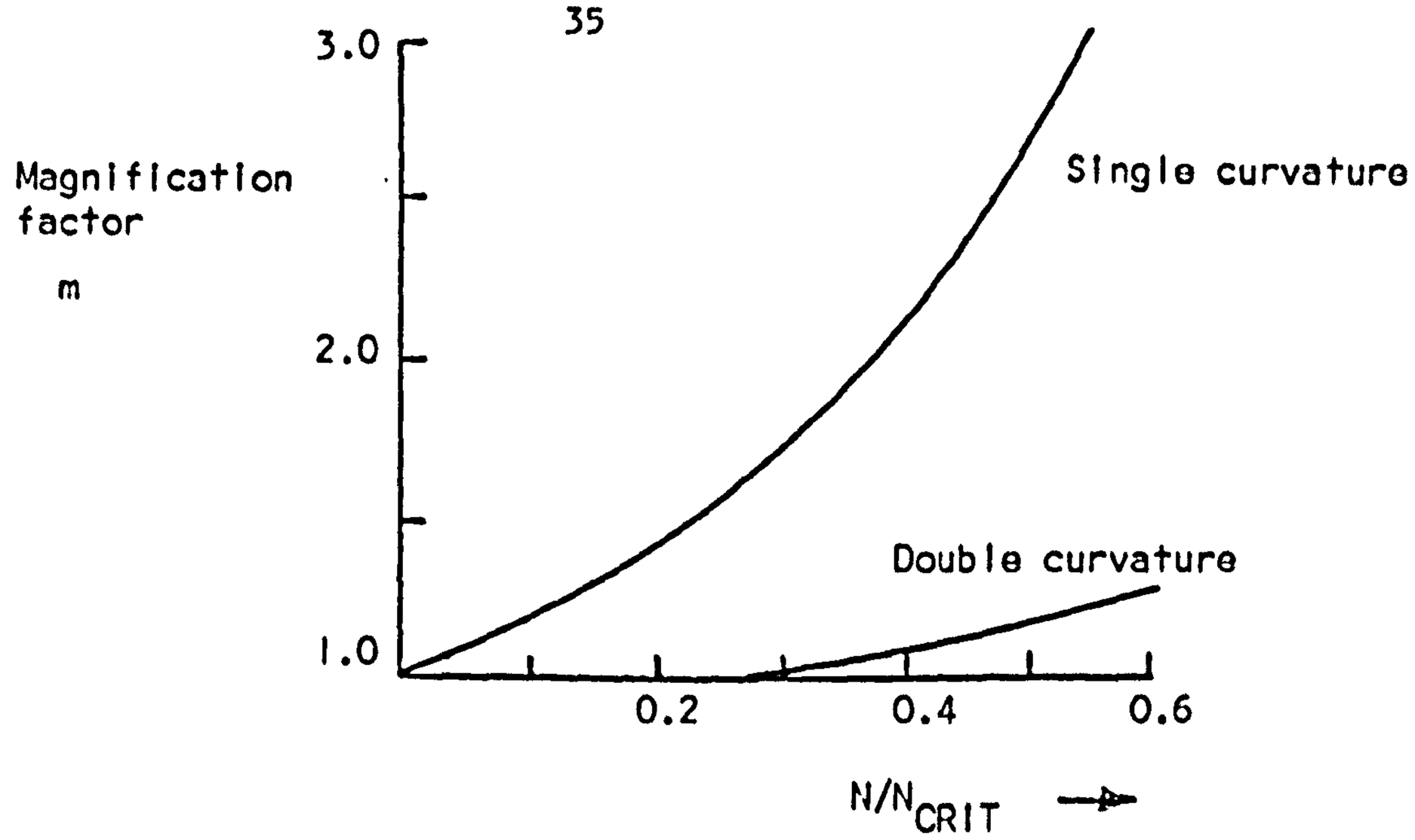

FIG. 1.10 MAGNIFICATION OF BENDING MOMENTS DUE TO AXIAL LOAD

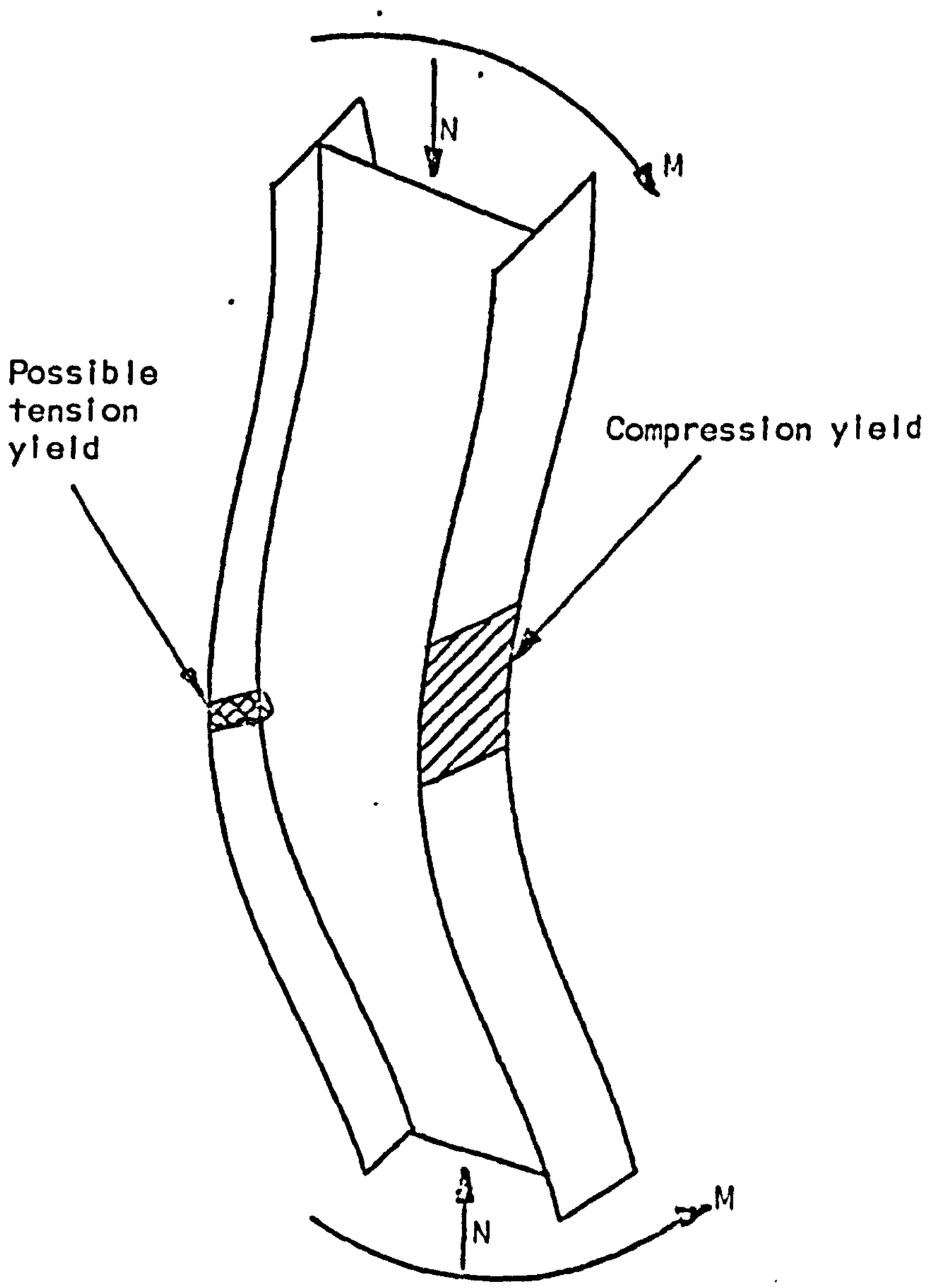

FIG. 1.11 YIELDING OF COLUMN WITH SINGLE CURVATURE BENDING ABOUT THE MAJOR AXIS.

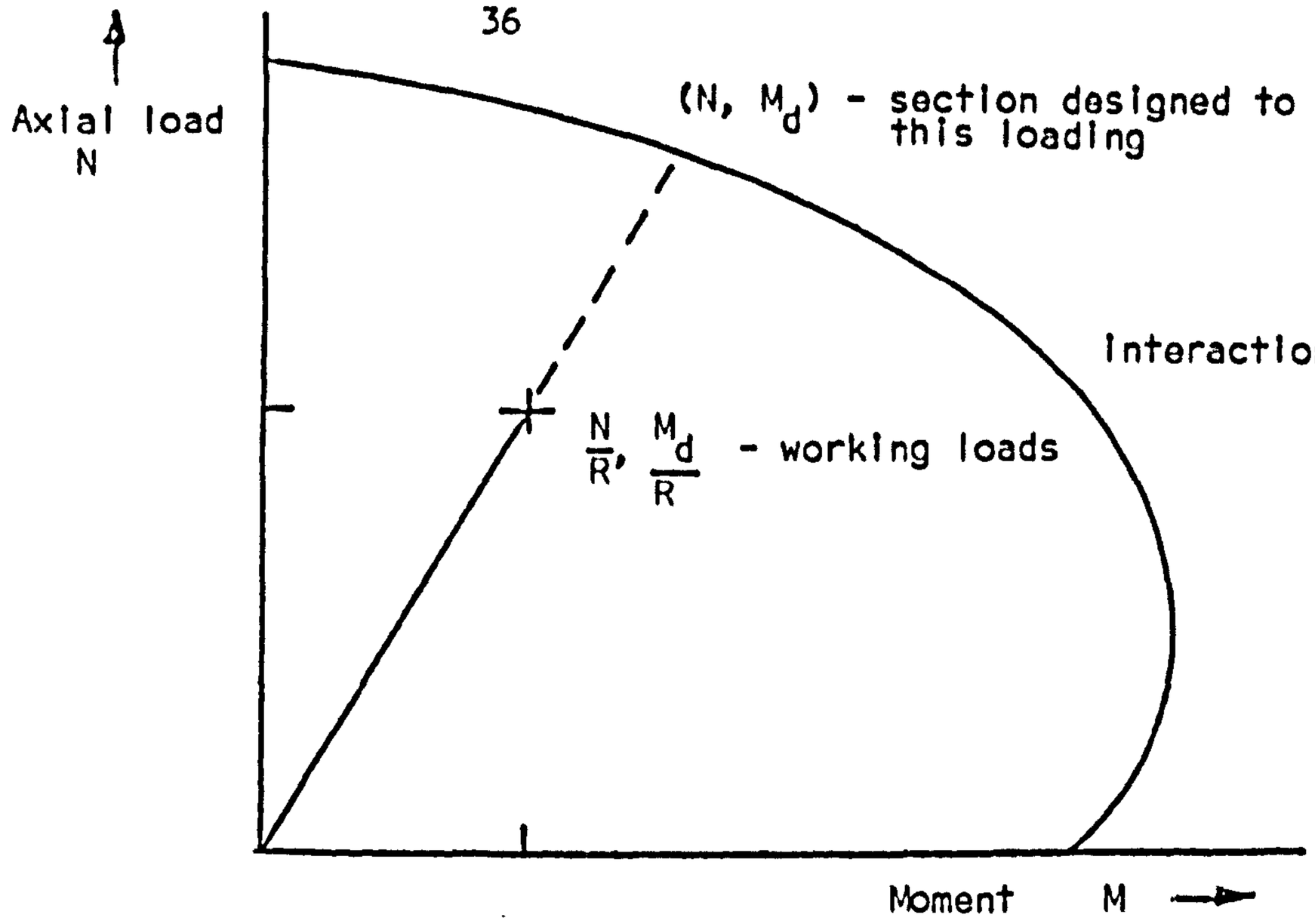

FIG. 1.12 REDUCTION FACTOR DESIGN

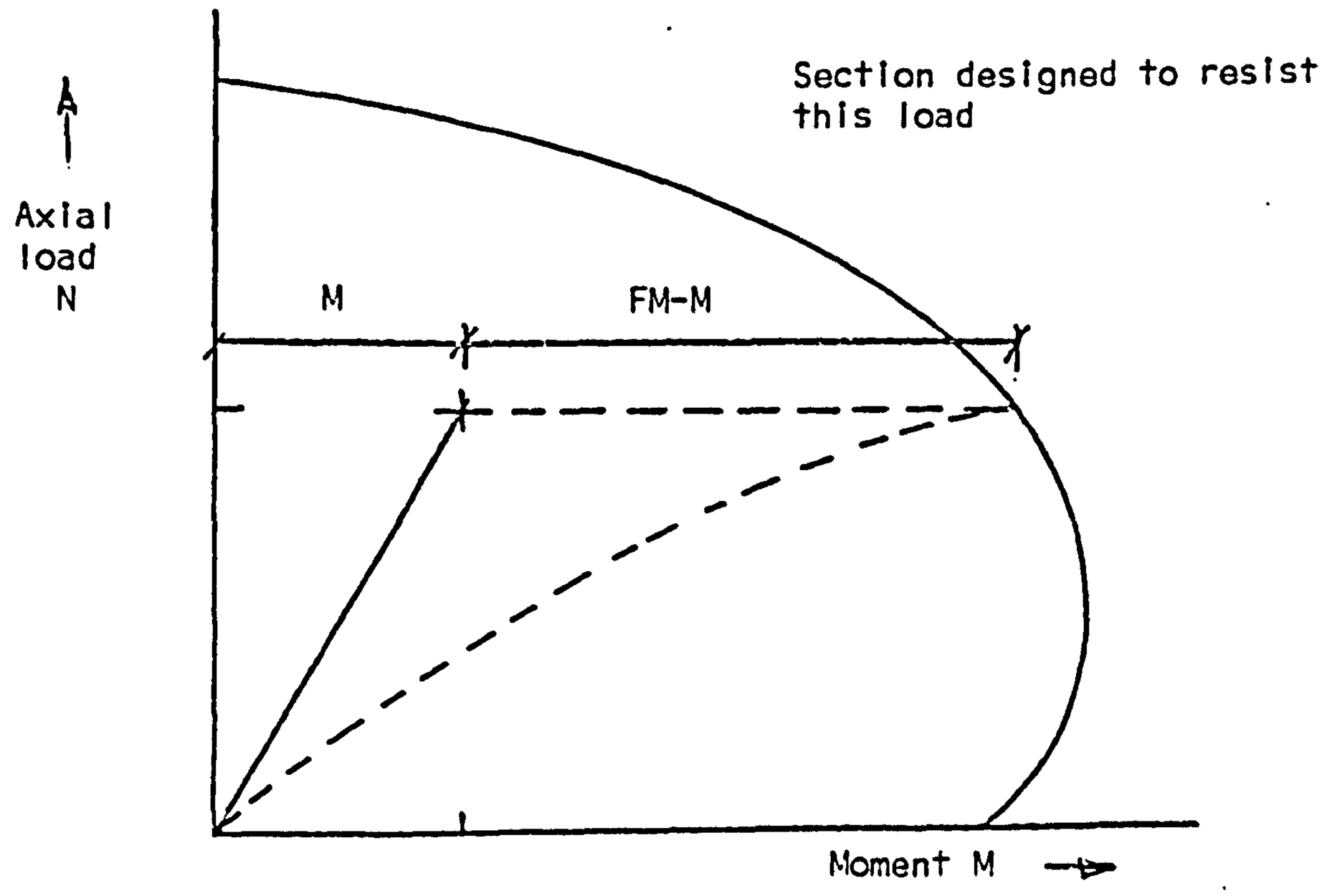

FIG. 1.13 MAGNIFICATION FACTOR METHOD

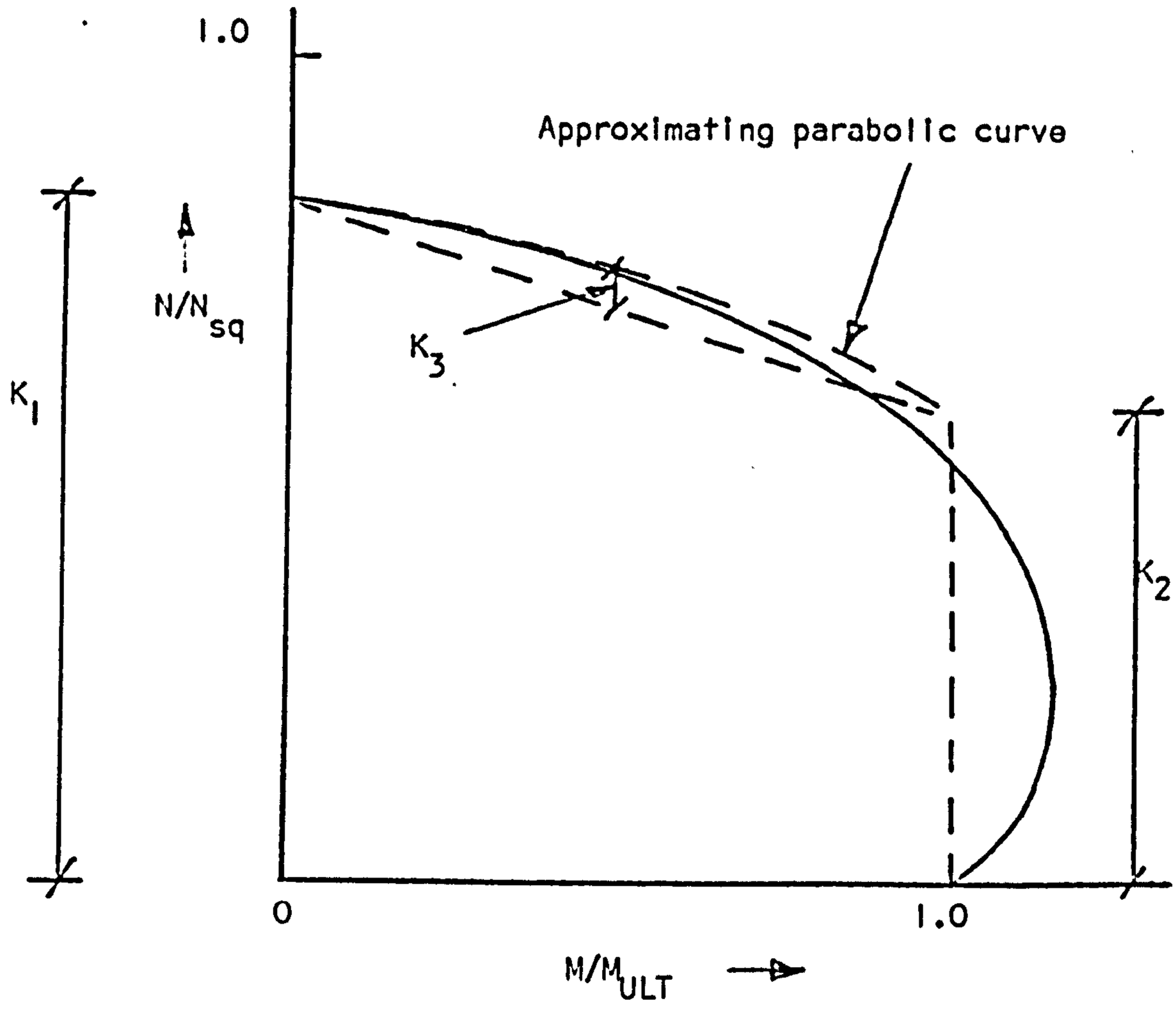

FIG. 1.14 TYPICAL INTERACTION CURVE AND APPROXIMATE CURVE

CHAPTER 2. THEORY FOR THE ANALYSIS OF BIAXIALLY RESTRAINED COLUMNS

2.1 Introduction

In the last ten years a number of computer analyses have been proposed for biaxially loaded columns. These have been reviewed in Chapter 1. Most of these analyses start with an initially estimated deflected shape and subsequently check and correct deflections. The analysis described in this chapter uses a technique of forward integration and has the advantage that at the end of each iteration the column is in equilibrium and thus, with a small correction, details of which are given in Section 2.5.1, can be modified to suit any set of axes.

In Appendix A2 and Appendix A3 two further methods of column analysis which have been tried are described.

2.2 Moment-axial load-curvature relationships

Before the analysis of a column can be carried out, relationships between moments, axial load, and curvatures are required. Because of the non-linearity of stress-strain curves and the make up of the cross-section, exact analytic solutions are not possible and more general numerical solutions have to be resorted to.

2.2.1 Materials properties

2.2.1.1 Concrete encased steel composite columns

For the composite cross-sections the assumed stress strain curves are shown in Fig. 2.1. The concrete stress-strain curve is a polynomial of the form

$$\frac{\sigma}{\sigma_u} = \sum_{i=1,2\ldots}^{n} C_i \left(\frac{\varepsilon}{\varepsilon_u}\right)^i \qquad (2.1)$$

where σ and σ_u are the stress and its maximum value respectively and ε and ε_u are the corresponding strains. The degree, n, of polynomial is taken as 4 and the values of the coefficients C_1, C_2, C_3 and C_4 are 2.41, -1.865, 0.5 and -0.045. The values of these coefficients were obtained by Basu[48] from tests carried out by Barnard and Johnson[66]. The value of ε_u is generally taken as 0.0025 and the crushing strain of concrete generally as 0.0035.

The steel is assumed to have a bi-linear stress-strain relationship, with a yield stress σ_y and corresponding strain ε_y. Strain-hardening has been ignored in the analyses described but could be easily included.

2.2.1.2 Reinforced concrete columns

For the analysis of reinforced concrete cross-sections, the curve adopted by Warner[67] has been used as shown in Fig. 2.2.

The curve is given by

$$\frac{\sigma}{\sigma_u} = \gamma\left(\frac{\varepsilon}{\varepsilon_u}\right) + (3-2\gamma)\left(\frac{\varepsilon}{\varepsilon_u}\right)^2 + (\gamma - 2)\left(\frac{\varepsilon}{\varepsilon_u}\right)^3 , \qquad (2.2)$$

where γ is a constant,

for $0 \leq \frac{\varepsilon}{\varepsilon_u} \leq 1.0$

and

$$\frac{\sigma}{\sigma_u} = 1 - \frac{1 - 2\left(\frac{\varepsilon}{\varepsilon_u}\right) + \left(\frac{\varepsilon}{\varepsilon_u}\right)^2}{1 - 2\gamma_2 + (\gamma_2)^2} \qquad (2.3)$$

for $1.0 \leq \frac{\varepsilon}{\varepsilon_u} \leq \gamma_2$

where $\gamma_2 = \frac{\varepsilon_f}{\varepsilon_u}$.

and ε_f = maximum concrete strain.

For the reinforcement a curve similar to that in Fig. 2.1 has been used.

2.2.2 Method of solution

Figure 2.3 shows a typical encased section in biaxial bending for which relationships are required between bending moment, M, axial load N, and curvature ϕ; these will be referred to as M-N-ϕ data.

For any given values of orientation of neutral axis, θ, depth of neutral axis, Z_n and principal curvature ϕ the cross section is divided into a grid of small elements. The strain profile for the cross-section has thus been described. The solution used is similar to that proposed by Sharples[52].

The distance from the centroid of the (i,j)th element, z_{ij}, to the neutral axis is given by

$$z_{ij} = u_{ij} \cos\theta + v_{ij} \sin\theta \qquad (2.4)$$

where u_{ij} is the co-ordinate along the x axis and v_{ij} is the co-ordinate along the y axis of the (i,j)th element, Fig. 2.3.

Hence the strain, ε_{ij}, on the (ij)th element is given by

$$\varepsilon_{ij} = (\phi \times z_n)\left(1 - \frac{z_{ij}}{z_n}\right) . \qquad (2.5)$$

Knowing the stress-strain curves for all elements the elemental stress, σ_{ij}, can be calculated

$$\sigma_{ij} = \varepsilon_{ij} \times f(E) \qquad (2.6)$$

where f(E) is the relationship to convert strain to stress.

Hence the elemental axial load, n_{ij}, and moments, $(m_x)_{ij}$ and $(m_y)_{ij}$, can be calculated knowing the area, A_{ij}, of the element.

$$n_{ij} = \sigma_{ij} \times A_{ij}$$

$$(m_x)_{ij} = n_{ij} \times u_{ij} \qquad (2.7)$$

$$(m_y)_{ij} = n_{ij} \times v_{ij}$$

The cross-section load, N, and moments, M_x and M_y, are then calculated.

$$N = \sum_{i=1}^{i=m} \sum_{j=1}^{j=n} n_{ij}$$

$$M_x = N \times \frac{D}{2} - \sum_{i=1}^{i=m} \sum_{j=1}^{j=n} (m_x)_{ij} \qquad (2.8)$$

$$M_y = N \times \frac{B}{2} - \sum_{i=1}^{i=m} \sum_{j=1}^{j=n} (m_y)_{ij}$$

where m and n are the number of elements along the x and y axes respectively, B, the breadth and D the depth of the cross-section, Fig. 2.3.

To obtain the values of curvature associated with particular values of moments M_x, M_y and axial load N Equations 2.4 to 2.8 are used with the Newton-Raphson procedure.

The load and moments on any cross-section in biaxial bending can be expressed as

$$N = f(\phi, z_n, \theta)$$
$$M_x = f(\phi, z_n, \theta) \qquad (2.9)$$
$$M_y = f(\phi, z_n, \theta)$$

Expanding Equation 2.9 and retaining linear terms gives

$$N = N_1 + \frac{\partial N}{\partial \phi}\delta\phi + \frac{\partial N}{\partial Z_n}\delta Z_n + \frac{\partial N}{\partial \theta}\delta\theta$$
$$M_x = M_{x1} + \frac{\partial M_x}{\partial \phi}\delta\phi + \frac{\partial M_x}{\partial Z_n}\delta Z_n + \frac{\partial M_x}{\partial \theta}\delta\theta \qquad (2.10)$$
$$M_y = M_{y1} + \frac{\partial M_y}{\partial \phi}\delta\phi + \frac{\partial M_y}{\partial Z_n}\delta Z_n + \frac{\partial M_y}{\partial \theta}\delta\theta$$

Where N_1, M_{x1} and M_{y1} are values corresponding to estimated values of θ_1, Z_{n1} and ϕ_1. $\delta\phi$, δZ_n and $\delta\theta$ are thus the corrections to be applied to give N_1 M_x and M_y.

Re-arranging equation 2.10 gives

$$\begin{bmatrix} \delta\phi \\ \delta Z_n \\ \delta\theta \end{bmatrix} = [E]^{-1} \begin{bmatrix} N - N_1 \\ M_x - M_{x1} \\ M_y - M_{y1} \end{bmatrix}$$

Where

$$[E] = \begin{bmatrix} \frac{\partial N}{\partial \phi} & \frac{\partial N}{\partial Z_n} & \frac{\partial N}{\partial \theta} \\ \frac{\partial M_x}{\partial \phi} & \frac{\partial M_x}{\partial Z_n} & \frac{\partial M_x}{\partial \theta} \\ \frac{\partial M_y}{\partial \phi} & \frac{\partial M_y}{\partial Z_n} & \frac{\partial M_y}{\partial_\theta} \end{bmatrix}$$

Thus a better estimation of the variables ϕ, Z_n and θ is given by

$$\begin{bmatrix} \phi_1 \\ Z_{n1} \\ \theta_1 \end{bmatrix} + [E]^{-1} \begin{bmatrix} N - N \\ M_x - M_{x1} \\ M_y - M_{y1} \end{bmatrix} \qquad (2.11)$$

The computational procedure is to estimate values of θ_1, Z_{n1} and ϕ_1 and calculate the corresponding values N_1, M_{x1} and M_{y1}. These values are compared with the required values N, M_x and M_y and if not within the required tolerances the partial differentials in Equation 2.10 are calculated. The orientation of the neutral axis θ is incremented to $\theta_1 + d\theta$ and the corresponding values N_2, M_{x2} and M_{y2} are calculated. Similarly Z_{n1} and ϕ_1 are incremented in turn to $Z_{n1} + dZ_n$ and $\phi_1 + d\phi$ and N_3, M_{x3} and M_{y3}, and N_4, M_{x4} and M_{y4} are calculated. Thus the differentials for the matrix E are given by

$$\frac{\partial N}{\partial \theta} = \frac{N_2 - N_1}{d\theta} \quad ; \quad \frac{\partial M_x}{\partial \theta} = \frac{M_{x2} - M_{x1}}{d\theta} \quad , \quad \frac{\partial M_y}{\partial \theta} = \frac{M_{y2} - M_{y1}}{d\theta}$$

$$\frac{\partial N}{\partial Z_n} = \frac{N_3 - N_1}{dZ_n} \quad ; \quad \frac{\partial M_x}{\partial Z_n} = \frac{M_{x3} - M_{x1}}{Z_{n_3} - Z_{n_1}} \quad , \quad \frac{\partial M_y}{\partial \theta} = \frac{M_{y3} - M_{y1}}{Z_{n3} - Z_{n1}}$$

$$\frac{\partial N}{\partial \phi} = \frac{N_4 - N_1}{d\phi} \quad ; \quad \frac{\partial M_x}{\partial \phi} = \frac{M_{x4} - M_{x1}}{\phi_4 - \phi_1} \quad , \quad \frac{\partial M_y}{\partial \phi} = \frac{M_{y4} - M_{y1}}{\phi_4 - \phi_1}$$

The analysis is repeated with the new values of ϕ , Z_n and θ .

When the required degree of convergence on to M_x, M_y and N has been achieved the curvatures, ϕ_x and ϕ_y about the x and y axes respectively, are calculated from

$$\phi_x = \phi \sin\theta$$

and $$\phi_y = \phi \cos\theta$$

2.3 Analysis using forward integration.

The method of analysis is a forward integration technique with subsequent corrections using the second order Newton-Raphson procedure. The length of the column to be analysed is split into a number of elements so that with use of central differences the second order flexural differential equations can be solved step by step. To commence an analysis estimations have to be made of some starting values.

The analysis will be described as applied to a uniaxially loaded pin-ended column before its application to the case of biaxially restrained columns is discussed.

2.3.1 Assumptions

The following assumptions are made in the analysis.

(i) Plane sections remain plane

(ii) Deflections are small and hence curvature can be represented by $\frac{d^2y}{dx^2}$ where the x and y axes are as Fig. 2.4.

(iii) Stress-strain curves for steel and concrete are reversible.

(iv) Shear stresses are small and do not affect deflections or yield of the materials.

(v) Torsion is ignored.

2.3.2 Uniaxial Analysis.

Fig. 2.4a shows a column of length L split into elements each of length ℓ and the scheme of differences used if the deflections at

nodes 1, 2, ... $l-1$, l, are v_1, v_2, ... v_{l-1}, v_l .... etc. The external applied loads are as shown in Fig. 2.4b.

If a value of deflection is assumed for node 2 then the moment at node 2 can be calculated using

$$M_2 = M_1 + Nv_2 + S_1\ell \tag{2.12}$$

where M_1 is the applied end moment

M_l is the moment at node l

N is the axial load

and S_1 is the shear applied at node 1.

Given the moment and axial load, the curvature $(d^2y/dx^2)_2$ is found from the M-N-ϕ data.

Using the finite difference expression for curvature,

$$\phi_2 = \frac{v_1 - 2v_2 + v_3}{\ell} \tag{2.13}$$

then the deflection at node 3 is given by

$$v_3 = 2v_2 - v_1 - \ell^2\left(\frac{d^2y}{dx^2}\right)_2 \tag{2.14}$$

The process is repeated at each node in turn until v_n, the deflection at the bottom end, has been calculated. The misclose in deflection, $\bar{M}$, which is the difference between the calculated deflection, v_n, and the required deflection, v_{req}, is found

$$\bar{M} = v_n - v_{req}. \tag{2.15}$$

In the case of a no-sway column then v_{req} is equal to zero. If the misclose is not within the required tolerance the initial estimation of deflection at node 2 is altered to $v_2 + \partial v_2$ and the procedure repeated to obtain new values of bottom end deflection, $v_n + \partial v_n$, and the misclose $\bar{M} + \partial\bar{M}$

The Newton-Raphson technique is then used to obtain a revised estimation of the deflection at node 2, v_{R2}, such that

$$v_{R2} = v - \frac{\partial v_2}{\partial \bar{M}} \qquad (2.16)$$

to be used in place of v_2.

The analysis is repeated until the required degree of convergence is obtained.

The effect of initial lack of straightness is accounted for in the analysis by including an additional curvature term $\left(\frac{\partial^2 y}{\partial x^2}\right)_{ic}$

$$\text{i.e.} \quad v_n = 2v_{n-1} - v_{n-2} - \ell^2 \left(\left(\frac{\partial^2 y}{\partial n^2}\right)_2 + \left(\frac{\partial^2 y}{\partial x^2}\right)_{ic} \right) \qquad (2.17)$$

2.3.3 Extension of analysis to biaxially restrained sway and no-sway columns.

It has been shown[68] that for pin-ended composite columns failure occurs in a predominantly flexural mode. Gent[26] has shown that the effect of torsion on elastically restrained H steel columns is of little importance. The analysis that follows therefore neglects torsion and also axial shortening although these can be easily included.

The method is similar to that for pin-ended columns except that four end conditions have to be satisfied compared with the one

for the uniaxially loaded pin-ended column. The variables chosen are the two rotations and two sway displacements at the far end of the column.

The main steps in the method, for given axial load and beam loadings, are

(1) The column is split into a number of elements, each of length ℓ.

(2) The end rotations for both axes at the top and the bottom of the column θ_{tx1}, θ_{ty1}, θ_{bx1} and θ_{by1} are estimated.

The subscript 1 referring to analysis 1.

(3) Given the moment-rotation characteristic for each restraining beam the applied end moments M_{tx}, M_{ty}, M_{bx} and M_{by} are found.

(4) The shear force and the relative displacement of the top and the bottom of the column are calculated. In the general case of a column with beams of shear stiffness $\bar{s}_1$ and $\bar{s}_n$ at the top and bottom of the column Fig. 2.5 ,

$$S_1 = S_n = \bar{s}_1 \delta_1 = \bar{s}_n \delta_n$$

$$\delta = \delta_1 + \delta_n$$

$$S_1 = \frac{\delta}{\frac{1}{\bar{s}_1} + \frac{1}{\bar{s}_n}}$$

Taking moments about the bottom of the column gives

$$N(\delta_1 + \delta_n) + S_1 L = M_2 - M_1 \quad .$$

Hence $$\delta = \frac{M_2 - M_1}{N + \frac{L}{\left(\frac{1}{\bar{s}_1} + \frac{1}{\bar{s}_n}\right)}} \qquad (2.18)$$

In the case of a no-sway column

$$\bar{s}_1 \text{ and } \bar{s}_n \to \infty$$

hence $\delta = 0$

and $$S_1 = \frac{M_2 - M_1}{L}$$

for a column with no shear restraint

$$\bar{s}_1 = \bar{s}_n = 0$$

hence $$S_1 = S_n = 0$$

and $$\delta = \frac{M_2 - M_1}{N}$$

Thus by using Equation 2.18 about each axis in turn the values of deflection required at node n, U_n and V_n, and the shears, S_x and S_y, can be calculated.

(5) The moment curvature routine is entered to find the curvatures ϕx and ϕy at node I.

(6) Using the finite-difference approximation for rotations, Fig. 2.4a,

$$\theta_1 = \frac{w_2 - w_1}{2\ell} \qquad (2.19)$$

Where w_1 is the deflection at node I, and for curvatures,

$$\phi_1 = \frac{w_2 - 2w_1 + w_o}{\ell^2} \qquad (2.20)$$

about each axis the deflections, u_2 and v_2 at node 2 are found.

(7) The moments are then calculated at node 2, using Equation 2.12, and then the curvatures are found from the $M - N - \phi$ routine.

(8) The deflections at node 3, u_3 and v_3, are found, equation 2.14, steps 7 and 8 are repeated for each node up to and including node n at the bottom.

(9) The miscloses in deflection and rotation at node n are calculated, the subscript, p, being the number of the analysis.

$$\overline{M1}_p = u_{np} - U_{np}$$

$$\overline{M2}_p = v_{np} - V_{np}$$

$$\overline{M3}_p = \frac{u_{(n-1)p} - u_{(n+1)p}}{2\ell} - \theta_{bxp} \qquad (2.21)$$

$$\overline{M4}_p = \frac{v_{(n-1)p} - v_{(n+1)p}}{2\ell} - \theta_{byp}$$

If $p = 1$ the four miscloses are compared with the allowable tolerances to check if the required degree of convergence has been obtained, if not the analysis is continued.

(10) The end rotations are incremented in turn and steps 2-9 repeated.

Thus for analysis number 2, i.e. $p = 2$, the end rotations are

$$\theta_{tx2} = \theta_{tx1} + d\theta_{tx}$$

$$\theta_{ty2} = \theta_{ty1}$$

$$\theta_{bx2} = \theta_{bx1}$$

$$\theta_{by2} = \theta_{by1}$$

and for analysis 3, i.e. p = 3,

$$\theta_{tx3} = \theta_{tx1}$$

$$\theta_{ty3} = \theta_{ty1} + d\theta t_{y1}$$

$$\theta_{bx3} = \theta_{bx1}$$

$$\theta_{by3} = \theta_{by1}$$

For analysis 4, i.e. p = 4,

$$\theta_{bx4} = \theta_{bx1} + d\theta_{bx1}$$

and for analysis 5, i.e. p = 5,

$$\theta_{by5} = \theta_{by1} + d\theta_{by1}$$

all other rotations being equal to those in analysis 1.

(11) Using a similar method to that used for the $M - N - \phi$ relationships it is found that better estimates of the end rotations are given by

$$\begin{bmatrix} \theta_{tx} \\ \theta_{ty} \\ \theta_{bx} \\ \theta_{by} \end{bmatrix} = \begin{bmatrix} \theta_{tx1} \\ \theta_{ty1} \\ \theta_{bx1} \\ \theta_{by1} \end{bmatrix} + [E]^{-1} \begin{bmatrix} \overline{M1}_1 \\ \overline{M2}_1 \\ \overline{M3}_1 \\ \overline{M4}_1 \end{bmatrix} \qquad (2.22)$$

Where

$$[E] = \begin{bmatrix} \frac{\partial \overline{M1}}{\partial \theta_{tx}} & \frac{\partial \overline{M1}}{\partial \theta_{ty}} & \frac{\partial \overline{M1}}{\partial \theta_{bx}} & \frac{\partial \overline{M1}}{\partial \theta_{by}} \\ \frac{\partial \overline{M2}}{\partial \theta_{tx}} & \frac{\partial \overline{M2}}{\partial \theta_{ty}} & \frac{\partial \overline{M2}}{\partial \theta_{bx}} & \frac{\partial \overline{M2}}{\partial \theta_{by}} \\ \frac{\partial \overline{M3}}{\partial \theta_{tx}} & \frac{\partial \overline{M3}}{\partial \theta_{ty}} & \frac{\partial \overline{M3}}{\partial \theta_{bx}} & \frac{\partial \overline{M3}}{\partial \theta_{by}} \\ \frac{\partial \overline{M4}}{\partial \theta_{tx}} & \frac{\partial \overline{M4}}{\partial \theta_{ty}} & \frac{\partial \overline{M4}}{\partial \theta_{bx}} & \frac{\partial \overline{M4}}{\partial \theta_{bu}} \end{bmatrix}$$

and

$$\frac{\partial \overline{M1}}{\partial \theta_{tx}} = \frac{\overline{M1}_2 - \overline{M1}_1}{d\theta_{tx}}, \frac{\partial \overline{M1}}{\partial \theta_{ty}} = \frac{\overline{M1}_3 - \overline{M1}_1}{d\theta_{ty}}, \frac{\partial \overline{M1}}{\partial \theta_{bx}} = \frac{\overline{M1}_4 - \overline{M1}_1}{d\theta_{bx}}, \frac{\partial \overline{M1}}{\partial \theta_{by}} = \frac{\overline{M1}_5 - \overline{M1}_1}{d\theta_{by}},$$

$$\frac{\partial \overline{M2}}{\partial \theta_{tx}} = \frac{\overline{M2}_2 - \overline{M2}_1}{d\theta_{tx}}, \frac{\partial \overline{M2}}{\partial \theta_{ty}} = \frac{\overline{M2}_3 - \overline{M2}_1}{d\theta_{ty}}, \frac{\partial \overline{M2}}{\partial \theta_{bx}} = \frac{\overline{M2}_4 - \overline{M2}_1}{d\theta_{bx}}, \frac{\partial \overline{M2}}{\partial \theta_{by}} = \frac{\overline{M2}_5 - \overline{M2}_1}{d\theta_{by}},$$

$$\frac{\partial \overline{M3}}{\partial \theta_{tx}} = \frac{\overline{M3}_2 - \overline{M3}_1}{d\theta_{tx}}, \frac{\partial \overline{M3}}{\partial \theta_{ty}} = \frac{\overline{M3}_3 - \overline{M3}_1}{d\theta_{ty}}, \frac{\partial \overline{M3}}{\partial \theta_{bx}} = \frac{\overline{M3}_4 - \overline{M3}_1}{d\theta_{bx}}, \frac{\partial \overline{M3}}{\partial \theta_{by}} = \frac{\overline{M3}_5 - \overline{M3}_1}{d\theta_{by}},$$

$$\frac{\partial \overline{M4}}{\partial \theta_{tx}} = \frac{\overline{M4}_2 - \overline{M4}_1}{d\theta_{tx}}, \frac{\partial \overline{M4}}{\partial \theta_{ty}} = \frac{\overline{M4}_3 - \overline{M4}_1}{d\theta_{ty}}, \frac{\partial \overline{M4}}{\partial \theta_{bx}} = \frac{\overline{M4}_4 - \overline{M4}_1}{d\theta_{bx}}, \frac{\partial \overline{M4}}{\partial \theta_{by}} = \frac{\overline{M4}_5 - \overline{M4}_1}{d\theta_{by}}.$$

The analysis is then repeated using the new values of rotations.

When convergence has been achieved the loads are increased and the analysis repeated. When convergence is unobtainable at a particular load level the increment of load is reduced and the analysis repeated. Thus any degree of accuracy for a failure load can be obtained.

2.4 Verification of computer programs

The verification of the computer programs has been carried out in two stages.

2.4.1 Verification of the biaxial moment-thrust-curvature relationships and

2.4.2 Verification of the column analysis program.

2.4.1 The moment curvature relationships

These have been checked against results obtained by Basu[48] for a concrete encased I section. Details of the cross-section are given in Fig. 2.6. The results are plotted on Fig. 2.7 and Fig. 2.8.

It can be seen that agreement is extremely good. The relationships have also been tested for a reinforced concrete section against results obtained by Warner[67]. Details are given in Fig. 2.9 and results plotted in Fig. 2.10, Fig. 2.11, Fig. 2.12 and Fig. 2.13. Again agreement is extremely good.

2.4.2 The column analysis.

The biaxial restraint analysis has been checked against a number of published results.

2.4.2.1 Encased composite column in uniaxial bending.

Basu and Hill[49] presented details of the analysis of a pin-ended composite column with minor axis bending. The column properties and the results of the present analysis are given in Fig. 2.14, from which it can be seen that the agreement between deflections is good.

2.4.2.2. Encased composite in biaxial bending.

Virdi[55] carried out theoretical analyses of the columns he tested. One column has been selected and the column properties and the results using the present analysis are given in Fig. 2.15, from which it can be seen that agreement is again very good. The analysis carried out by Virdi included residual stresses and, since the proposed analysis ignores these, it can be seen that they have little effect on the behaviour of this column.

2.4.2.3 Bare steel column in biaxial single curvature bending.

Birnstiel tested a number of columns in single curvature. The details and the experimental results and the results using the proposed analysis are shown in Fig. 2.16, also plotted are

results obtained by Vinnakota [24] using an analysis which includes the effects of torsion. Agreement between analyses and test is good.

2.4.2.4 Bare steel column in biaxial double curvature bending.

This is similar to the problem in section 2.4.2 but the column is bent in double-curvature. Vinnakota has also analysed this column and gives reasons for the discrepancies between calculated and experimental deflections. The details of the specimens and the results are shown in Figs. 2.16 and 2.17.

2.4.2.5 Steel column with elastic restraints.

The column selected is one of those tested by Gent and Milner[26]. The details of the test rig and specimens and the results of Column A4 are shown in Fig. 2.18. The calculated values of major and minor axis moments and deflections are also shown in Fig. 2.18, with the corresponding experimental values. It can be seen that agreement between experimental and computed results is reasonably good. The difference being probably due to the ignoring of strain hardening in the analysis and the possibility of initial curvature and slight eccentricity of loading giving beneficial effects in the tests.

2.4.2.6 Elastically restrained column free to sway.

Baker Horne and Heyman[11] give details of a series of tests of model columns in single and double no-sway bending. Wood[84] subsequently carried out a theoretical analysis of two of these columns with (a) no sway allowed and (b) sway allowed. Details of the column analysed using the proposed analysis are given in Fig. 2.19. The analysis has been carried out in two stages

(a) an elastic computer analysis which has been compared with the theoretical results obtained using stability functions[85], Fig. 2.19

(b) an elastic plastic analysis the results of which are compared with Wood's results.

It can be seen from Fig. 2.19 that agreement between the theoretical predictions and the proposed analysis is extremely close. Slight discrepancies exist between Wood's results and the results from the proposed analysis. A possible reason for this is that the

$$\text{ratio } \frac{K_c}{\Sigma K} = \frac{\text{column stiffness}}{\text{total stiffness}}$$

at the joint is equal to 0.11 using the given beam and column properties If, however, the effect of the stub-stanchion is included the effective stiffness of the beam is reduced but the reduction is dependent on axial load, Equation A5.2 Appendix 5. Wood has allowed for this by making $\frac{K_c}{\Sigma K} = 0.13$ approximately. This value has been used in the analysis. However the failure load is sensitive to the value of $\frac{K_c}{\Sigma K}$ used, Fig. 2.19.

2.5 Extension of analysis

The method used for analysis is flexible enough to allow extensions for various other effects such as torsional effects, and axial shortening. Inclusion of these effects increases the size of the error matrix, Equation 2.22.

2.5.1 Production of moment-rotation characteristics.

Since each iteration is a solution of a column analysis, such that internal and external equilibrium are satisfied on each iteration, conversion of the results to a set of no-sway axes can be carried out. If a column in uniaxial bending is considered, Fig. 2.20 with an end sway of δ_2 then the forces can be resolved to new no-sway axis X - X.

The axial load, N_A, is given by

$$N_A = N \cos \frac{\delta_2}{L} + S_2 \sin \frac{\delta_2}{L} \text{ given by} \qquad (2.23)$$

and the shear, S_A, is

$$S_A = S \cos \frac{\delta_2}{L} - N \sin \frac{\delta_2}{L}. \qquad (2.24)$$

The moments remain the same.

The rotation at end 1 becomes

$$\theta_A = \theta_1 - \frac{\delta_2}{L} \qquad (2.25)$$

The only load that can affect the analysis is the axial load N, since the curvature is a function of N and M, but if δ_2/L is small then $\cos \frac{\delta_2}{L} \rightarrow 1$ and $\sin \frac{\delta_2}{L} \rightarrow 0$ and thus $N_A \rightarrow N$.

Hence at the end of any iteration in the analysis the results of that iteration can be transferred to a set of no-sway axes, using Equations 2.23, 2.24 and 2.25.

2.5.2 Dealing with symmetrical columns.

When a column is loaded in uniform single curvature about bothaxes it is possible to take advantage of the symmetry of behaviour about the centre of the column. In a restrained column analysis this reduces the size of the error matrix from 4×4 to 2×2 and approximately halves the number of entries into the moment-curvature relationships for the derivation of any term in the matrix. Thus this reduces the computer time required for any analysis to about 30% of the time required by the full analysis. Additionally convergence can be speeded up due to the reduced size of the error matrix.

The steps in the analysis are in general similar to those for the full analysis described in Section 2.3.3 and the list below discusses those which differ.

(1) as previous.

(2) Because of symmetry the top and bottom beams rotations about either axis will be equal in magnitude.

(3) - (6) as previous.

(7) Steps (6) and (7) are repeated for each node up to the centre node only, node i, Fig. 2.21, and the deflection at node $i + 1$ is calculated.

(8) The errors are now considered as $v_{(i+1)} - v_{(i-1)}$ about each axis and would be equal to zero for full convergence. These errors are, however, checked against the required degree of convergence; if this is not achieved the analysis is continued.

(9) Steps (2) to (8) are repeated incrementing, in turn, the top major and minor axis end rotations.

(10) A 2×2 error matrix is constructed and solved to give better estimations of the two end rotations and the analysis is repeated until the required degree of convergence is obtained.

2.6 Discussion of analysis.

The advantages of the method of analysis described are

(a) The use of small error matrices

(b) That each iteration satisfies equilibrium.

(c) The possibility of inclusion of torsion, axial shortening etc.

Hutchings[69] has stated that large error matrices can cause problems because of ill-conditioning and hence difficulties in the solution of equation 2.22.

The way in which any iteration can be transferred to an arbitrary set of axes has been discussed in Section 2.5.1 and can be seen to be an obvious advantage, for the preparation of design-charts, end moment-rotation relationships, etc., over methods which do not have all iterations in equilibrium. In methods dependent on an initially estimated deflected shape which is used to obtain curvatures equilibrium is only satisfied at the last iteration. In all of the previous iterations, of which six or more have been required, equilibrium does not exist and thus the results are of no use.

The main disadvantage of the analysis is the fact that moment-curvature relationships are entered with two moments and the axial

load. It is felt, however, that the advantage of equilibrium outweighs this disadvantage.

2.7 Convergence of analysis

Generally convergence is rapid, one or two applications of the error equation 2.22 for either the moment-curvature relationships or the column analysis. Occasionally problems can arise in the moment-curvature relationships for steel sections when most of the cross-section is plastic but this can be overcome by additional elements in the cross-section.

2.8 Accuracy of analysis.

The accuracy to which the failure load, deflections, etc., are calculated using the proposed analysis are dependent on two factors:

(1) The fineness of the mesh and the tolerances used in the calculation of the moment curvature relationships.

(2) The number of elements into which the column is divided and the tolerances used in the analysis.

Warner[67] and Sharples[52] have both investigated the first factor and their recommendations have been used in the choice of mesh and tolerances in the moment-curvature relationships.

Virdi[55] has discussed the division of the column length for pin-ended columns with applied end-moments and axial load. He concluded that for columns loaded in uniform single curvature 8 elements gave a conservative estimation of the ultimate load to within 0.1% of the exact ultimate load. For columns loaded in

double curvature, however, he found that with 16 elements errors, on the unsafe side, of about 6% occurred and that 25 or more segments were required before errors of less than 1% existed.

The case of a rotationally restrained column is now considered. The problem is more complex than that of the pin-ended column because the applied end moment is dependent, partly, on the deflected shape of the column

$$\text{i.e.} \quad M = f(\theta) \tag{2.26}$$

where M is the end moment

and θ is the end rotation of the column.

If the restraint is elastic then

$$M = M_f - k\theta \tag{2.27}$$

where M_f is the beam fixed end moment and k is a measure of the beam stiffness.

If the column has initial imperfections in the form of a pre-deflected shape then even if no beam loads are applied end moments exist as the axial load increases. Equation 2.27 then becomes

$$M = -k\theta$$

We can now see that if the beam is very stiff, i.e. $k \to \infty$, then small changes in θ give large moments, and hence accuracy of the calculated θ needs to be considered.

The finite difference approximation used for θ is derived in Appendix 4 and shows that an error of

$\frac{-\ell^2}{3!} f_o^{111} - \frac{\ell^4}{5!} f_o^{v}$, where f_o^{111} and f_o^{v} are the third and fifth derivates of the displacement function respectively, exists. The effect of this error can be reduced by two methods.

(1) by the use of cycling; that is a value of θ is obtained using the normal expression and the corresponding moment is obtained from the beam moment-rotation relationships. This is used to calculate the deflections using the forward integration method until enough deflections have been calculated so that f_o^{111} can be found.

A revised estimate of θ is made including the term $\frac{-\ell^2}{3!} f_o^{111}$ and compared with the previous value of θ If the required degree of accuracy has been attained the analysis is continued,

or (2) the number of elements along the column is increased, e.g. doubling the number of elements will reduce the error term $\frac{\ell^2}{3!} f_o^{111}$ by a factor of 4.

The computer analysis described here has used the second approach.

To illustrate the accuracy of the method for a restrained column an investigation using a slender column with an initially deflected shape, loaded externally by axial load only, and with stiff elastic restraint, Fig. 2.22, was carried out. The results are given in Fig. 2.22. On first inspection the results do not appear to conform with Virdi's findings since the initial loading

is uniform single curvature one would expect the results for 8 elements to be more accurate. However, as the load is increased, the column approaches a double curvature situation because the moments are restraining moments.

Therefore in an analysis of a column with end restraints consideration has to be given to the final deflected shape when deciding on how many elements to use. In general, however, unless extremely large beam to column stiffness ratios exist the ratio of end moments will determine the number of elements to be used.

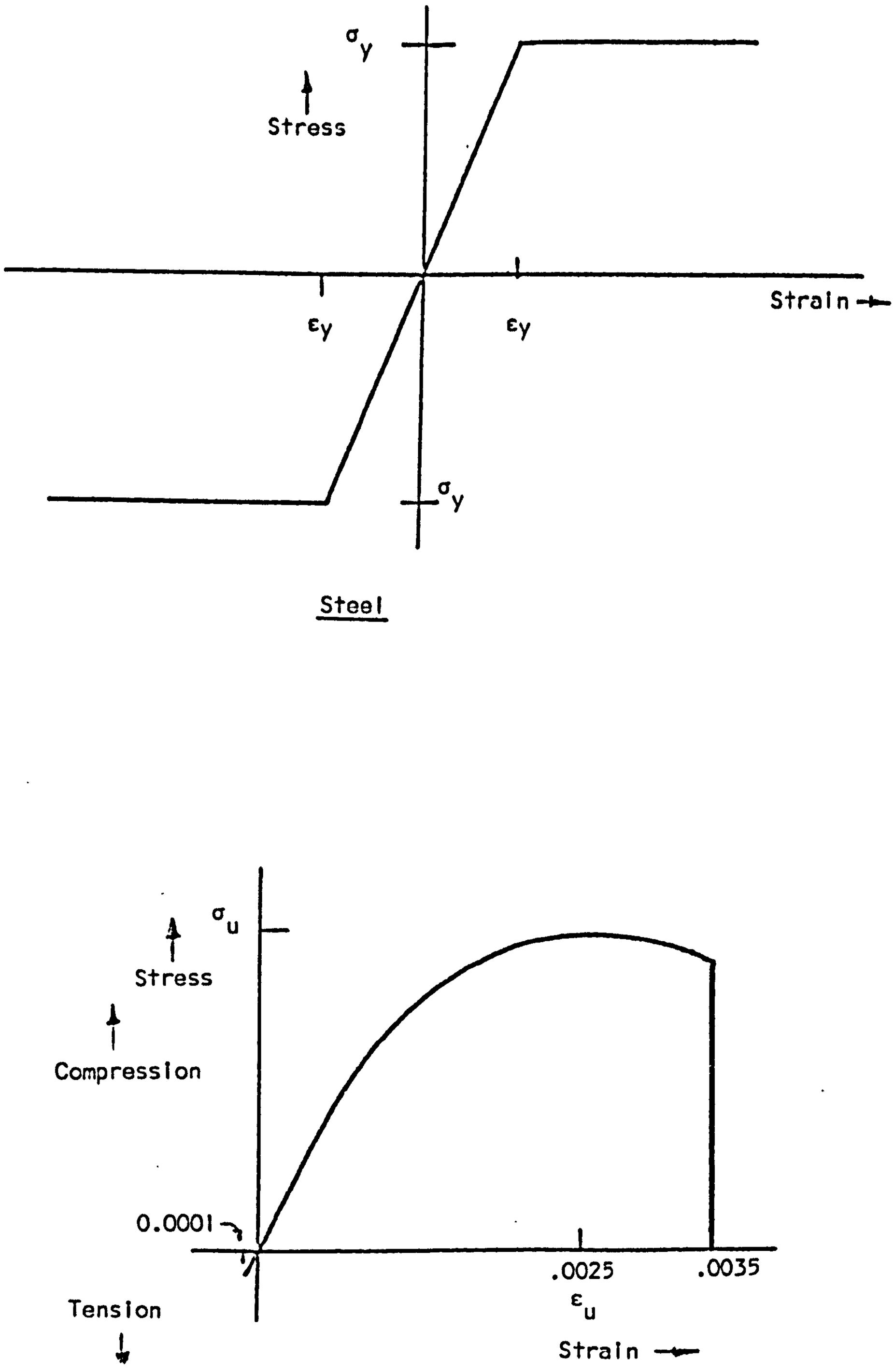

FIG. 2.1 STEEL AND CONCRETE STRESS-STRAIN CURVES FOR COMPOSITE CROSS-SECTIONS.

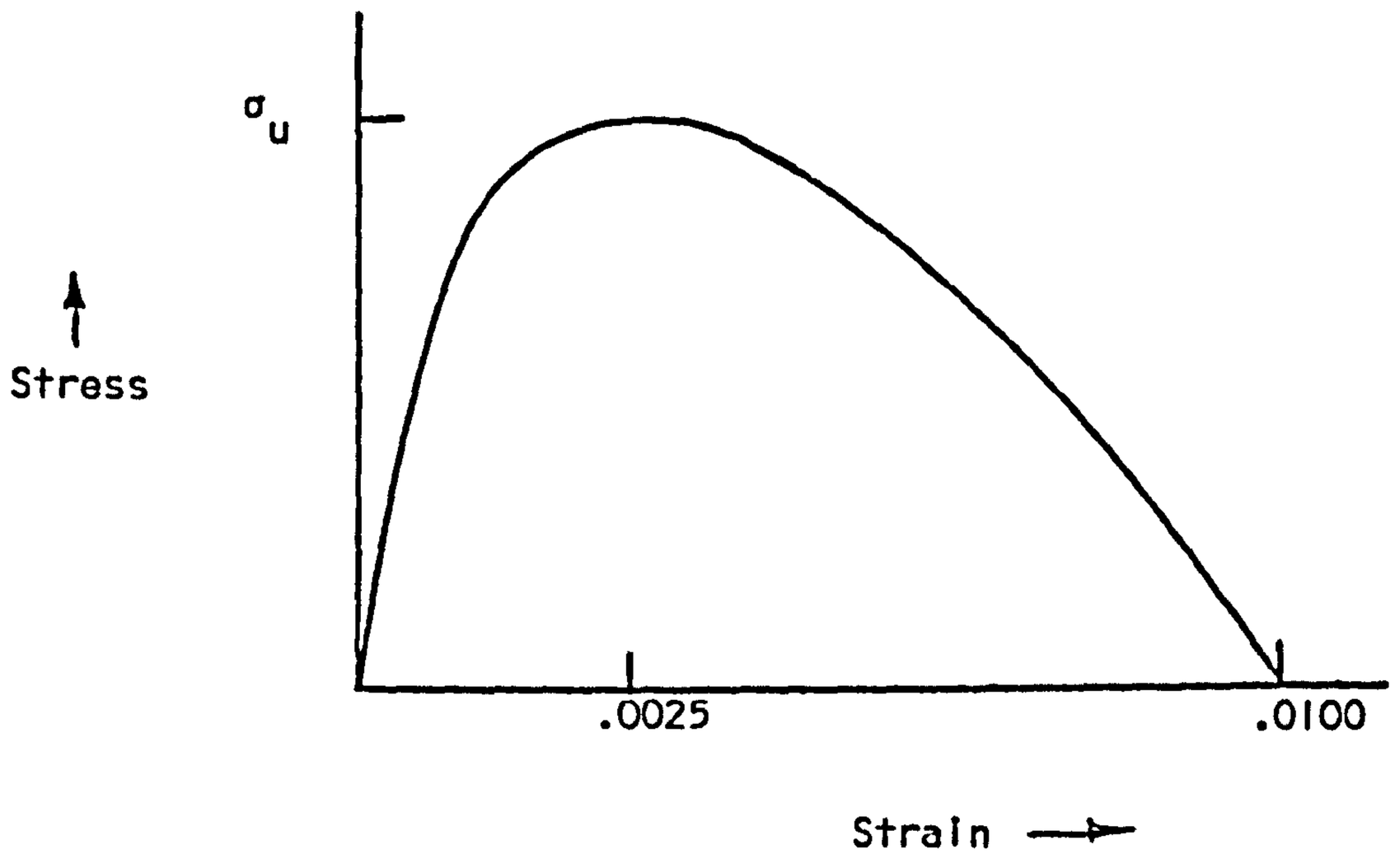

FIG. 2.2 CONCRETE STRESS-STRAIN CURVE FOR REINFORCED CONCRETE CROSS-SECTION.

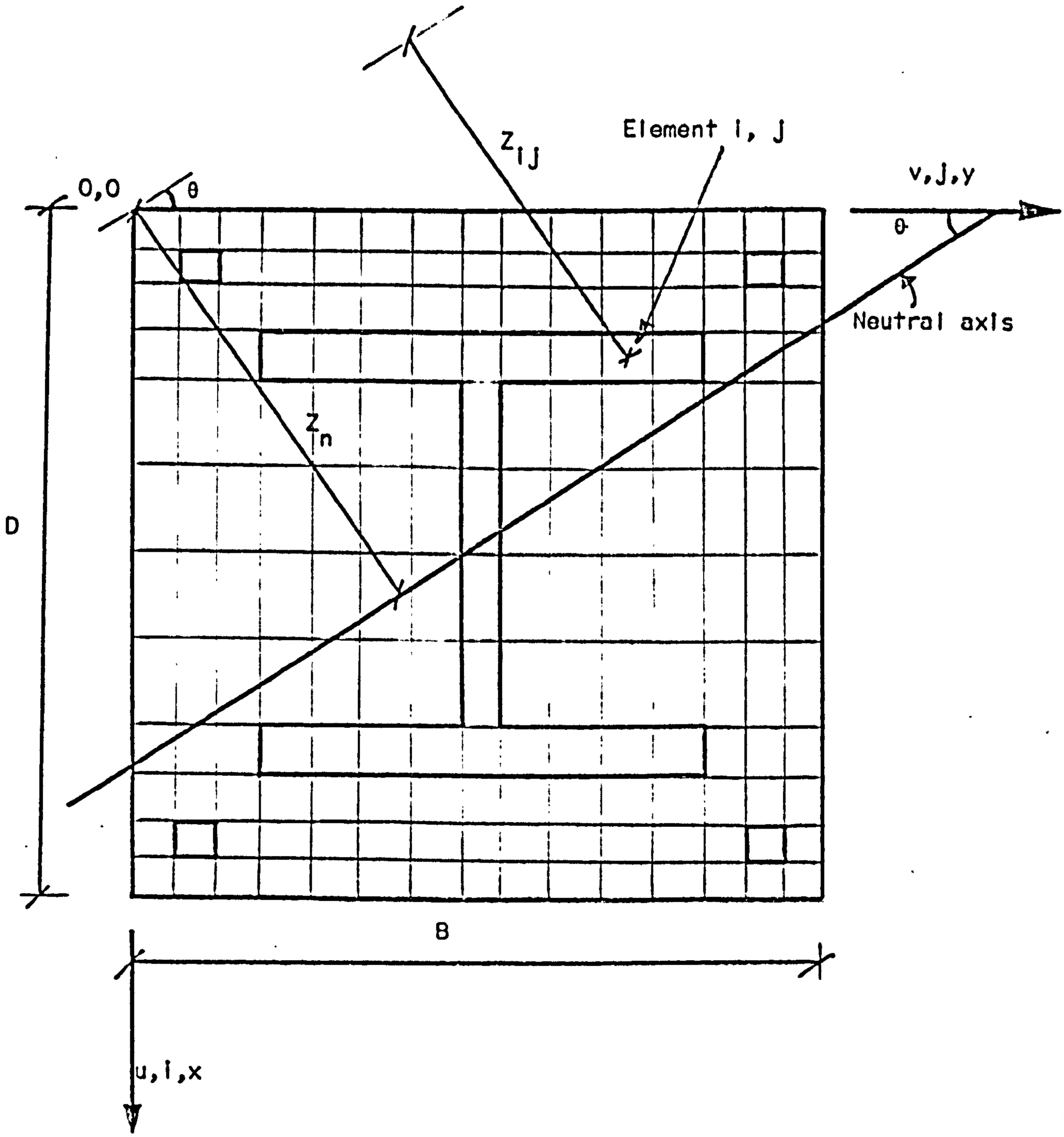

FIG. 2.3 SUB-DIVISION OF CROSS-SECTION FOR CALCULATION OF AXIAL LOAD AND MOMENTS.

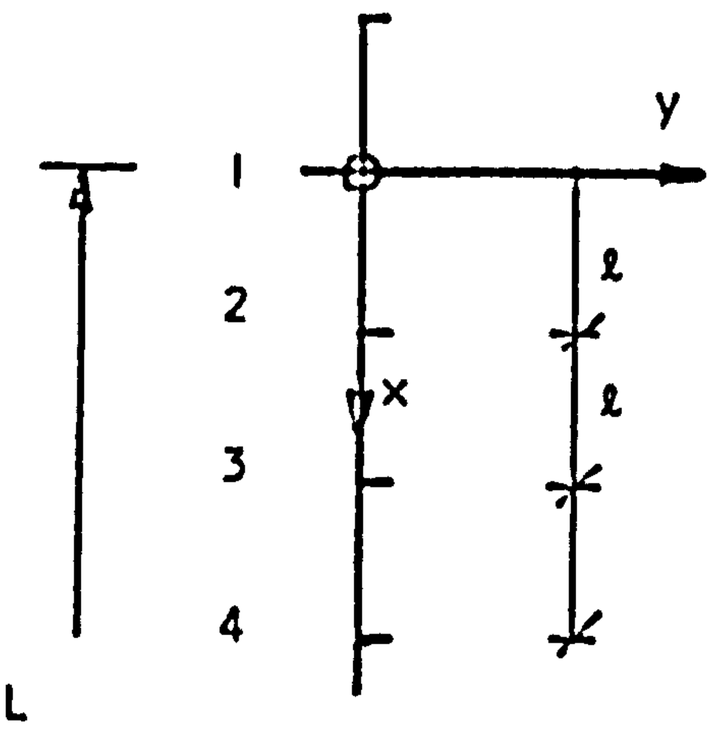

Node 1

$$\left(\frac{dy}{dx}\right)_1 = \frac{v_{1+1} - v_{1-1}}{2\ell}$$

$$\left(\frac{d^2y}{dx^2}\right)_1 = \frac{v_{1+1} - 2v_1 + v_{1+1}}{\ell^2}$$

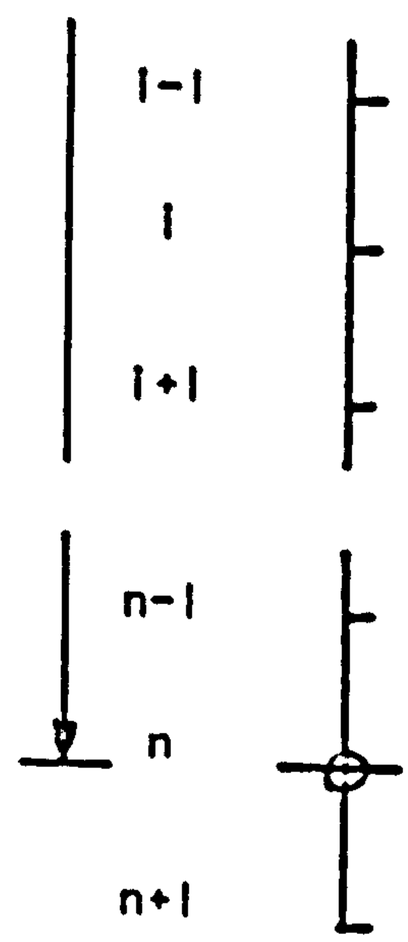

(a)

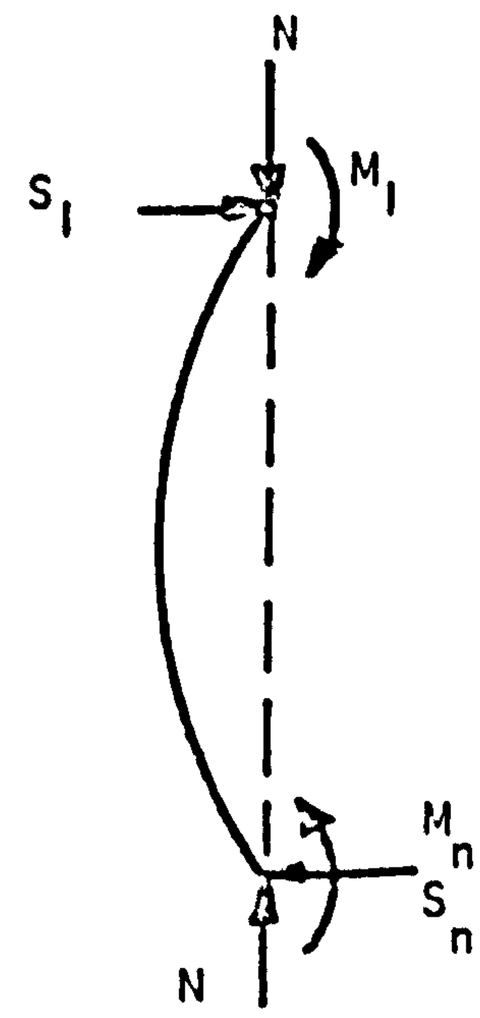

(b)

FIG. 2.4 FINITE DIFFERENCE EXPRESSIONS USED IN ANALYSIS

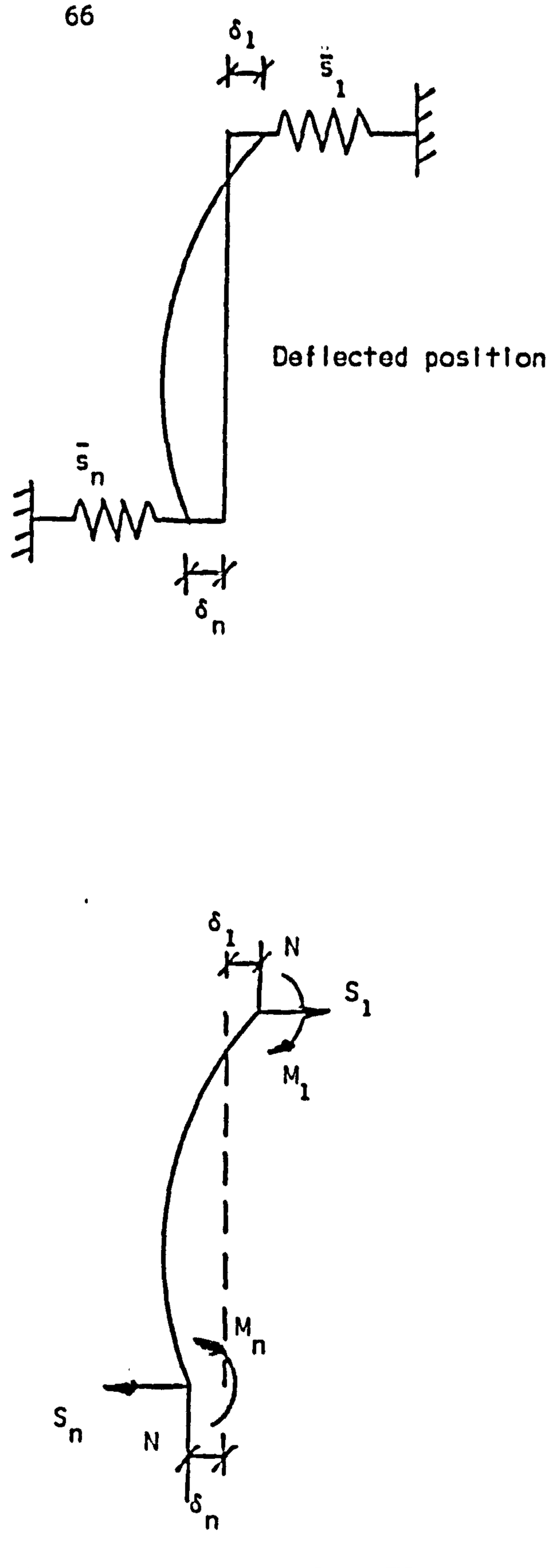

FIG. 2.5 COLUMN WITH DIRECTIONAL RESTRAINTS

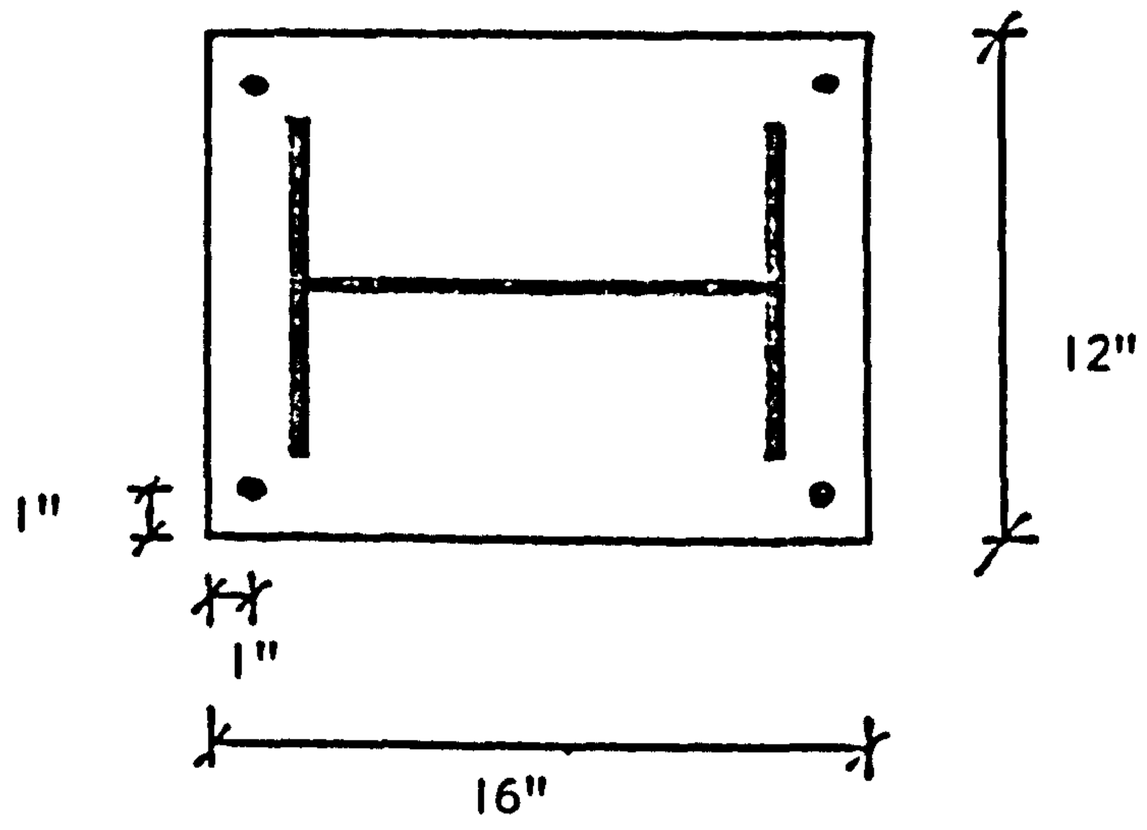

Steel: 4 - ½" Diameter bars

12" x 8" x 65lb R.S.J.

σ_y = 14.7 tons per sq.inch

ε_y = 0.001116

Concrete:

σ_u = 1.34 tons per sq. inch

ε_u = 0.0025

FIG. 2.6 DETAILS OF COMPOSITE SECTION ANALYSED

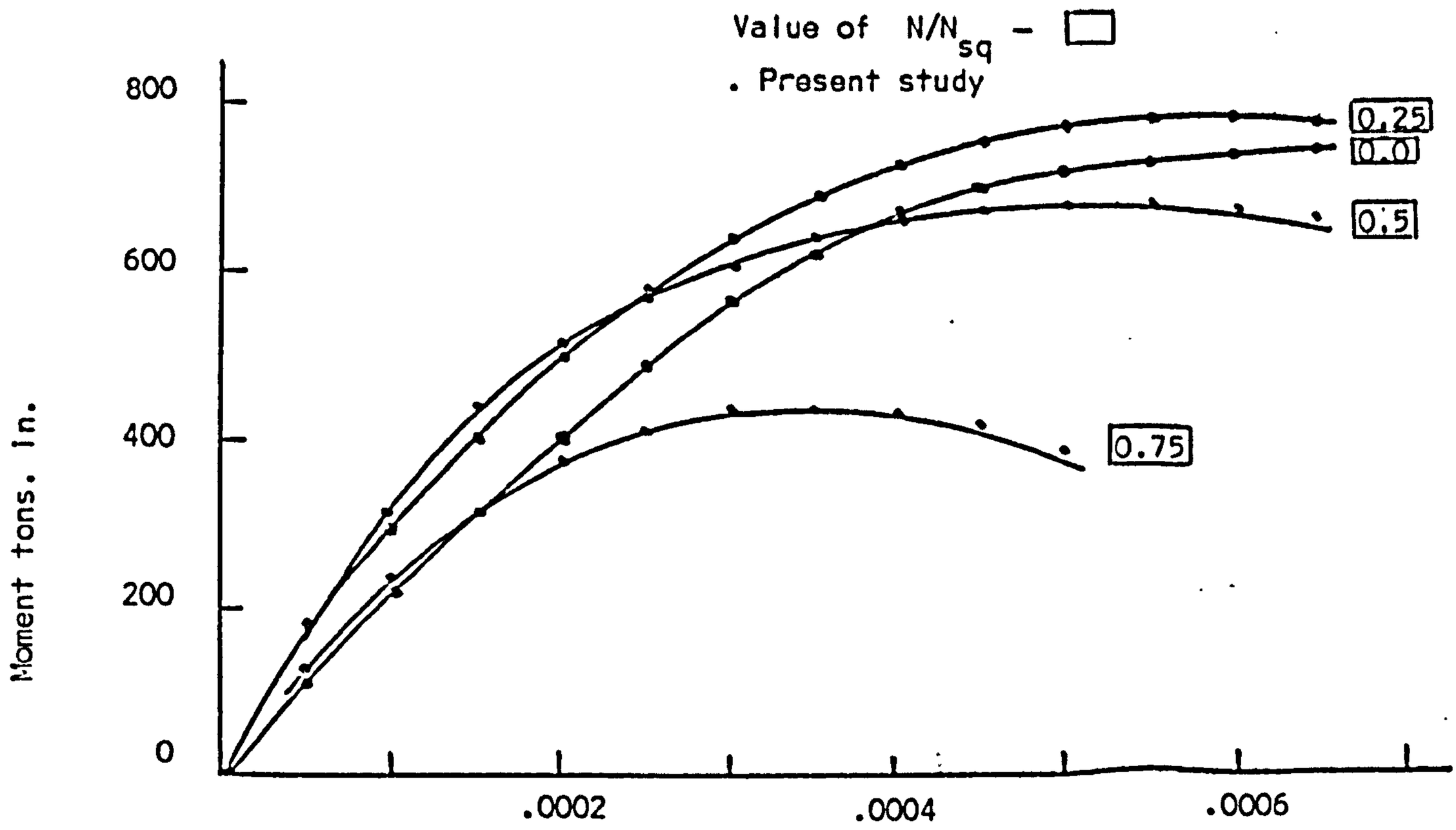

FIG. 2.7 MOMENT-CURVATURE CURVES FOR MINOR AXIS BENDING

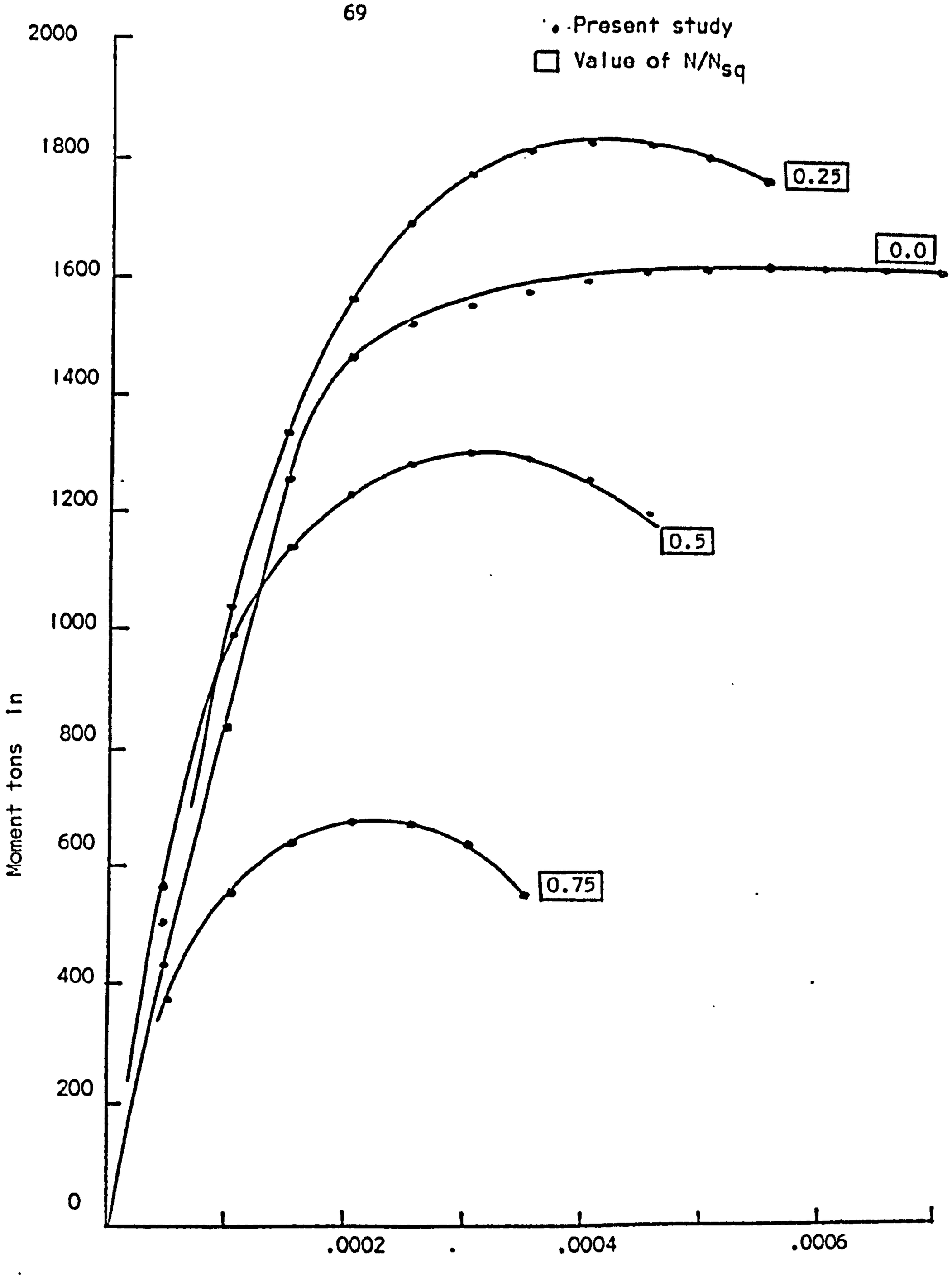

FIG. 2.8 MOMENT-CURVATURE CURVES FOR MAJOR AXIS BENDING

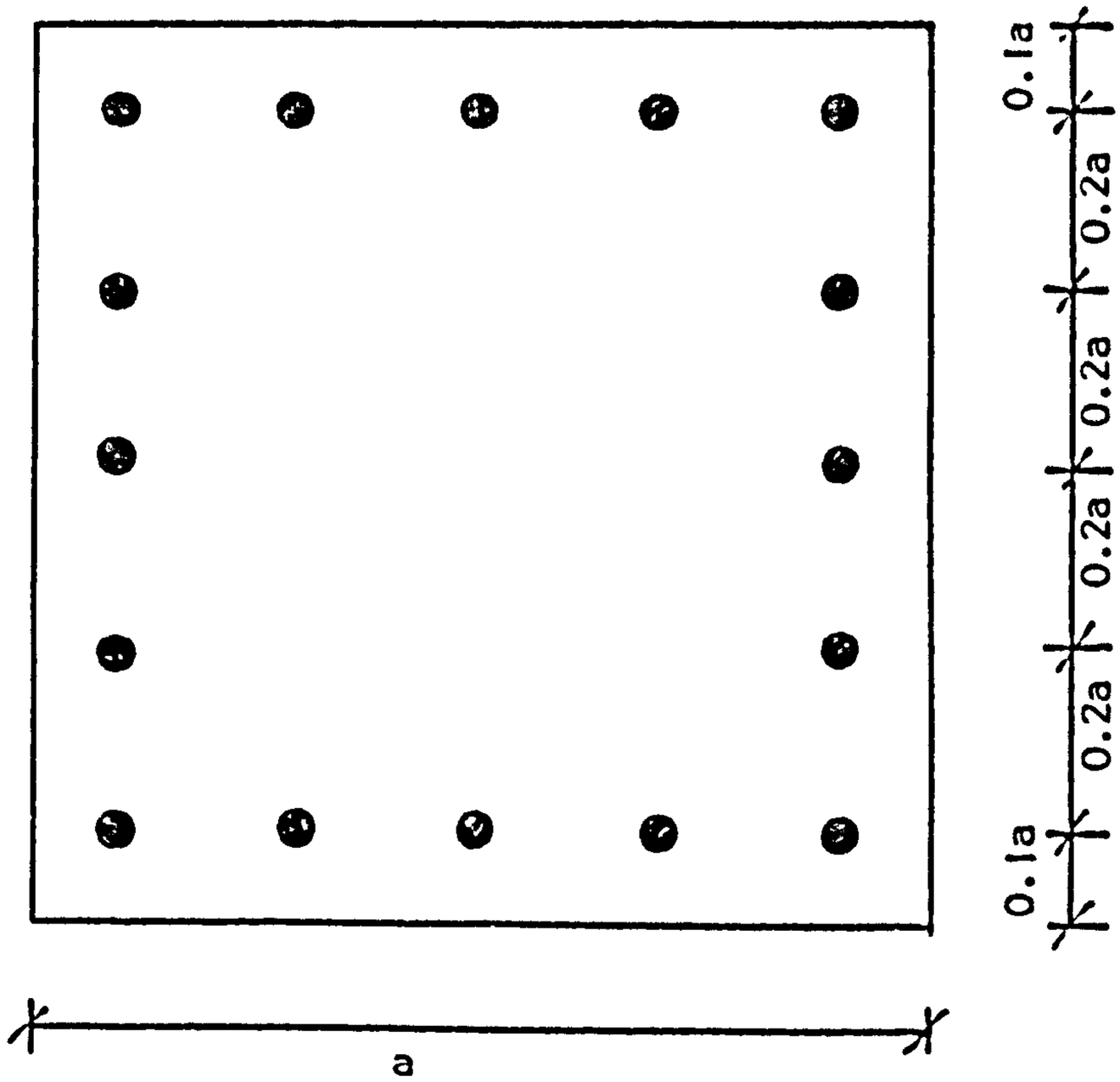

$$\frac{A_s\ \sigma_y}{A_c\ \sigma_u} = 0.5$$

$$\frac{\Sigma_y}{\Sigma_u} = 0.5$$

$$\gamma_1 = 2.2$$

$$\gamma_2 = 4.0$$

FIG. 2.9 DETAILS OF REINFORCED CONCRETE CROSS-SECTION ANALYSED.

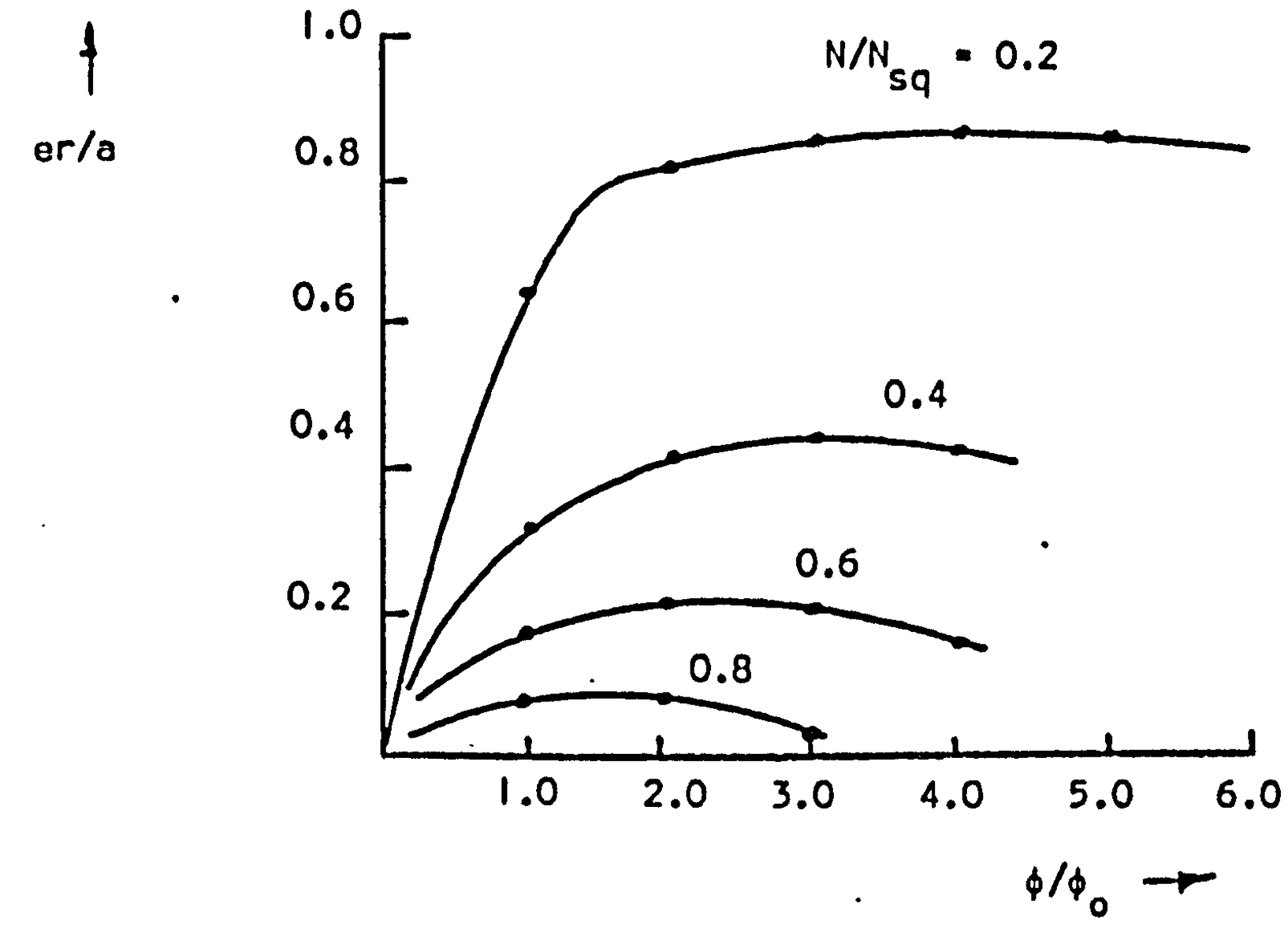

FIG. 2.10 MOMENT CURVATURE RELATIONS $\theta = 0^{\circ}$

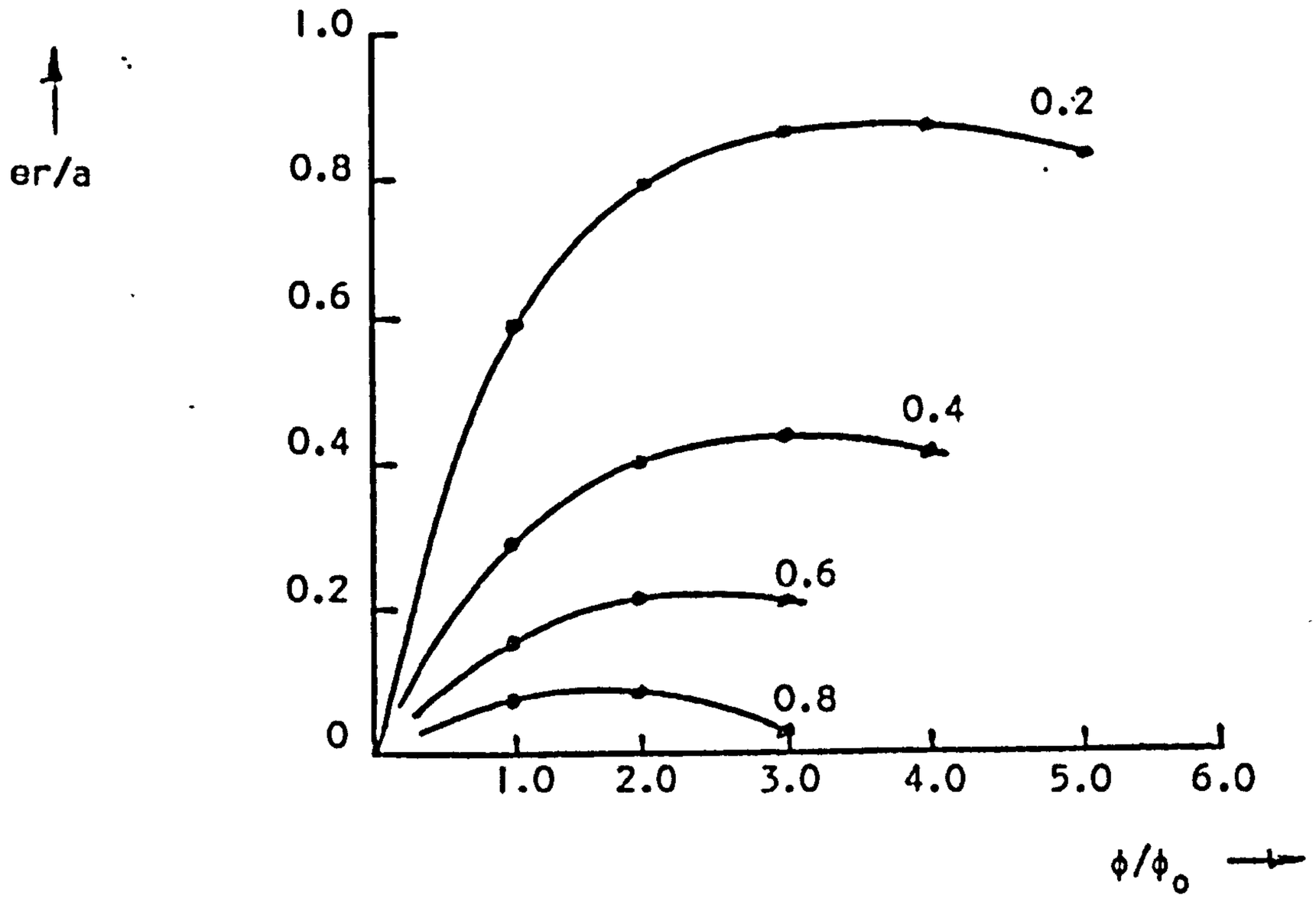

FIG. 2.11 MOMENT CURVATURE RELATIONS $\theta = 15^{\circ}$

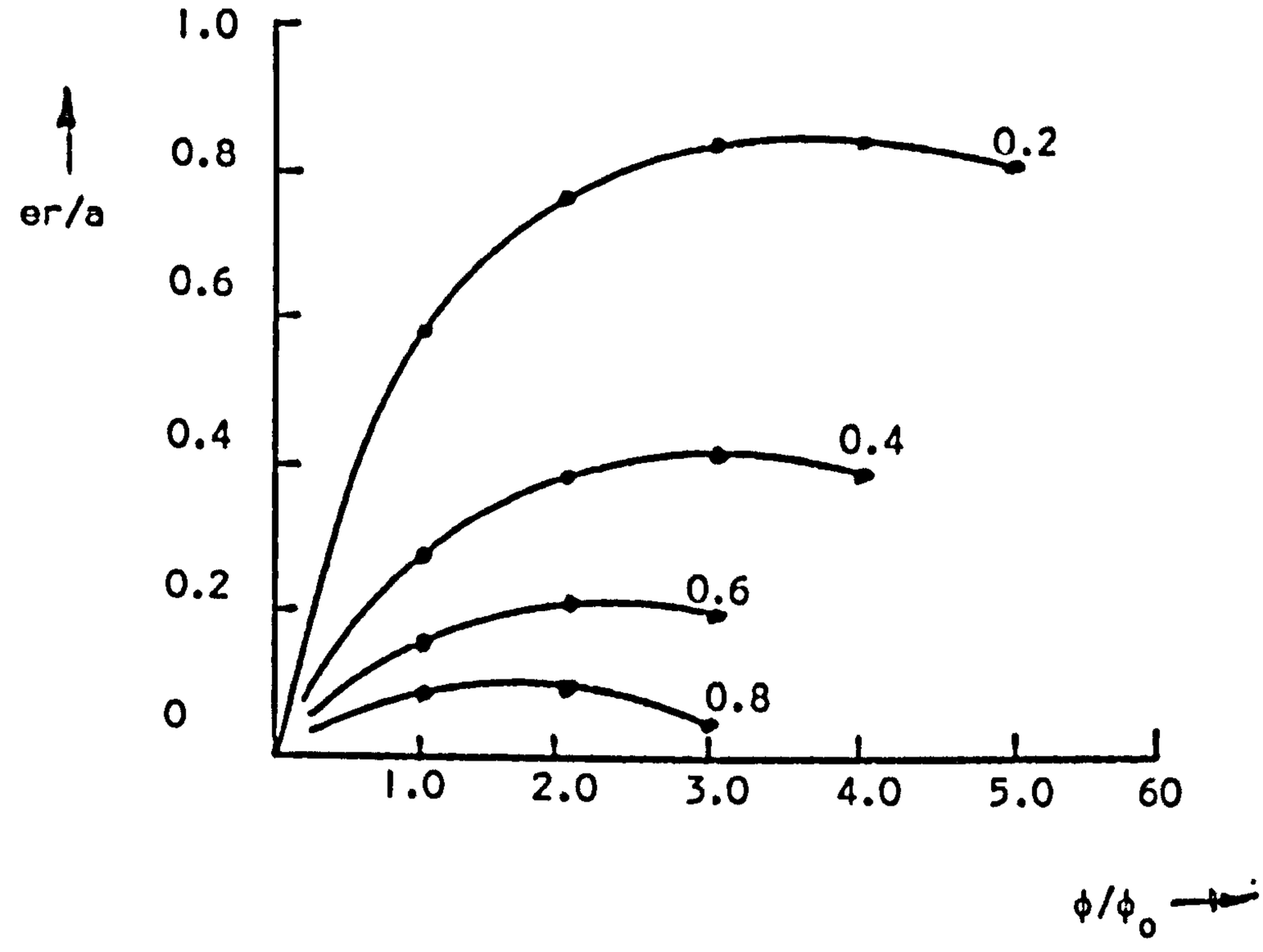

FIG. 2.12 MOMENT CURVATURE RELATIONS $\theta = 30^0$

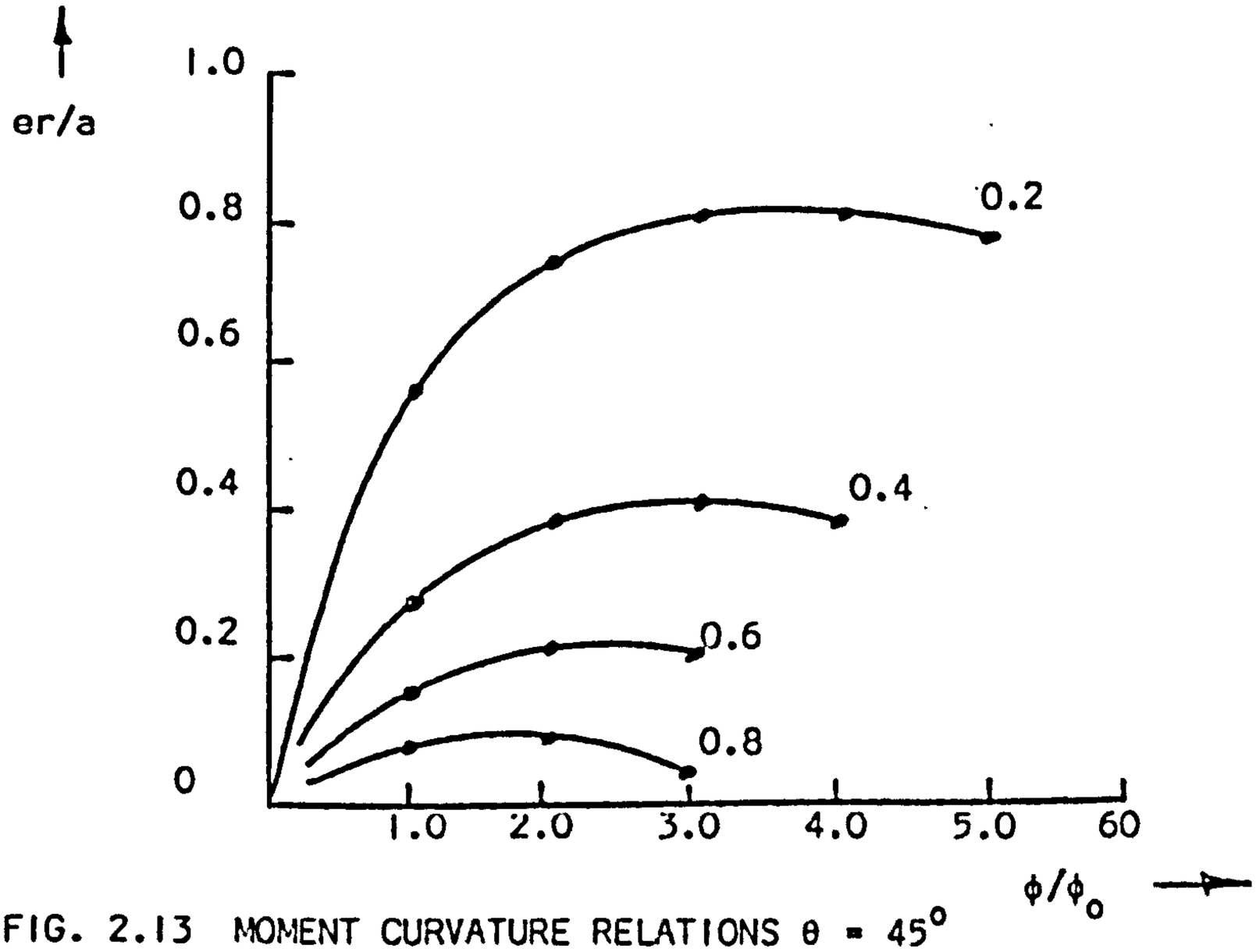

FIG. 2.13 MOMENT CURVATURE RELATIONS $\theta = 45^0$

Node No.		0	1	2	3	4	5	6	7
Deflection	Basu & Hill[7]	0	.1395	.2666	.3741	.4558	.5070	.5244	.5070
	Author	0	.1417	.2710	.3804	.4635	.5155	.5332	.5155
	% Diff.	0	1.58%	1.65%	1.68%	1.69%	1.68%	1.68%	1.68%

Cross-section as Fig. 5. Minor axis bending

Length 180 in.

P/P_{ULT} = 0.65

eccentricity = 0.1689 Single curvature bending β = 1

Number of elements = 12.

FIG. 2.14 RESULTS OF COLUMN ANALYSIS

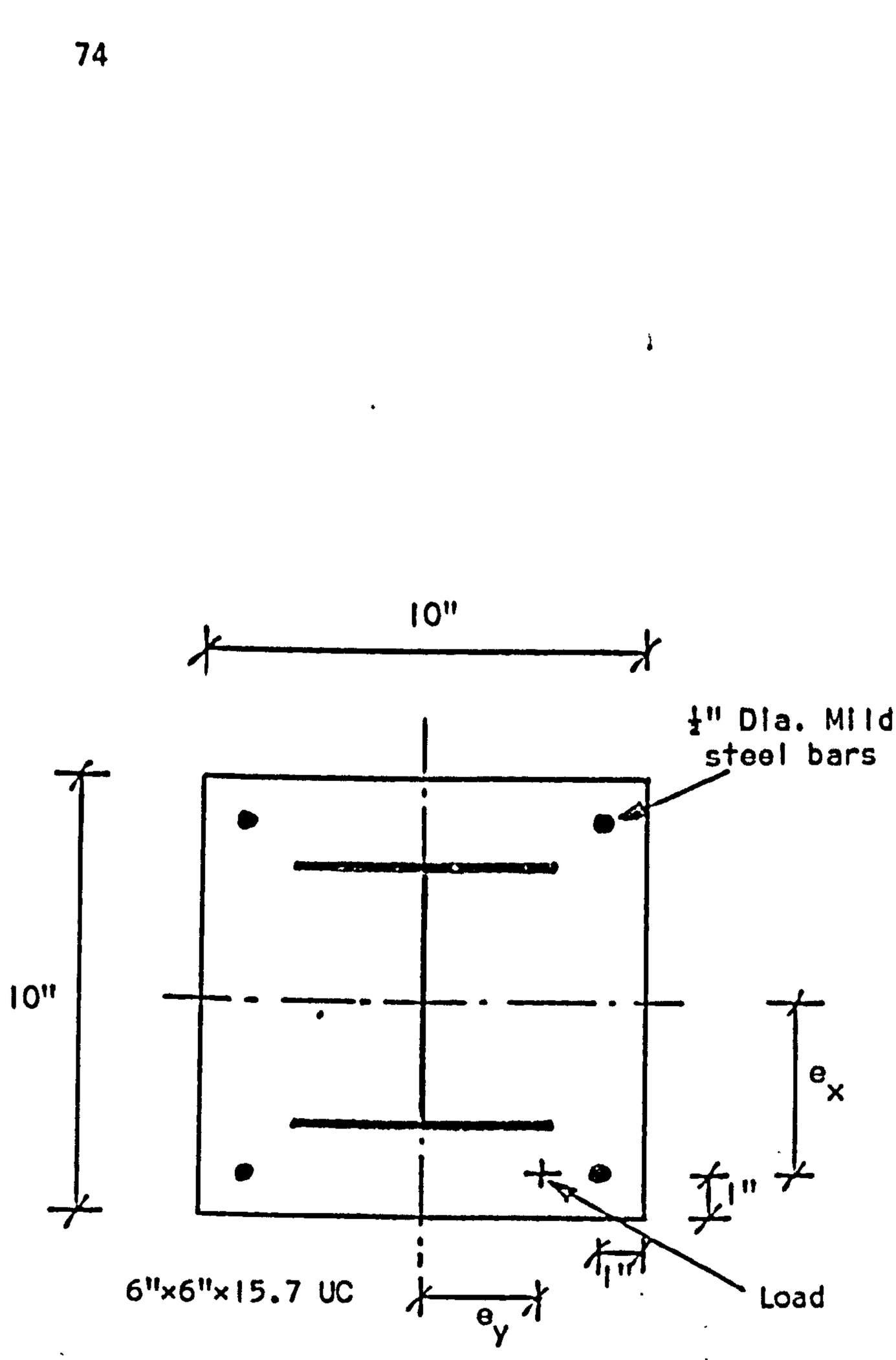

Length	144"
e_x	5"
e_y	2.9"
σ_u	2.56514 Tonf/sq.in.
σ_y	20.37 Tonf/sq.in.
ϵ_y	0.00155

INITIAL MIDSPAN IMPERFECTIONS L/1000

Fig. 2.15 Cont...

Continuation

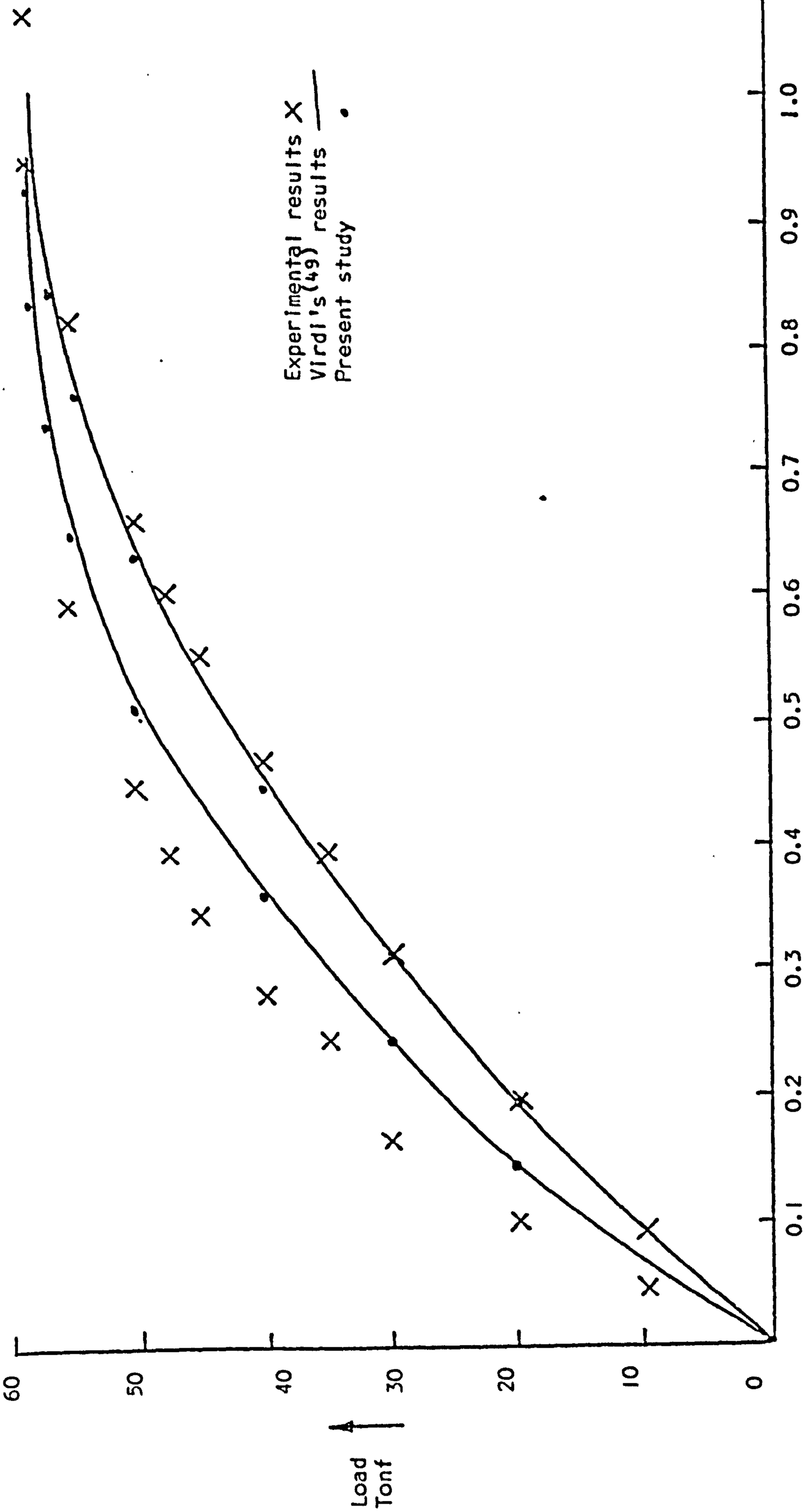

FIG. 2.15 COMPARISON OF RESULTS FOR COMPOSITE COLUMN

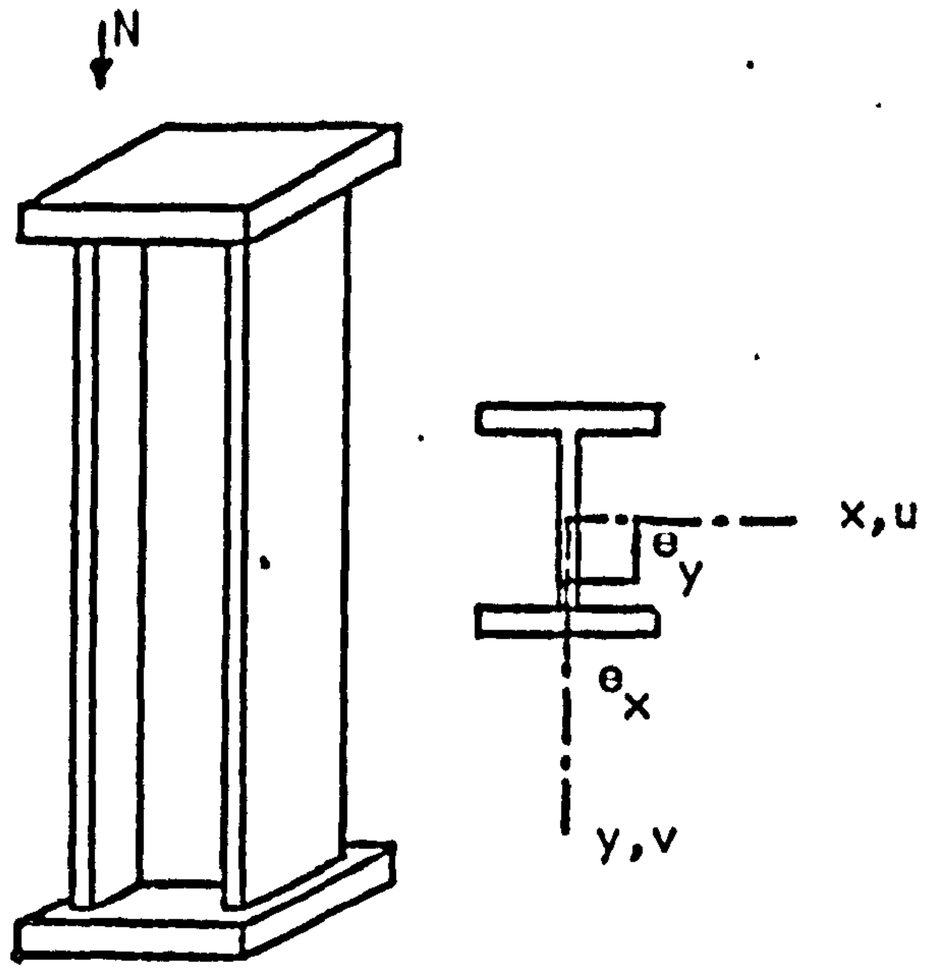

TEST SPECIMEN OF ISOLATED COLUMN
REFERENCE 20

	SPEC. No. 4	SPEC. No. 15
L	2440 mm	3050 mm
σ_y	0.0251 t/mm^2	0.0453 t/mm^2
e_{x1}	42.4 mm^2	44.5 mm^2
e_{x2}	42.2 mm^2	-37.3 mm^2
e_{y1}	74.9 mm^2	75.2 mm^2
e_{y2}	74.9 mm^2	-75.2 mm^2

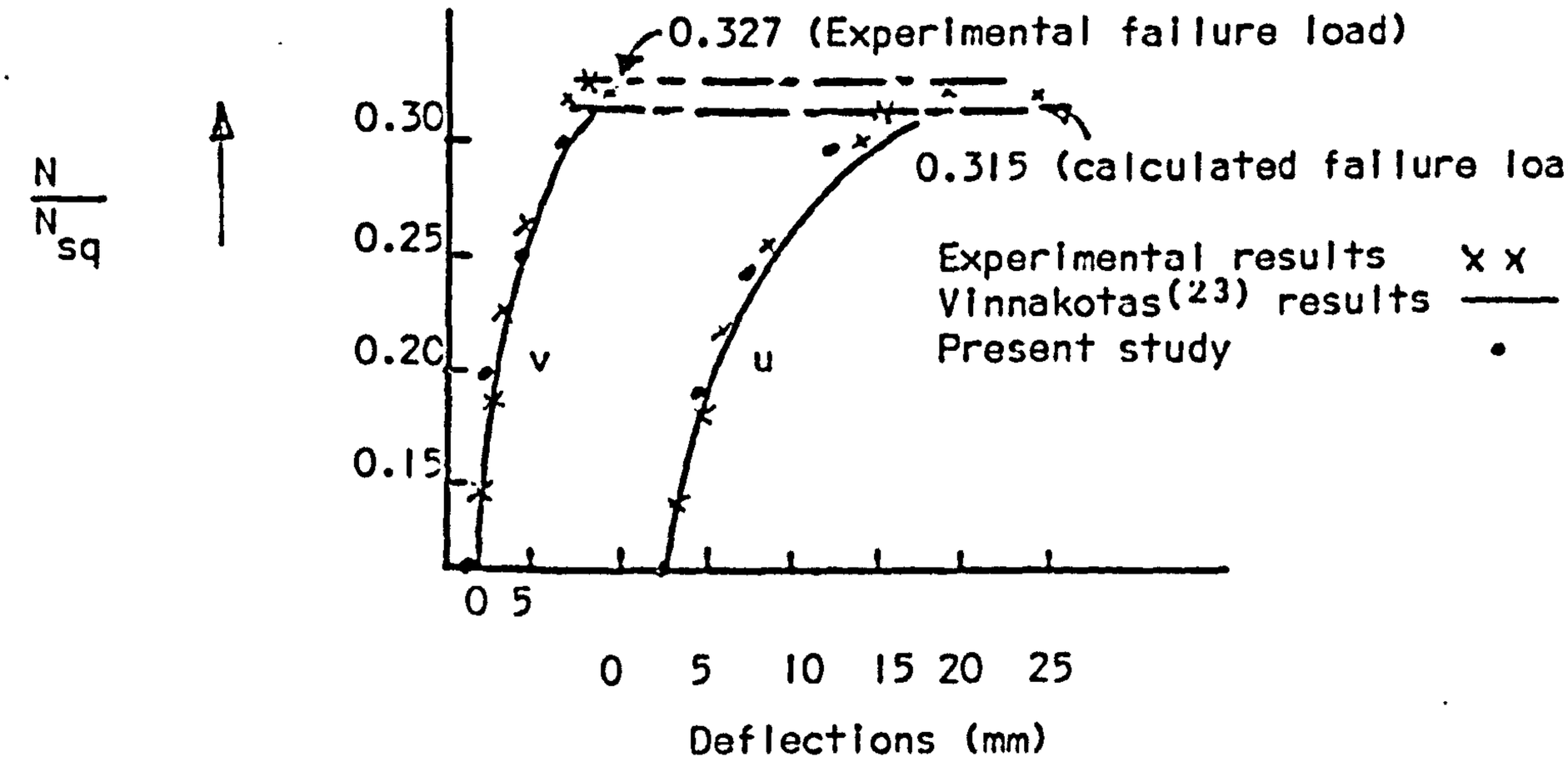

FIG. 2.16 COMPARISON OF RESULTS FOR COLUMN NO.4 REFERENCE 20

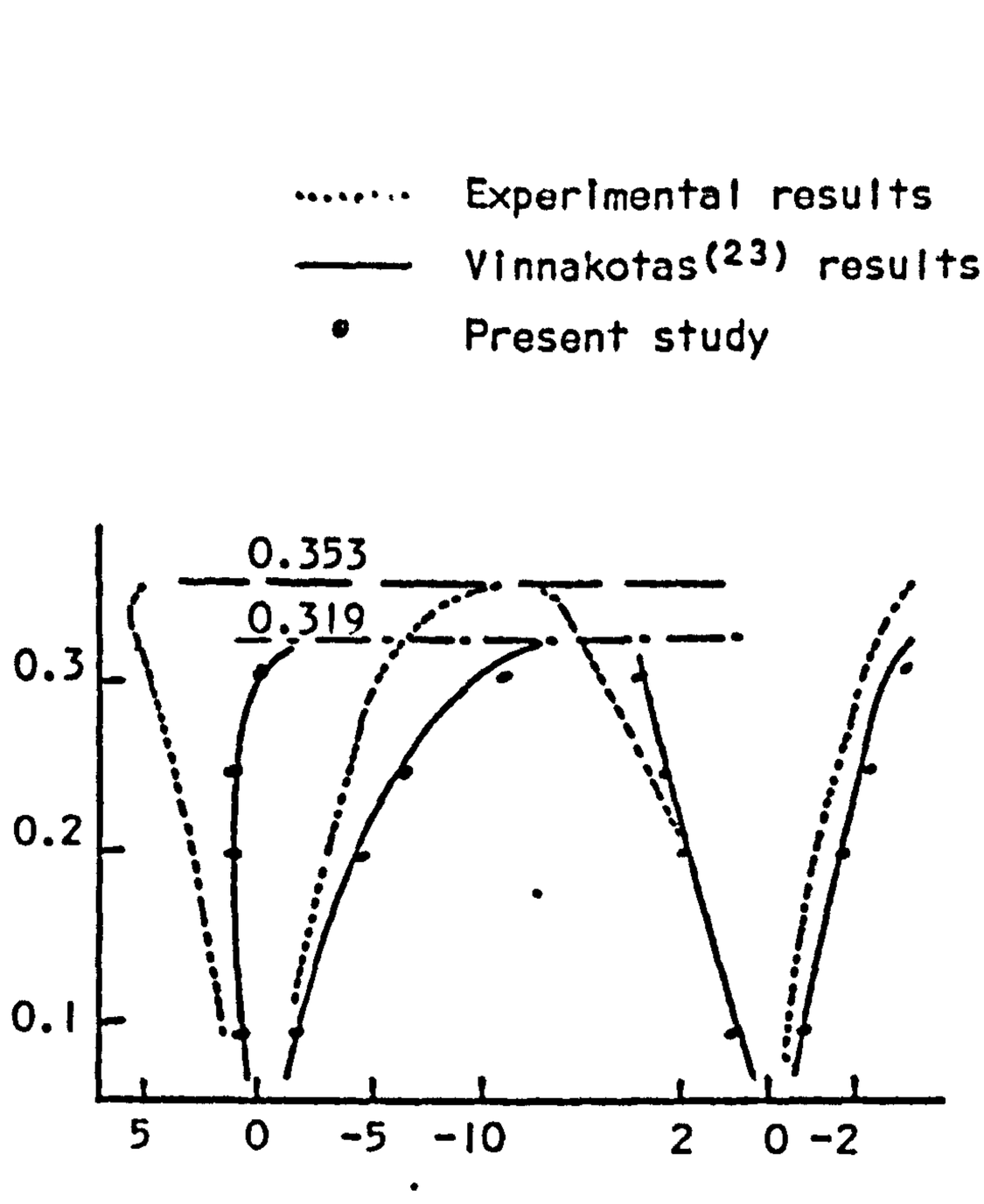

FIG. 2.17 COMPARISON OF RESULTS FOR COLUMN NO. 15 REFERENCE 20

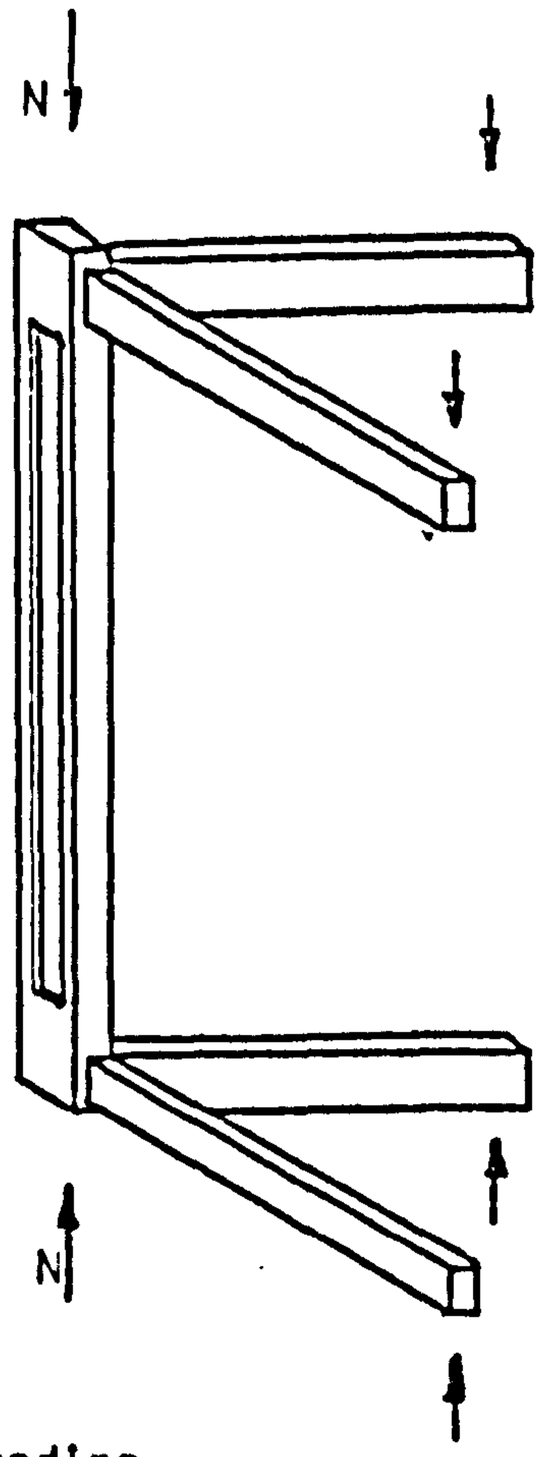

Beam-column sub assemblage and loading

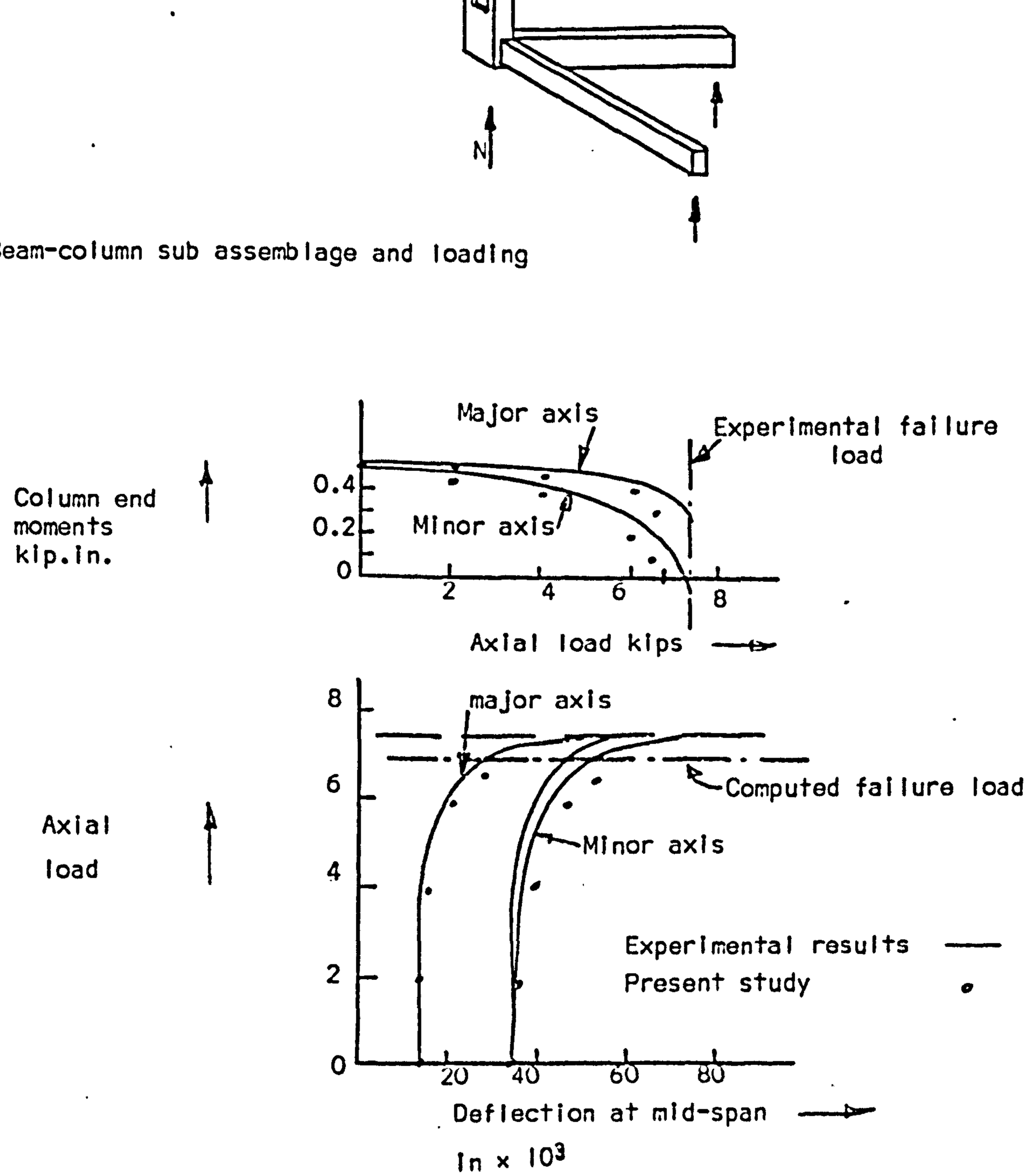

FIG. 2.18 COMPARISON OF RESULTS FOR SPECIMEN A4 OF REFERENCE 21

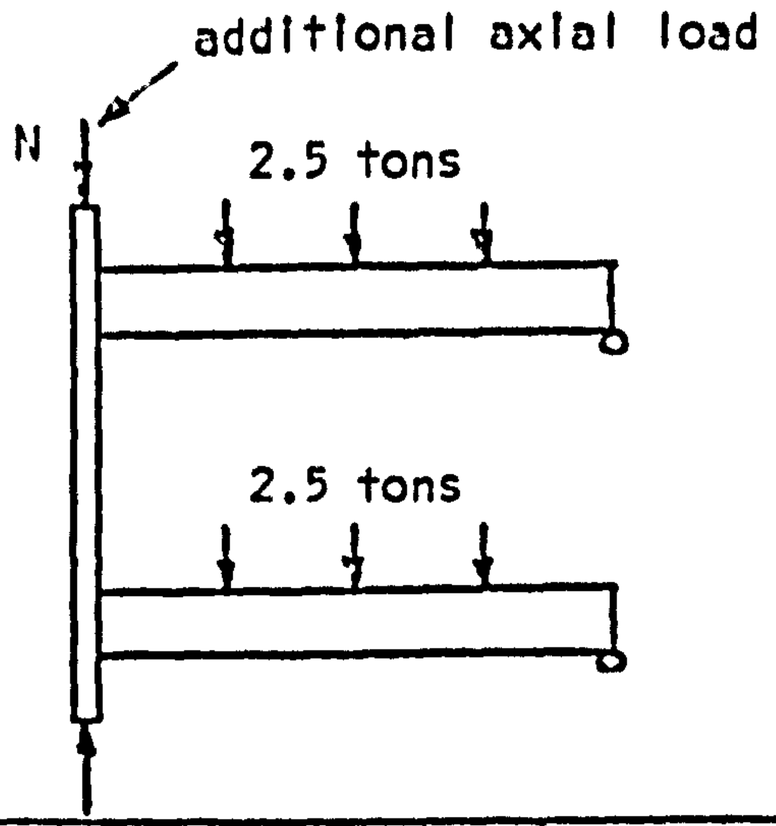

	Elastic critical load	Direct load first yield	Collapse load	$\frac{K_c}{\Sigma K}$
Wood	6.0	2.0	2.4	0.13
Present analysis		2.0	2.5	0.13
		2.4	2.8	0.11

Results for elastic plastic analysis (Tons)

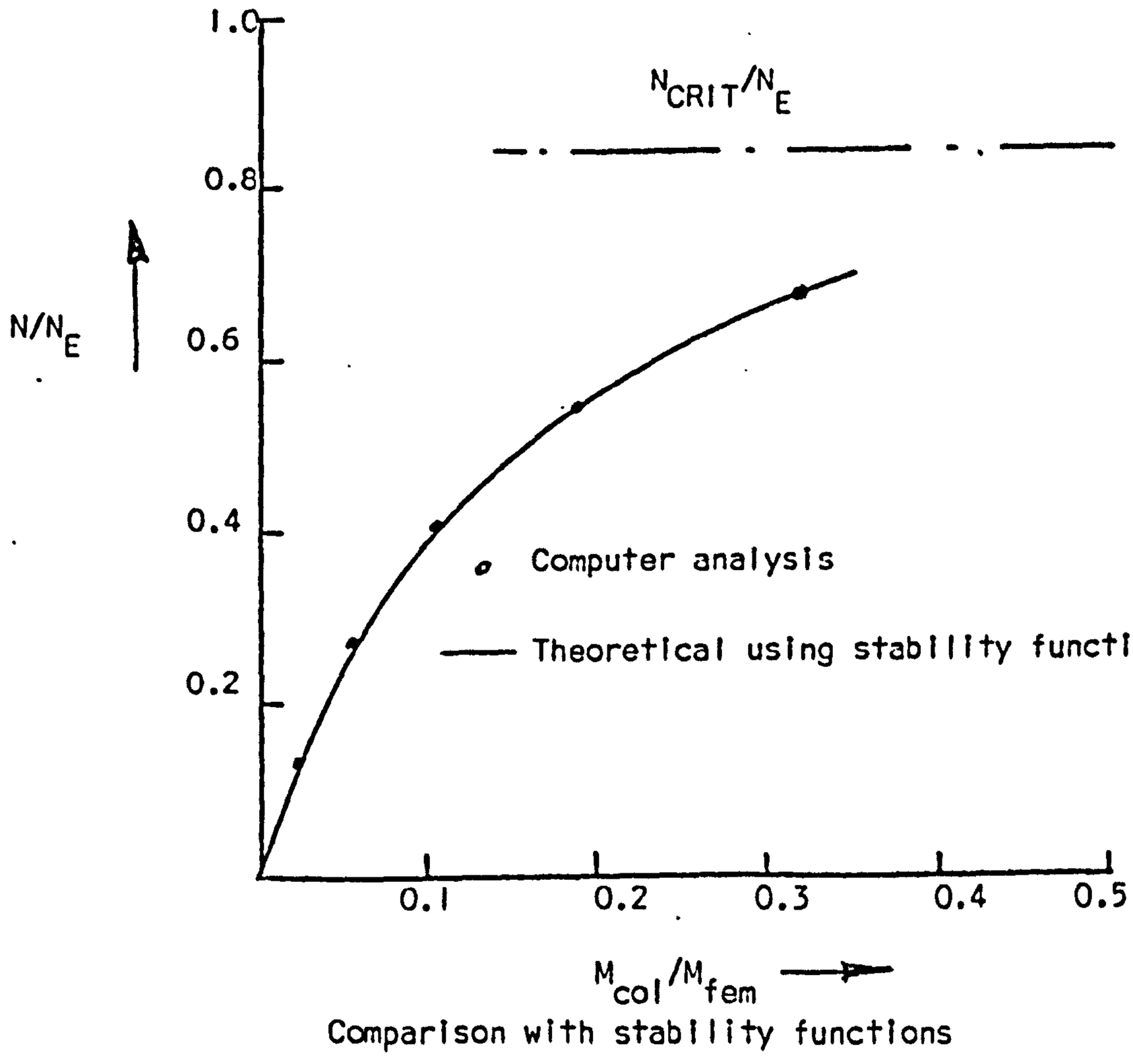

FIG. 2.19 ANALYSIS OF SWAY FRAME

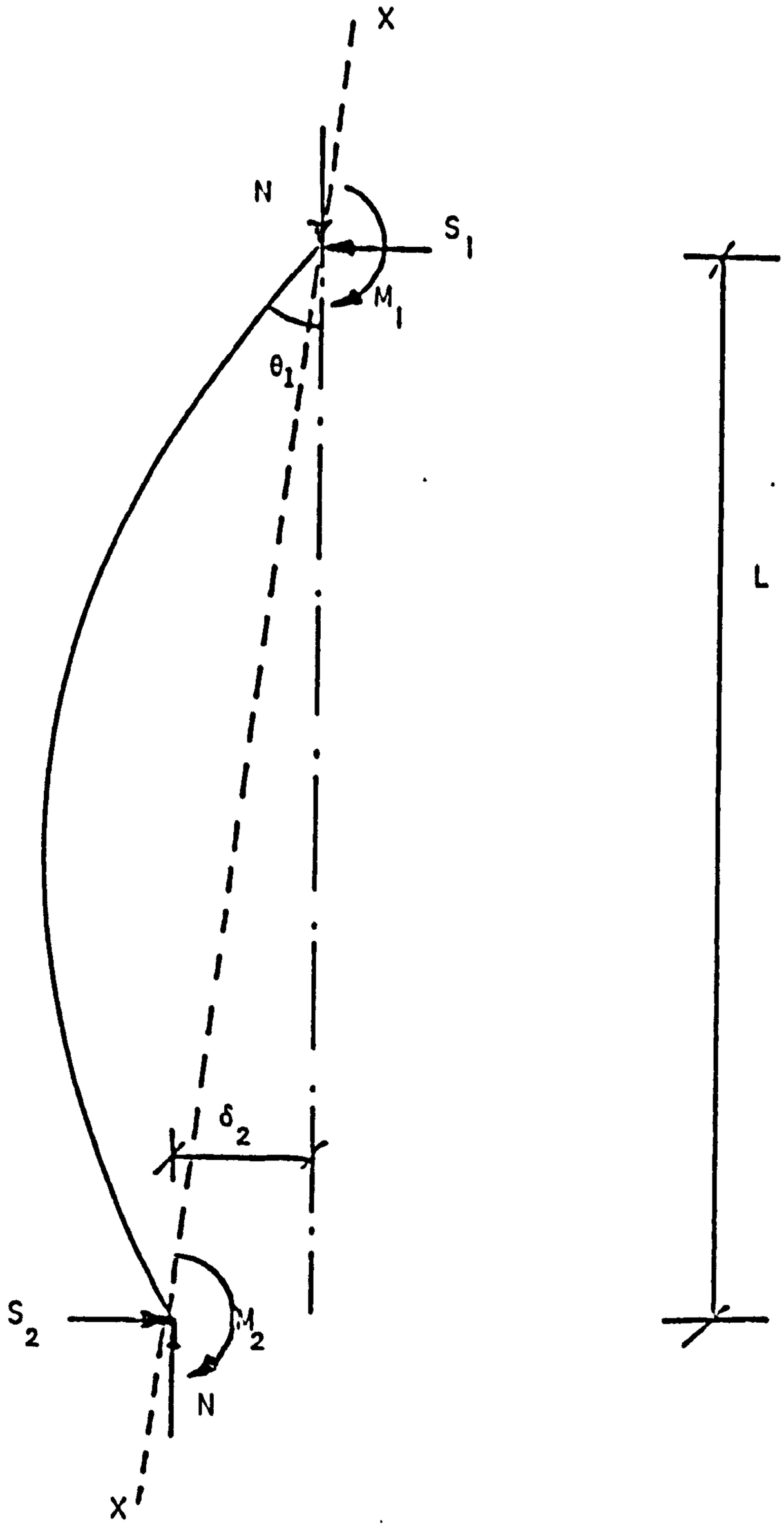

FIG. 2.20 FORCES AND DISPLACEMENTS ON A COLUMN IN UNIAXIAL BENDING

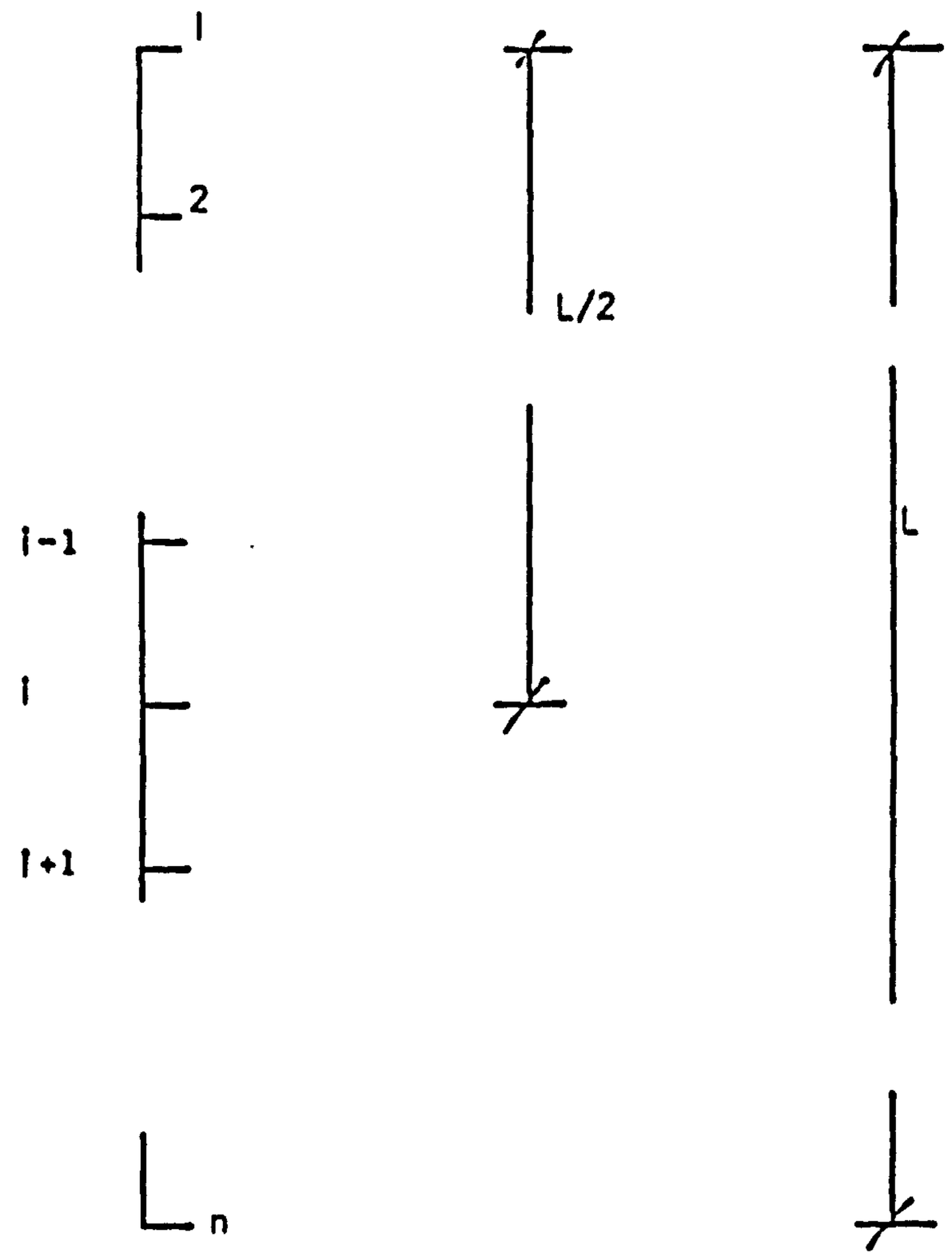

FIG. 2.21 NODE NUMBERING USED IN SYMMETRICAL CASES

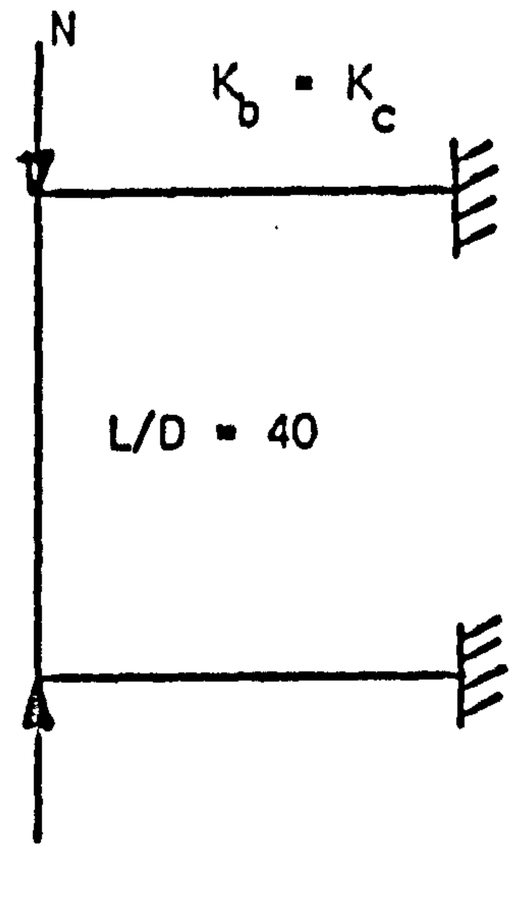

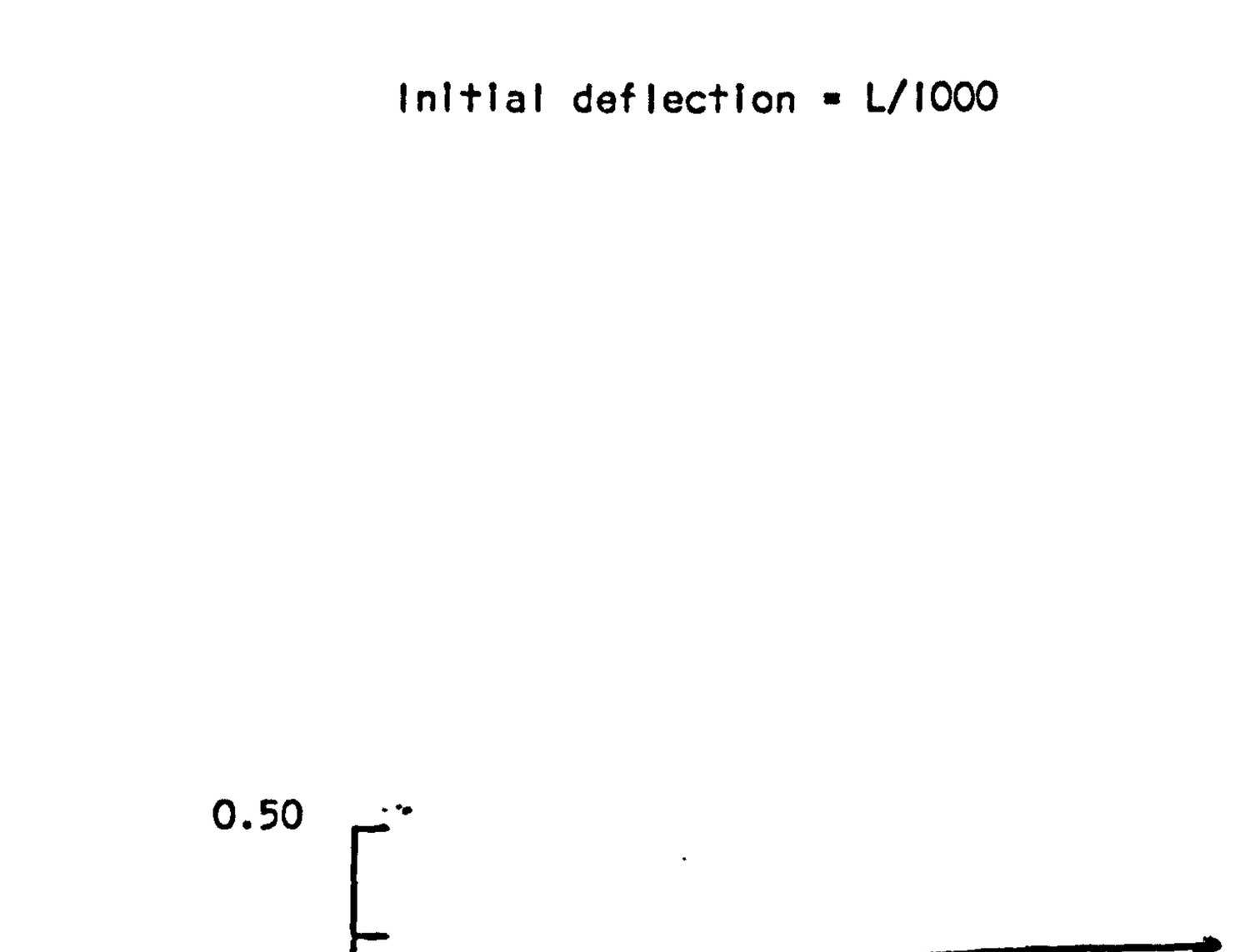

FIG. 2.22 CONVERGENCE OF ANALYSIS

CHAPTER 3. THE BEHAVIOUR OF THE LIMITED SUBSTITUTE FRAME.

3.1 Introduction.

The object of this Chapter is that, before discussing the design of the test rig and test specimens, Chapter 4 and Chapter 5, a review is made of the behaviour of columns with elastic and elastic-plastic restraint. The method of 'beam-lines' has been used and an extension to enable elastic-plastic beams to be included is examined. Further discussion of the behaviour of restrained columns is included in Chapter 8.

As discussed in Chapter 1 many design methods for columns within rigid-jointed frames recommend the use of the limited substitute frame, Fig. 3.1, for the design of columns within no-sway frames. The fixed remote ends of the beams in the limited substitute frame have been chosen to avoid undue conservatism due to the interaction between beams and slabs[70] in multi-storey buildings. A further simplification of the frame is to remove the upper and lower columns and, for design, to use half of the calculated beam stiffnesses[83] for the adjoining beams.

This frame, Fig. 3.3(a) gives slightly lower failure loads, and will be used to examine the behaviour of limited substitute frames.

3.2 Behaviour of isolated columns.

The behaviour of the initially straight, axially loaded, elastic pin-ended column is shown in Fig. 3.2. The failure load N_f is equal to the Euler load N_E if deflections are small

$$\text{i.e.} \quad N_f = N_E = \frac{\pi^2 E I}{L^2} \tag{3.1}$$

where E is the Young's modulus of the material

I is the second moment of area

and L is the length of the column.

If the ends of the column are fully restrained against rotation then the failure load is given by

$$N_f = 4\, N_E = \frac{4\pi^2 E I}{L^2} \tag{3.2}$$

Columns within rigid-jointed frames have a degree of restraint between the two extremes of pinned and fixed and additionally have end moments applied due to beam loadings.

3.3 Behaviour of rotationally restrained columns.

In the frame of Fig. 3.3(a), which is loaded to give uniform single curvature bending, the value of M_{col}, Fig. 3.4 the moment acting on the column, when $N = 0$ can be calculated, e.g. by moment distribution. As the axial load is increased the stiffness of the column falls and hence the relative stiffness of beams and columns changes. The moment M_{col} thus reduces. At the Euler load the stiffness of the column is zero and therefore M_{col} must equal zero. Any additional load causes negative stiffness in the column and therefore M_{col} .is required to reverse sign, Fig. 3.3(b), and stabilize the column, such that M_{col} tends to act as a restraining moment and stops the column from buckling, Fig. 3.4.

At some value of axial load the total stiffness of the beam-column assemblage becomes equal to zero and any further increase in axial load causes a total negative stiffness for the frame and hence collapse.

The problem becomes further complicated in practical columns because of the effects of non-linear stress-strain curves, plasticity and initial imperfections in the column.

3.4 The use of beam-lines to investigate frame behaviour.

A graphical method of investigating the behaviour of columns with non-linear moment-rotation characteristics is that of superimposing beam-lines on the moment-rotation relationships.

3.4.1 End-moment-end-rotation relationships.

Before beam-lines can be used end-moment-end-rotation relationships for columns are required. For an elastic, initially straight, strut loaded with terminal couples, M, and axial load, N, the end rotation, θ, is given by

$$\theta = \frac{M}{N}\sqrt{\frac{N}{EI}}\tan\left(\frac{L}{2}\sqrt{\frac{N}{EI}}\right) \qquad 3.3$$

Thus for a given axial load, N_a,

$$M = C\theta \qquad 3.4$$

Where C is a constant for the given axial load and is equal to $\dfrac{1}{\sqrt{\frac{N_a}{EI}}\tan\frac{L}{2}\left(\sqrt{\frac{N_a}{EI}}\right)}$

Equation 3.4 gives the moment rotation curves as shown on Fig. 3.5.

If however plasticity and initial out-of-straightness are included, then the relationship between moment and rotation ceases to be linear and is of the form shown in Fig. 3.6.

3.4.2 Addition of beam-lines to end-moment-end-rotation relations.

On Fig. 3.7 the curves 1-5 are the end-moment-end-rotation curves for a given column under increasing axial load P. The beam-line, ABCD, for an elastic beam, is based on the fact that the end-moment is the fixed end-moment, M_F when the rotation is zero and decreases linearly when rotation is allowed.

It can be seen that if the axial load is such as to give curve (1) then for this combination of beam and axial loads, the joint rotation is given by θ_1 and the column end moment by M_1.

Similarly for axial loads corresponding to curves (2) and (3) the moments are rotations can be obtained from Fig. 3.7.

The point C on curve (4) gives the failure load since any further increase in axial load does not give an equilibrium position, e.g. curve (5).

The column moment-rotation relationships can include the effects of initial imperfections, non-linear stress-strain relations, etc.

3.5 Inclusion of elastic-plastic beams.

If the beams are such that a plastic hinge develops at M_p then this can be included by modifying the beam-lines, Fig. 3.8, by inclusion of lines EF and GH, assuming equal value of plastic moments for the development of positive and negative hinges.

3.6 Behaviour of the limited substitute frame.

The rotational restraint offered by the beams in a rigidly jointed frame is usually considered to be either

(1) Elastic

or (2) Elastic-plastic.

Hence the effects of either of these types of restraint on the behaviour of columns will be analysed. To simplify the problem a symmetric limited substitute frame loaded to give uniform single-curvature bending in the column will be used.

3.6.1 Columns restrained by elastic beams.

The end-moment-end-rotation relationships for a short column and the beam-line for an elastic rotational restraint are shown on Fig. 3.9. Since failure occurs when beam line is tangential to the moment rotation curve, point F, the moment acting on the column at failure is still positive and therefore moment reversal has not occurred.

If however a more slender column is used, Fig. 3.10, then moment reversal does occur and hence the elastic beams are applying restraining moments to the column.

3.6.2 Columns restrained by elastic-plastic beams.

Details of the forces acting on the column are shown in Fig. 3.11(b). As the axial load is increased the column moment $M_p - M_d$ reduces and hence M_d increases, Fig. 3.11(c). If beams are symmetric the maximum value M_d can take is M_p and

when M_d is equal to M_p a hinge forms adjacent to the column in the lightly loaded beam and the moment acting on the column is zero.

If the column is short the behaviour is similar to that of the short column with elastic beams and failure occurs before the restraining beam becomes plastic, Fig. 3.12. However for the slender column Fig. 3.13, before moment reversal can occur the restraining beam has developed a plastic hinge adjacent to the column and failure occurs at the load which gives the end-moment-end-rotation curve that passes through point F.

3.6.3 Summary of failure modes.

It has been shown in Sections 3.6.1 and 3.6.2 that for symmetric frames with patterned loading collapse of the column can occur

(a) in frames with elastic restraint (Section 3.6.1)
either (1) before moment reversal
or (2) at or after moment reversal
and (b) in frames with elastic-plastic restraint (Section 3.6.2)
either (1) before the lightly loaded beam develops a plastic hinge
or (2) after the development of a hinge in the lightly loaded beam and thus at zero applied end moment on the column.

3.7 Out-of-plane failure.

Up to now only the in-plane failure of columns has been considered. However, in steel frames using standard rolled sections for the columns failure often occurs about the minor axis although heavy beam loads may be applied about the major axis. The reason for this is that the major axis Euler load

N_{EX} is usually about three times as large as the minor axis Euler load N_{EY}. Therefore to attain values of axial load near N_{EX} rotational restraint has to be applied about the Y axis, using beams which are NOT allowed to become plastic.

Design methods such as the Variable Stiffness Method[58] therefore allow plastic design of major axis beams and have elastic minor axis beams rigidly jointed to the column, P_xE_y.

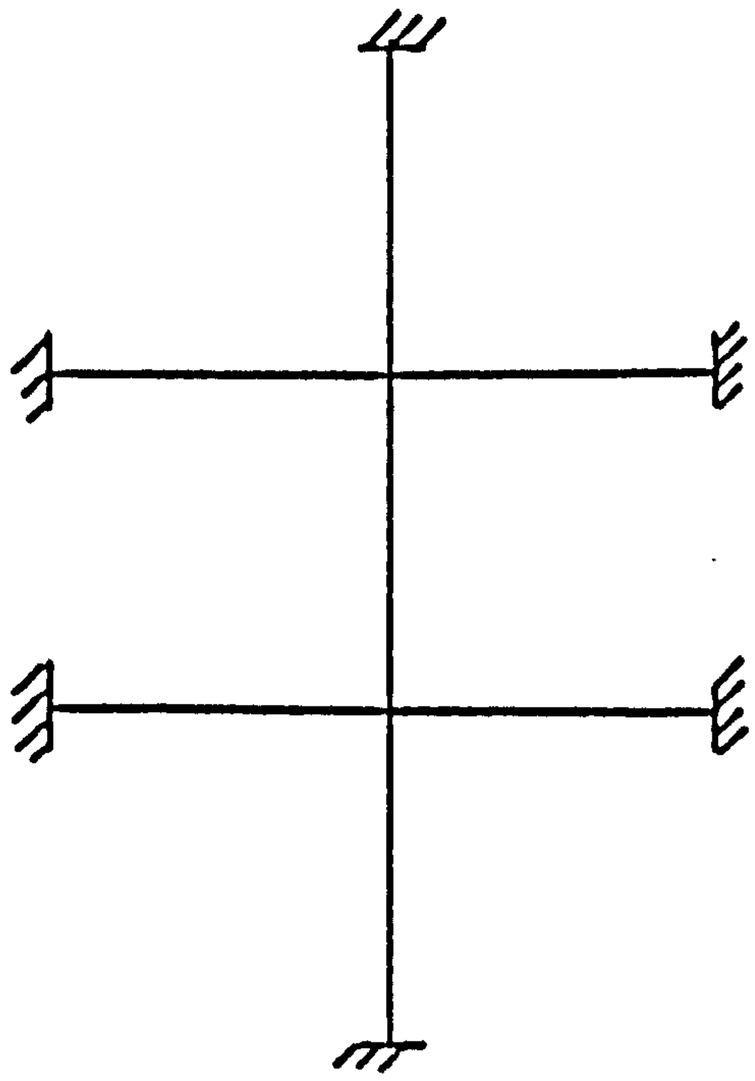

FIG. 3.1 LIMITED SUBSTITUTE FRAME

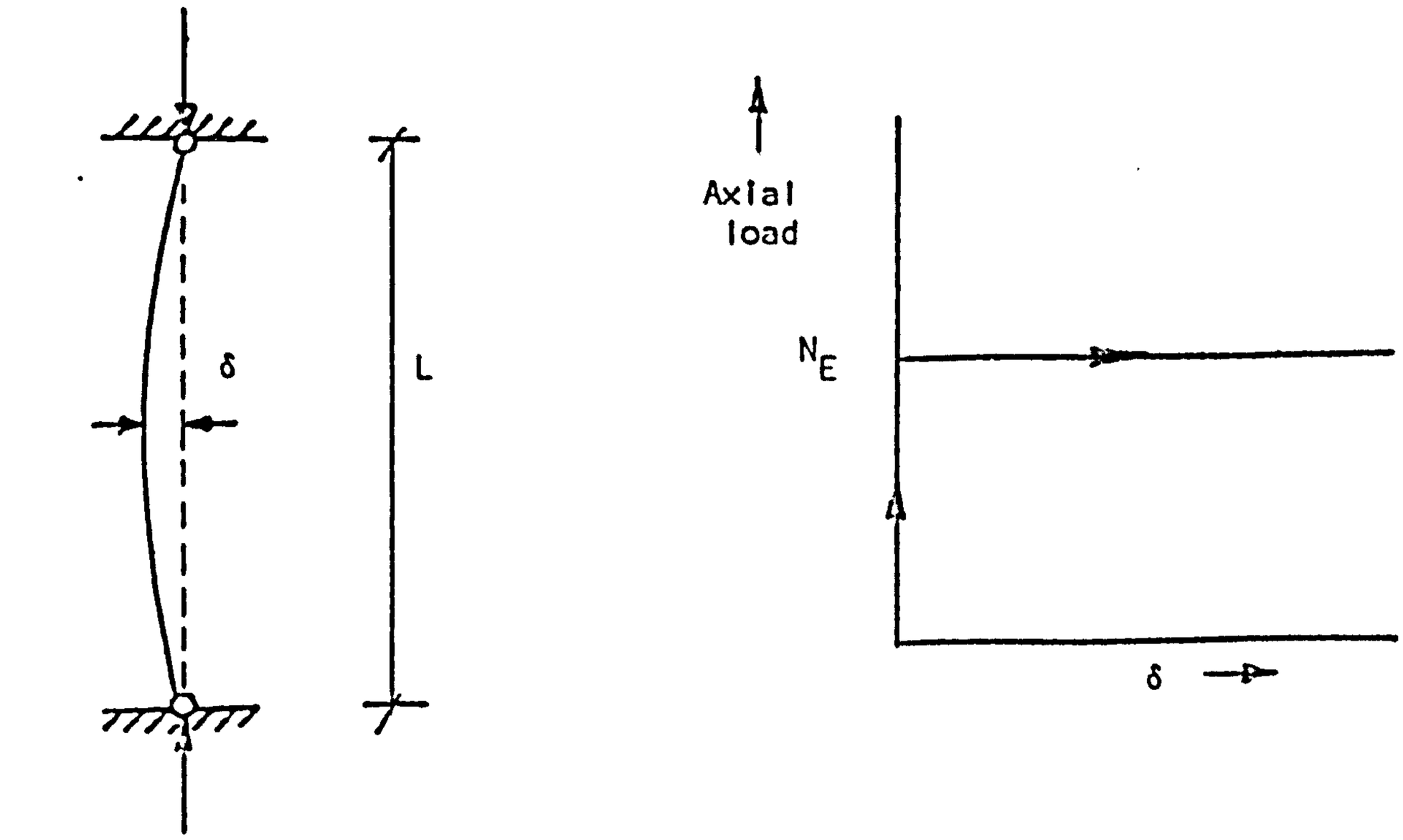

FIG. 3.2 BEHAVIOUR OF PIN-ENDED COLUMN

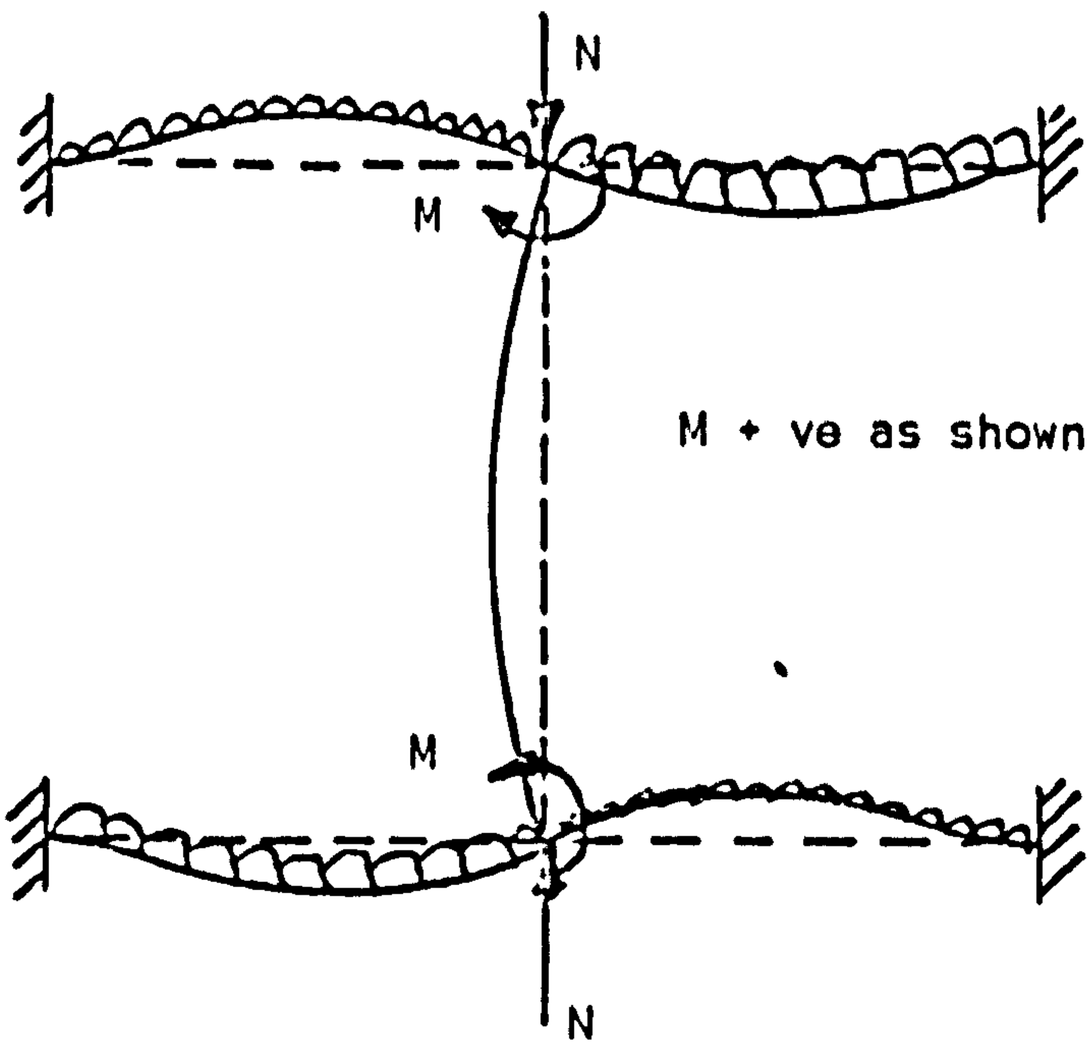

(a)

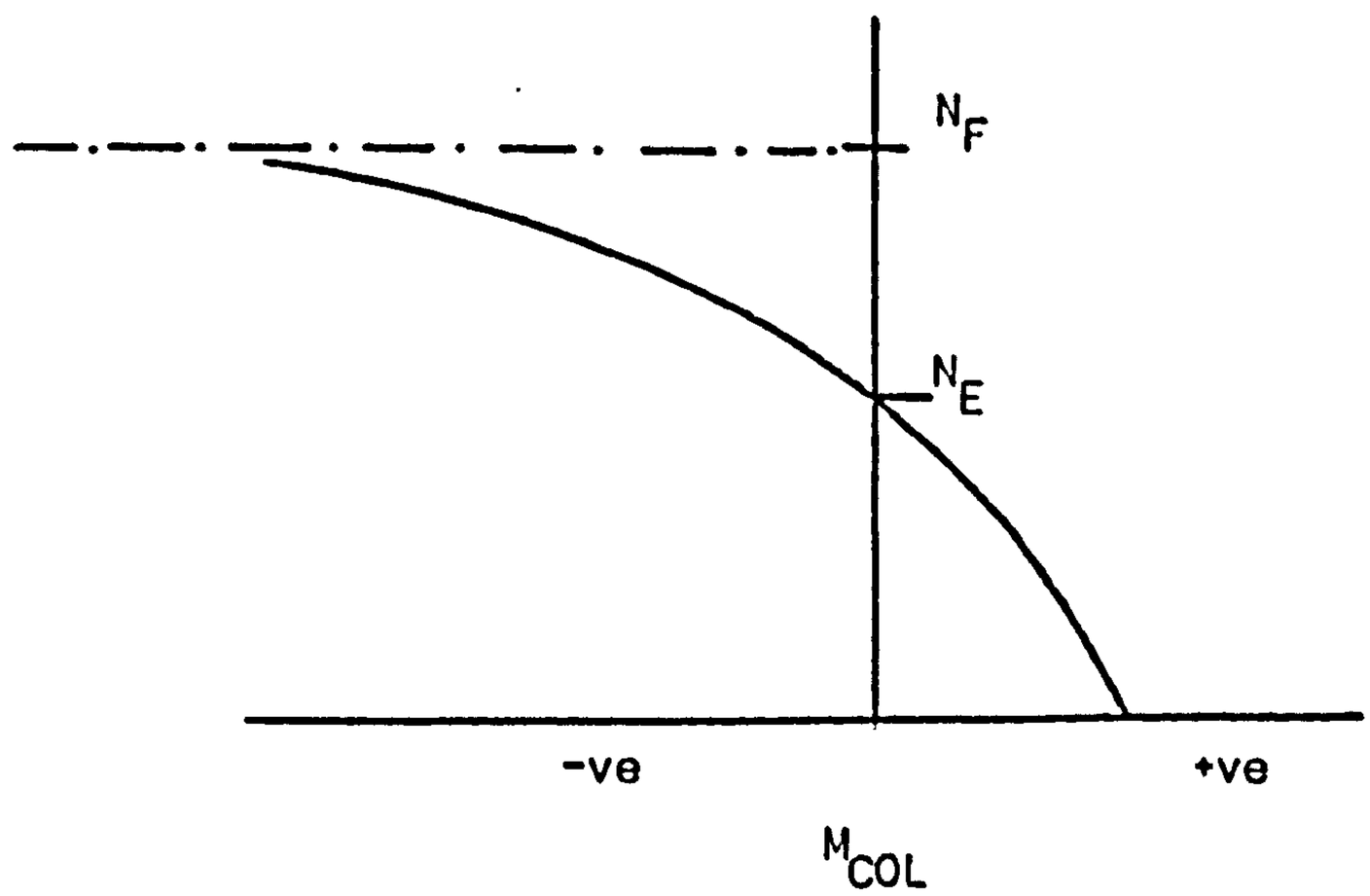

(b)

FIG. 3.3 BEHAVIOUR OF ELASTICALLY RESTRAINED COLUMN

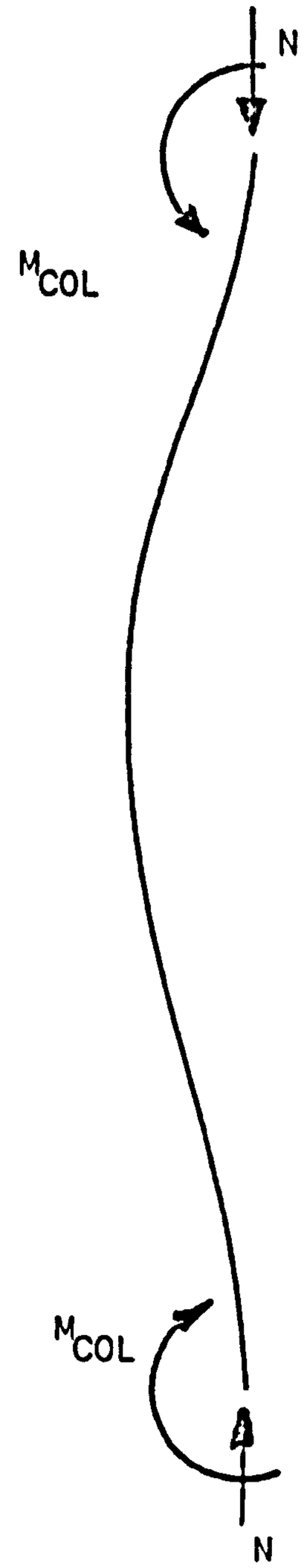

$N > N_E$

FIG. 3.4 FORCES AND MOMENTS ON COLUMN

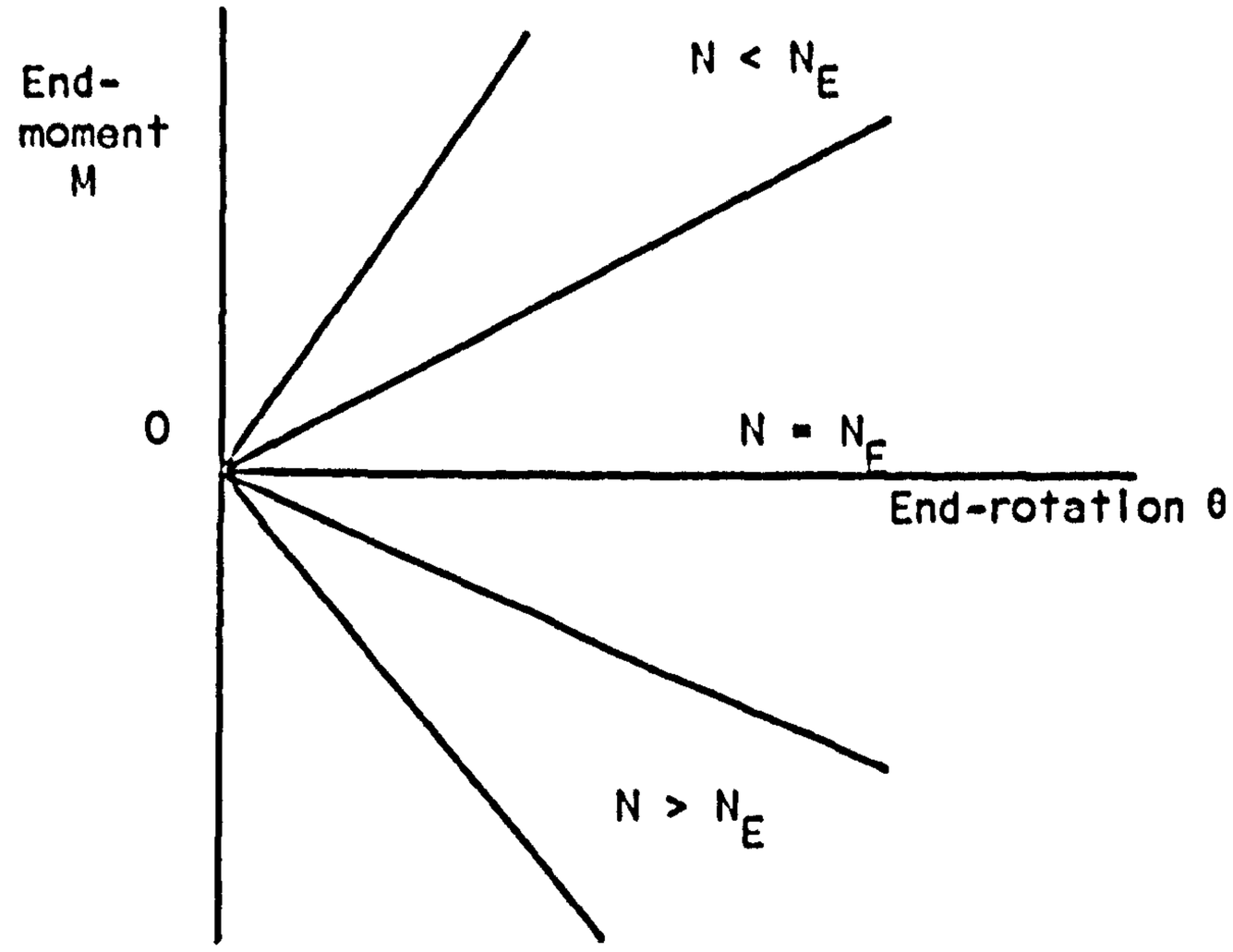

FIG. 3.5 END-MOMENT-END-ROTATION RELATIONSHIPS FOR AN INITIALLY STRAIGHT ELASTIC COLUMN

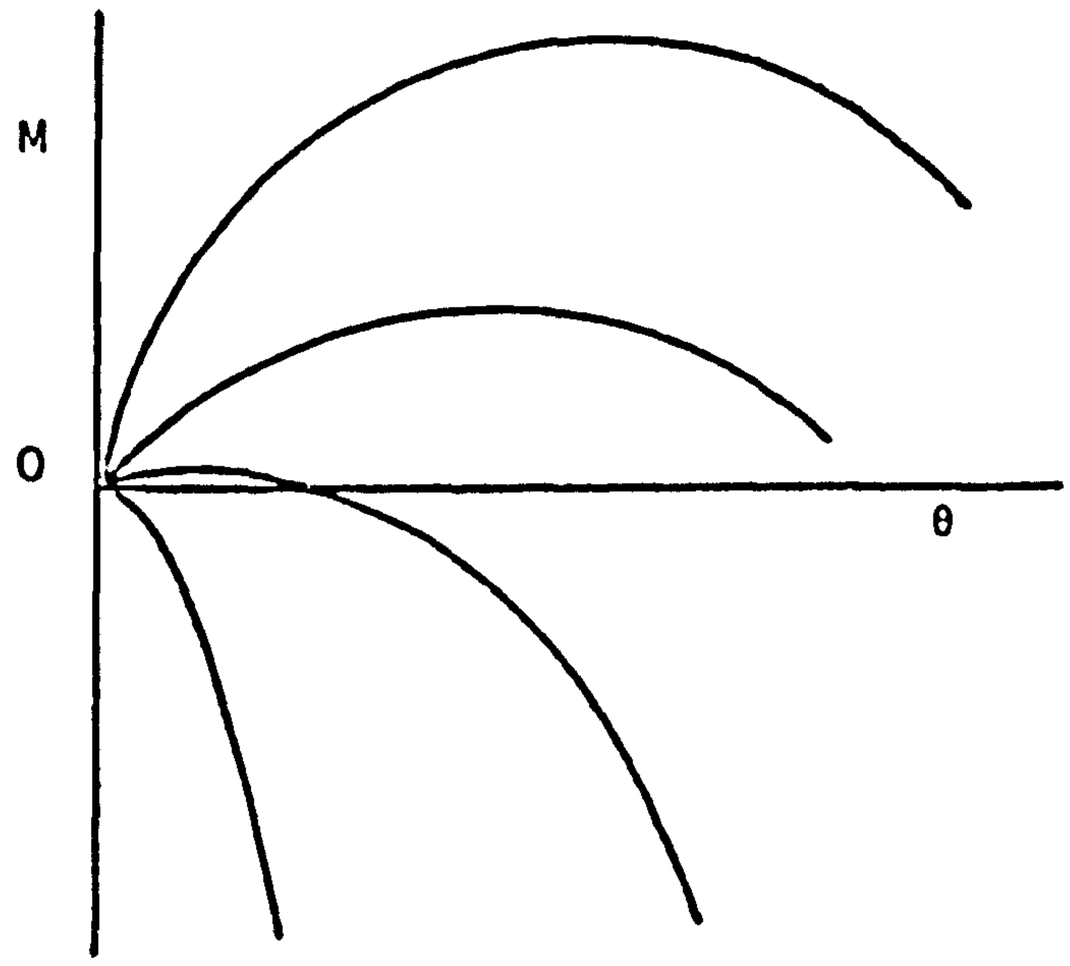

FIG. 3.6 END-MOMENT-END-ROTATION RELATIONSHIPS FOR AN INELASTIC COLUMN

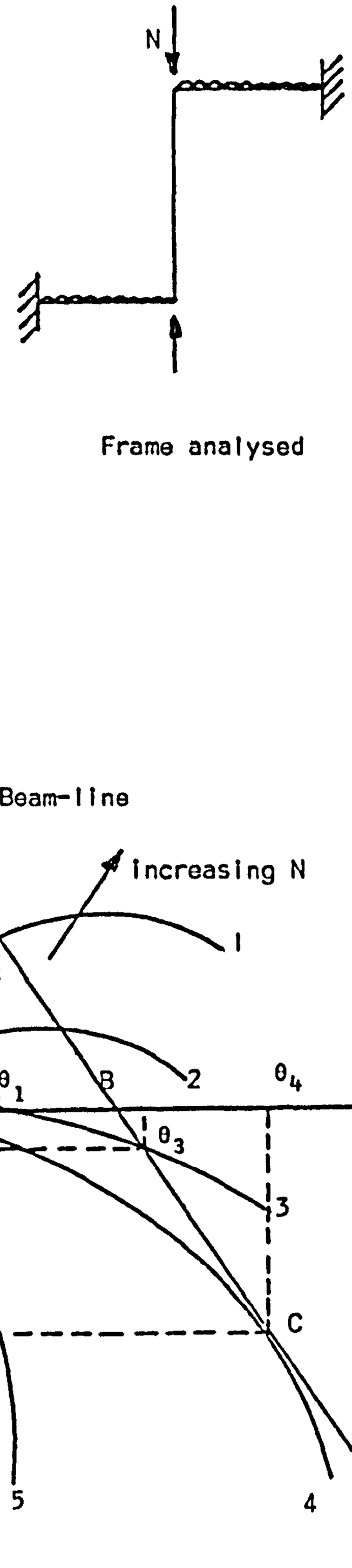

FIG. 3.7 THE USE OF BEAM-LINES

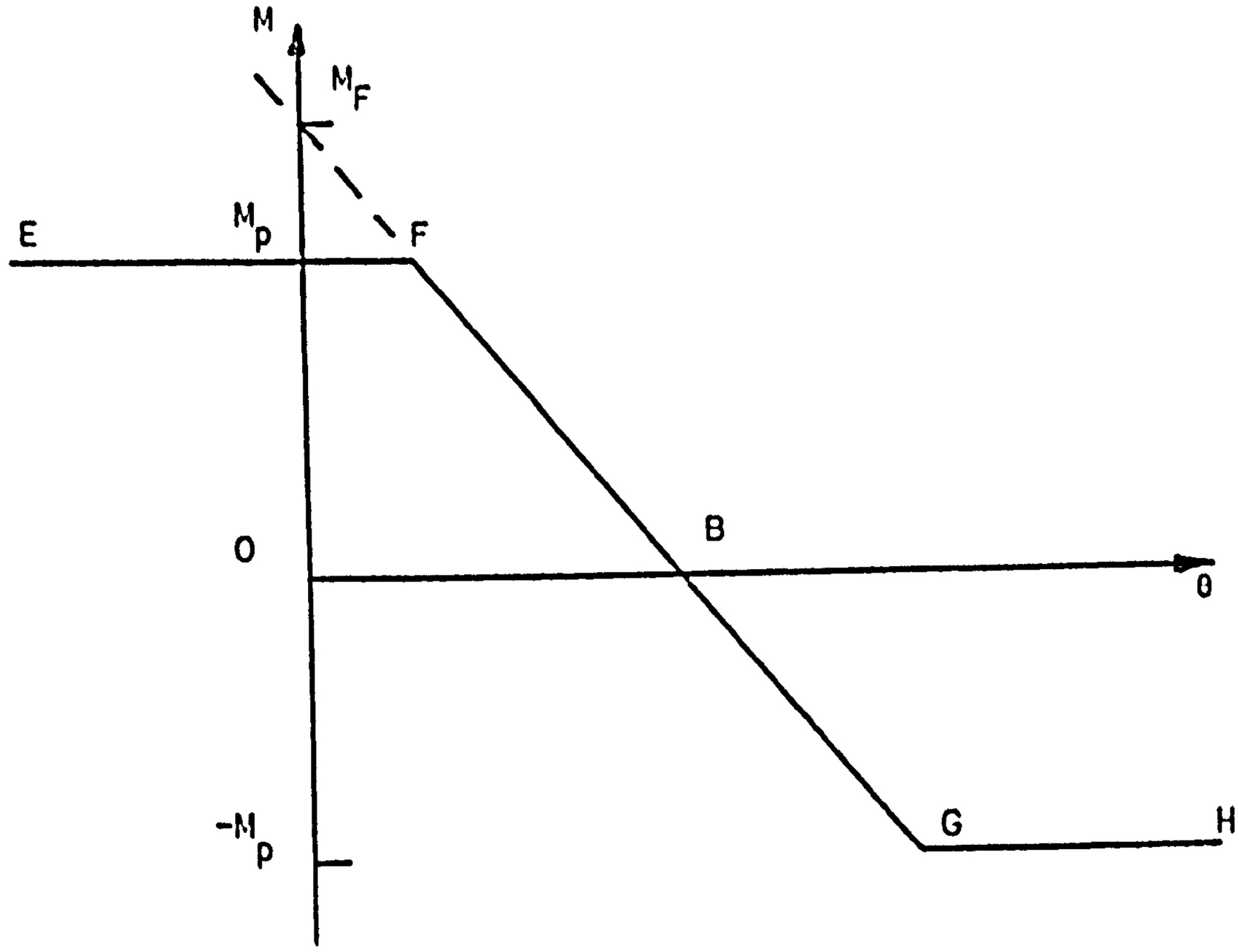

FIG. 3.8 INCLUSION OF PLASTIC HINGES IN BEAMS

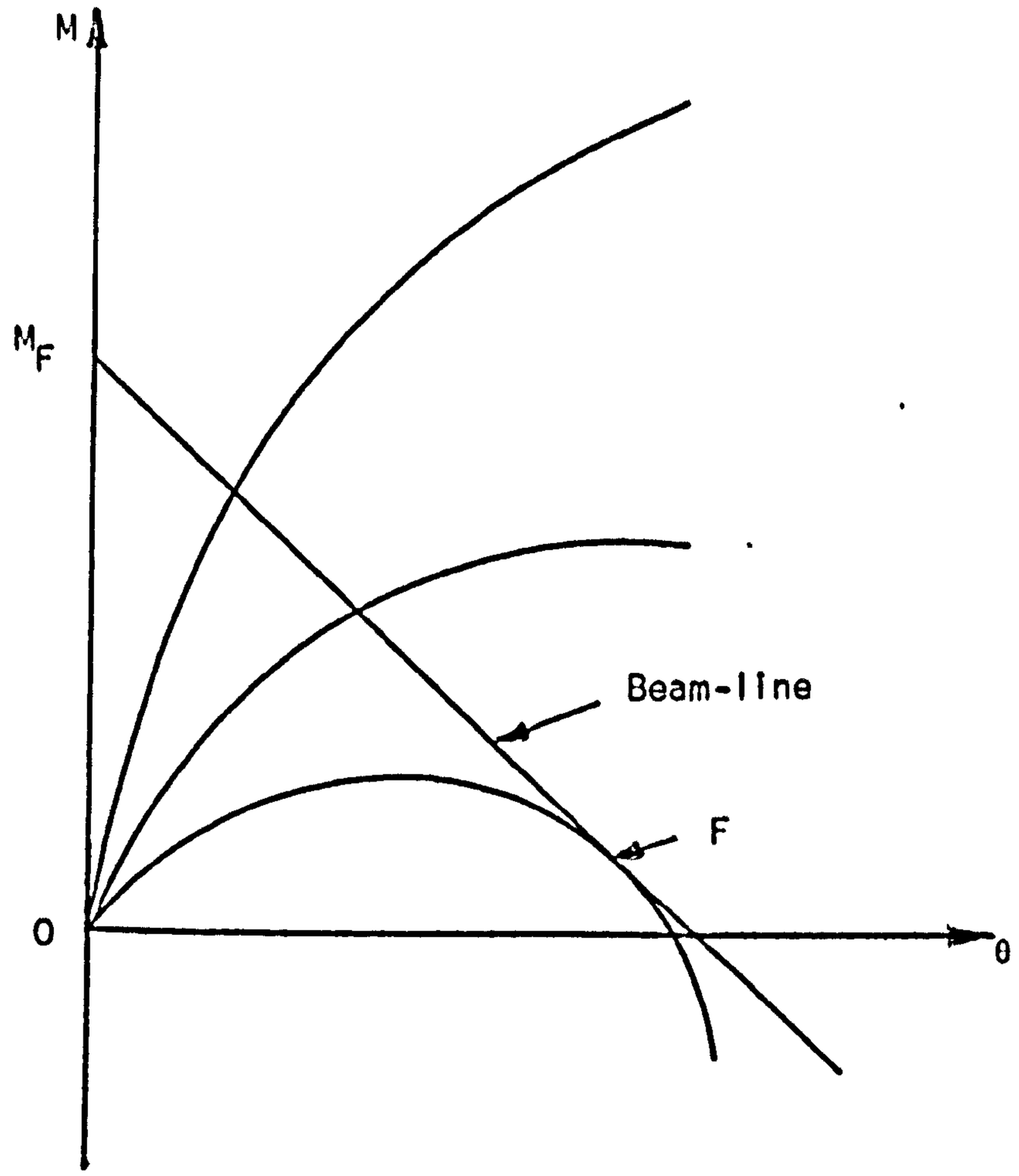

FIG. 3.9 BEHAVIOUR OF SHORT ELASTICALLY RESTRAINED COLUMN

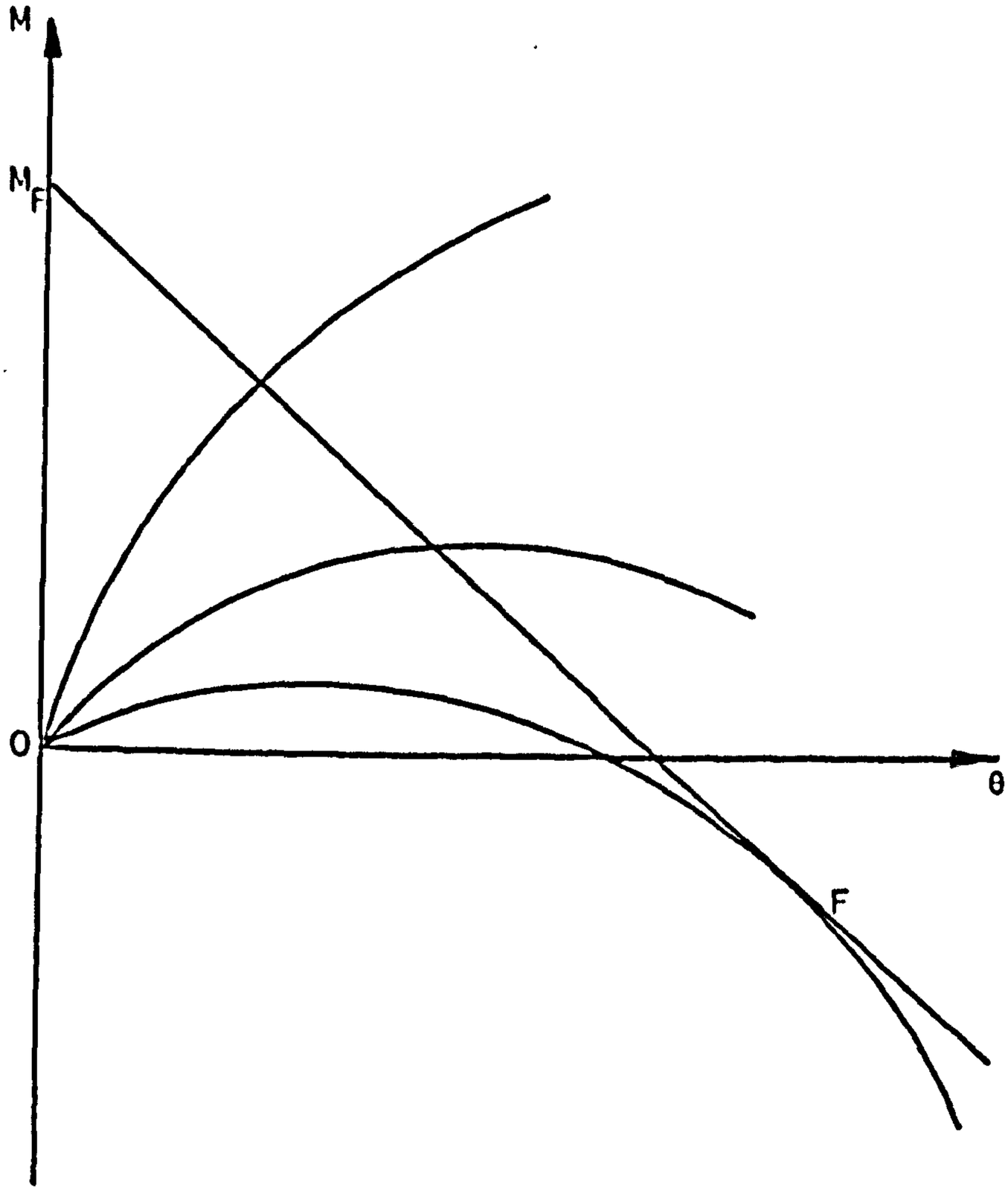

FIG. 3.10 BEHAVIOUR OF SLENDER ELASTICALLY RESTRAINED COLUMN

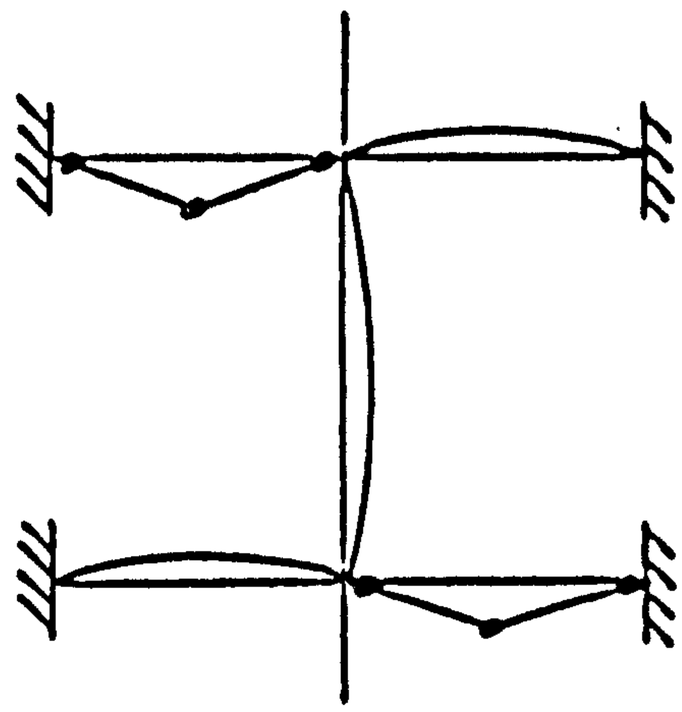

(a)

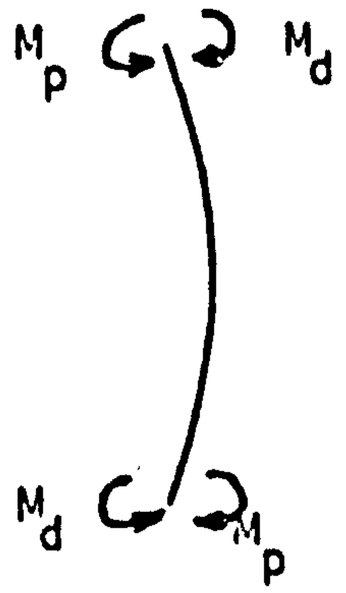

(b)

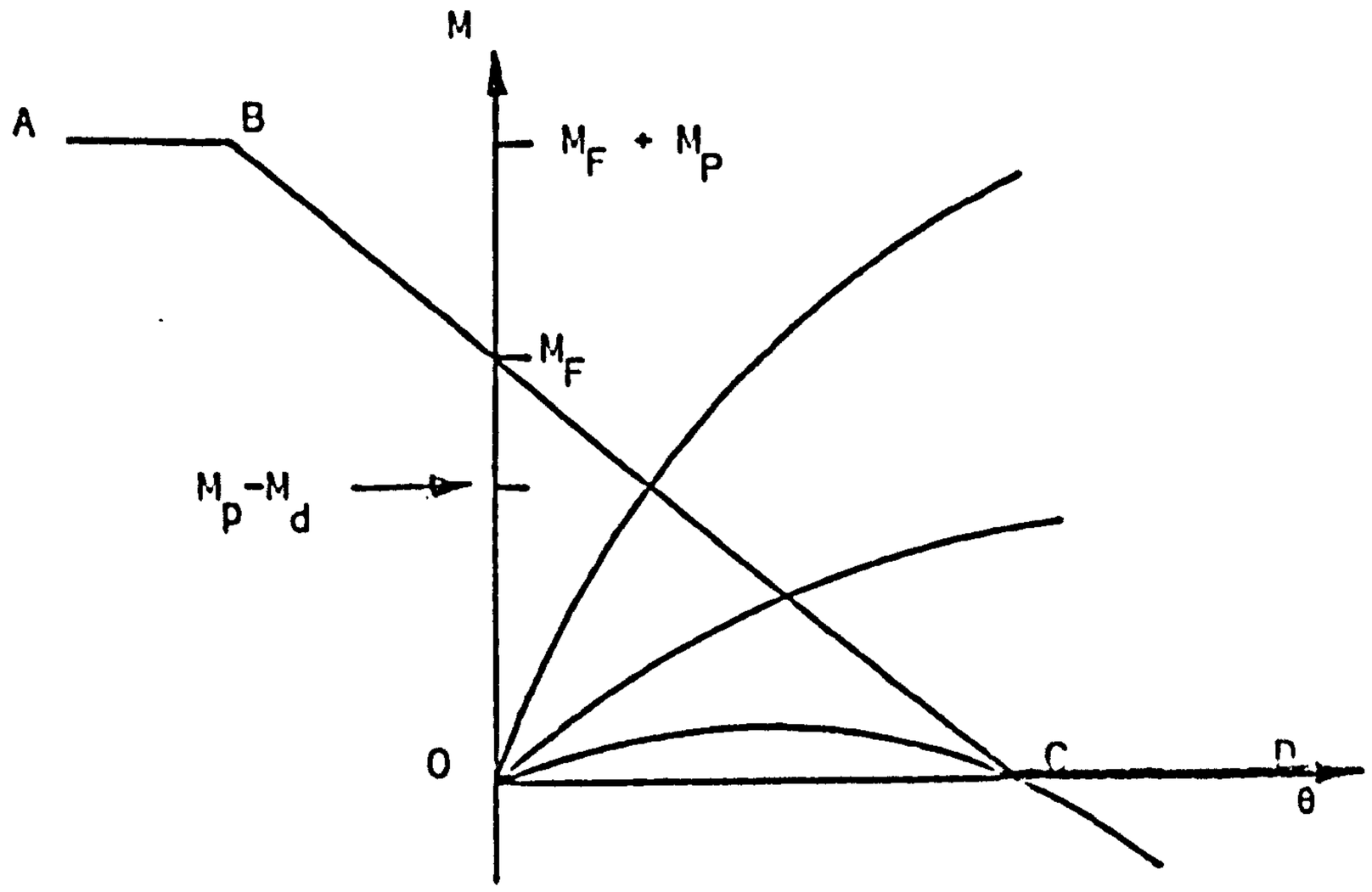

(c)

FIG.3.11 BEHAVIOUR OF A LIMITED SUBSTITUTE FRAME

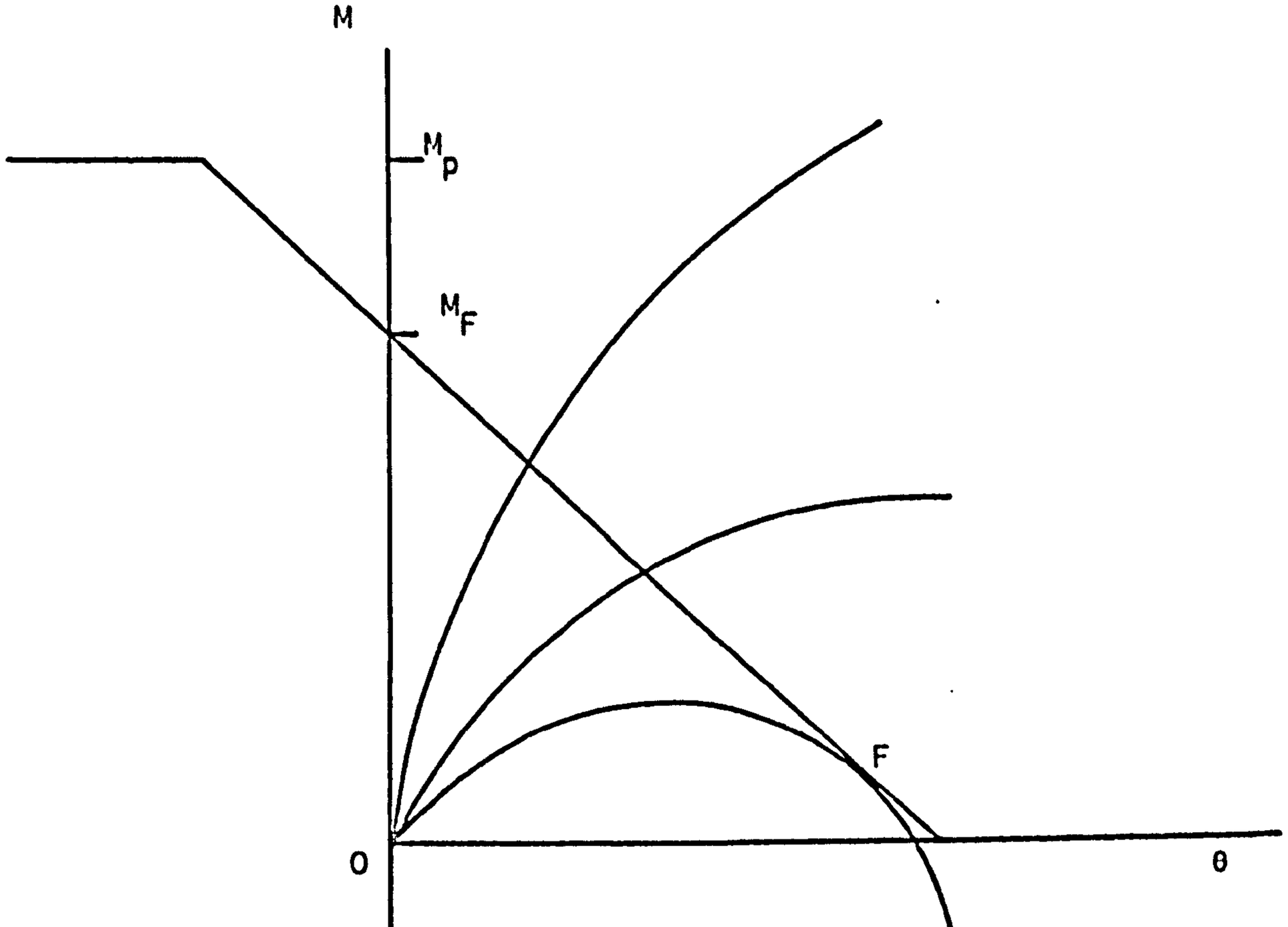

FIG. 3.12 BEHAVIOUR OF SHORT ELASTIC-PLASTICALLY RESTRAINED COLUMN

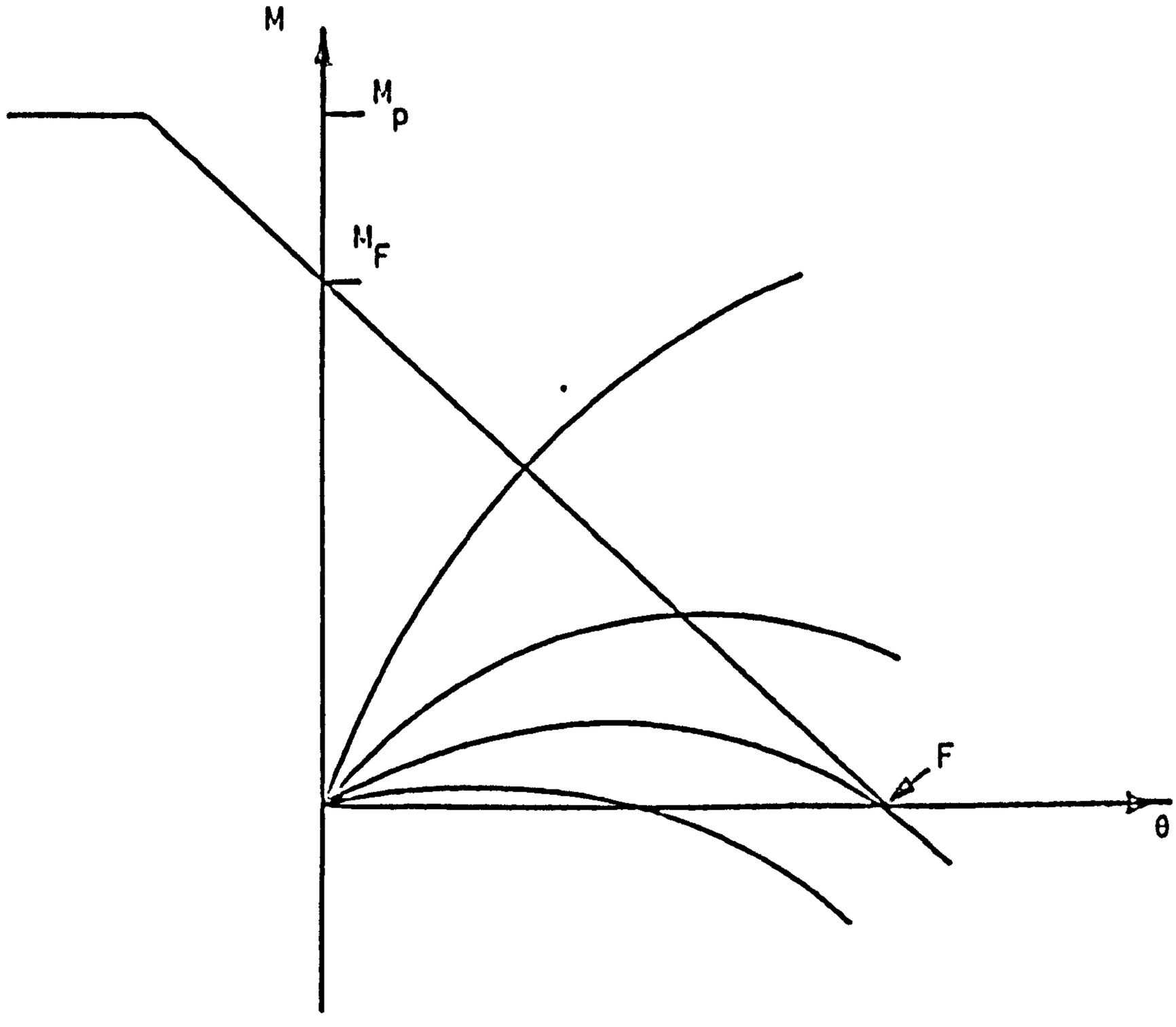

FIG. 3.13 BEHAVIOUR OF SLENDER ELASTIC-PLASTICALLY RESTRAINED COLUMN

CHAPTER 4. THE TEST RIG

4.1 Introduction

Most experimental research[25][46][54] into the behaviour of columns has concentrated on isolated pin-ended columns under axial loads with uniaxial or biaxial bending. Recently investigations [26][69] have been more concerned with the effects of beam restraint on the behaviour of bare steel columns and the complex interaction within frames[59][60][71]. Most of the test rigs used have been capable of applying loads of up to only 500 kN and have usually been restricted to testing a maximum length of column of about 3.5 m. Therefore before tests on restrained composite columns could be carried out, a test rig with a larger axial load capacity and the capability of testing columns of any length was required.

4.2 Choice of specimens

In Chapter 3 use of the limited substitute frame for the design of columns was discussed.

The frame chosen for testing comprises part of this frame, Fig. 4.1 except that the remotes ends of the beams are pinned, so that the behaviour of the column under investigation can be easily seen. For design, limited substitute frames are often used about both axes; hence the experimental frame can have beams about both axes. During testing the beams can remain either linear-elastic, or linear-elastic-plastic. The test columns were manufactured using standard rolled sections and a medium strength concrete mix, because of the difficulties involved in simulating residual stresses in the steel and obtaining concrete with comparable properties in

reduced scale tests. With a universal column section of the smallest size rolled and a medium strength concrete mix, a minimum axial load capacity of approximately 1.5 MN was required.

The size of the specimens and the ease with which instrumentation could be mounted determined that the tests should be carried out horizontally, Fig. 4.2. A description of the various elements of the rig now follows.

4.3 Axial load system.

The fundamental part of the test rig is the axial load system which is shown in Fig. 4.2 and schematically in Fig. 4.3. The system is loaded, Fig. 4.4, by a 2 MN hydraulic jack, with electric pump, through crossed knife edges, Fig. 4.5, which are contained in a box to which the column and beams under test are bolted, Fig. 4.4. The axial load on the column is measured at the opposite end to the jack, after passing through a second set of crossed knife edges, by a 2 MN strain-gauged load cell. The forces from jack and load cell are transferred to the tie-rods, Fig. 4.3, by stiff steel sandwich plates and grillages, Fig.4.4. Either four or six 32 mm dia. Lee Mc-Call prestressing bars (characteristic load 800 kN each) are used, depending on the force to be resisted, Fig. 4.2.

The fixed grillage, Fig. 4.3, is bolted to the strong floor whilst the sliding grillage is free to move along the axis of the column only, to take up strains within the bars.

4.3.1 The crossed knife edges.

The crossed knife edges, Fig. 4.5, are designed for working loads of up to 2 MN. They provide rotational freedom about both

major and minor axis, but do not give torsional freedom, as Proctor[68] has shown that torsional failure of composite sections is unlikely to occur and Gent[26] has shown that failures of restrained steel H columns are also unlikely to have a torsional component. Additionally, most columns within rigid frameworks can be considered to be torsionally fixed at their ends due to the rigidity of beams framing into the joint.

Prior to the construction of these knife edges the maximum load applied through crossed knife edges was about 600 kN by Hutchings[69].

Several models of the knife edges were made and tested before the manufacture of the full size set. The main problem was the choice of the thickness of the centre plate.

The ideal solution for the knife edges would have been to have had the two centres of rotation coincident; however, it was found from the model tests that if the distance between the knives was too small, (less than 40 mm), then the centre plate split.

A second problem was the choice of the area of contact of the knife edge on the centre plate. Ideally, the knives would have had line contact only. Initially, therefore the tips of the knife edges had only a 2.5 mm radius and sat in a 120^{o} groove with a 10 mm radius. Under test, however, it was found excessive local yielding occurred causing binding of the knife edges.

In the full size set, therefore, the knives have a 10 mm radius at the tip and sit in a 120^{o} groove 5 mm deep with a 10 mm radius, Fig. 4.5. The average bearing stress, at the knife edge tips, for the maximum working load, 2 MN, is of the order of

400 N/mm^2 although stresses near the centre of the knife will be higher.

The plates and knives are all manufactured from grade EN32 case-hardening steel with a yield stress of 500 N/mm^2. The knives were case-hardened using the carburising process to a depth of approximately 0.5 mm.

Each knife edge is bolted into its plate and the top and bottom plates are attached by keeper plates to the centre plate. The entire set of knife edges are bolted within the beam-column joint boxes and the top plates are attached to either jack or load cell.

4.3.2 Column-beam boxes.

One of the problems that is often encountered in tests on restrained columns if the "sub-stanchion" effect. The stub-stanchions are the column lengths often used for loading, Fig. 4.6, which modify the effective stiffness of the restraining beams as shown in Appendix A5. The ideal solution, to avoid translation of the beam-column joint, is to have the axial load applied at the intersection of the beam and column centre-lines.

Hutchings[69] solved this problem by column-beam boxes in which to place the knife edges and this method has been used in this test rig. A small stub-stanchion effect does still exist due to the offset centres of rotation in the crossed knife edges; however, this is small compared to the lengths of columns tested, the stub length being ± 20 mm, less than ± 2% of the shortest column length.

One of the boxes is shown in Fig. 4.4. The major and minor axis beams and the column under test are bolted to the machined faces of these boxes. The boxes have been designed to act as rigid extensions to the beams and columns and thus the working stresses due to transfer of the bending moments from beam to column have been kept below approximately a quarter of the yield stress.

4.4 Beam restraint and loading system.

If the behaviour of columns with the limited substitute frame of Fig. 3.1 is to be investigated experimentally it is useful to simplify the frame further.

In the case of a column with linear elastic beams carrying loads of w_1 and w_2, and with stiffnesses K_1 and K_2 repsectively, Fig. 4.7(a), the two beams can be replaced with an equivalent single beam of stiffness $K_1 + K_2$ with load $w_2 - w_1$. If, however, the loading w_1 is increased to cause a plastic mechanism in the beam, Fig. 4.7(b), then it will contribute no stiffness to the system and the equivalent single beam will have stiffness K_2 and load $w_2 - w_1$. Thus the limited frame is simplified to that shown in Fig. 4.1.

The requirements of the beam loading and restraint system are that they provide

1) a method of application of a beam load or end-moment equivalent to a set of given beam loadings which may be from two elastic beams or one elastic and one plastic beam, Fig. 4.7.

2) the ability to measure the applied moment on the column which can, with elastic restraint, change sign.

and 3) the ability to provide elastic or elastic-plastic restraint to the column.

The application of the beam loading is accomplished by using an equivalent fixed end-moment which is applied by deflecting the end of the beam, Fig. 4.8, by δ. Knowing the flexural rigidity of the beam, EI/L, the fixed end-moment, $\frac{3EI\delta}{L^2}$, can be calculated. This moment obviously remains constant as long as the deflection of end B relative to A is kept constant, although the actual end-moments on column and beam will be dependent upon the stiffness of the column and beam also.

The size of the moment is measured by determining the reaction, R, at the end B of the beam, Fig. 4.8.

The major axis beam deflections are applied by means of a threaded rod and nut arrangement, Fig. 4.9. The beam is deflected by tightening the nut "A", Fig. 4.10, against the rigid reaction block. If elastic restraint is required and moment reversal is expected the nuts "A" and "B" are locked either side of the reaction block, Fig. 4.10. If it is required, as in a symmetric frame with elastic and plastic beams, that the moments should not change sign then nut "B" is not used and hence elastic-plastic behaviour is simulated.

Axial shortening of the column during a test is measured using displacement transducers. This of course affects the beam deflections which can be adjusted if necessary.

The reactions in the links are measured using strain-gauged

tension-compression load cells.

The arrangement for application of the minor-axis loads is shown schematically in Fig. 4.11. The two beams are connected by a link which contains a turnbuckle to deflect the minor axis beams, and a tension-compression load cell to measure the force in the link. At present there is no capability, about the minor axis, of simulating elastic-plastic beams simply.

Because the two major axis beam loading systems are independent of each other, either or both can be moved along the beam to give various beam stiffness ratios. They can also be loaded to give any required moment ratio. It is also easy to change the sections used for the beams.

The minor axis loading system is such that at the present time only symmetric single curvature loading is applied. Variations of stiffness ratio can be accommodated by using beams of differing section and moment ratios by moving the point of application of the load. It is envisaged that minor axis restraint should remain elastic.

4.5 Geometry of deformations.

A problem of major importance in any column testing rig is the introduction of the requisite degrees of freedom whilst maintaining the overall stability of the rig. The section that now follows discusses the geometry of the deformations following the application of moments and explains the choice of suitable bearings.

Initially, the centres of rotation of the end of the column about both major and minor axes are assumed to be coincident. One

centre of rotation is the origin for x, y and z axes, Fig. 4.12, with corresponding displacement u, v and w, and rotations θ_x, θ_y and θ_z respectively; this origin is taken to be at the fixed end of the test rig, Fig. 4.3.

The knife edges have been designed to cater for rotations θ_y and θ_z however, the torsional rotation of the column, θ_x, is not allowed. No translations are allowed.

At the other end of the column a centre of rotation exists at the second set of knife edges; the same rotational degrees of freedom are allowed and in addition translation along the x axis is available to cater for axial shortening of the column.

If the major axis beams are deflected at end 1 by u_1 Fig. 4.13 because no translation is allowd at the origin an additional displacement v_1 occurs, and also a rotation θ_{z1}. The corresponding rotation at the end of the minor axis beam point 2, Fig. 4.13, is θ_{z1}.

The effects of the application of a displacement to minor axis beam whilst maintaining the major axis beam displacement, Fig. 4.14, is now considered. If the displacement is u_2 then, because of bending and translation of the beam, a displacement w_2 occurs and additionally a rotation θ_{y2} of the major axis beam, Fig. 4.14. The rotations of the major and minor axis are now θ_{z1} and θ_{y2}.

Thus the degrees of freedom required at the ends of the beams are:-

Bearing 1	translations	x, y
	rotations	θ_z, θ_y
Bearing 2	translations	z, x
	rotations	θ_z, θ_y

The problem is further complicated because at the beam-column boxes each of the two beams rotates about a different point due to the arrangement of the knife edges, Section 4.3.2. This is equivalent to the two beams having axes that are offset from each other, Fig. 4.15. Consider the effects on the minor axis knife edge and bearing 1 due to the application of a minor axis displacement. If the minor axis rotation is θ_{y2} and the stub stanchion length is ℓ then the points O and B move relative to each other $\ell\theta_{y2}$ Point O, however, is fixed in the z direction and therefore point B must be able to move. Application of a displacement, u_1, to the major axis beam will cause a displacement of v_B along the y axis at the point B.

Because the two minor axis beams are interconnected and different values of y displacement can occur at each end, freedom is also required for a θ_x displacement at the ends of the beams.

Therefore for the bearings the following degrees of freedom are required

Bearing 1.	x, y.
	θ_z, θ_y.
Bearing 2.	x, y, z.
	θ_x, θ_y, θ_z.

Knife edges	
"Fixed end"	y, z.
	θ_y, θ_z.
"Free end"	x, y, z
	θ_y, θ_z.

4.6 Overall stability of rig and specimens.

The schematic drawing of the rig, Fig. 4.16, shows the axial load system to be a pin-jointed frame and hence any small movement such as that shown will cause instability of the rig; If moments are taken about M a clockwise out of balance moment of SL exists, which makes the rig unstable. It is therefore necessary to provide restraints, at each end, to movements caused by the shear forces S. The rig is therefore stabilised in the horizontal plane by fitting the grillage at end A within slides, Fig. 4.17.

A similar problem exists in the vertical plane but is not so critical because any instability moment must first overcome the moment due to the self weight of the test rig and specimen. However in the vertical plane the end A is stabilised by slides and rollers, Fig. 4.17.

The only mode of instability likely to occur on the specimen is due to the application of unequal end moments causing shear forces at the ends of the columns. These are resisted by long pin-ended links connected to the strong floor and capable of taking axial tension or compression only, Fig. 4.2. They are partly hidden by the major axis beams in Fig. 4.2.

4.7 Instrumentation.

The instrumentation provided is for

1) Deflection measurement

and 2) Load measurement.

The frame used to carry the deflection measuring equipment is shown in Fig. 4.2. The frame is mounted in such a way as to give deflection measurements of the column relative to the axis through the longitudinal centreline of the column under test.

Consider Fig. 4.18, with the axes x, y and z as shown and the origin at the centre of rotation of end B, the fixed grillage end, Fig. 4.18. The instrumentation frame is mounted so that it remains in the same relative position to the x axis throughout a test, and that no displacements are allowed along the y and z axes. The frame must however be capable of following the x axis movement at end A; thus sliding bearings are provided at end A of the instrumentation frame.

Small displacements of the fixed grillage are followed by mounting the frame onto the grillage. At the free end the frame is also mounted on the grillage. Theoretically the grillages should not rotate, and thus θ_x, θ_y and θ_z are zero, however small changes are likely to take place and are catered for in the bearings. To allow differential rotations of θ_x and θ_z at the two grillages the instrumentation frame was made torsionally flexible, by using very little cross-bracing, and spherical bearings were used. The spherical bearings are easily capable of allowing θ_y rotations.

The arrangement of bearings is shown in Fig. 4.19.

Thus the measurements taken using this frame system are relative to the initial shape of the columns under test, assuming no translation of the load cell, jack, knife edges and boxes relative to the grillages takes place.

All deflections were measured using linear voltage displacement transducers of various stroke lengths, dependent on expected movements and required accuracy. End-rotations of the column were also calculated from measurements from these displacement transducers.

The axial load was measured using a 2MN strain-gauged load cell. The beam loads were measured using tension-compression links with capacities, of 20 kN, 45 kN and 100 kN.

Readings from strain gauges, displacement transducers and load cells were recorded using a Solartron-Schlumberger data-logger and PDP11 8K computer. Software was written for the computer in BASAC language to give an output of strains, loads, deflections and end-rotations. Data was also output on to punched paper tape for subsequent analysis on the University Computer.

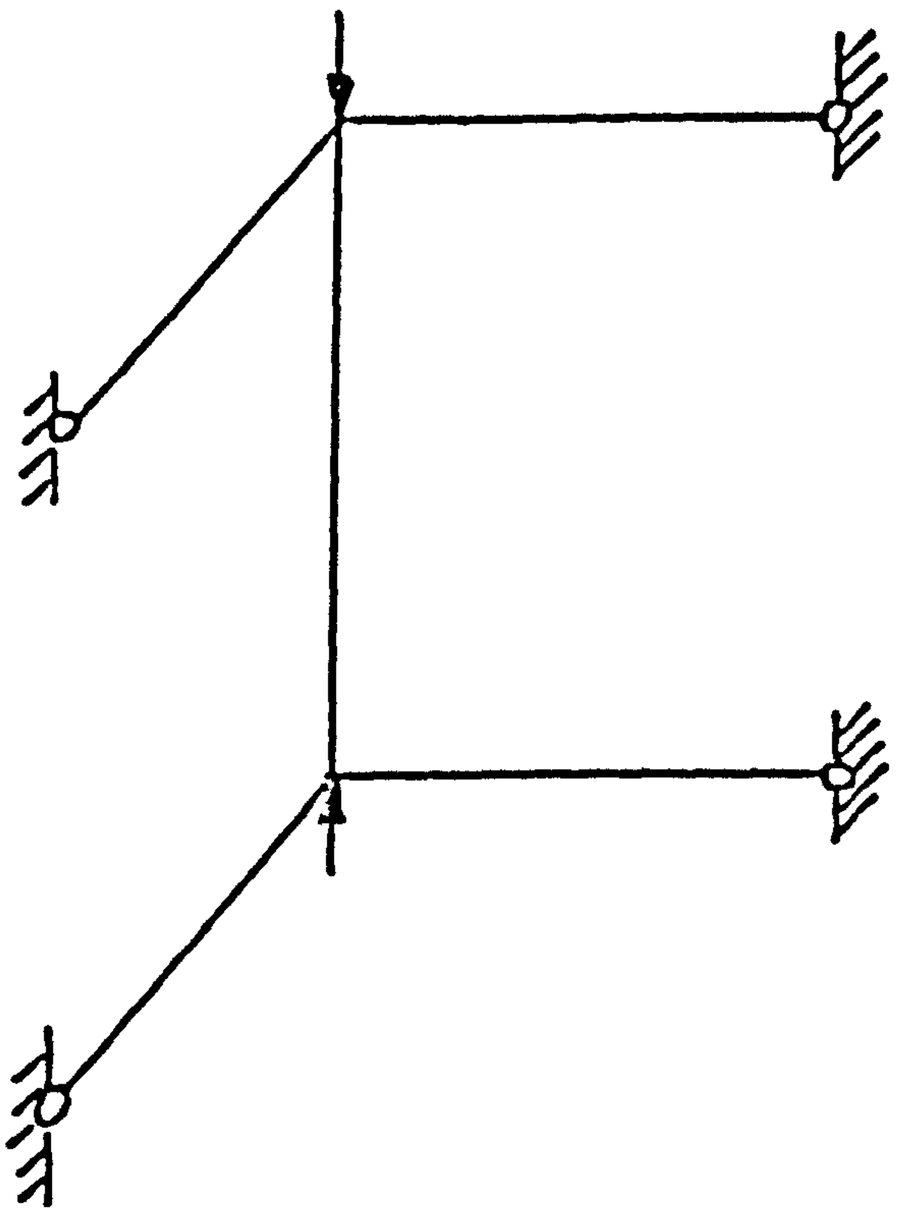

FIG. 4.1 FRAME USED FOR TESTS

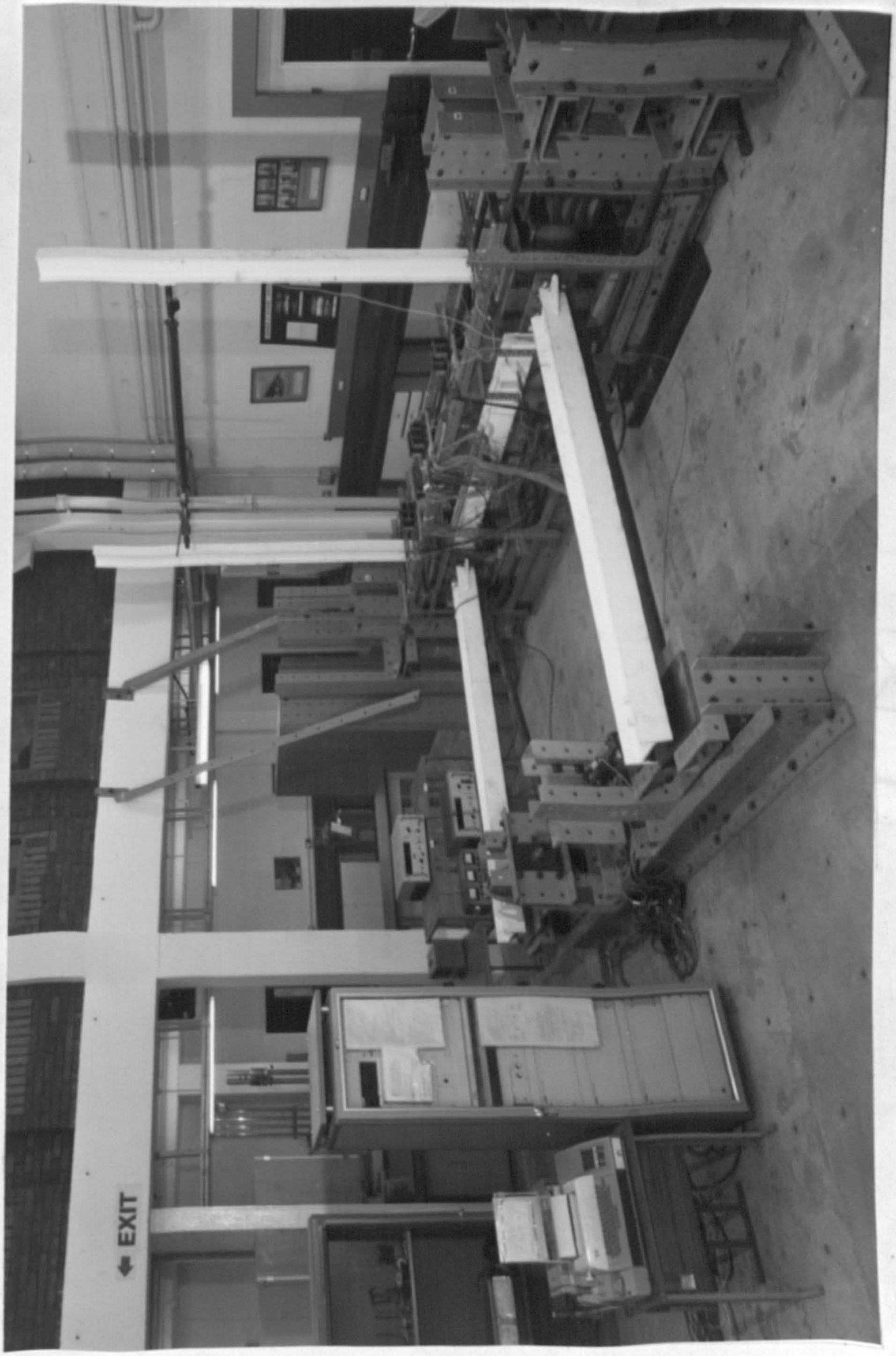

FIG. 4.2 GENERAL VIEW OF BIAXIAL COLUMN TESTING RIG

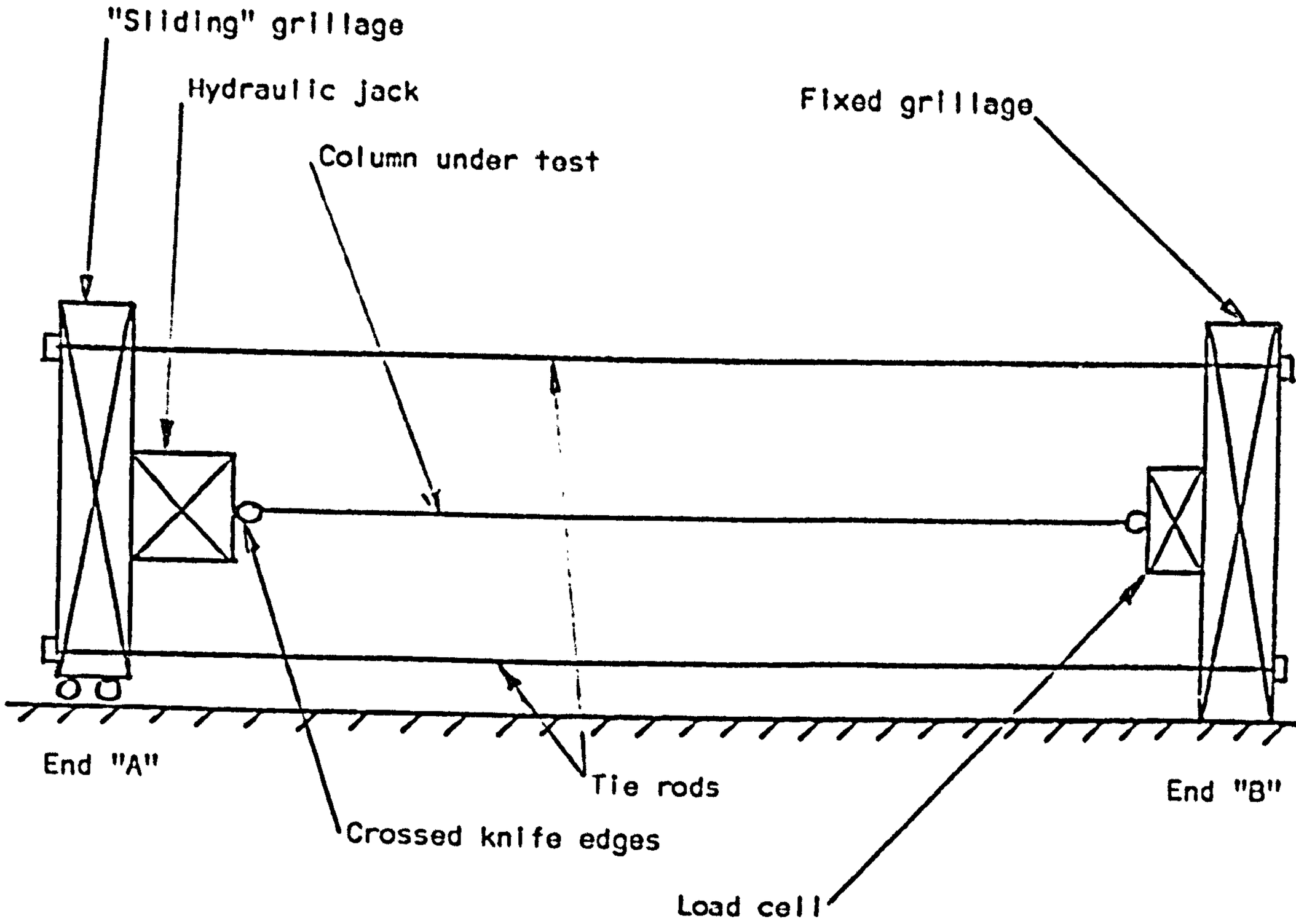

FIG. 4.3 SCHEMATIC REPRESENTATION OF TEST RIG.

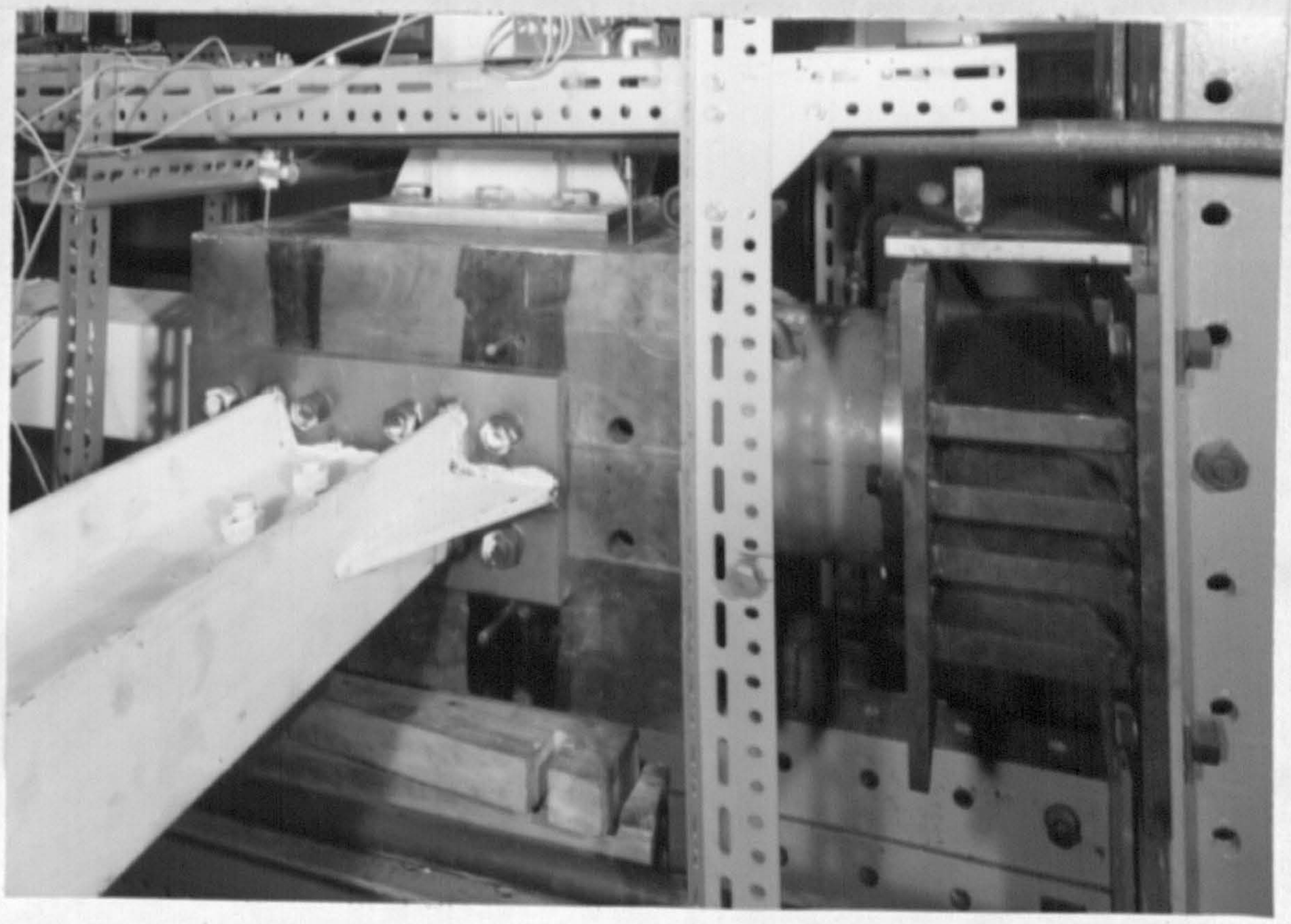

FIG. 4.4 LOADING SYSTEM - AXIAL LOADS

FIG. 4.5 CROSSED KNIFE EDGES

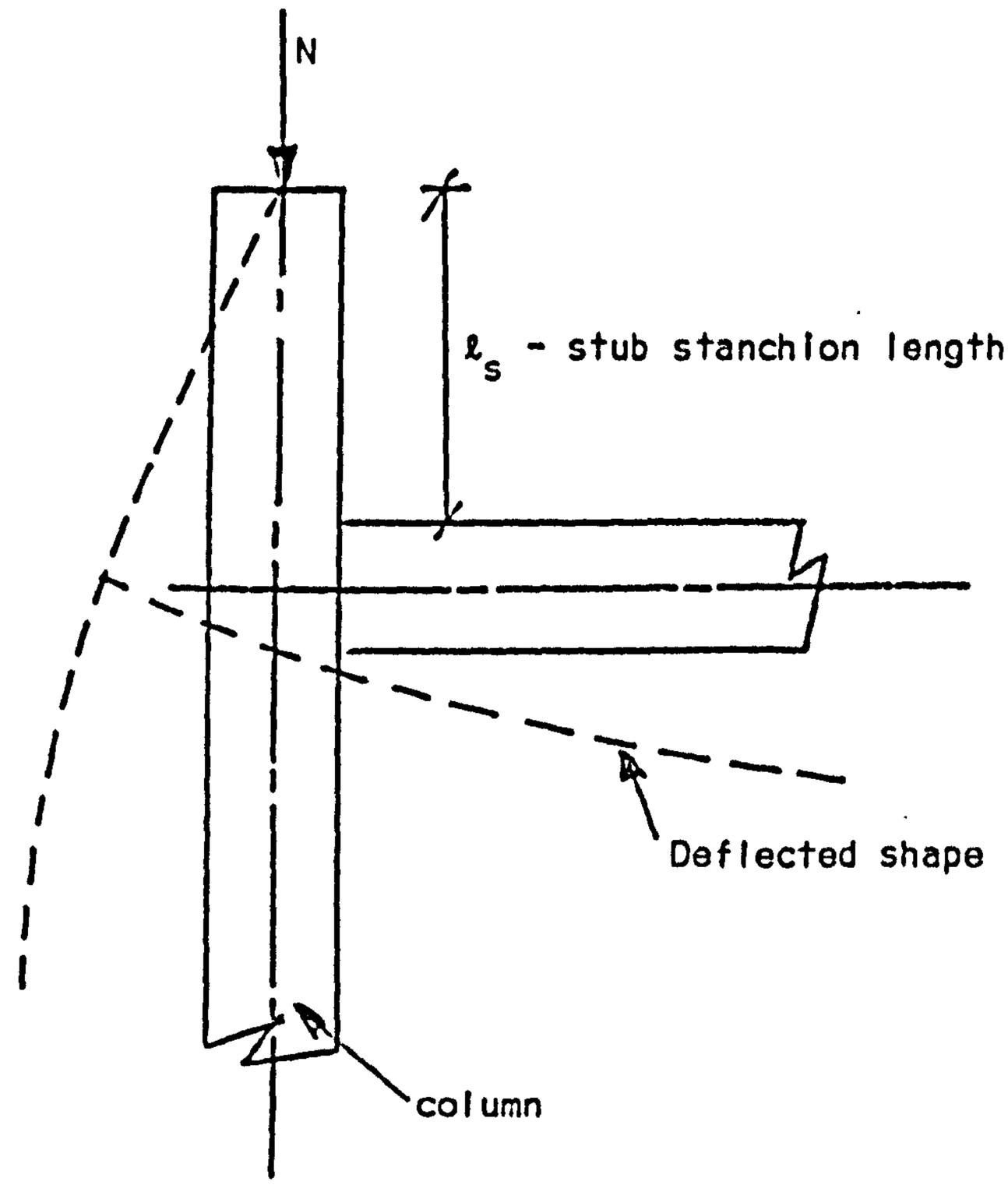

FIG. 4.6 THE "STUB STANCHION" EFFECT IN COLUMN TESTING

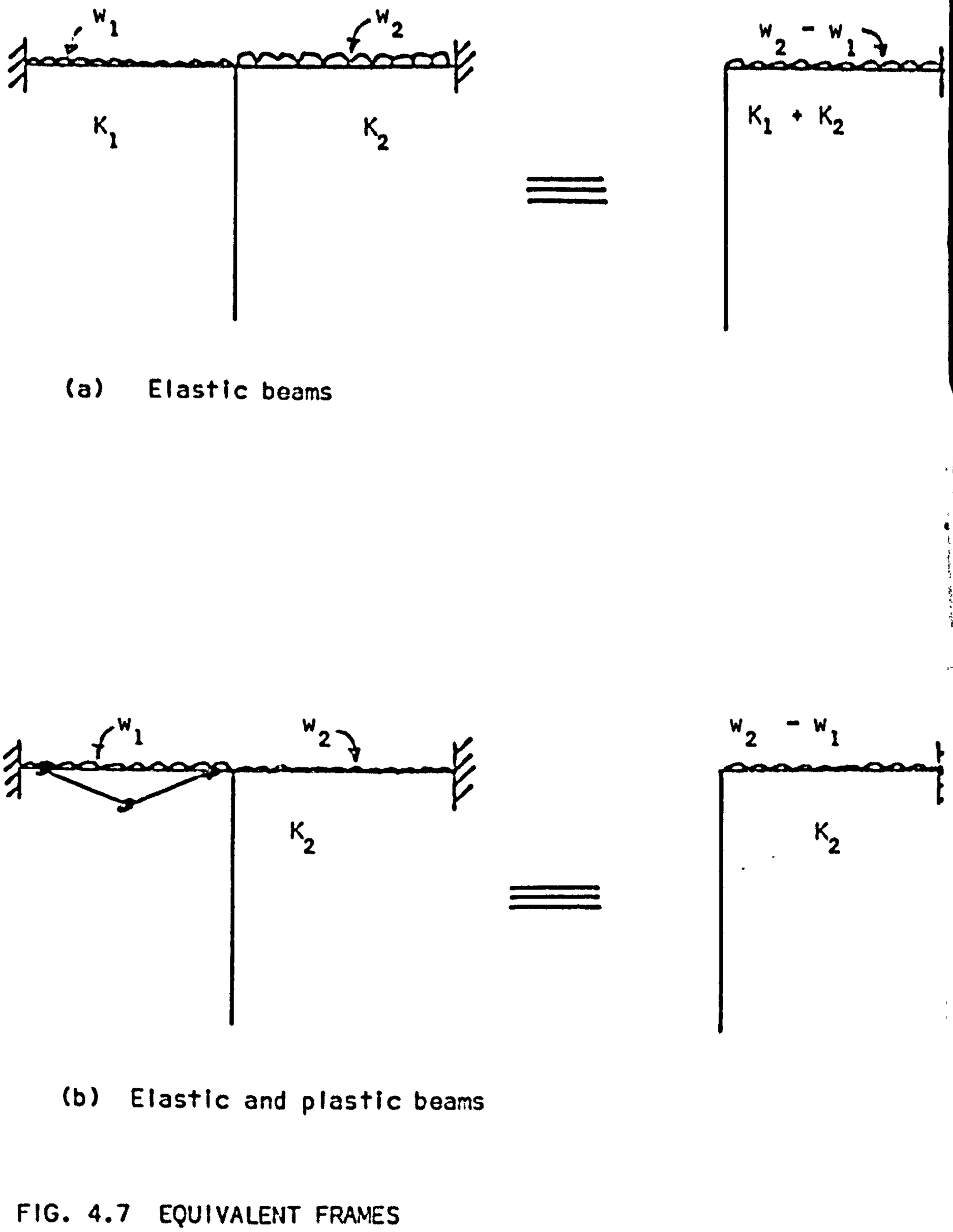

(a) Elastic beams

(b) Elastic and plastic beams

FIG. 4.7 EQUIVALENT FRAMES

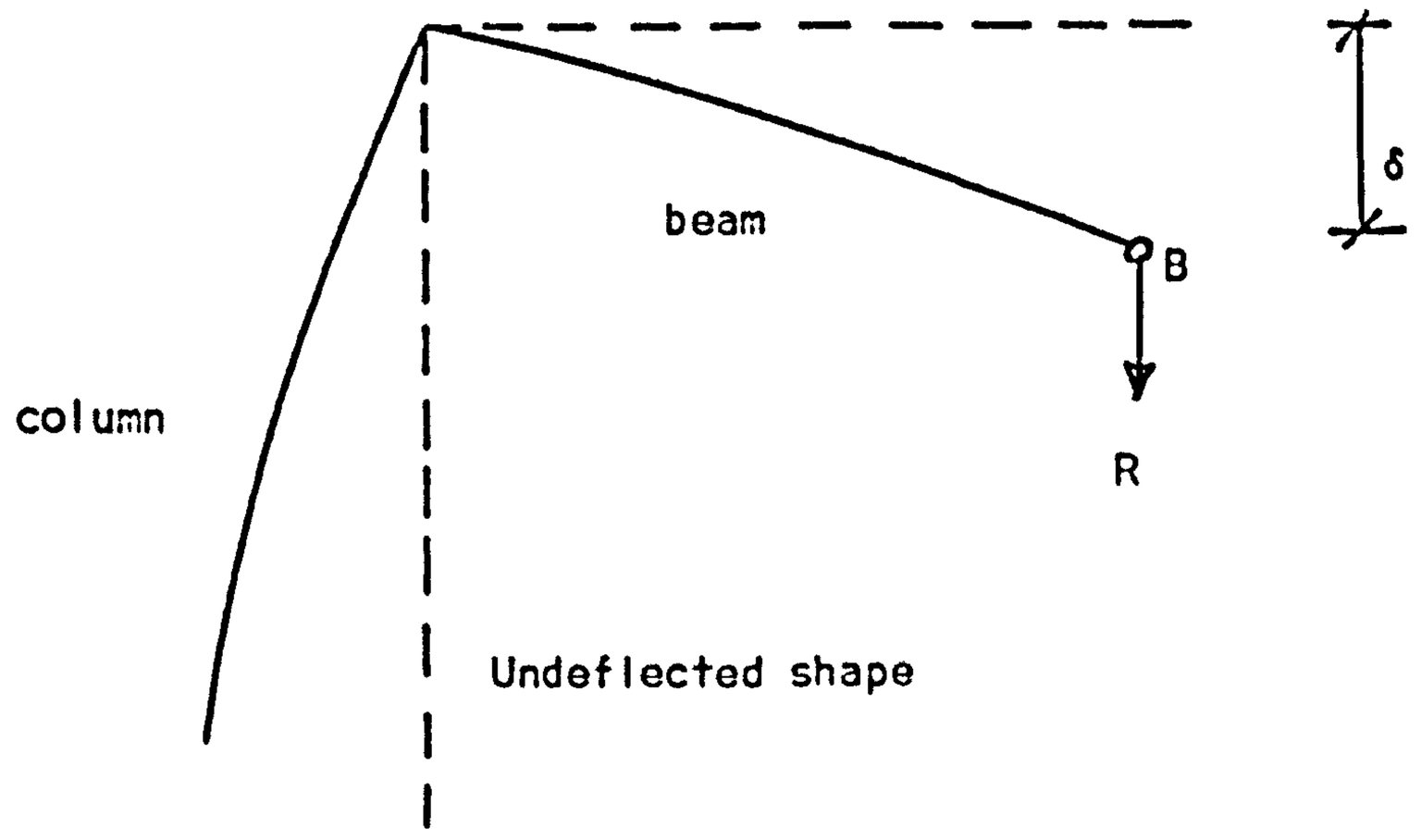

FIG. 4.8 APPLICATION OF BEAM LOADS

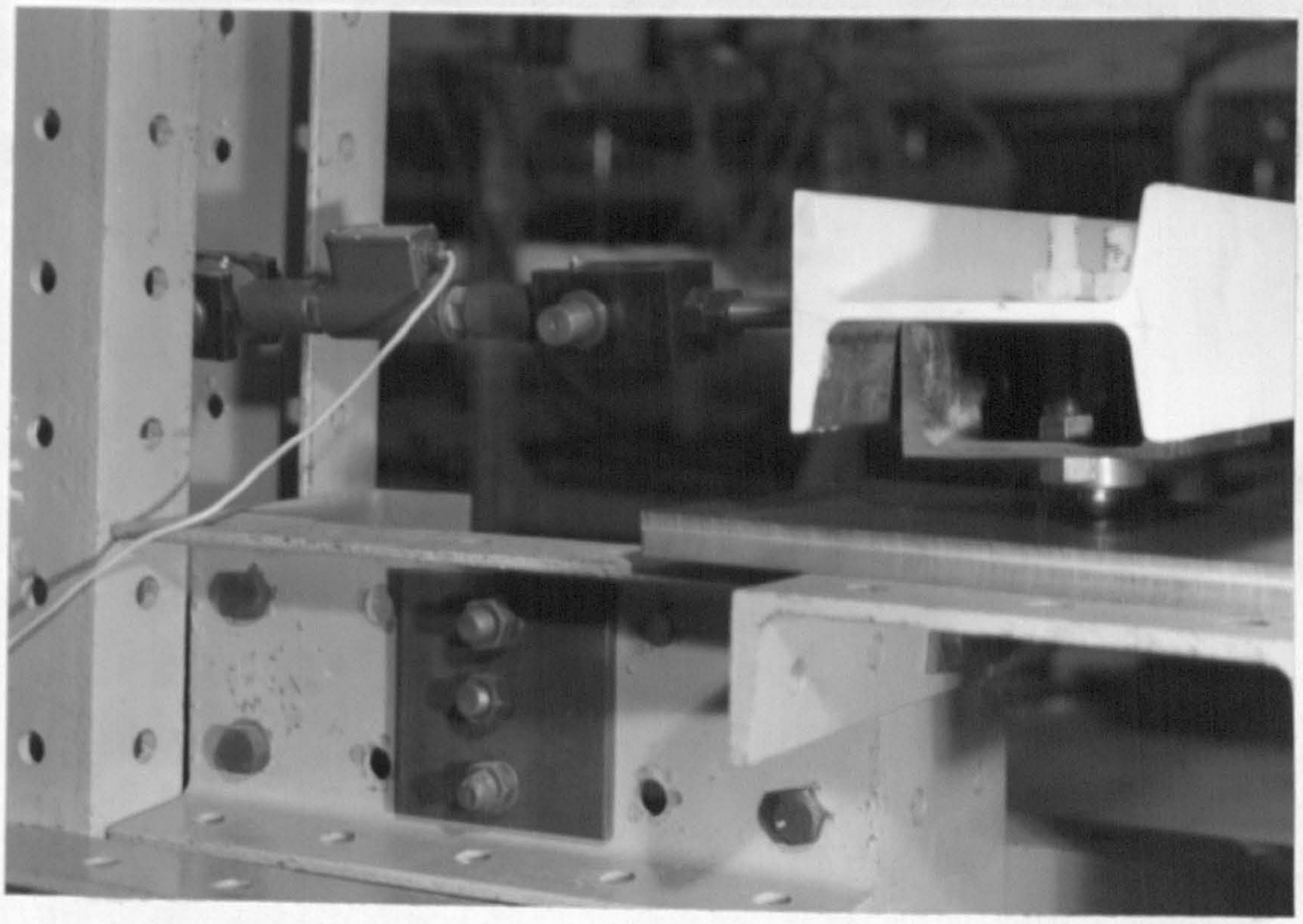

FIG. 4.9 DETAIL OF MAJOR AXIS LOADING SYSTEM

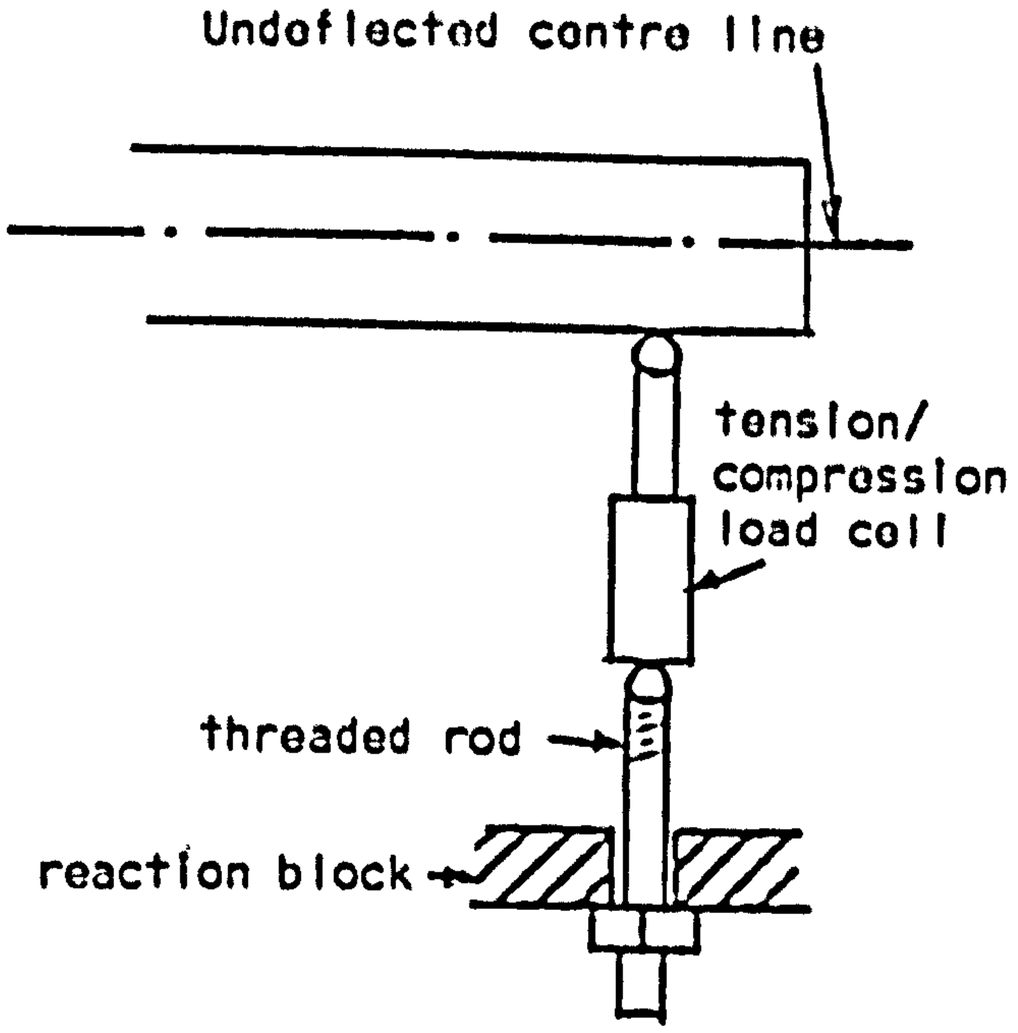

(a) System with zero deflection

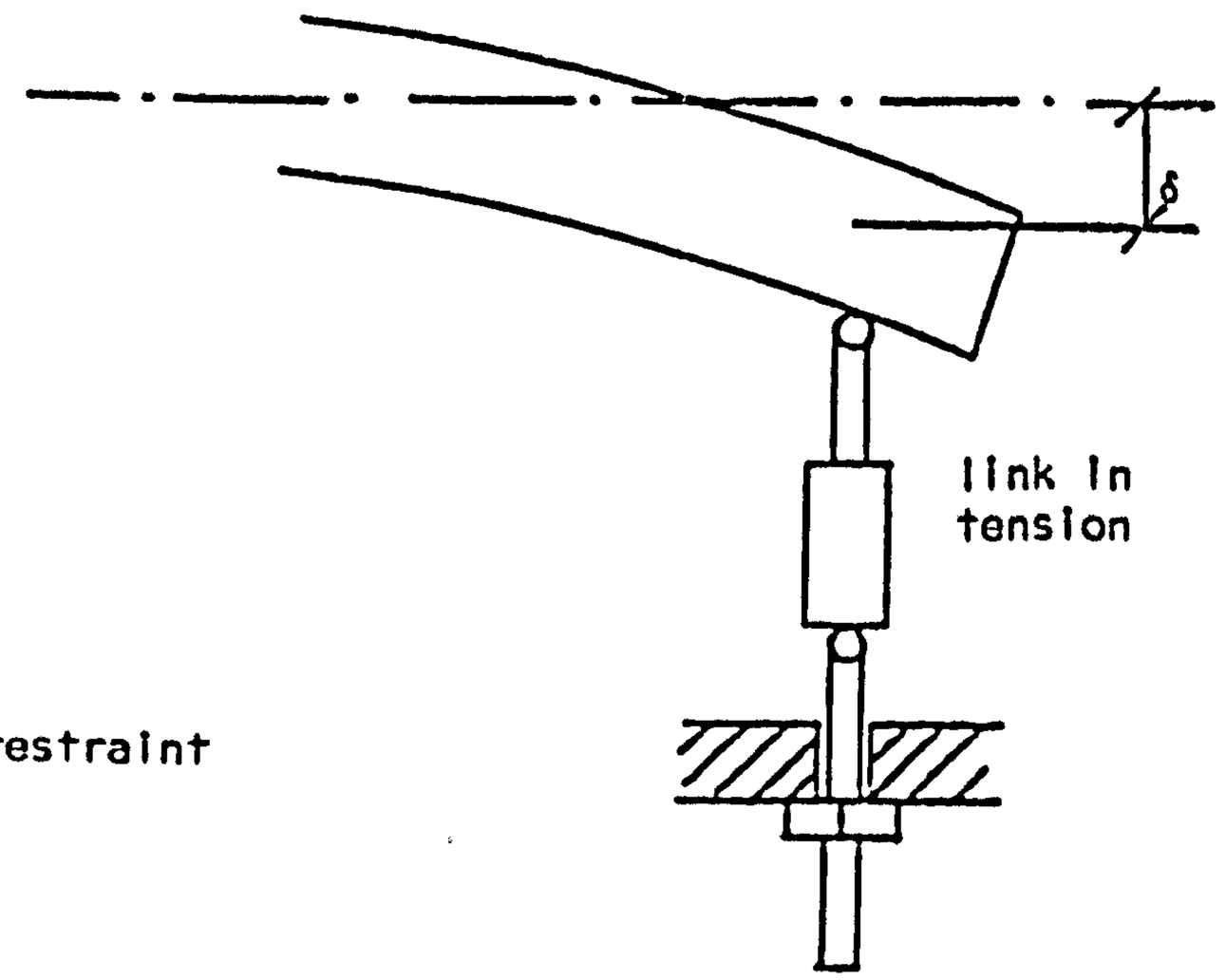

(b) Elastic-plastic restraint

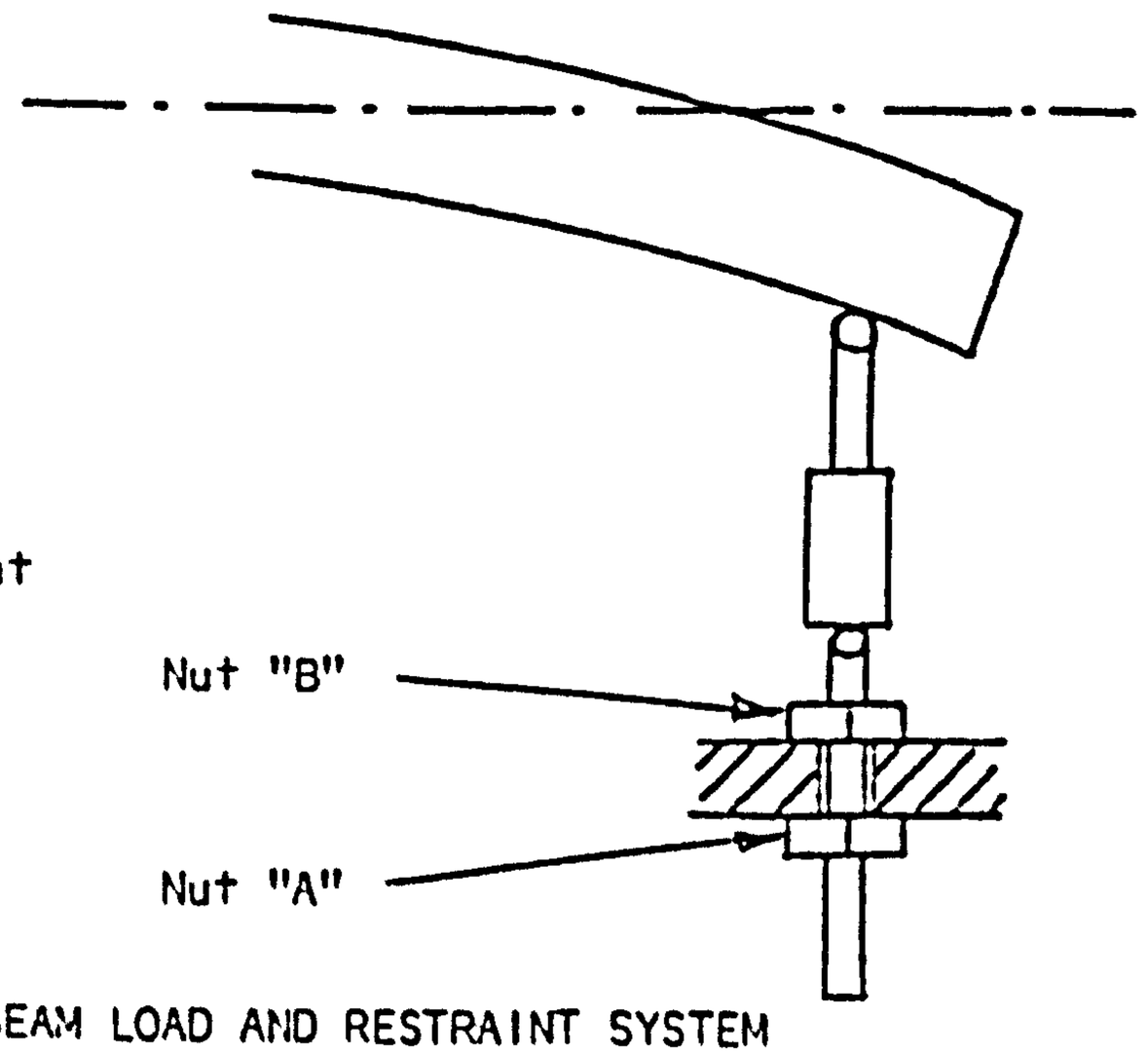

(c) Elastic restraint

FIG. 4.10 DETAILS OF BEAM LOAD AND RESTRAINT SYSTEM

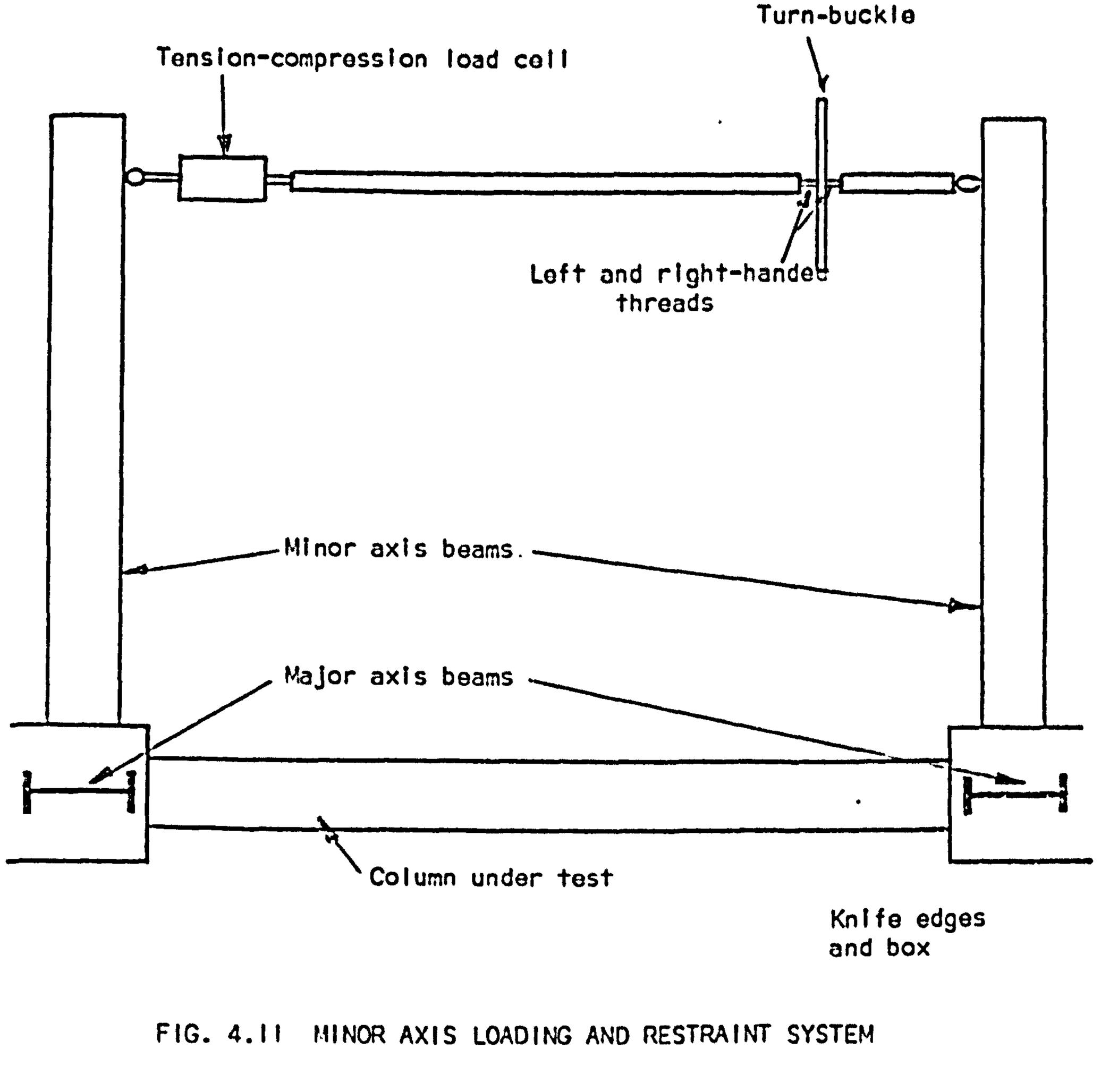

FIG. 4.11 MINOR AXIS LOADING AND RESTRAINT SYSTEM

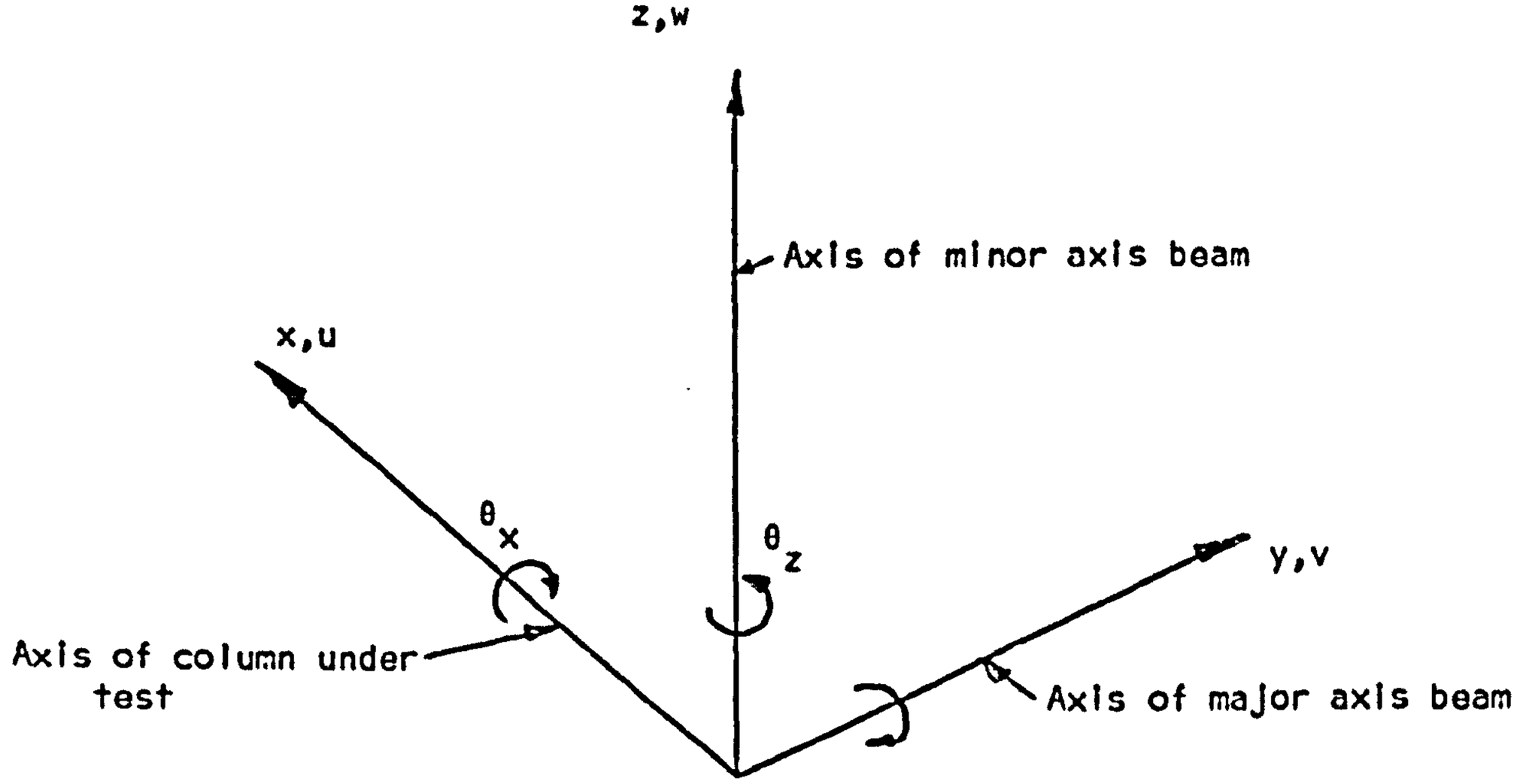

FIG. 4.12 CO-ORDINATE AXES USED TO DESCRIBE DEFORMATIONS.

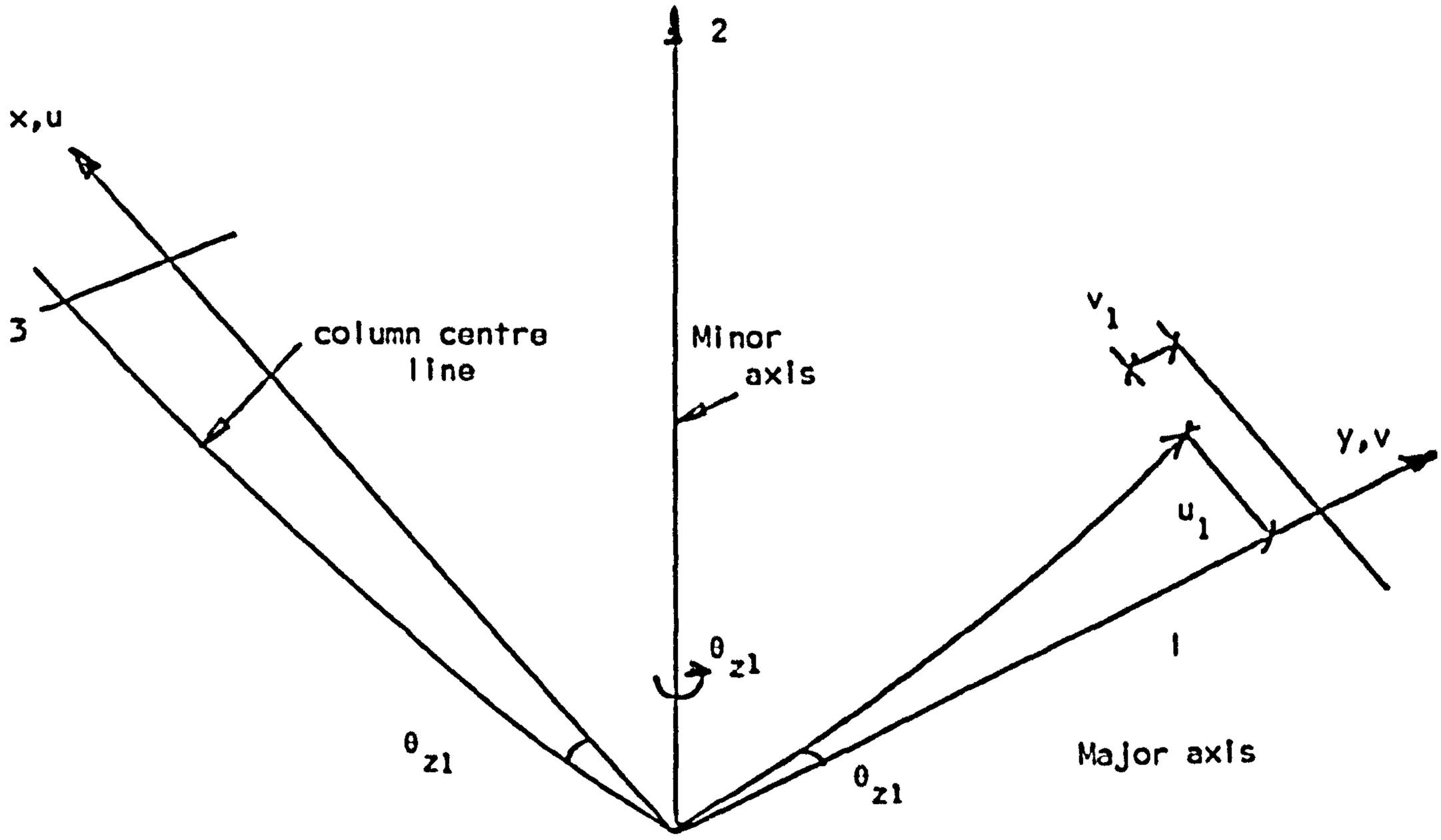

FIG. 4.13 APPLICATION OF DISPLACEMENT TO MAJOR AXIS

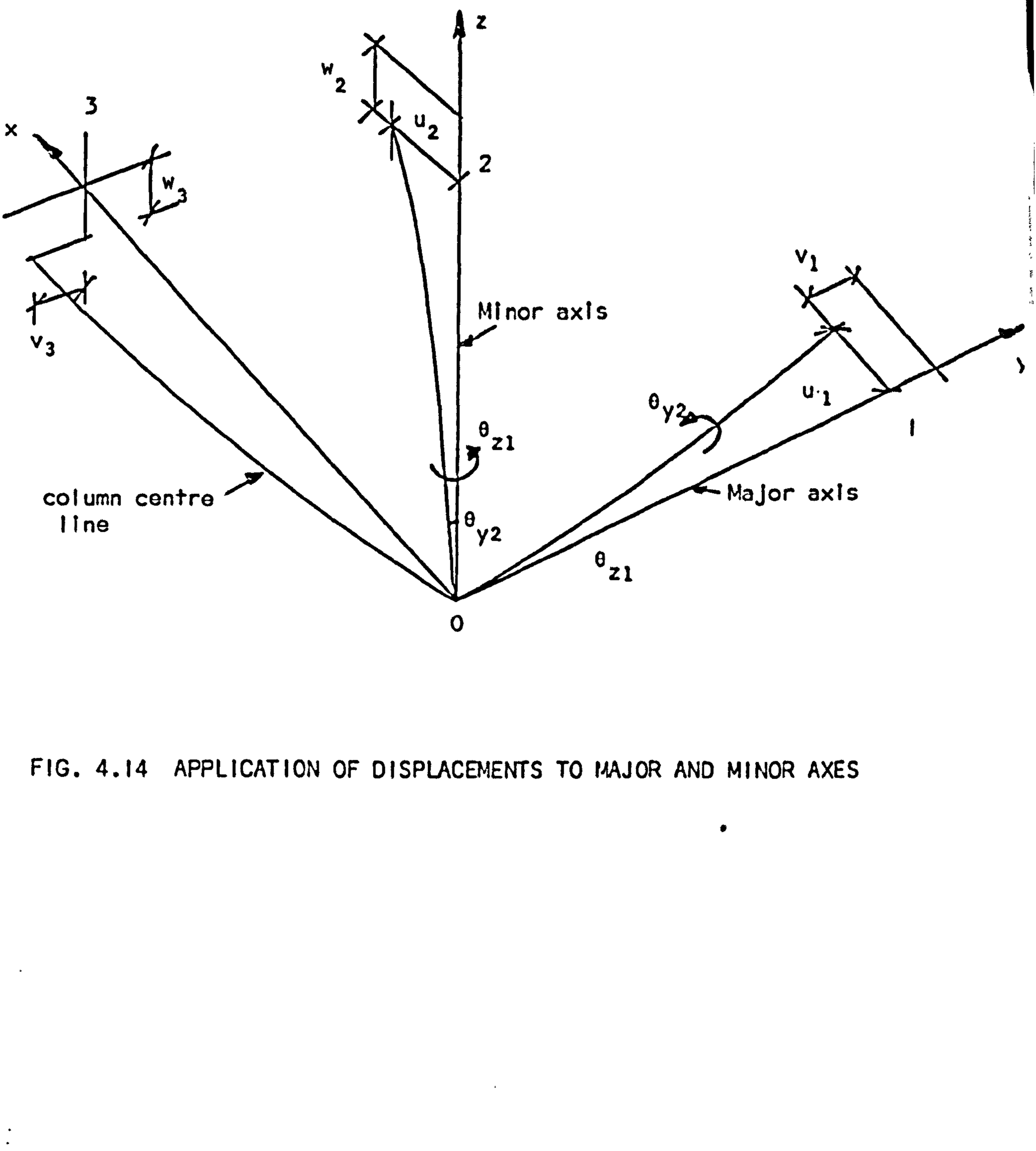

FIG. 4.14 APPLICATION OF DISPLACEMENTS TO MAJOR AND MINOR AXES

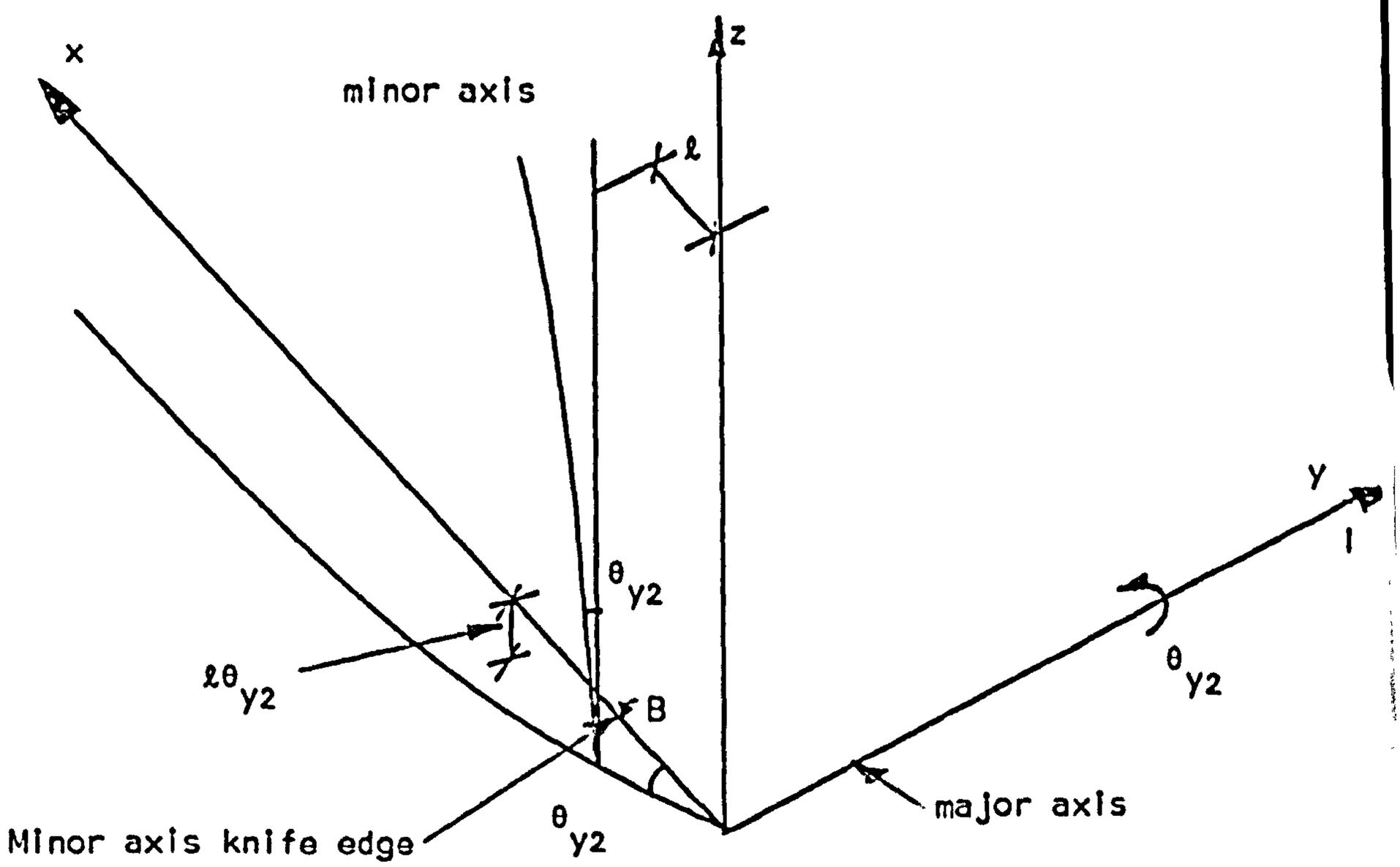

FIG. 4.15 GEOMETRY OF DEFORMATIONS WITH OFFSET MINOR AXIS

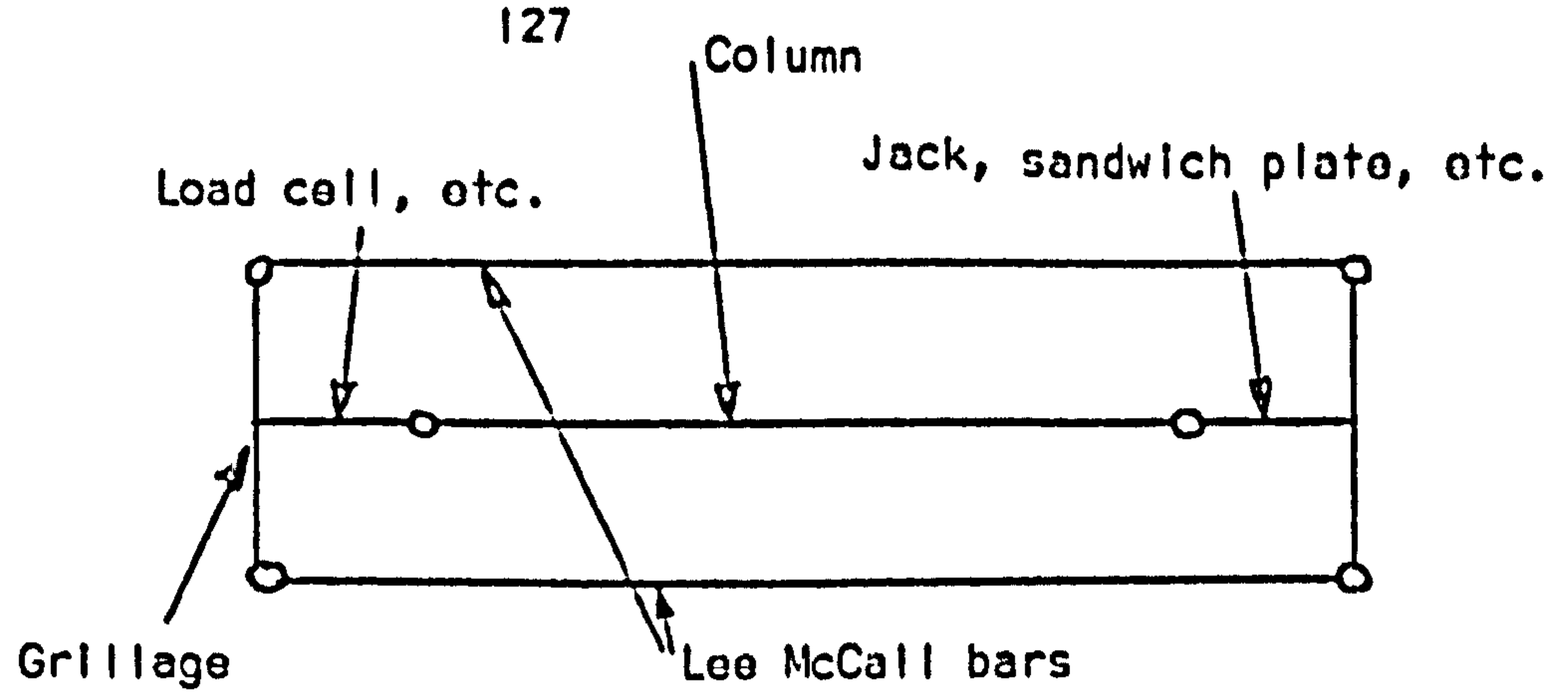

Plan of axial load system

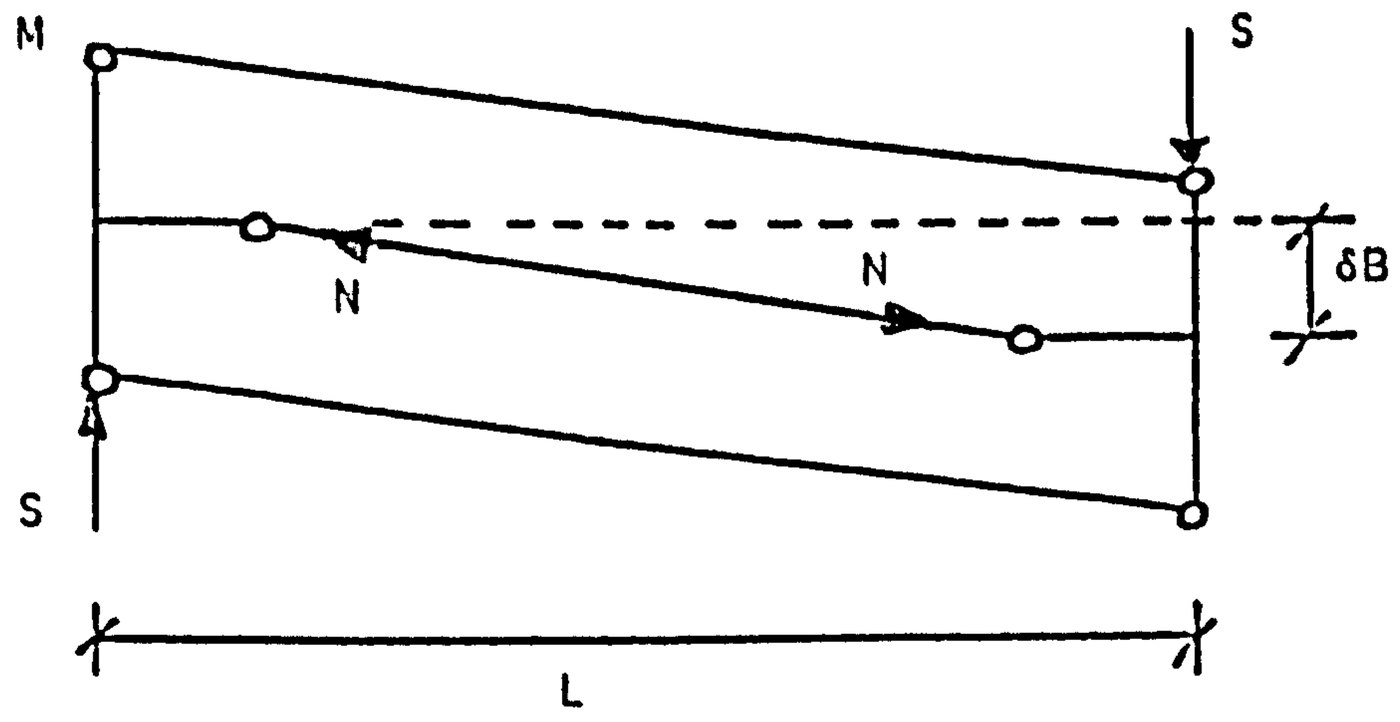

Forces on test rig due to small displacement

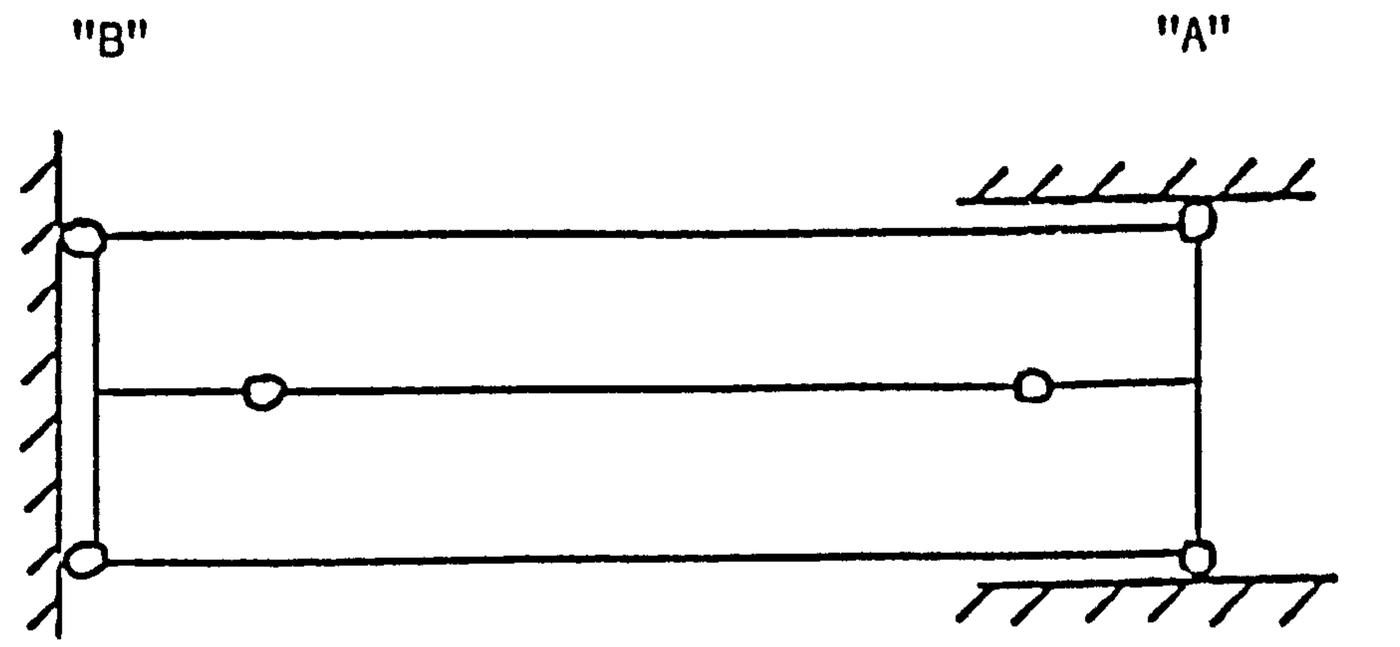

Plan of restraints provided to stabilise system

FIG. 4.16 STABILITY OF AXIAL LOAD SYSTEM.

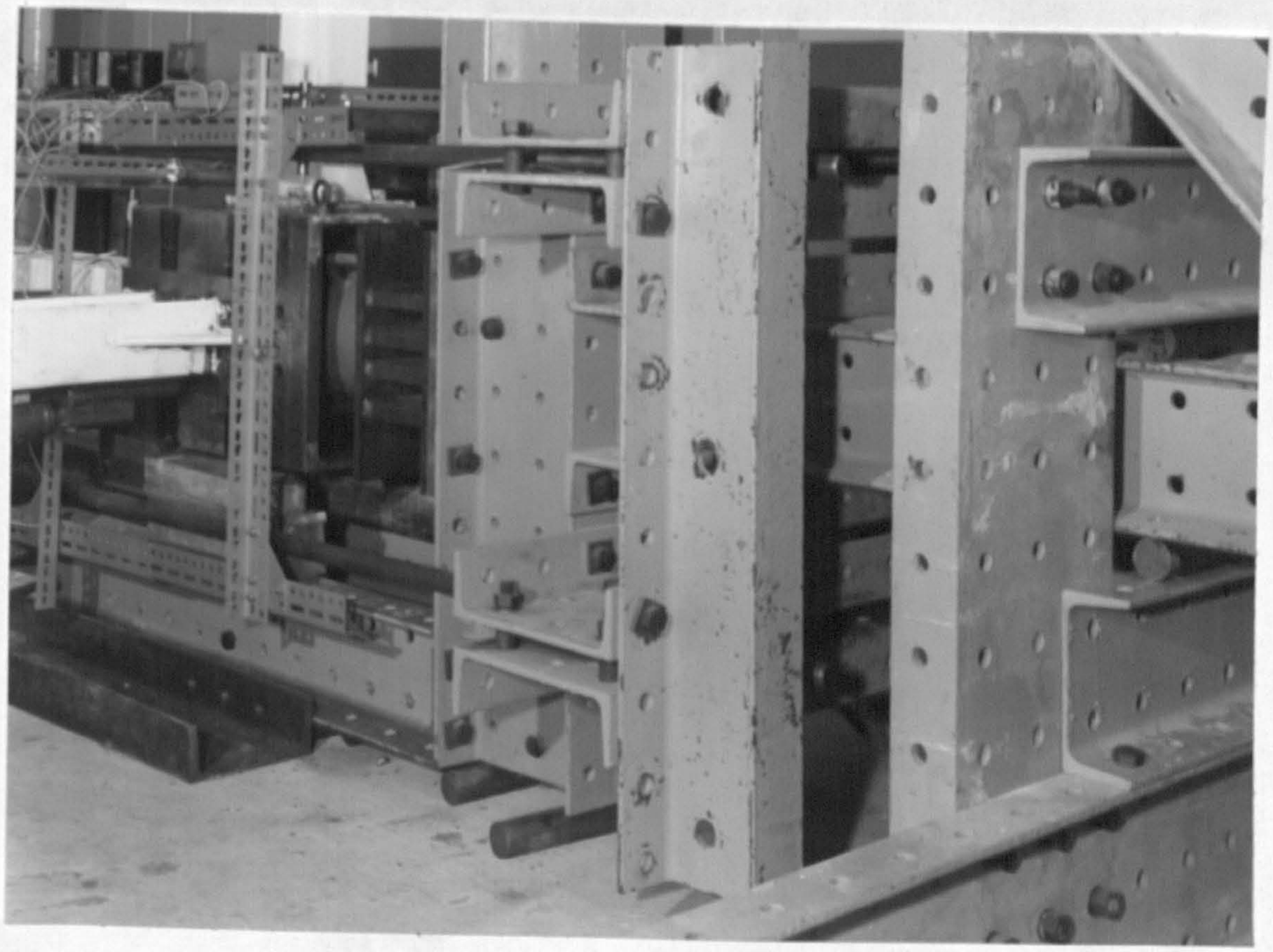

FIG. 4.17 DETAILS OF SLIDES AND ROLLERS

(a) Elevation

(b) Plan

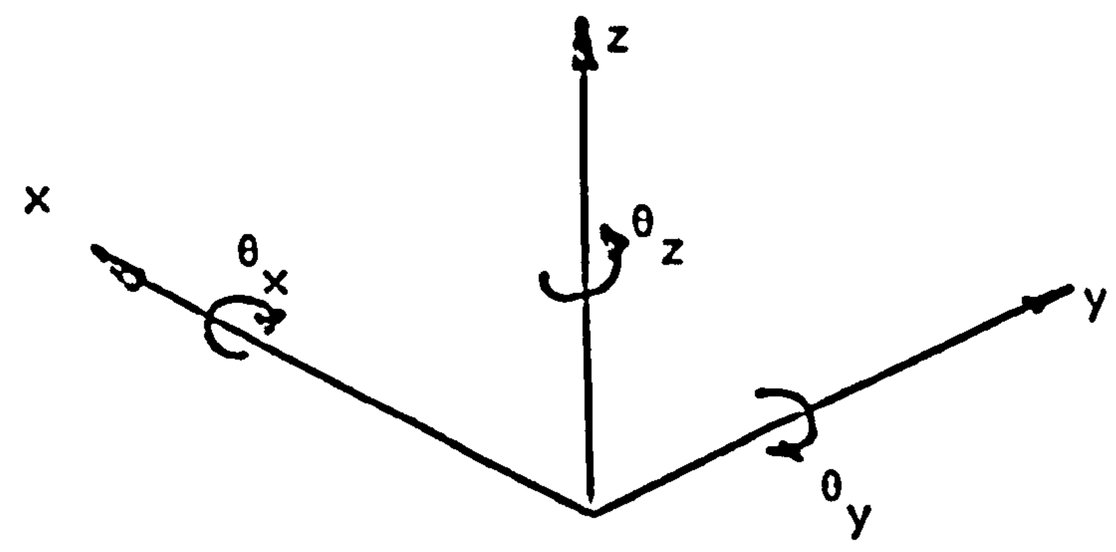

(c) Co-ordinate system

FIG. 4.18 DEGREES OF FREEDOM FOR INSTRUMENTATION RIG.

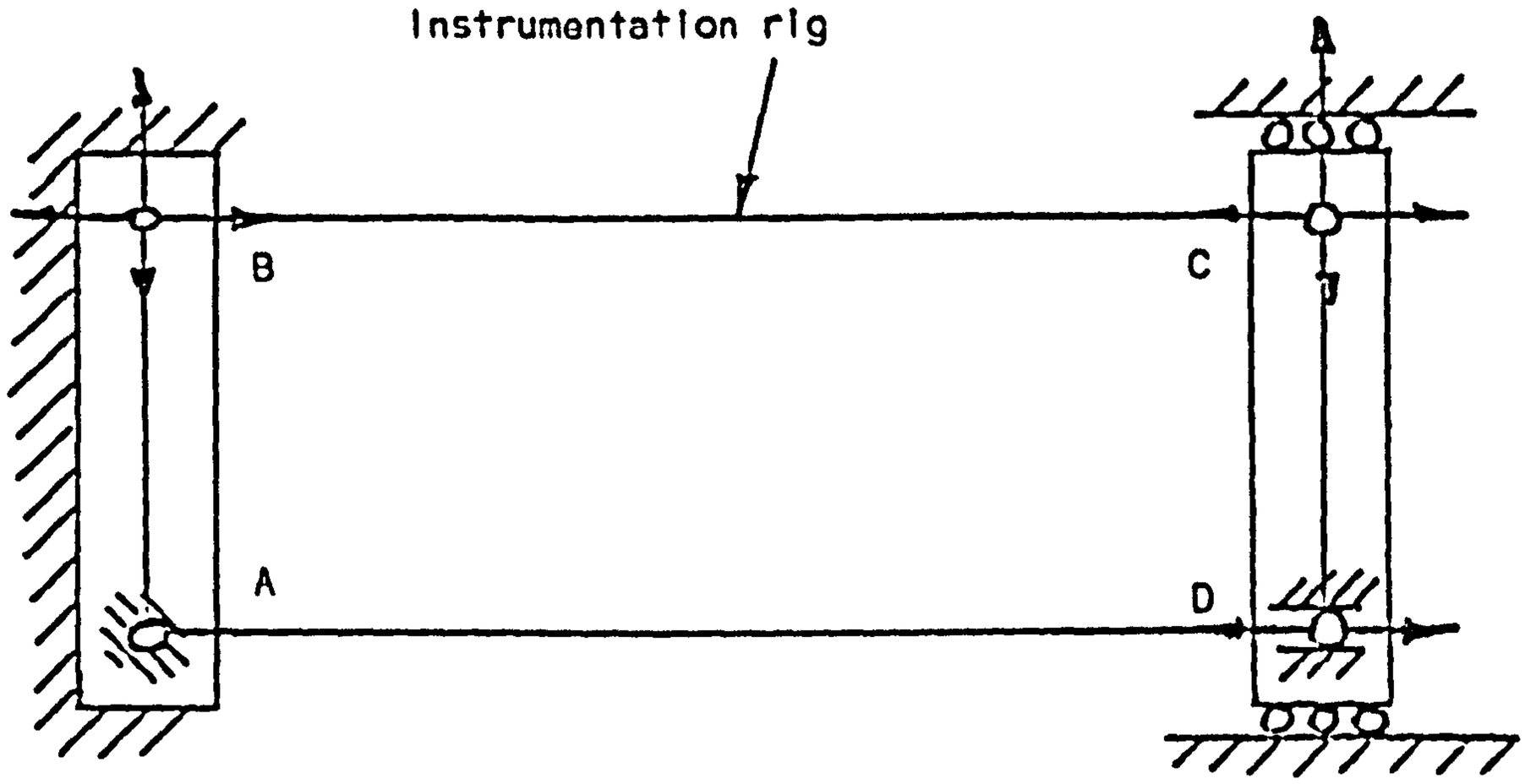

Bearings A, B, C and D are rotationally free

FIG. 4.19 PLAN OF INSTRUMENTATION RIG SHOWING DEGREES OF FREEDOM OF BEARINGS.

CHAPTER 5. CHOICE AND MANUFACTURE OF TEST COLUMNS.

5.1 Introduction

To enable the theoretical work to be checked and to assist in the development of design methods for composite columns a series of tests was carried out. This Chapter discusses the choice of tests, the instrumentation and manufacture of the specimens, and the auxiliary tests carried out. Chapter 6 gives a description of the behaviour of the columns under test, and Chapter 7 gives comparisons with the theoretical predictions.

5.2 Choice of test specimens.

5.2.1 Practical slenderness ratios.

In Chapter 1 Section 1.5.3 it was stated that a survey of reinforced concrete no-sway multi-storey frames showed that 90% of the columns within them had a slenderness ratio L/D of less than 10. Since composite columns generally have a larger steel to concrete ratio and hence a larger axial load capacity than reinforced concrete columns it is likely that for a given loading a composite column will tend to be slightly more slender, possibly 10% more.

Composite columns of slenderness greater than 25 are unlikely to occur in many buildings. The majority of the slender columns are used at ground-floor level in multi-storey buildings when a higher ceiling may be required. If the column height is 8 m and L/D equals 25 then the overall depth of the column will be 320 mm. The new BS.449 is likely to require[72] a minimum of 50 mm cover for fire-resistance and thus the steel section will be 220 mm which is a fairly light section.

Thus a slenderness of 25 is unlikely to be exceeded by many columns in buildings and in most cases is likely to be less than about 12. In the tests the range of slendernesses tested was 13-26. Stockier columns were not tested because instability effects are not likely to be very marked.

5.2.2 Specimens used.

There were three groups of tests:

(1) uniaxial tests on short columns (RC1, RC2, and RC3);

(2) uniaxial test on slender columns (RC4 and RC5); and

(3) biaxial tests (BC1, BC2 and BC3).

In group 1 the tests were carried out using stocky columns, 2.6 m long with $L/D = L/B = 13$, restrained and bent about the major axis but free to fail about the unrestrained minor axis. Test specimens RC1 and RC3 were both loaded in single curvature with $\beta = 1$ and end-moments M/M_p approximately 0.5, where M_p is the moment of resistance of the cross-section with zero axial load. In test RC1 a loss of stiffness due to the formation of cracks on the initial application of moments occurred. To assist in the evaluation of this effect in the test of specimen RC3 the end-moments were applied at a higher axial load level.

Column RC2 was tested in single curvature with $\beta = \frac{1}{2}$ and the maximum applied M/M_p approximately 0.7.

The two tests, RC4 and RC5, in group 2 were carried out on columns 5.3 m long with $L/D = L/B = 26$. Both tests were carried out with columns restrained and loaded about one axis but free to

fail about either axis. In test RC4 the restraint was about the columns major axis and in test RC5 it was about the minor axis of the column.

The columns in group 3, BC1, BC2 and BC3 were all tested with loading and restraint about both axes. All three columns had slenderness ratios of $L/D = 19$ and $L/B = 13$.

The columns were all loaded with similar major axis applied moments, of about $0.5\ M_p$.

Tests on columns BC1 and BC3 had similar loading about the minor axis, $0.5\ M/M_p$, for three reasons:-

(1) In test BC1 an instability failure of the link used to apply the minor axis moments, Fig. 4.2, had occurred at the failure load of the column. The link had been modified but some doubt remained about the result of the test.

(2) Two similar test were required to check if repeatable results could be obtained.

(3) Test BC1 had displayed extensive spalling of the concrete along the corner in maximum compression over the middle half of the column at loads of 70% of the failure load.

Column BC3 had similar major axis moments as columns BC1 and BC3 but had a smaller minor axis moment, $0.35\ M/M_p$.

5.3 Manufacture of specimens.

Columns RC1 to RC5 were manufactured from $152 \times 152 \times 23$ kg/m universal column sections of Grade 43 steel, in BC1, BC2, and BC3

152 × 89 × 17.1 kg/m rolled steel joists of Grade 43 steel were used. The steel sections were wire brushed to remove loose rust and scale and steel plates were welded to each end. Links of 4 mm. diameter mild steel were placed at 150 mm. centres 6 mm diameter high yield steel was used for the longitudinal bars in the RC tests and 4 mm diameter mild steel in the BC tests. Medium strength concrete was used for the casing. Cross-sections are shown in Fig. 5.1.

Details of the concrete mixes used are given in Table 5.1. The aggregate used had a maximum size of 10 mm and the mixes had medium workability. To keep the cube strength down, for tests RC1, RC2, and RC3, whilst giving a practical proportion of cement size particles, 25% of the cement was replaced by pulverised fuel ash (P.F.A.)

The concrete was mixed in batches of up to 80 kg and two 100 mm cubes were taken from each batch.

The columns were cast horizontally in plywood formwork mounted on a 305 × 89 channel strongback. A section is shown in Fig. 5.2.

To assist the placing of concrete and to avoid the trapping of air and free water beneath the flanges, the channel was placed on a series of rockers. These enabled the whole system to be rotated through 20^{o} during casting and vibration.

The moulds were placed on two vibrating tables during concreting and Kango hammers with rubber heads were used against the sides of the formwork.

The concrete was cured for 7 days beneath damp hessian, and the cubes, after demoulding, were stored under water until they were tested.

5.3.1 Instrumentation of specimens.

The location of strain gauges fixed to each flange and on the concrete cover is shown in Fig. 5.3. On both the steel section and concrete surfaces 120 ohm temperature compensated electrical resistance gauges were used. On the steel 10 mm long gauges were used, and were protected from the ingress of moisture during concreting with rubber coatings. On the concrete 60 mm long gauges were used.

5.4 Auxiliary tests.

5.4.1 Calibrations

All load cells were calibrated before and after testing. The transducers were calibrated before testing.

5.4.2 Materials tests.

Tension tests to BS18[73] were carried out on coupons cut from the Universal Column and Rolled Steel Joist sections. A cross-head speed of 0.5 mm/min. was used. Stress-strain curves were obtained using an autographic tensometer and XY plotter.

Two cross-sections were taken from the universal column sections designated A and B, Table 5.2. Similarly from the rolled steel joist sections two cross-sections C and D were taken. Typical

positions of coupons are shown in Figure 5.4 and results in Table 5.2.

The results of the compression tests on the concrete cubes, which were carried out at the same time as the main test, are given in Table 5.3.

5.4.3 Cross section dimensions

The cross-sectional area of each sample of the universal column and the rolled steel joist was found by weighing a known length and assuming a density for steel of 7840 kg/m^3. The dimensions of the cross-section were also checked at various positions as shown in Fig. 5.5. The average values for web and flange thickness, oversall dimensions and area are recorded in Table 5.4.

5.4.4 Residual stresses

Residual stresses in the universal column section were measured, full details can be found in Reference 74.Typical stresses from the rolling of universal column used are shown in Fig. 5.6.

5.4.5 Initial deflections

Initial deflections of the steel section relative to a straight line from end to end were recorded and are given in Table 5.5.

	RC1, RC2 & RC3	RC5 & RC6	BC1 & BC2	BC3
Ordinary Portland Cement	0.75	1.0	1.0	1.0
Pulverised fuel ash	0.25	0	0	0
⅜" Aggregate	2.08	1.30	1.43	1.43
Sand	3.14	2.55	2.76	2.76
Water	0.67	0.57	0.67	0.65

Proportions per batch

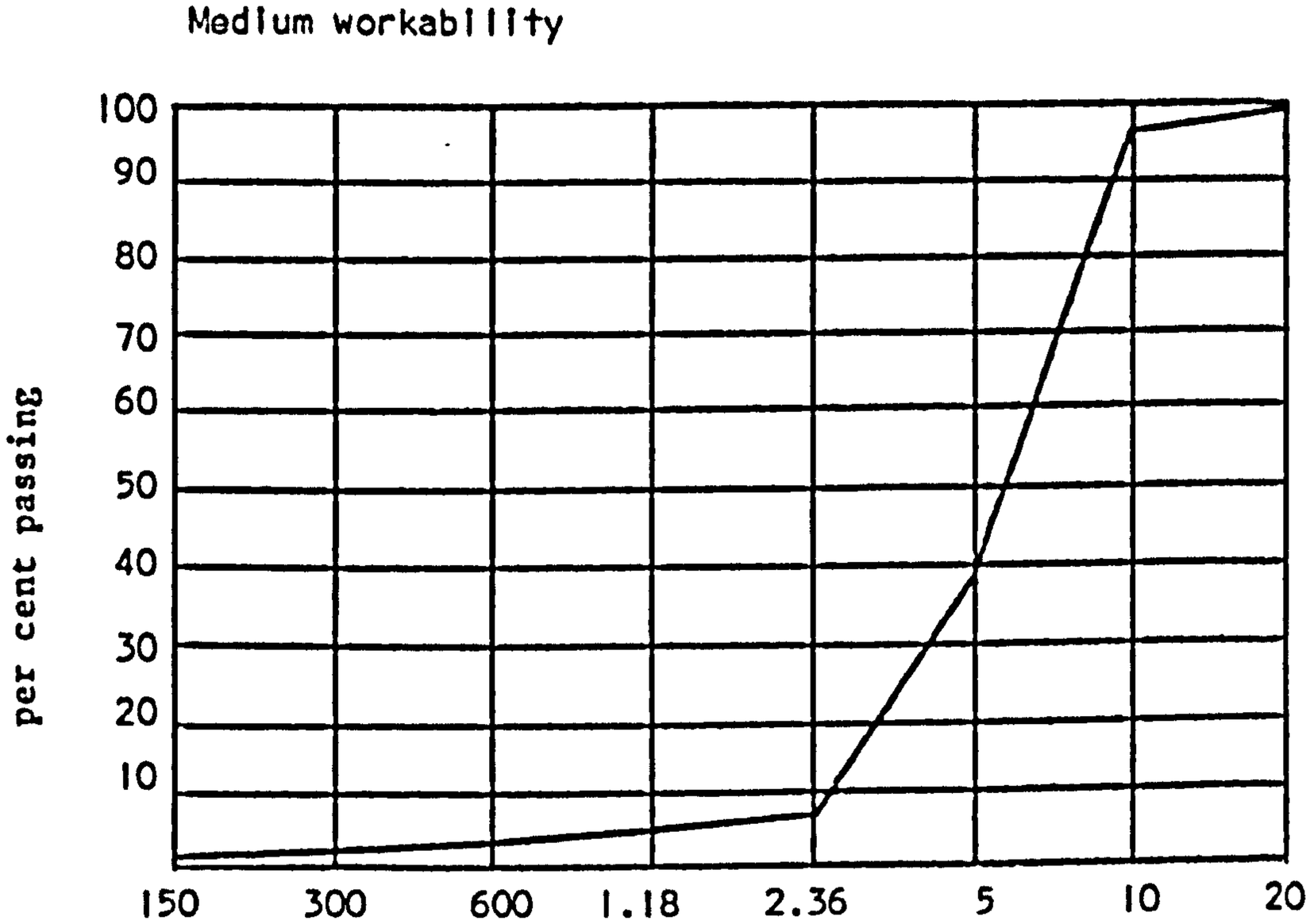

Grading curve for sand

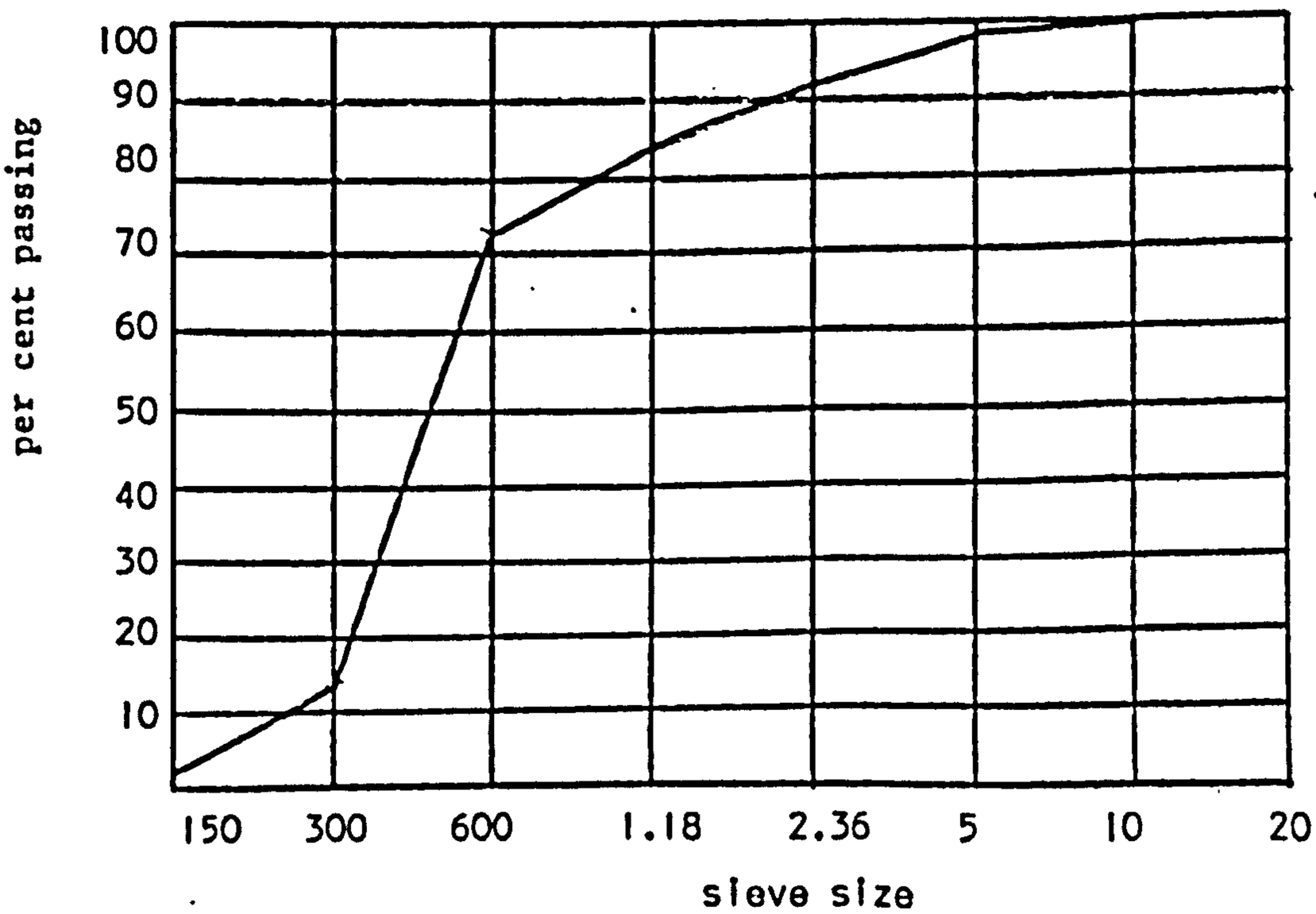

Grading curve for ⅜" aggregate

TABLE 5.1 MIX DETAILS

Section Details	Coupon No.	σ_y N/mm^2
152 x 152 UC23	F1	287
	F2	288
	F3	296
'A'	F4	293
	W1	286
	W2	288
	W3	302
Av. 291 N/mm^2		
'B'	F1	280
	F2	283
	F3	282
	F4	290
	W1	282
	W2	298
	W3	283
Av. 286 N/mm^2		
Average value of σ_y for "A" & "B"		288 N/mm^2
'C'	W1	273
	W2	289
	W3	281
	F1	282
	F2	274
	F4	261
Av. 277 N/mm^2		
'D'	W1	277
	W2	276
	W3	277
	F1	265
	F=	283
	F3	277
	F4	286
Av. 237 N/mm^2		
Average value of σ_y for "C" and "D"		277 N/mm^2

TABLE 5.2 RESULTS FROM TENSILE TESTS ON COUPONS

COLUMN NO.	CUBE STRENGTH N/mm²				
	BATCH NO.				AVERAGE
	1	2	3	4	
RC1	43.5	32.8	37.2	-	36.5
	-	32.0	37.1	-	
RC2	33.0	27.8	27.9	-	30.3
	35.1	28.8	29.5	-	
RC3	30.0	24.2	34.0	-	29.4
	30.5	25.6	32.2	-	
RC4	41.4	45.0	44.8	41.4	43.2
	39.1	45.6	44.1	44.4	
RC5	37.0	39.1	34.7	33.7	36.4
	36.7	37.2	37.6	35.0	
BC1	30.7	28.6	-	-	29.2
	29.2	28.5	-	-	
BC2	26.8	30.0	-	-	27.9
	27.8	26.9	-	-	
BC3	32.9	28.5	-	-	30.4
	-	29.7	-	-	

TABLE 5.3 RESULTS OF CONCRETE CUBE TESTS

LOCATION	DIMENSION				
	CS1	CS2	CS3	RSJ1	RSJ2
Flange (mm)	6.8	6.7	6.7	9.02	9.01
Web (mm)	6.4	6.2	6.2	5.48	5.54
W_1 (mm)	152	151.5	151.5	88	88
W_2 (mm)	152.5	152	152	88	88
D (mm)	150	154	154	154.5	154.5
Area (cm^2)	29.0	29.2	29.0	23.2	23.3

Dimensions used in analysis

	UC	RSJ
flange thickness	6.7 mm	9.0 mm
web thickness	6.1 mm	5.5 mm
overall depth (D)	152 mm	154.5 mm
overall width (W)	154 mm	88 mm

TABLE 5.4 CROSS-SECTION MEASUREMENTS

COLUMN NO.	AXIS	LOCATION		
		1	2	3
RC1	Major	0	+ 1.0 mm	+ 0.5 mm
	Minor	0	+ 1.5 mm	+ 1.5 mm
RC2	Major	0	+ 0.5 mm	+ 0.5 mm
	Minor	+1.5 mm	+ 1.5 mm	0
RC3	Major	0	- 0.5 mm	0
	Minor	+1.0 mm	+ 1.0 mm	+ 0.5 mm
RC4	Major	+ 1 mm	+ 1.5 mm	+ 1 mm
	Minor	- 1 mm	- 1 mm	+ 2 mm
RC5	Major	+ 1.0 mm	+ 1.5 mm	+ 1.0 mm
	Minor	+ 1.5 mm	+ 2.5 mm	+ 2.0 mm
BC1	Major	+ 0.1 mm	+ 0.2 mm	+ 0.1 mm
	Minor	+ 0.1 mm	0	0
BC2	Major	+ 0.1 mm	+ 0.1 mm	+ 0.1 mm
	Minor	+ 0.1 mm	+ 0.1 mm	0
BC3	Major	+ 0.3 mm	+ 0.5 mm	+ 0.4 mm
	Minor	+ 0.2 mm	+ 0.2 mm	+ 0.2 mm

Table 5.5 cont...

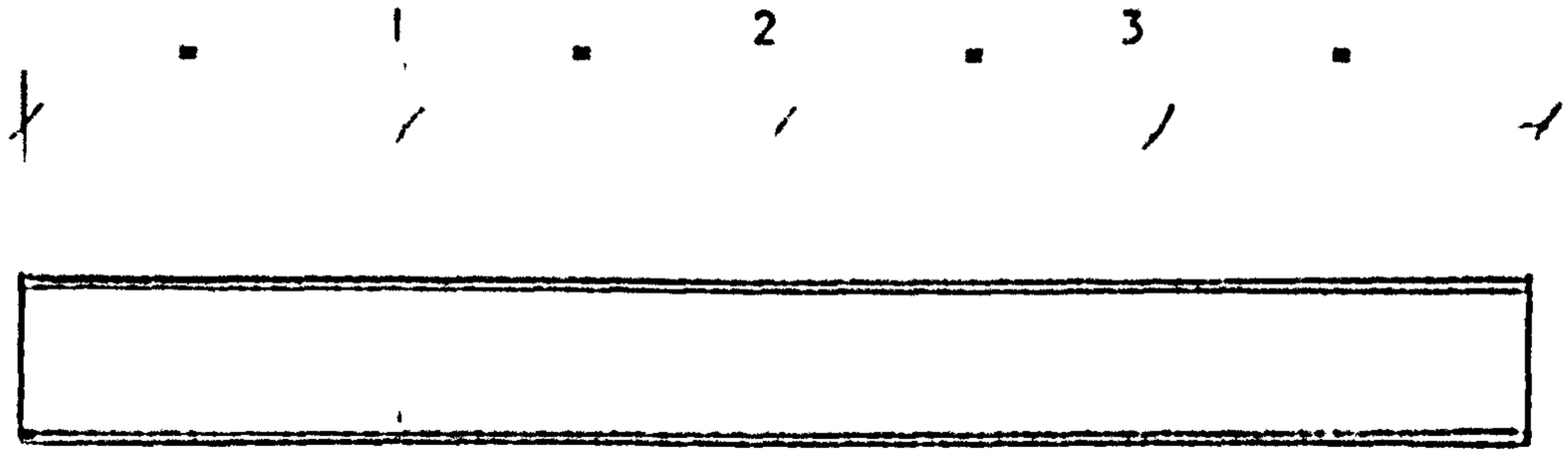

Locations

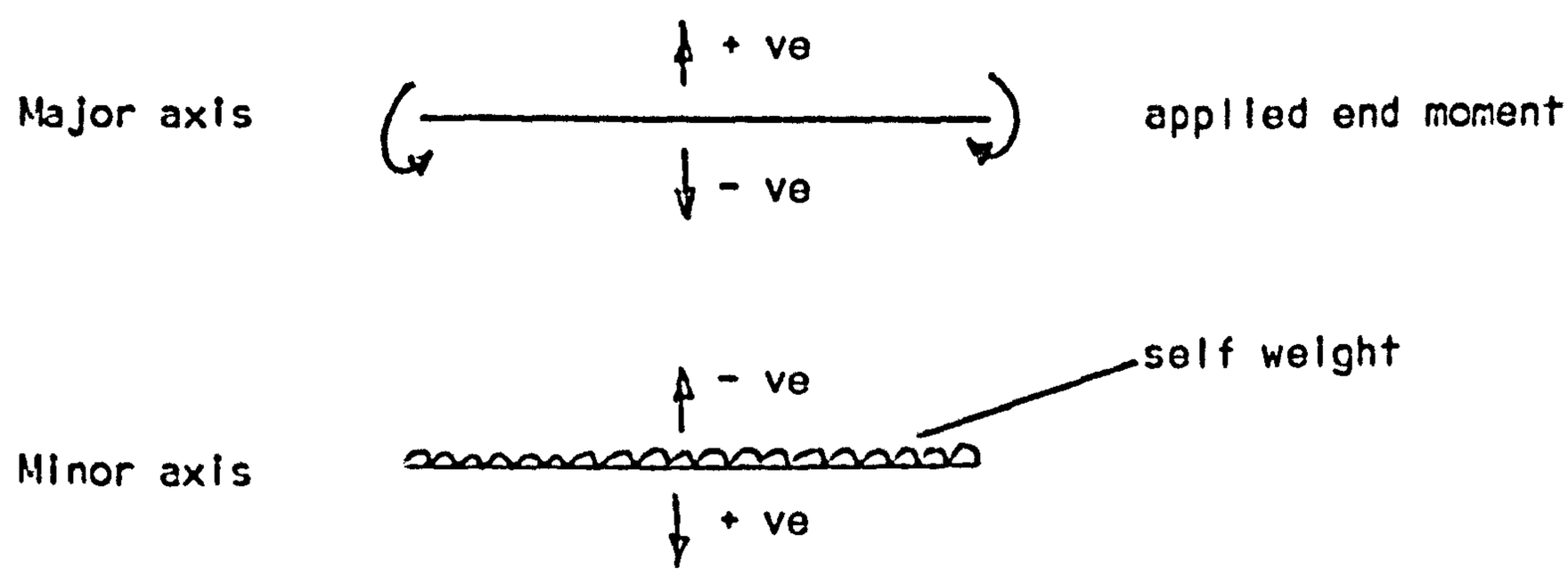

Signs of deflections

TABLE 5.5 VALUES OF INITIAL DEFLECTIONS

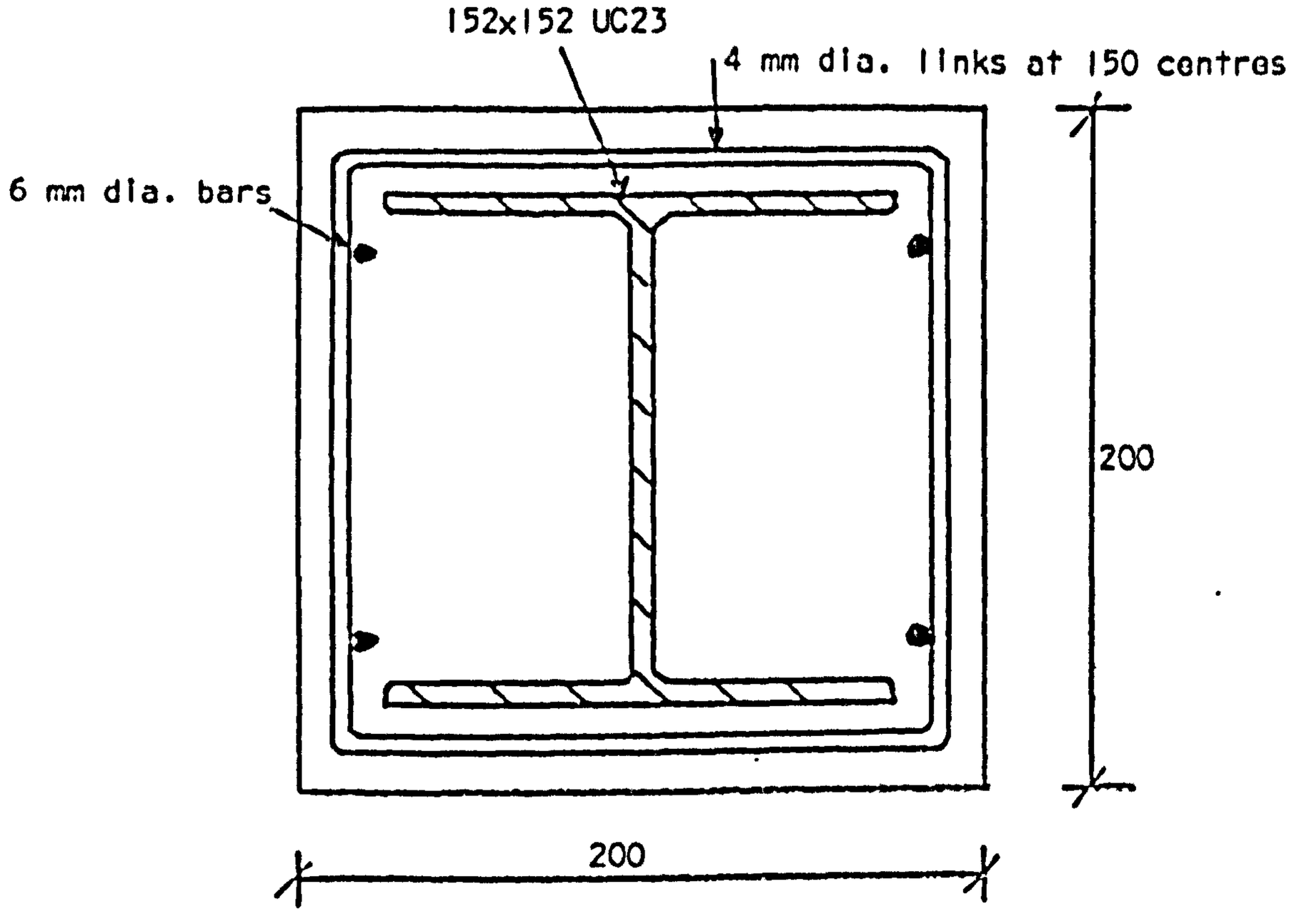

RC series

152 x 89 R.S.J.

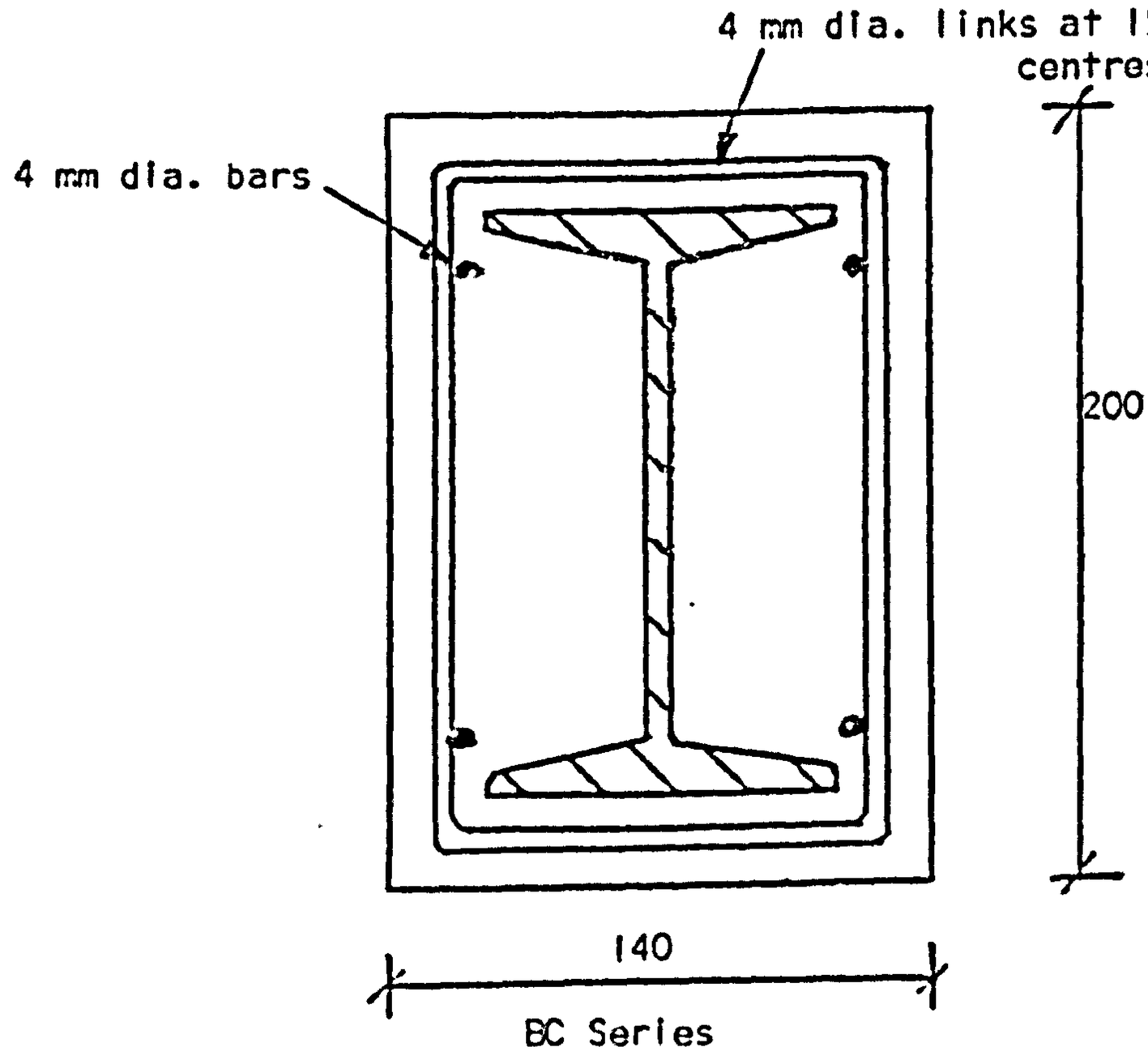

BC Series

FIG. 5.1 CROSS SECTION DETAILS

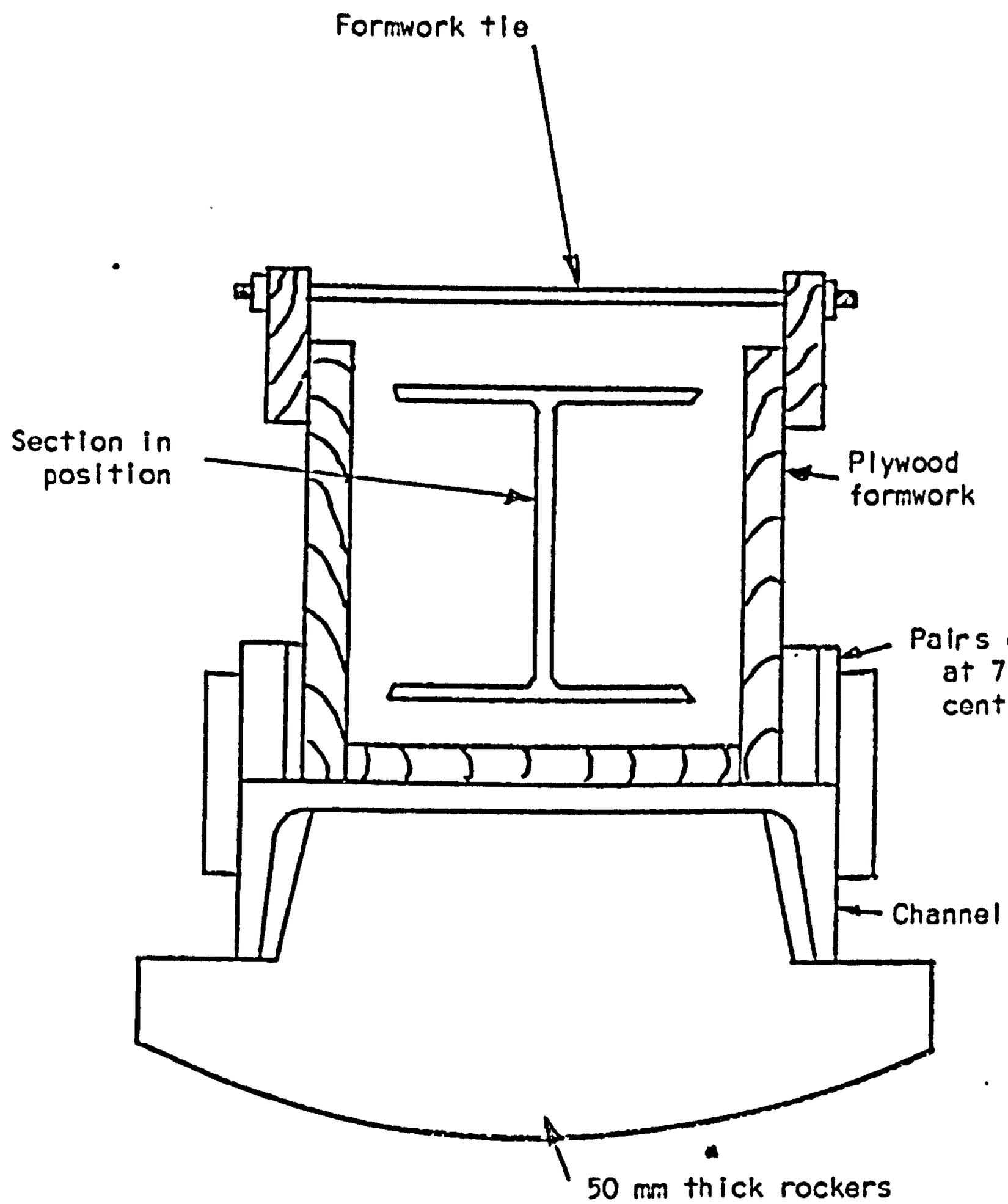

FIG. 5.2 SECTION THROUGH FORMWORK AND STRONGBACK

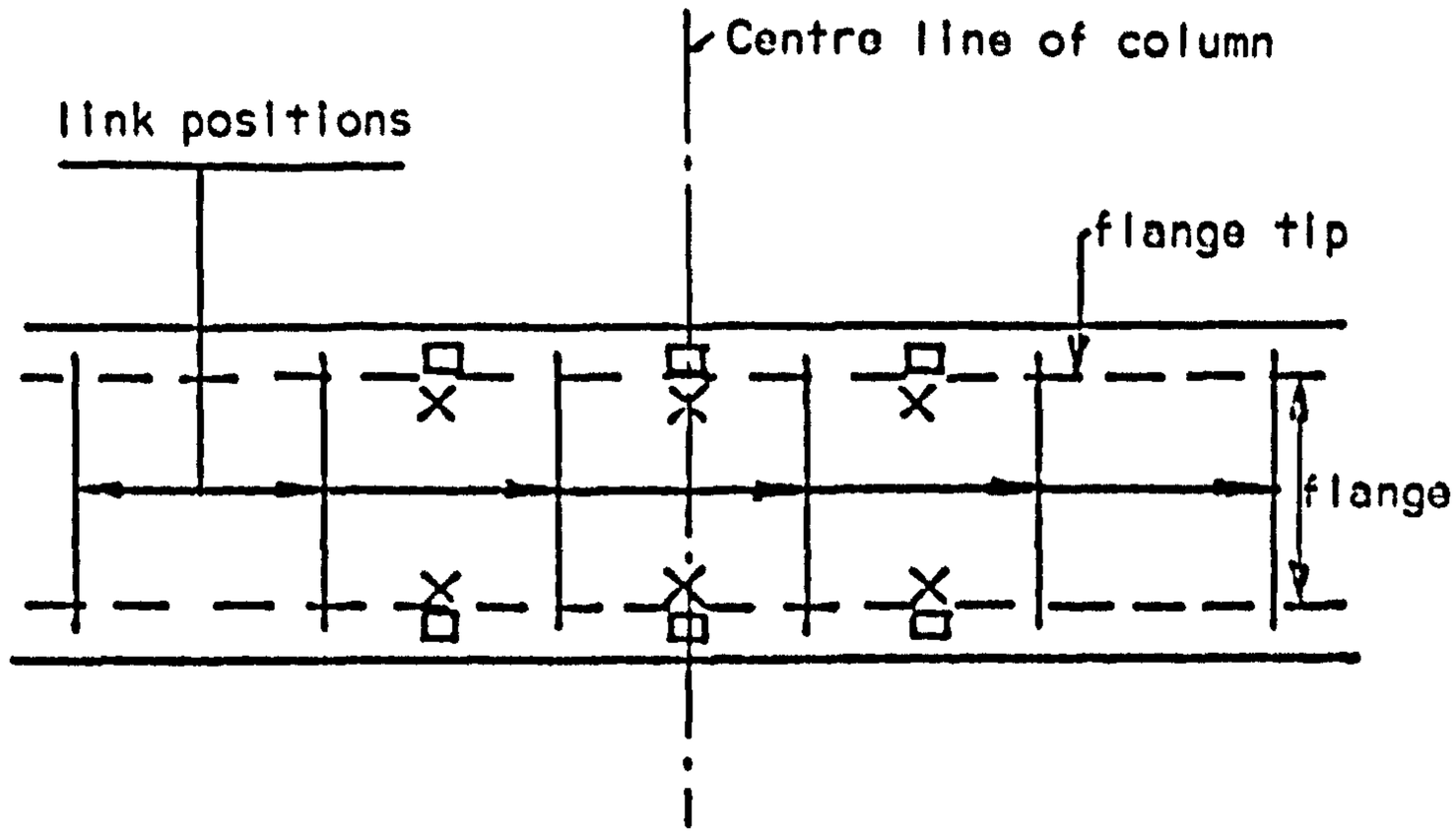

Column RC1

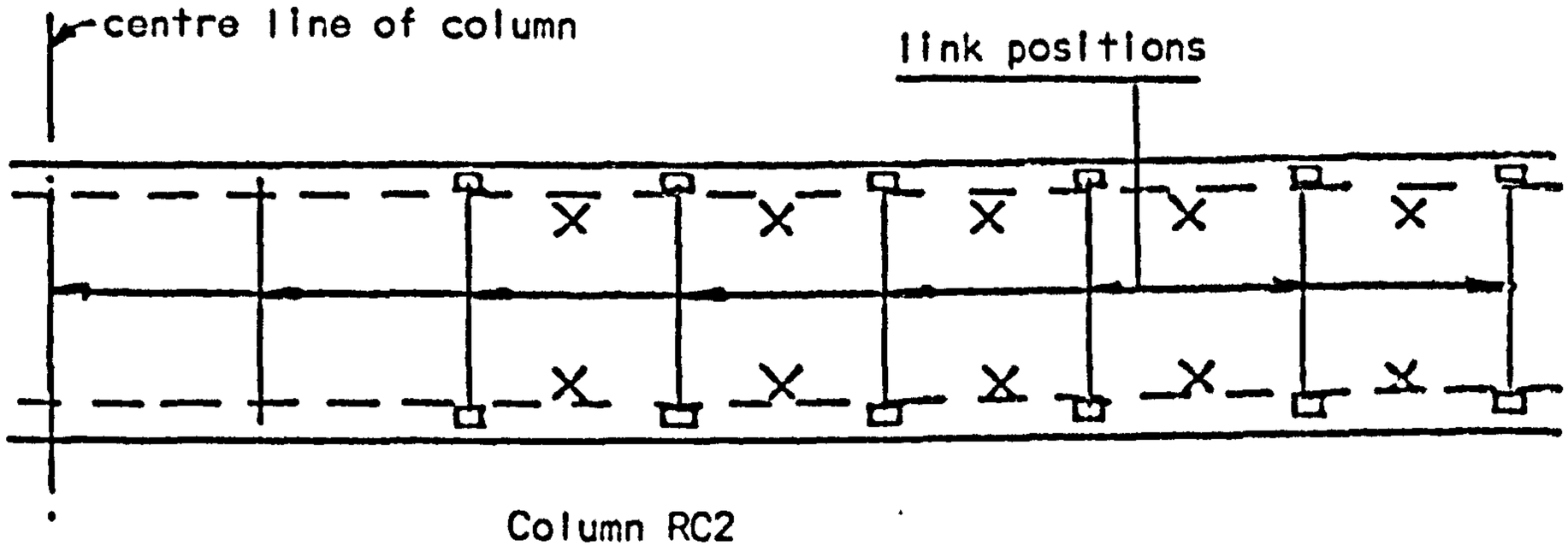

Column RC2

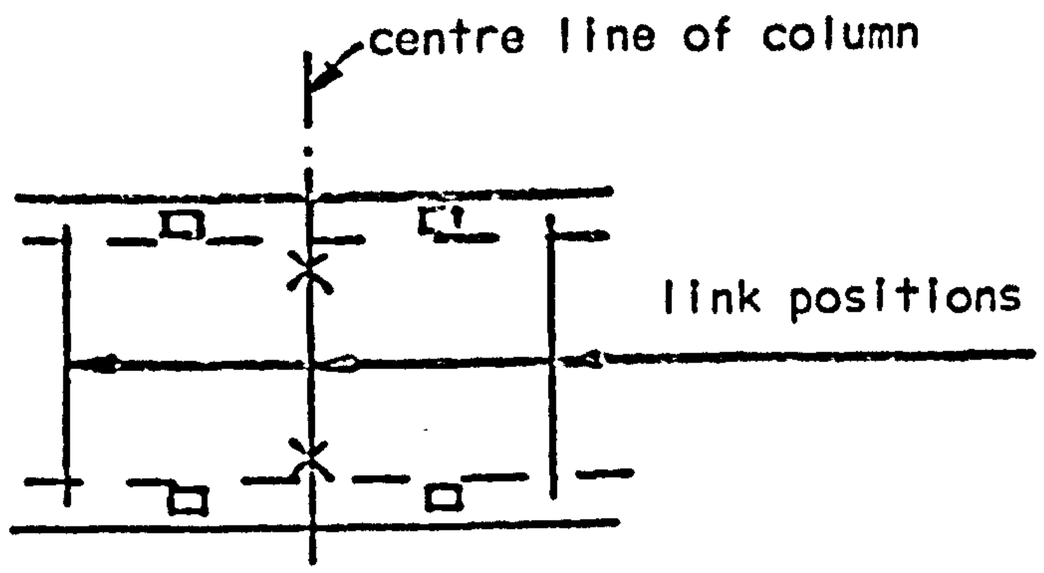

Column RC3

Fig. 5.2 cont....

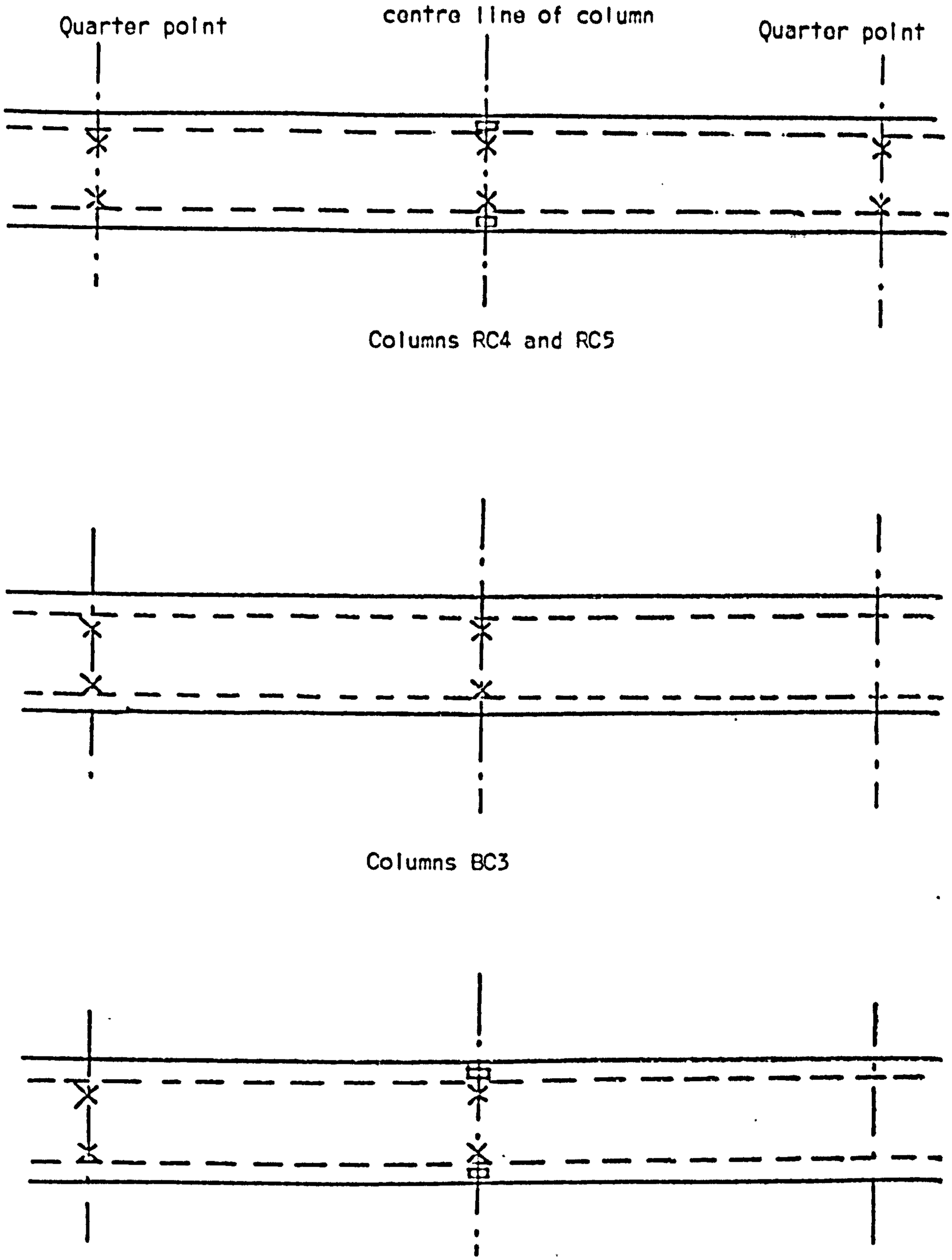

□ Strain gauge location on concrete

× Strain gauge location on steel

FIG. 5.3 LOCATION OF STRAIN GAUGES

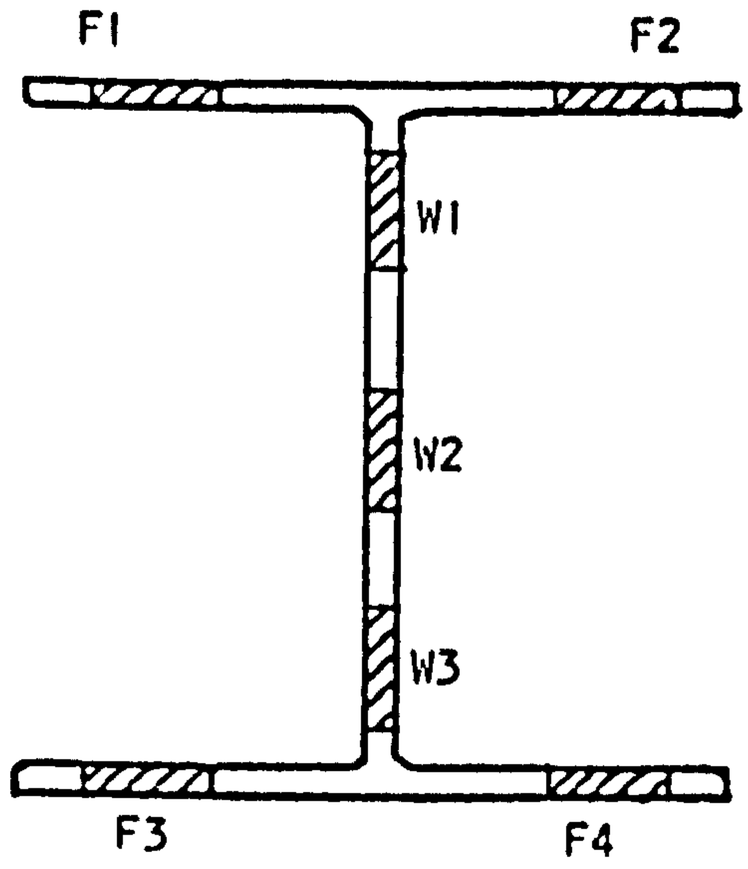

Universal column

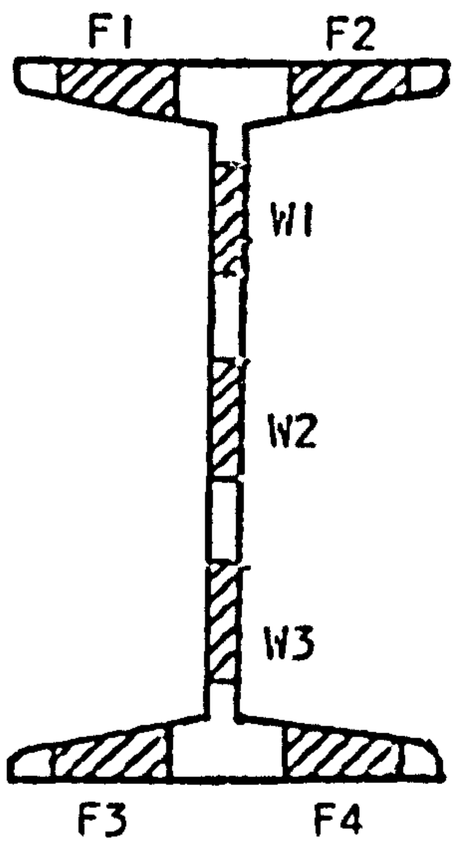

Rolled steel joist

FIG. 5.4 POSITION OF COUPONS FOR TENSILE TESTS

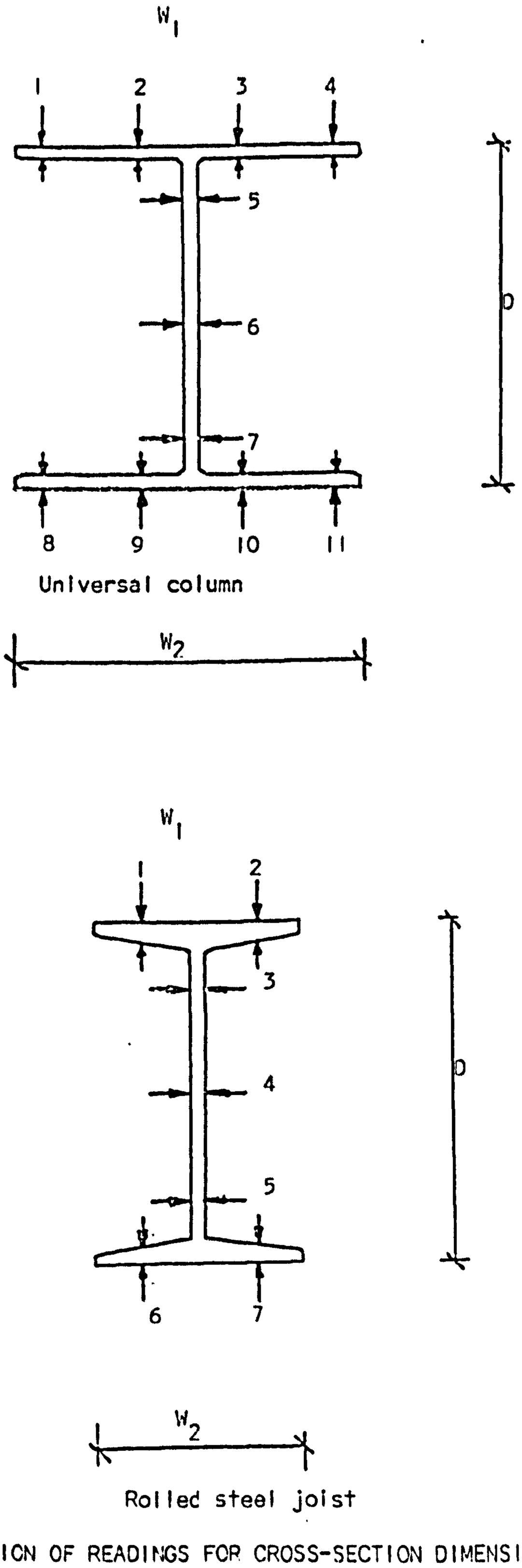

FIG. 5.5 LOCATION OF READINGS FOR CROSS-SECTION DIMENSIONS

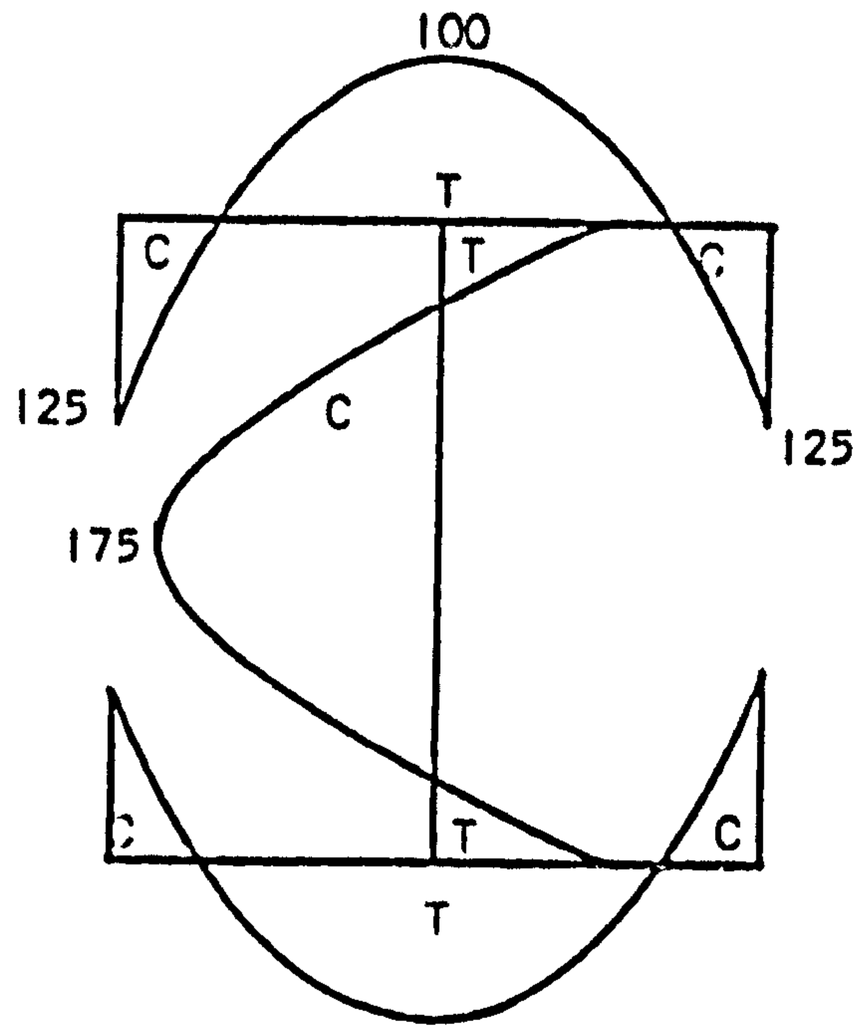

Pattern and values proposed by Young[75] (N/mm^2)

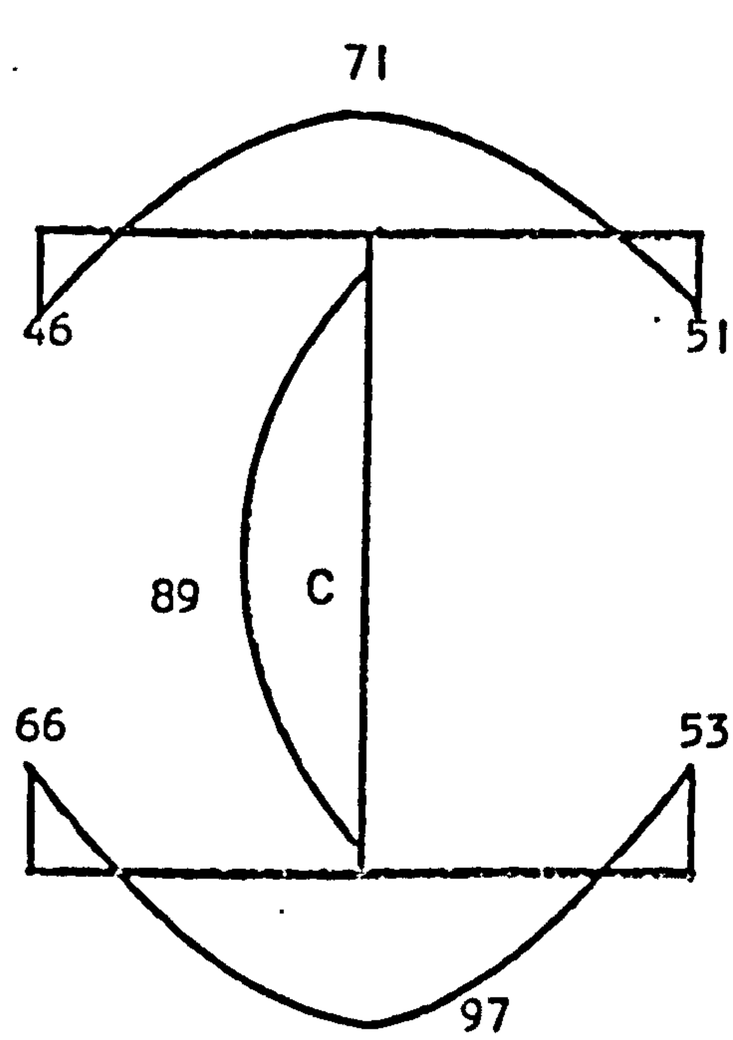

Typical measured values (N/mm^2)

FIG. 5.6 RESIDUAL STRESS MEASUREMENTS

CHAPTER 6 TEST RESULTS

6.1 Testing procedure.

The column to be tested was placed in the rig and bolted to the boxes containing the knife edges. The column was located in the correct vertical position by jacks beneath the boxes. The Lee McCall bars were tightened up until an axial load of about 2 kN had been applied to take the slack out of the rig.

An axial load of about 150 kN was applied and the changes in strain at a cross-section measured to check for eccentricity of loading. If the strains indicated an eccentricity of greater than 2.5 mm, assuming the column to be linear-elastic, then the positions of the boxes containing the knife edges were adjusted using the hydraulic jacks. The strains at the cross-section were then checked again for compliance with the above criterion. The load was cycled between 10 kN and 150 kN about six times and the strains checked each time.

An axial load of the order of 150 kN - 200 kN was then applied in 3 or 4 increments. This load was applied to stabilise the rig and to avoid extensive cracking of the column when the moments were applied. The moments were applied incrementally about one axis. When the required moment had been achieved the moment about the second axis, in the biaxial tests, was then applied. Axial load was then applied until failure took place, except in RC3 when additional moments were also applied to each end, Fig. 6.7.

The moments in the horizontal plane, (the major axis in all tests but RC5), were applied independently to each of the beams giving two moments, end 1 and end 2 on the Figures. End-moments in the vertical plane, in the biaxial tests, were applied by deflecting the beams with the screw jack in the link, Fig. 4.2, and so were the same at each end of the column.

Each test had between 20 and 40 separate load increments at which deflection, strain and load readings were taken.

6.2 Results of tests on columns RC1, RC2 and RC3.

6.2.1 Typical behaviour

The typical behaviour of a test specimen is described with respect to column RC1 as shown in Figs. 6.1, 6.2, and 6.3.

On initial loading the strains in both steel and concrete increased linearly and indicated plane sections remaining plane and virtually uniform compression, Fig. 6.3. Application of the moments caused cracking on the tension face of the column at every link position.

The addition of further axial load caused the cracks to close, the section to stiffen, the end-moments to increase and deflections to decrease, Figs. 6.1 and 6.2. Further increase in axial load caused the section to lose stiffness and the end-moments to fall.

Failure of the short columns commenced with indications of crushing along the compression face and longitudinal cracking on the compression face adjacent to the flange tips, Fig. 6.9.

Further axial load caused sections of the concrete cover to the flange to break off. Extensive yielding of the flange could then be seen. Final failure occurred with a snap through and an overall buckling failure about the minor axis with local buckling of the flanges between links and longitudinal bars occurring between stirrups. A typical failure zone is shown in Figs. 6.9 and 6.10.

6.2.2 Individual column behaviour

6.2.2.1 Column RC1

An axial load of 150 kN was applied initially. End-moments of 30 kNm, 0.5 M_p, were applied at each end of the column to give single curvature bending. The cracks at each link position extended approximately 60 mm into the section.

The axial load was increased and the cracks started to close. Fig. 6.1 shows the behaviour of the column end-moments under increasing axial load.

First signs of crushing occurred at an axial load of 1240 kN with signs of crushing along the entire compression face, especially close to end 2, and the start of longitudinal cracking on both faces adjacent to the flange tips. As the load was increased further more crushing appeared, followed by spalling of the concrete at a point about 500 mm from the centre of the column.

Failure of the section occurred at 1340 kN with an inelastic buckling failure about the minor axis, followed by the formation of a hinge at about 500 mm from the centre of the column.

An inspection of the specimen after failure showed extensive signs of crushing along the entire compression face, together with longitudinal cracking.

6.2.2.2 Column RC2.

An axial load of 150 kN was applied and end-moments of 40 kNm, 0.67 M_p, at end 1 and 20 kNm, 0.33 M_p, at end 2 to give unsymmetrical single curvature.

Cracks of up to 70 mm into the section occurred at the end with the larger applied moment.

Increasing axial load caused the cracks to close. Figs. 6.4 and 6.5 show the behaviour of the column under increasing axial load.

First signs of crushing and longitudinal cracking occurred at 1100 kN at a point about 750 mm from the centre of the column, Fig. 6.6.

Spalling started at a load of 1235 kN at the point where crushing had first been noted. Failure took place at 1270 kN with inelastic buckling about the minor axis.

6.2.2.3 Column RC3.

An axial load of 300 kN was applied and then end-moments of 15 kNm, 0.25 M_p, applied at each end to give uniform single curvature. Only short cracks, less than 10 mm long, appeared.

The axial load was then increased to 600 kN and the moments increased to 37 kNm, Fig. 6.7. Fine cracks, up to 25 mm deep,

appeared. On the addition of further axial load to 900 kN the crack lengths reduced to 10 mm and closed completely at 1050 kN.

The first signs of longitudinal cracking and crushing occurred at a load level of 1325 kN. These were followed by spalling and an inelastic buckling failure about the minor axis, Figs. 6.9 and 6.10 at 1360 kN.

6.3 Results of tests on columns RC4 and RC5.

6.3.1 Column RC4

On initial loading strains in both the steel section and the concrete encasement increased linearly and indicated plane sections remaining plane, and a small amount of bending due to initial imperfections. At an axial load of 200 kN the end-moments were applied in small increments up to a level of 33.5 kNm, 0.5 M_p, cracking occurred on the tension face at link positions.

Additional axial load caused the end-moments to fall off immediately, Fig. 6.13.

As the axial load was increased the minor axis deflections increased until, at about 600 kN, a rapid rate of change of minor axis deflections was noted, Fig. 6.11.

Failure occurred at 850 kN with a minor axis instability failure, Fig. 6.15, and with relatively small deflections about the major axis Figs. 6.12 and 6.14.

6.3.2 Column RC5.

An axial load of 200 kN was applied initially. End-moments of approximately 16.5 kNm, 0.4 M_p, were applied at each end incrementally to give single curvature bending. Cracking occurred on the tension

face at link positions.

Additional axial load caused an increase in deflections, Fig. 6.16, and a fall off in the end moments, Fig. 6.17 and reversal of end moments occurred at about 700 kN. First signs of crushing occurred near the hinge position at 750 kN.

Fine cracks appeared on the inside face at link positions near the beam-column joint just before failure, Fig. 6.19. Failure occurred with the formation of a hinge and minor axis instability at 825 kN, Fig. 6.18. Major axis deflections were relatively small, Fig. 6.20.

6.4 Results of biaxial column tests.

6.4.1 Column BC1

On initial loading the strain in the steel section increased linearly and indicated plane sections remaining plane and a small amount of bending due to initial imperfections and possibly a small eccentricity of loading. At an axial load of 200 kN the end-moments were applied in small increments. The minor axis moment of 4.5 kNm, approximately $0.45\ M_{py}$ was applied first followed by the major axis moment of 21.5 kNm, approximately $0.5\ M_{px}$, where M_{py} and M_{px} are the minor and major axis ultimate moments at zero axial load. On application of the minor axis moment cracking occurred on the tension face at link positions. When the major axis moment was applied additional cracks appeared and others started to close as areas changed from tension to compression.

Additional axial load caused the minor axis end-moments and

one of the major axis moments to fall off. The other major axis end moment increased slightly, Figs. 6.21 and 6.22, but started to decrease at about 300 kN.

At a load of about 450 kN a small amount of crushing appeared near the centre of the column in the compression zone. This crushing increased slightly with additional load.

At 650 kN the minor axis end-moment changed sign.

Extensive crushing along the compression corner occurred at 700 kN followed by the formation of a hinge, Figs. 6.23 and 6.24, and collapse at 742 kN.

During the test deflections were recorded at quarter points along the column about both axes, Figs. 6.25 and 6.26. The major axis deflections, Fig. 6.25 varied very little and gave little indication of the onset of failure. The minor axis deflections, Fig. 6.26, did increase more rapidly when an axial load of 700 kN had been reached.

6.4.2 Column BC2

The behaviour of BC2 was similar to BC1 up to 200 kN. The minor axis moment of 3.5 kNm, 0.35 M_{py}, was applied followed by the major axis moment of 20.5 kNm, 0.45 M_{px}. Cracking occurred at the link positions. Additional axial load, to a level of 300 kN, caused all applied moments, Figs. 6.27 and 6.28, to increase before falling off.

One of the major axis end-moments however increased until a

load of 450 kN after which, it also dropped.

No signs of distress were seen until about 700 kN when crushing occurred along the compression face near the centre of the column, Fig. 6.32. This crushing continued to increase until failure at 834 kN. Just prior to failure, crushing was observed at the ends of the column adjacent to the end-plates, Figs.6.31, 6.32 and 6.33, indicating large restraining moments from the minor axis beams.

The deflections were recorded at quarter points and the behaviour was as test BC1. The deflections at the mid-height of the column are given on Figs. 6.29 and 6.30.

6.4.3 Column BC3

The behaviour of BC3 was similar to BC1 and BC2 up to 200 kN. In this test the major axis moments of 22.6 kN, 0.55 M_{py}, were applied first. Cracking occurred at link positions and also longitudinal cracking, Fig. 6.40. The minor axis moment of 5 kNm, 0.55 M_{px}, was then applied, and some cracks closed leaving a crack pattern as Fig. 6.34.

Increasing axial load caused a fall off of minor axis moments, Fig. 6.36 and initially a slight increase in one of the major axis moments, Fig. 6.35. Further axial load caused all moments to fall.

At 550 kN spalling commenced along the compression tip of the column over the central half. This increased fairly slowly until about 675 kN when extensive crushing and cracking appeared. Failure occurred at 730 kN, Fig. 6.40 and 6.41.

As in column BC2 crushing occurred at the ends of the column, Fig. 6.39.

Deflections were recorded at quarter points and mid-height deflections are given in Figs. 6.37 and 6.38. As in test BC1 little prior indication was given by the deflections of the onset of failure.

6.5 Accuracy of experimental results.

6.5.1 Measurement errors.

The accuracy of the 2 MN load cell was 0.25% of full read out, (F.R.O) i.e. ± 5 kN, for a stabilised input. The input voltage was monitored throughout testing and found to vary up to 0.5% giving a maximum error of 0.75% of F.R.O. i.e. ± 15 kN. Hence the maximum error on ultimate load is about 2% (i.e. 15 kN on 750 kN). The tension-compression cells have a linearity of 0.1% of F.R.O, which can introduce an error of up to ± 0.26 kNm in the end-moments in tests RC1 to RC5, and ± 0.13 kNm in the major axis end-moments and ± 0.06 kNm in the minor axis end-moments in tests BC1 to BC3. The input voltage was monitored throughout testing and, as for the 2MN load cell, found to vary by ± 0.5%. Hence the moment can have an additional error of ± 0.5%.

The transducers are calibrated to 0.1% linearity, i.e. for ±50 mm transducers to 0.05 mm., and give stable results for voltages of 30 ± 3 volts.

The strain-gauges on the steel were in general reliable. The gauges on the concrete, however, failed to give consistent results.

6.5.2 Misalignment errors and rig defects.

The most likely source of misalignment errors was in the setting up of the knife edges, column, and load cell or jack. Any misalignment caused additional moments about either or both axes. If the axis had beam loading and restraint then the additional moment was automatically recorded on the tension-compression cell as a change of force in the link. Misalignment errors about an axis with pin-ends however caused additional moments which were not recorded and increased directly as axial load. Deflections about such axes were therefore recorded, Tests RC1, RC2, RC3, RC4 and RC5, and were found to be small until failure was imminent.

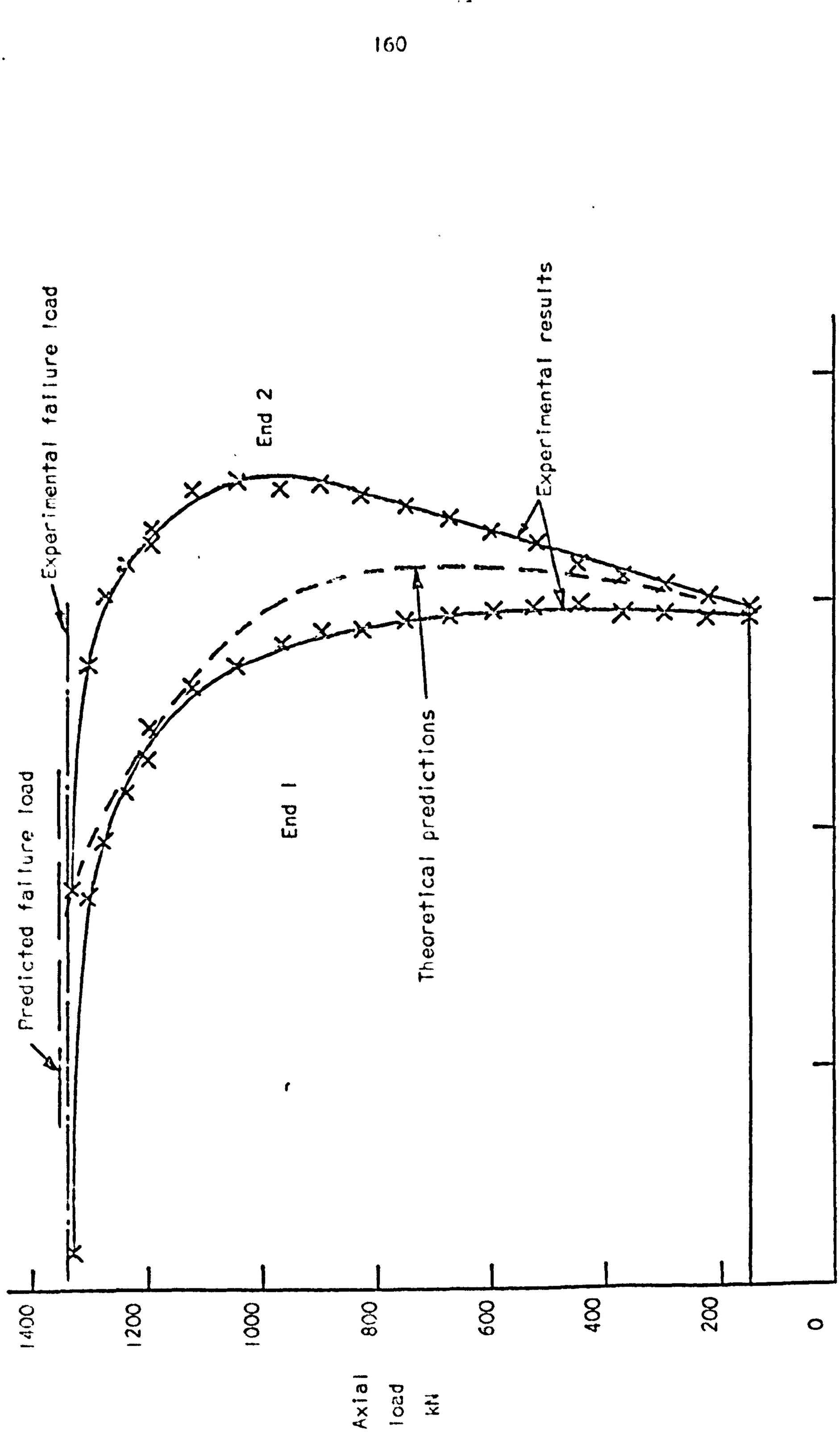

FIG. 6.1 COLUMN RC1 END-MOMENT - AXIAL LOAD CURVES

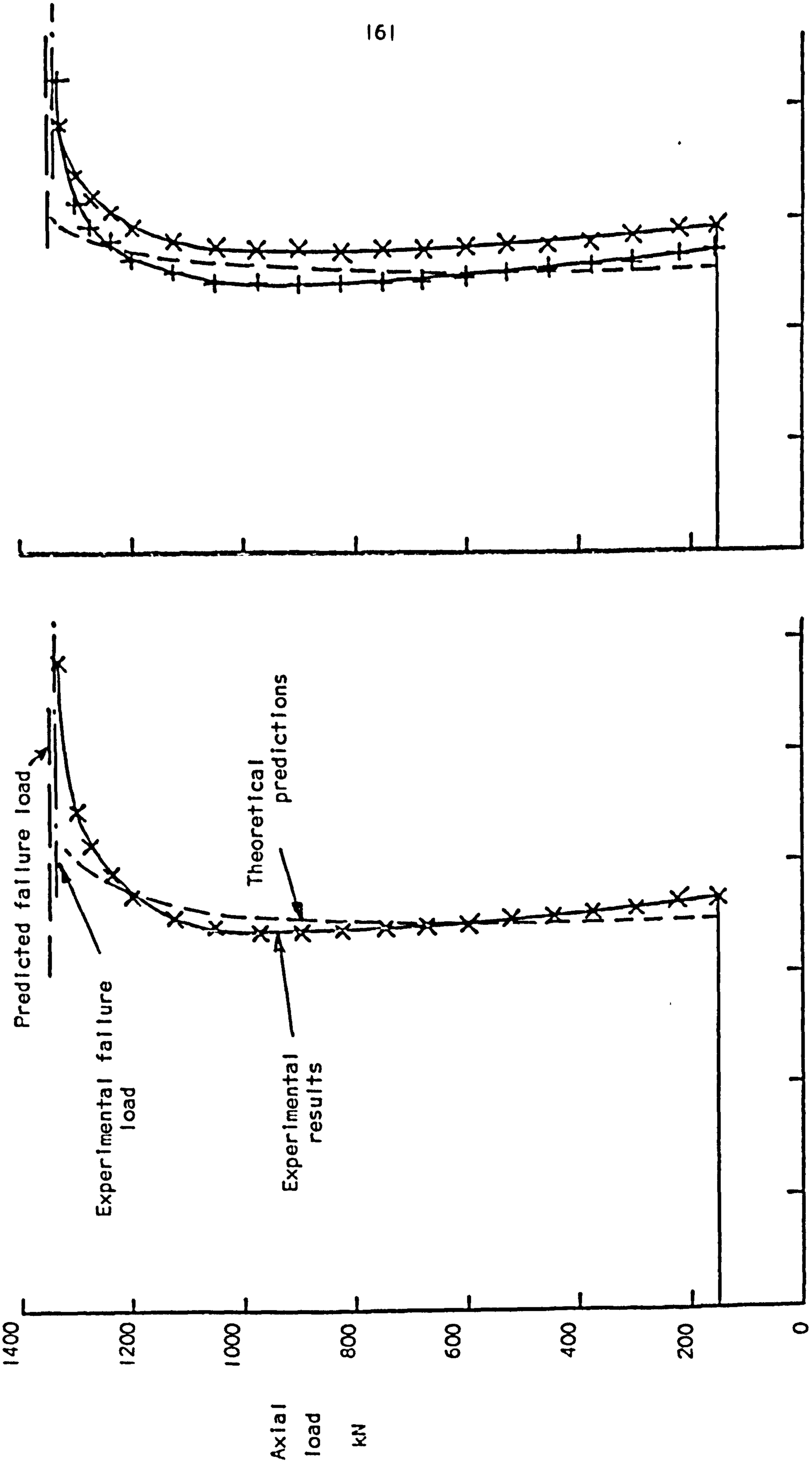

FIG. 6.2 COLUMN RC1 COMPARISON OF DEFLECTIONS AT QUARTER POINTS

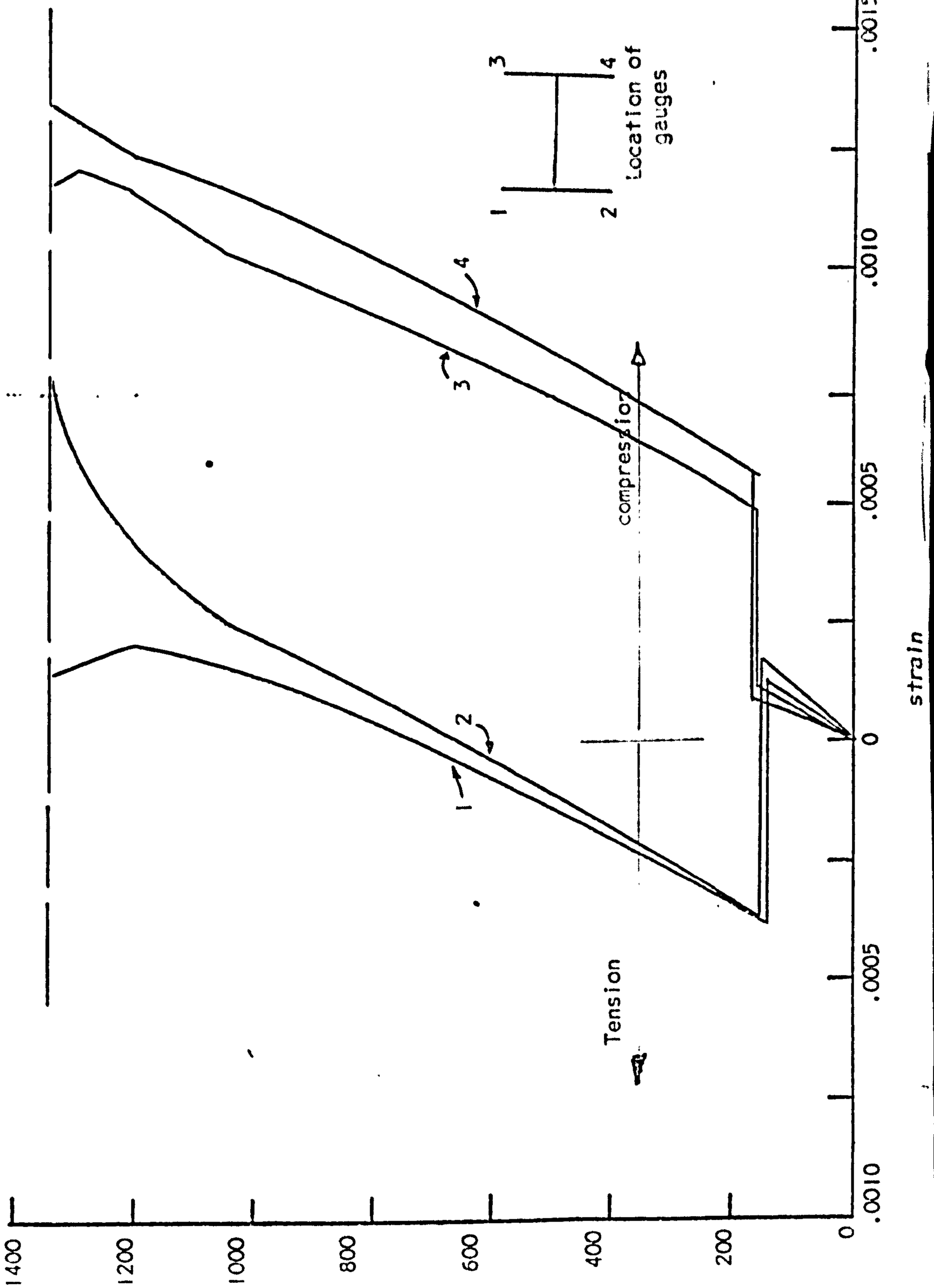

FIG. 6.3 COLUMN RC1 MEASURED STEEL STRAINS AT MID-HEIGHT

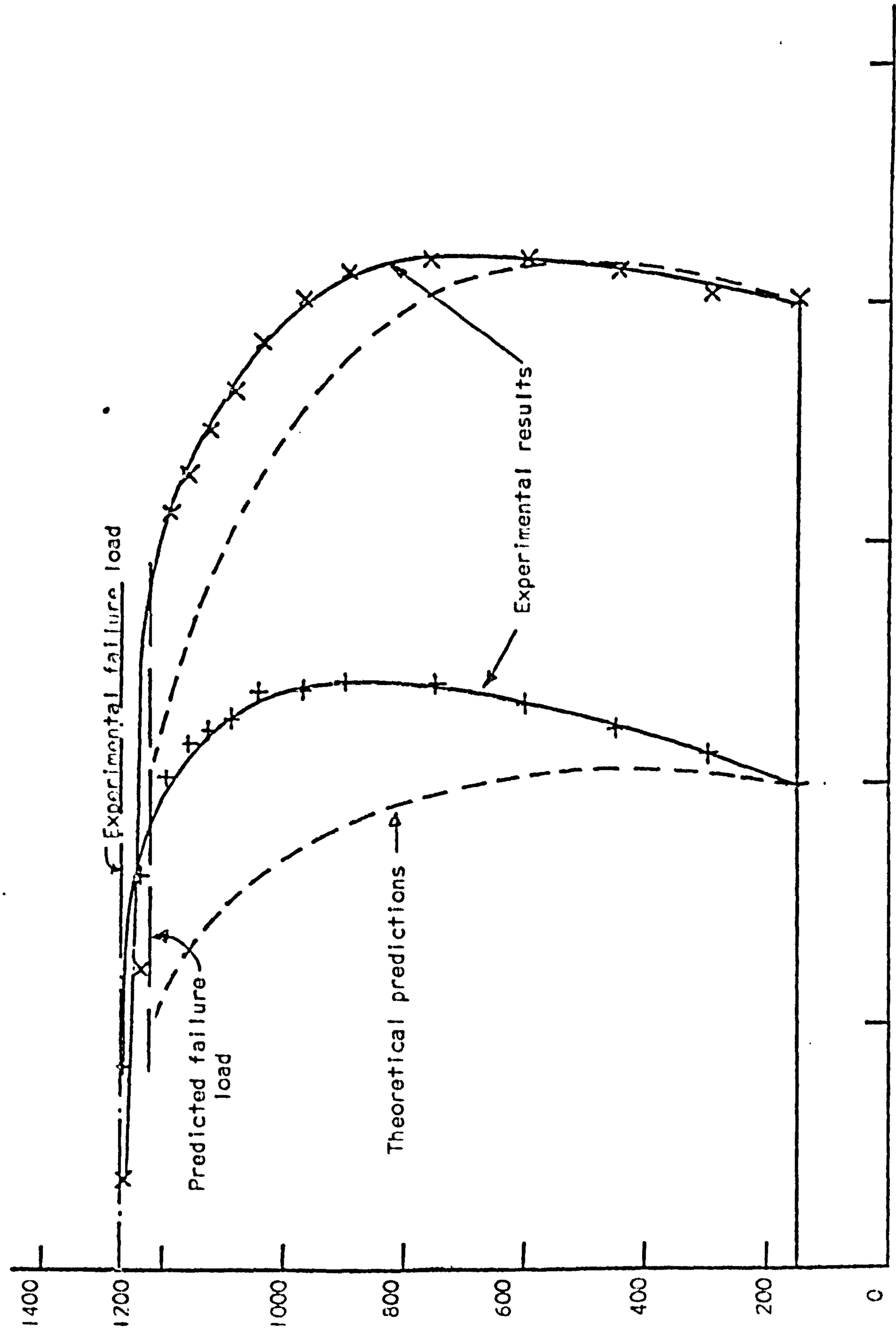

FIG. 6.4 COLUMN RC2 END-MOMENT-AXIAL LOAD CURVE

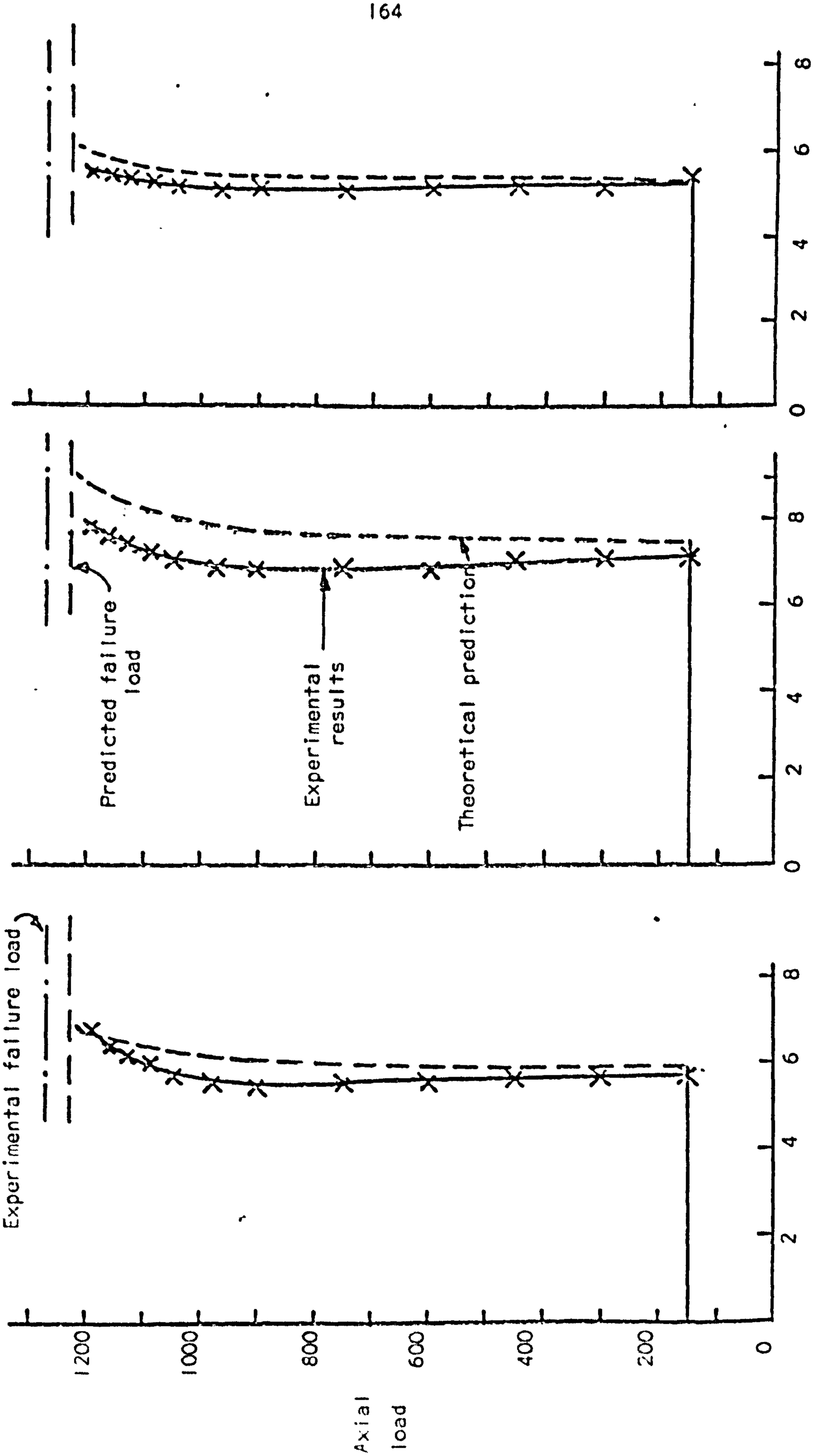

FIG. 6.5 COLUMN RC2 COMPARISON OF DEFLECTIONS AT QUARTER POINTS

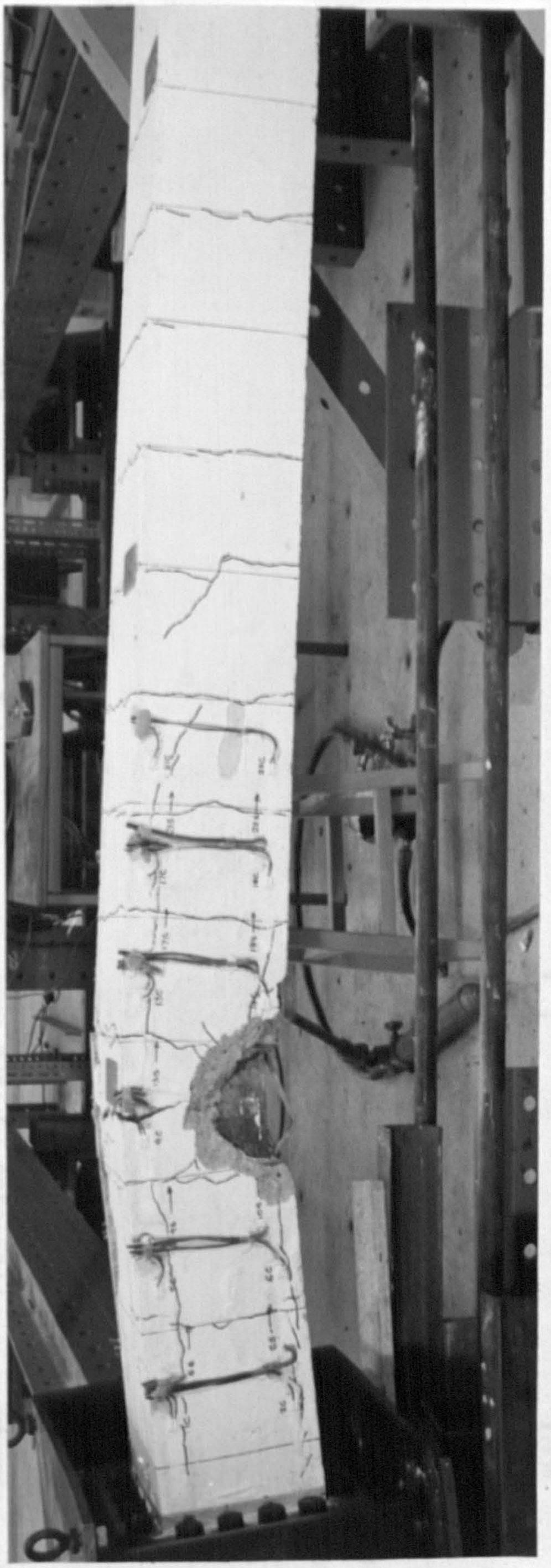

FIG.6.6 COLUMN RC2 - FINAL DEFLECTED SHAPE OF COLUMN

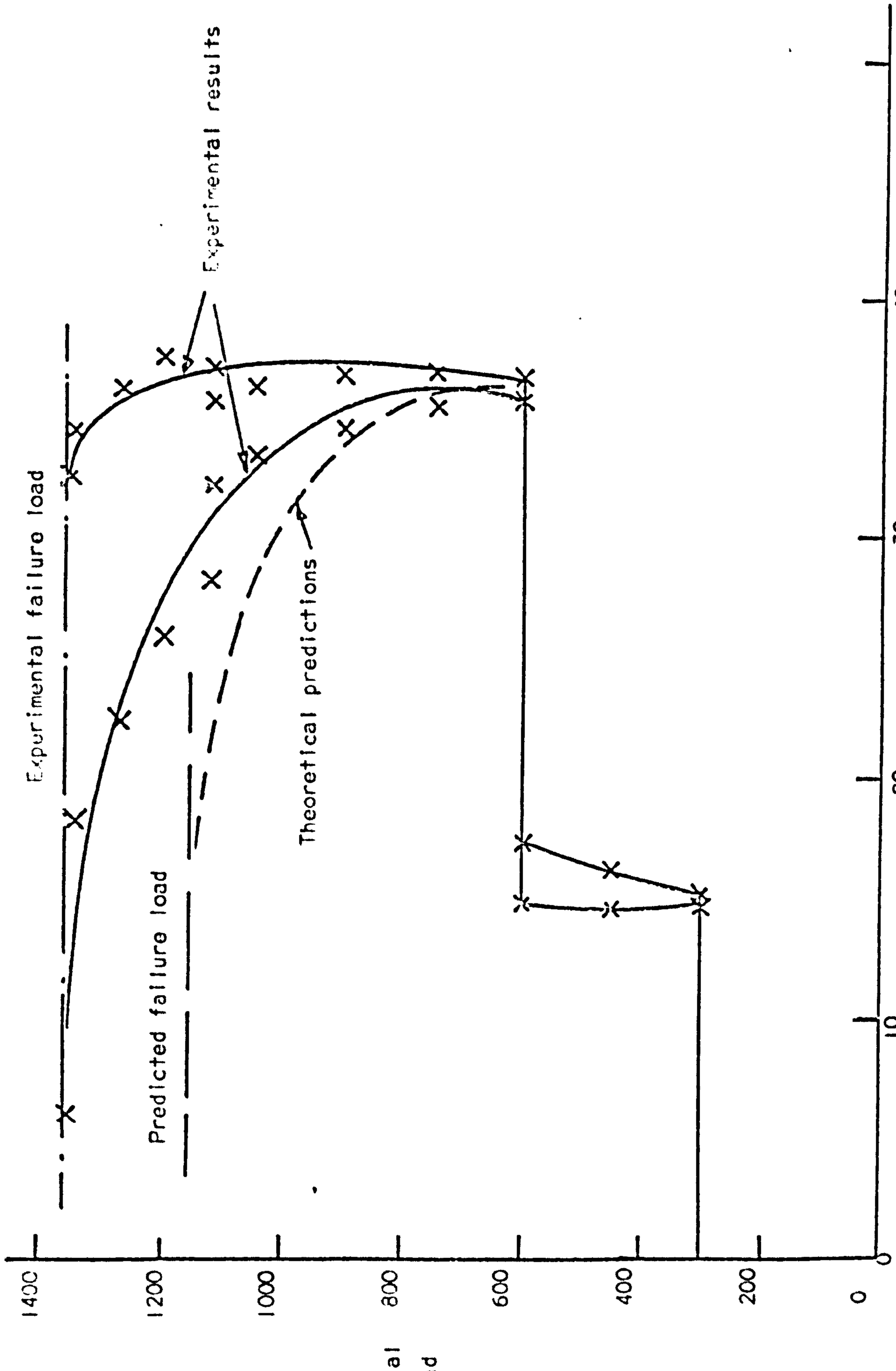

FIG. 6.7 COLUMN RC3 END-MOMENT-AXIAL LOAD CURVES

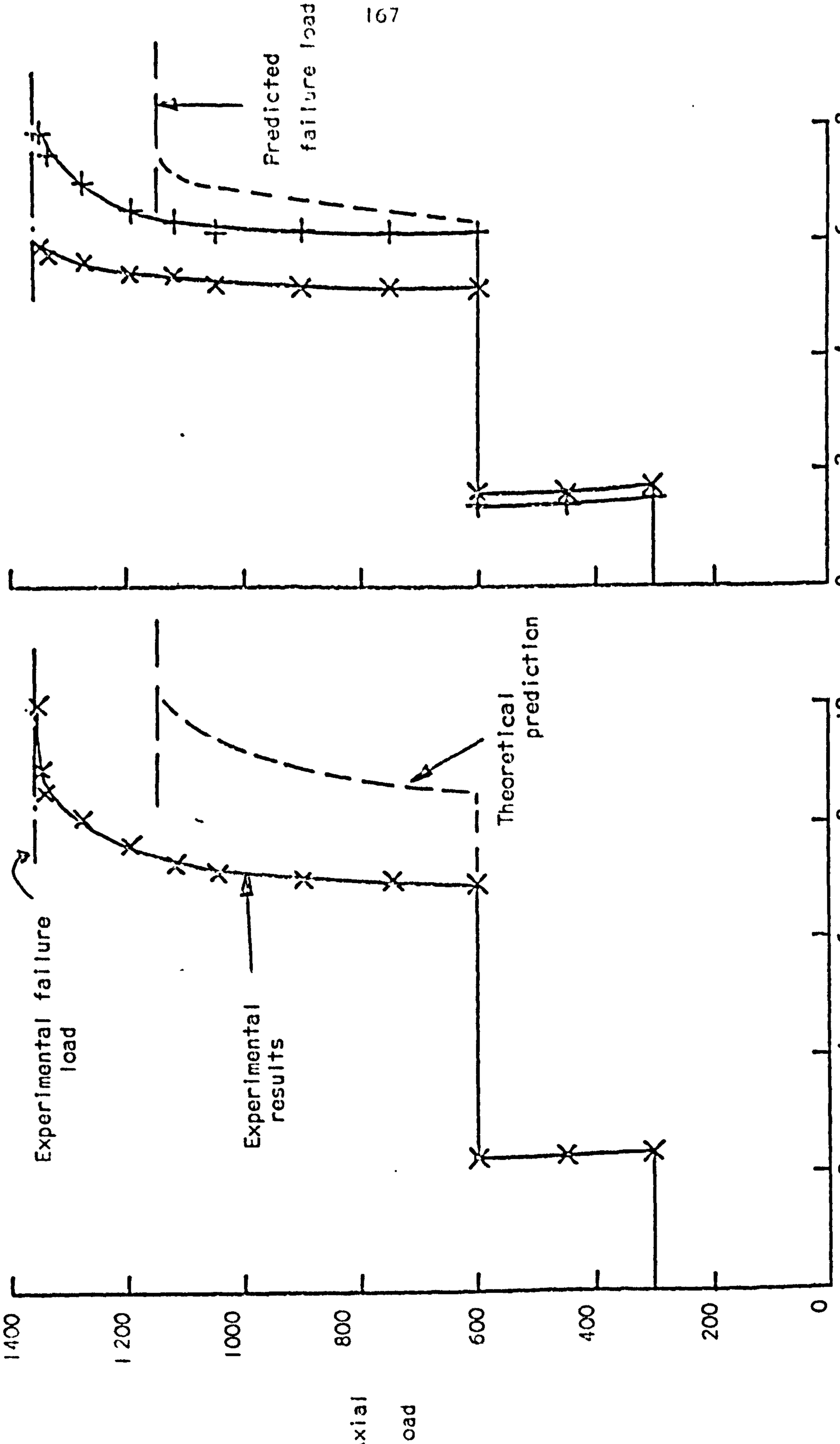

FIG. 6.8 COLUMN RC3 COMPARISON OF DEFLECTIONS AT QUARTER POINTS

FIG. 6.9 COLUMN RC3 - FAILURE ZONE VIEWED ABOUT MINOR AXIS

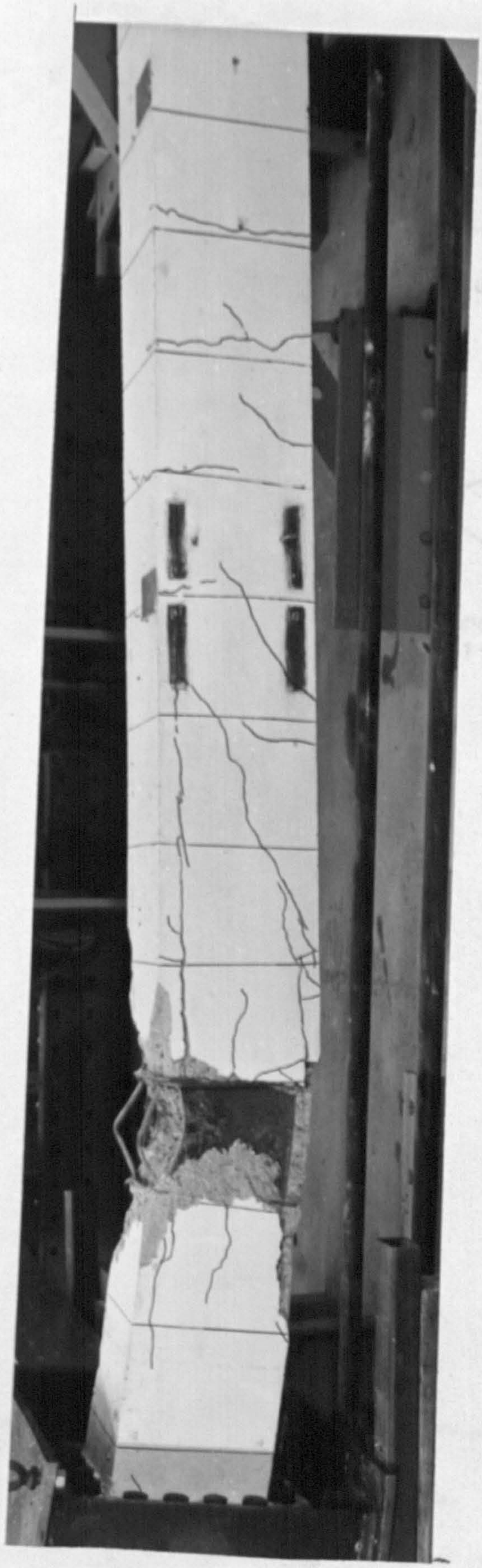

FIG. 6.10 COLUMN RC3 - FAILURE ZONE VIEWED ABOUT MAJOR AXIS

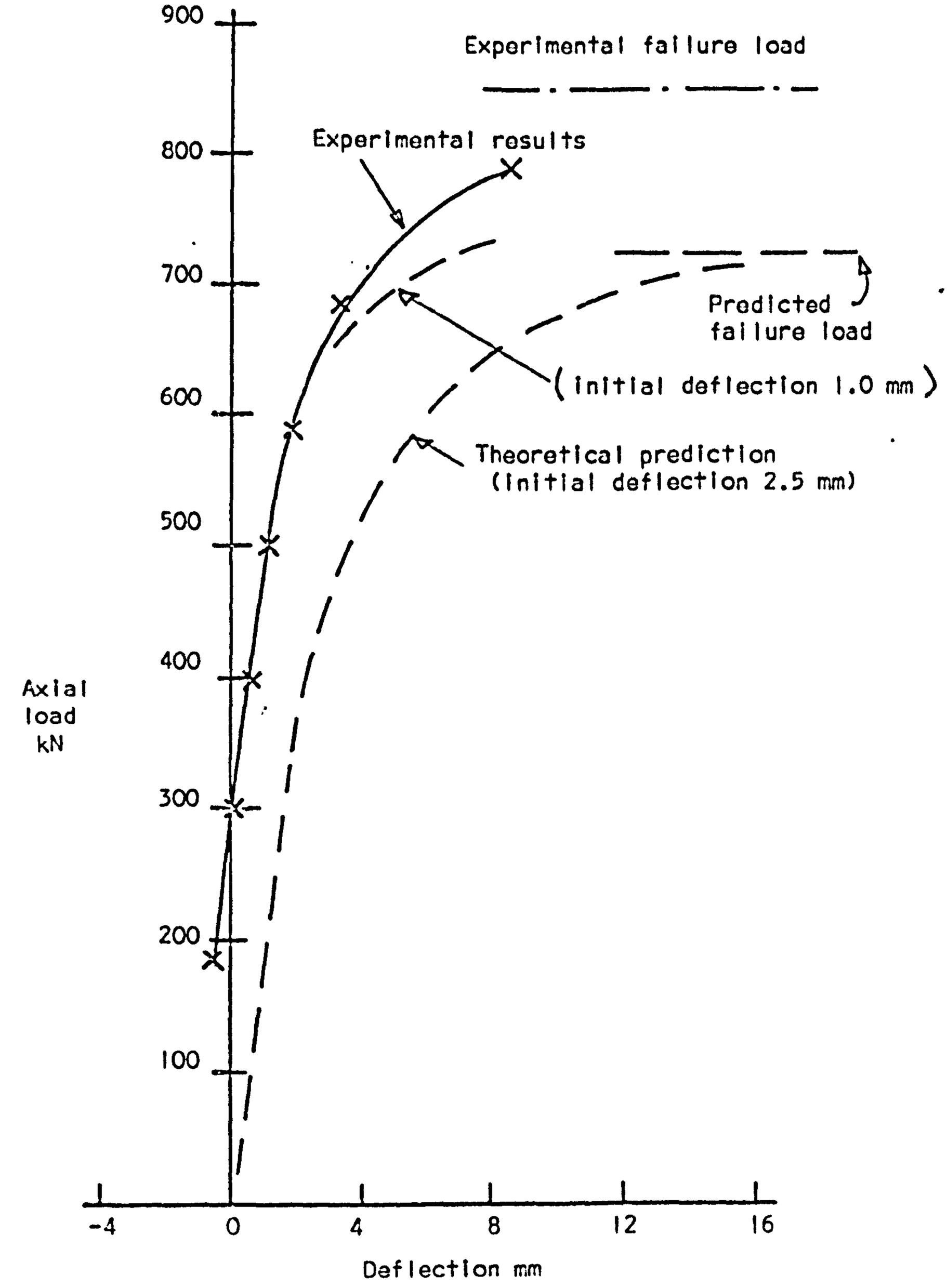

FIG. 6.11 COLUMN RC4 COMPARISON OF MINOR AXIS DEFLECTIONS AT MID-HEIGHT

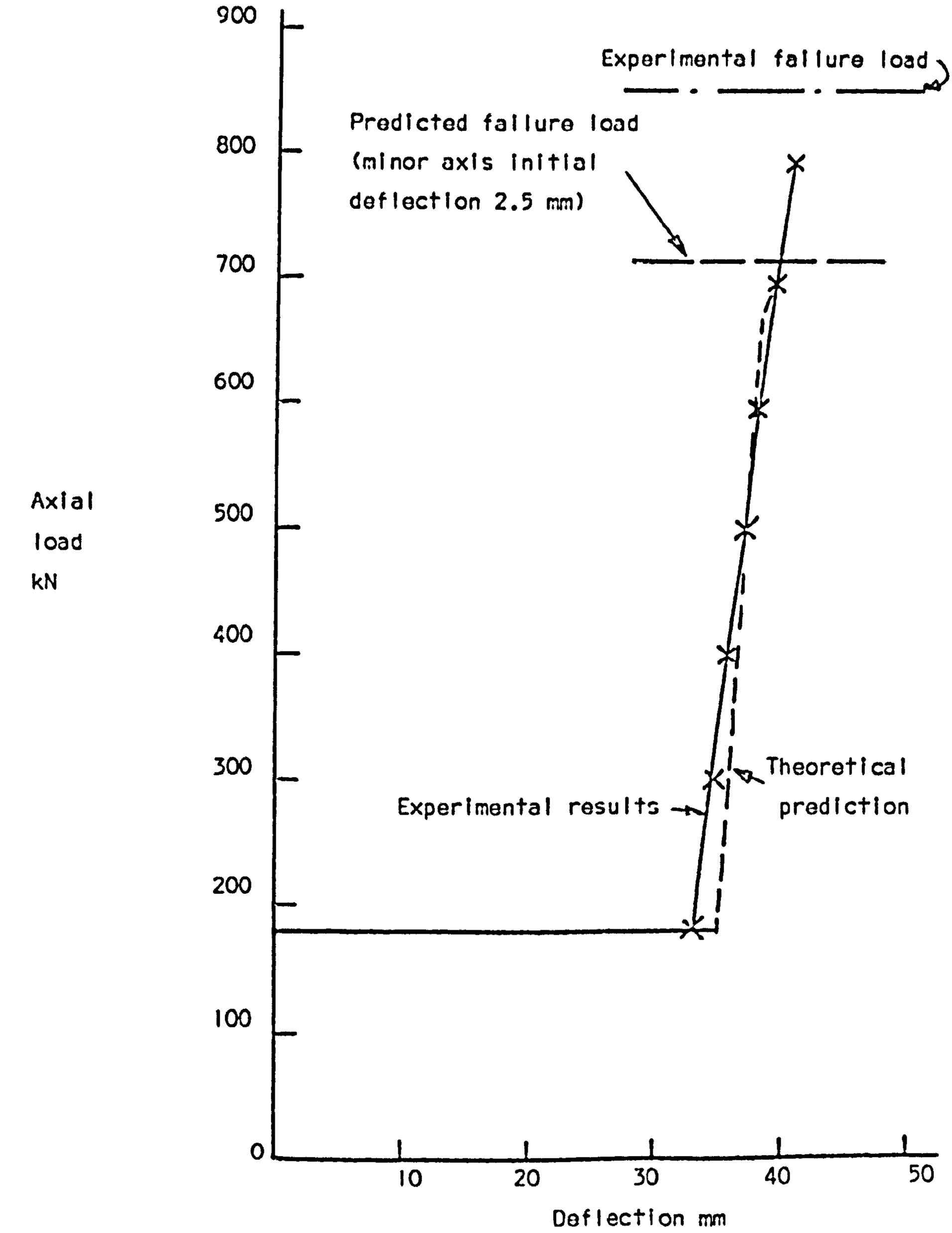

FIG. 6.12 COLUMN RC4 COMPARISON OF MAJOR AXIS DEFLECTIONS AT MID-HEIGHT

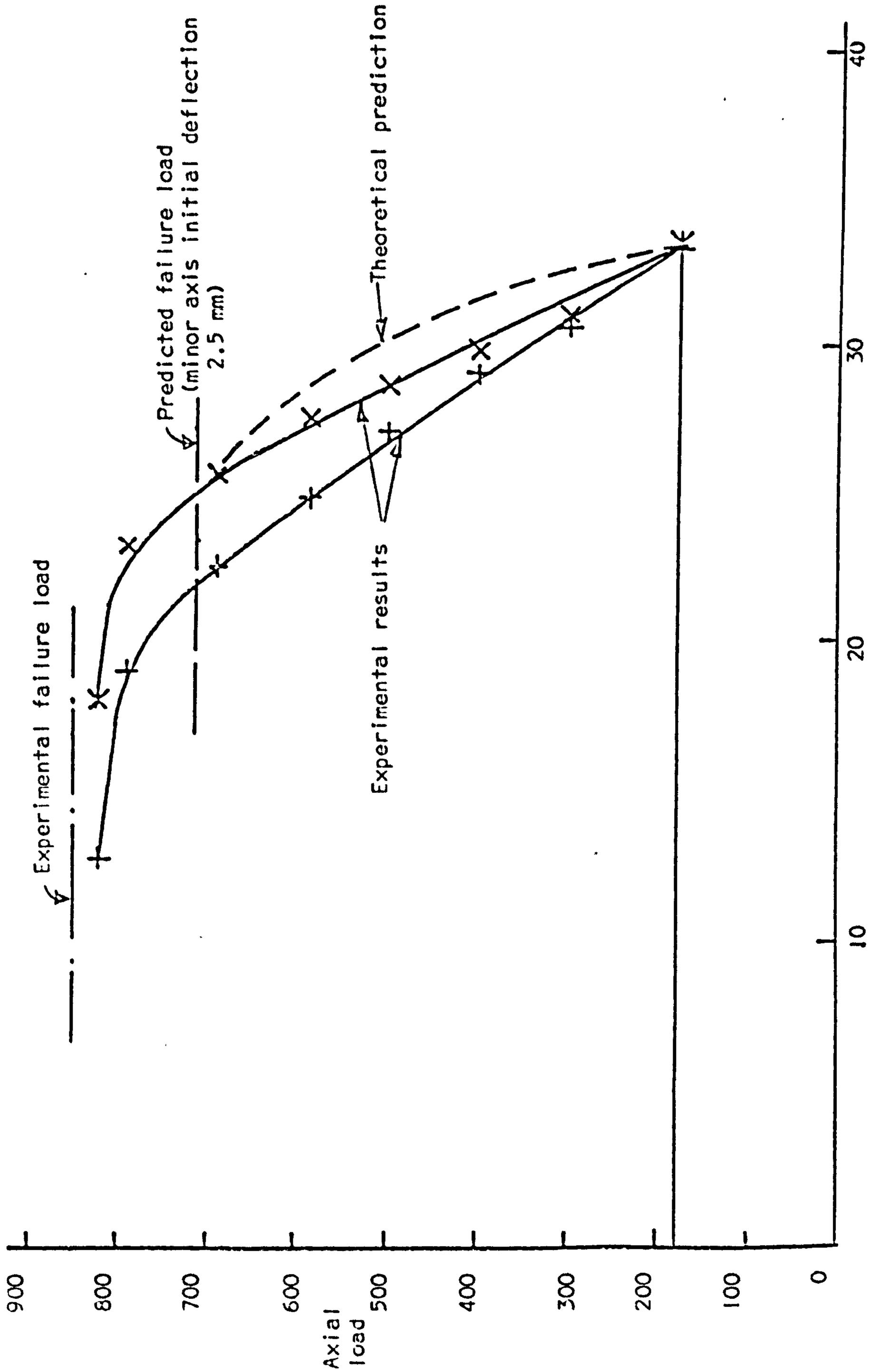

FIG. 6.13 COLUMN RC4 END-MOMENT-AXIAL LOAD CURVES

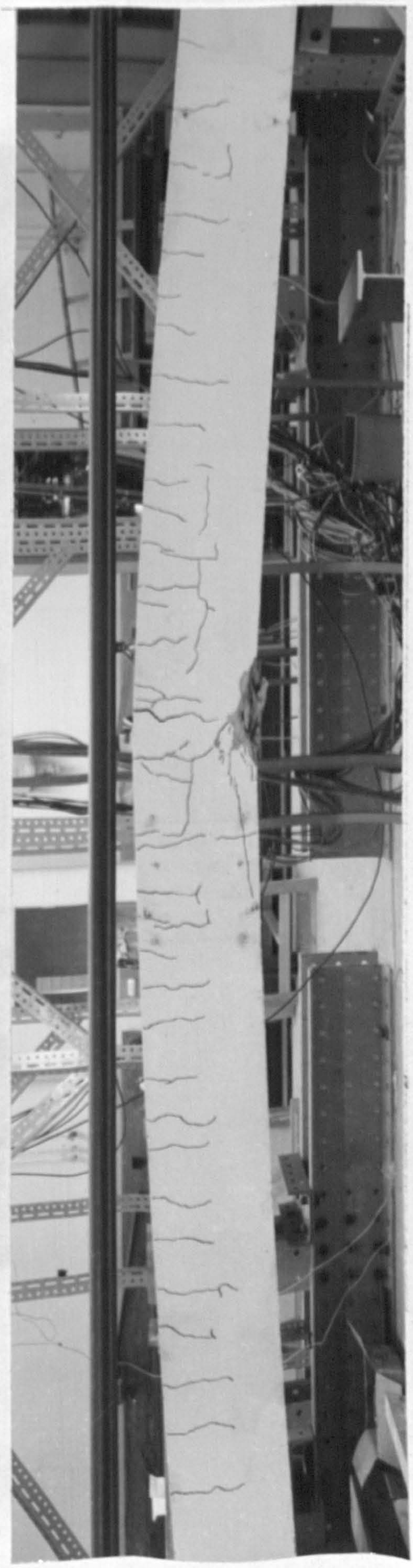

FIG. 6.14 COLUMN RC4 - FINAL DEFLECTED SHAPE VIEWED ABOUT MAJOR AXIS

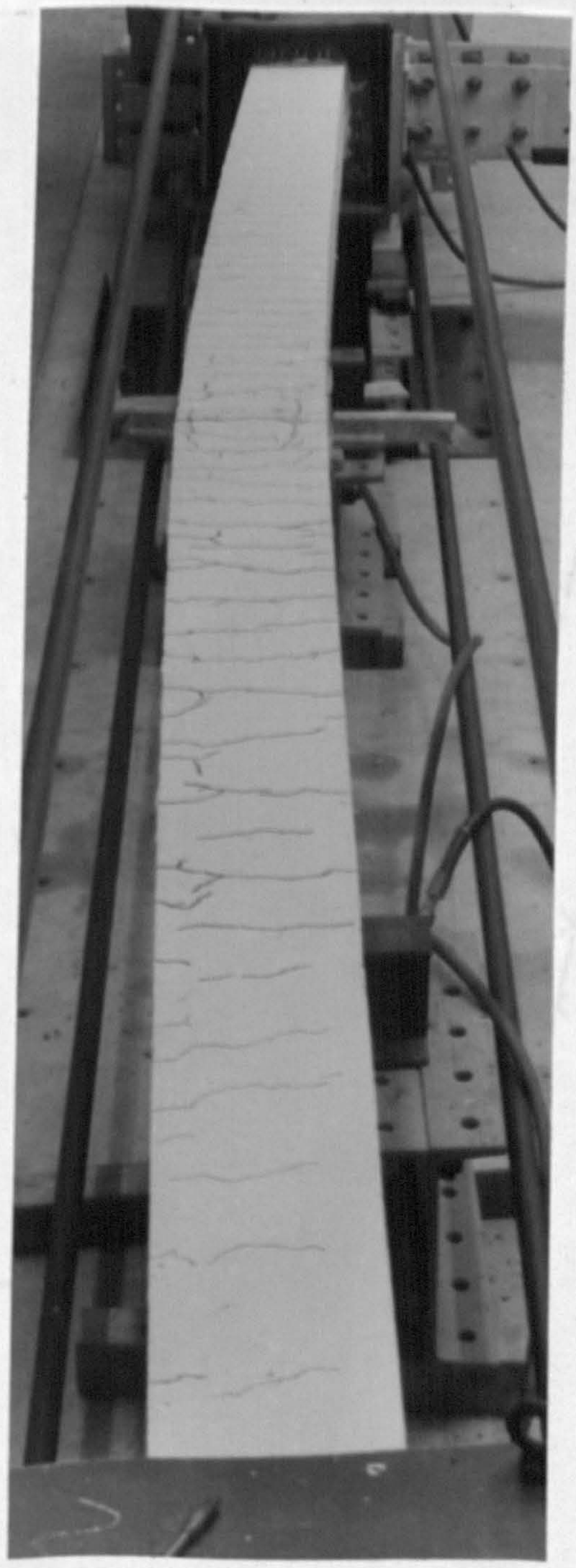

FIG. 6.15 COLUMN RC4 - FINAL DEFLECTED SHAPE VIEWED ABOUT MINOR AXIS

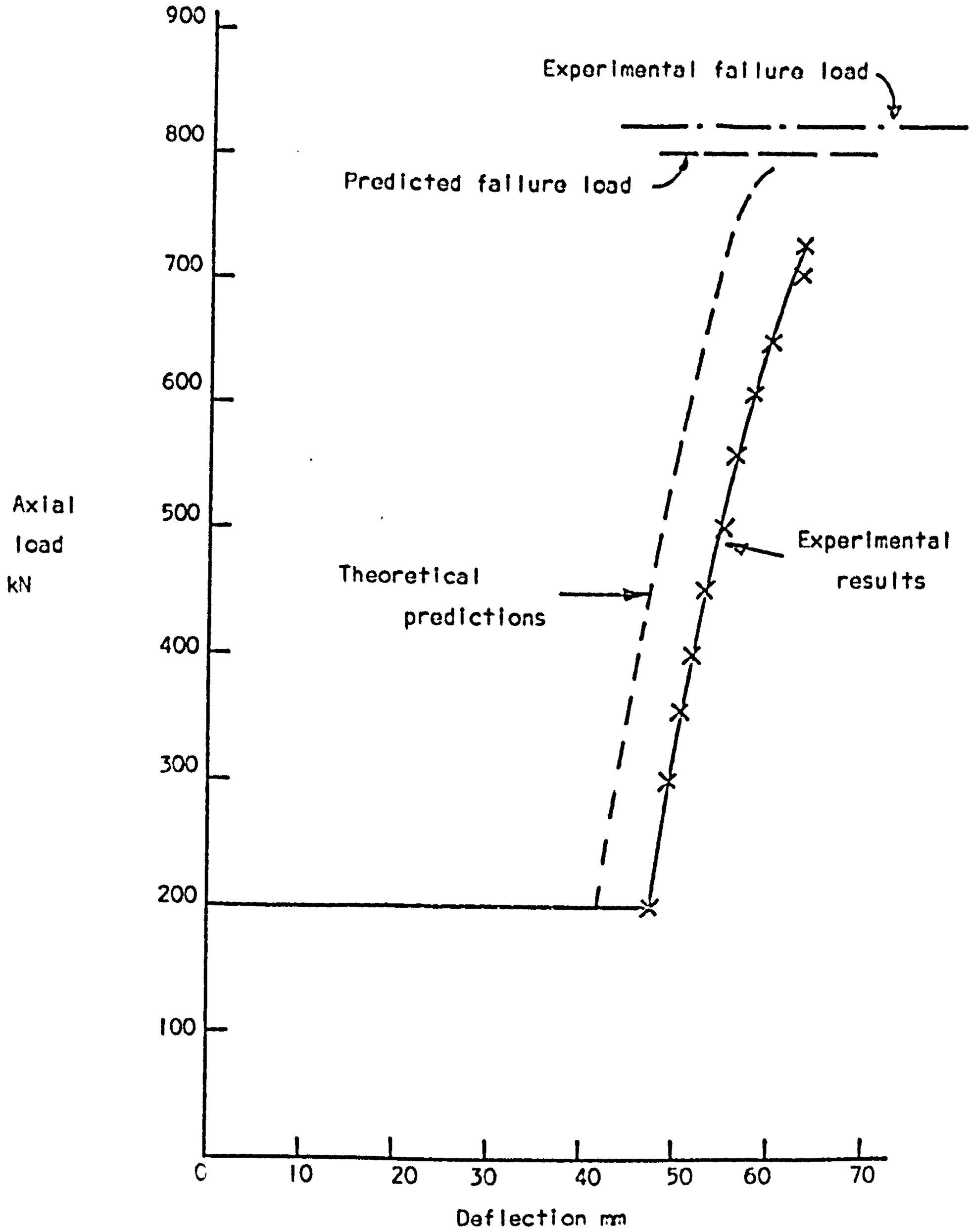

FIG. 6.16 COLUMN RC5 COMPARISON OF DEFLECTIONS AT MID-HEIGHT

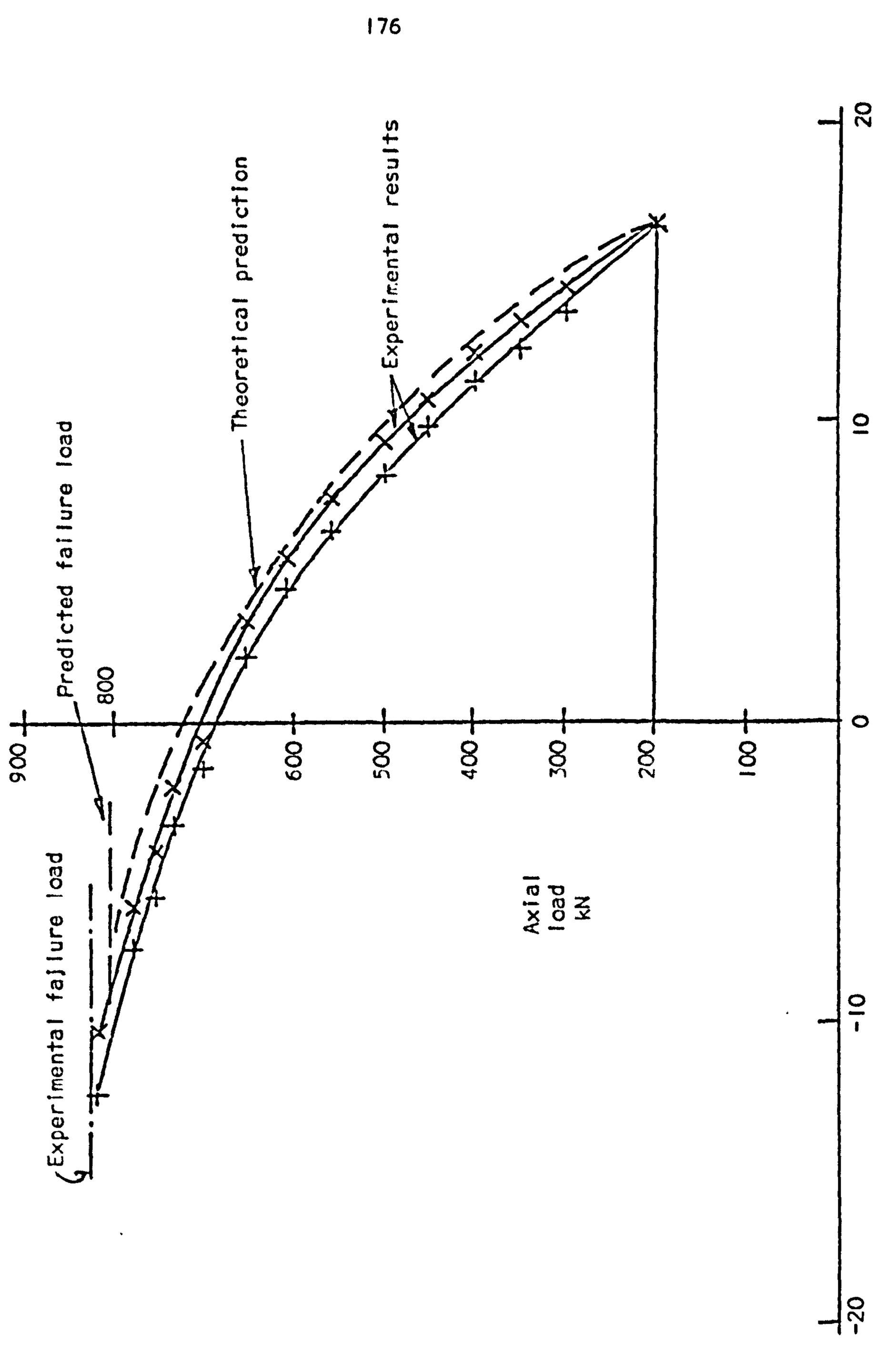

FIG. 6.17 COLUMN RC5 END-MOMENT-AXIAL LOAD CURVES

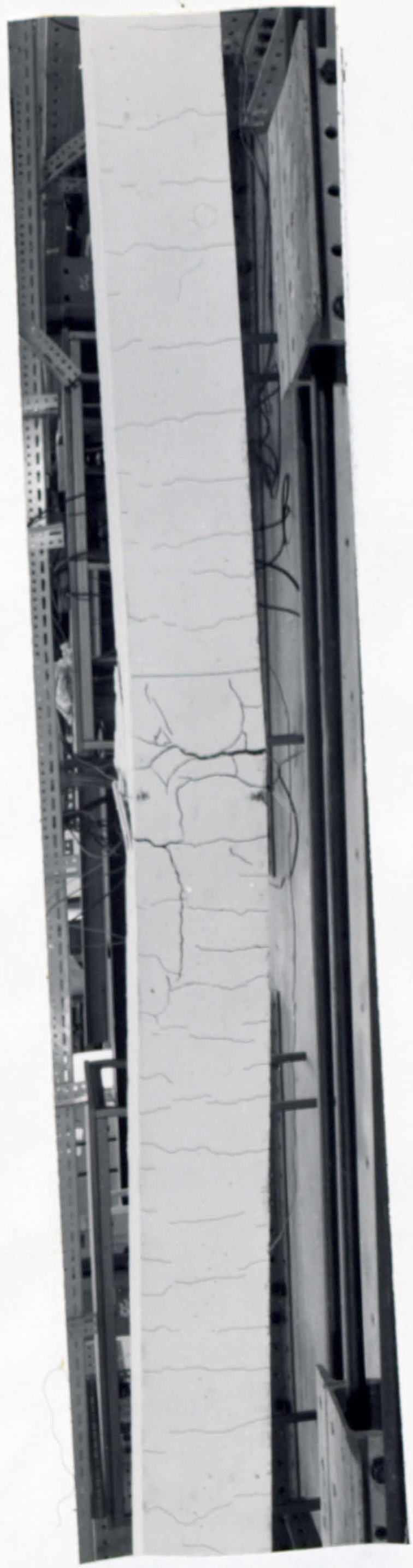

FIG. 6.18 COLUMN RC5 - FINAL DEFLECTED SHAPE VIEWED ABOUT MINOR AXIS

FIG. 6.19 COLUMN RC5 - EXTENT OF CRACKING NEAR BEAM-COLUMN JOINT

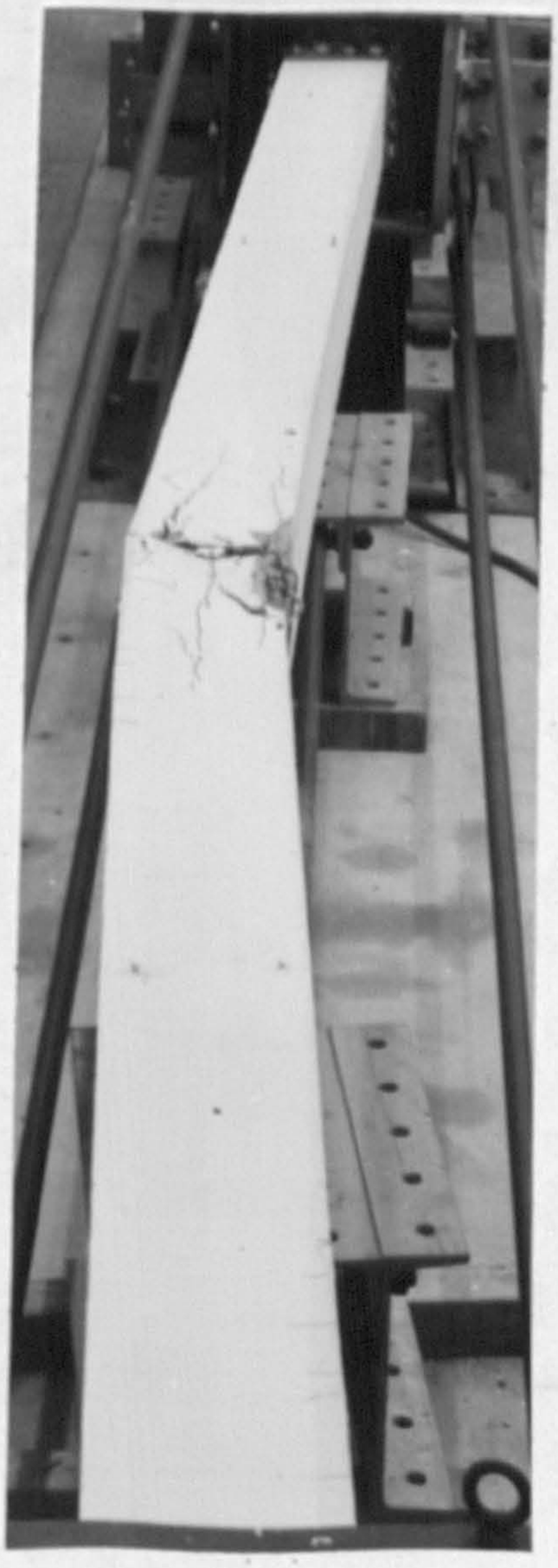

FIG. 6.20 COLUMN RC5 FINAL DEFLECTED SHAPE VIEWED ABOUT MAJOR AXIS.

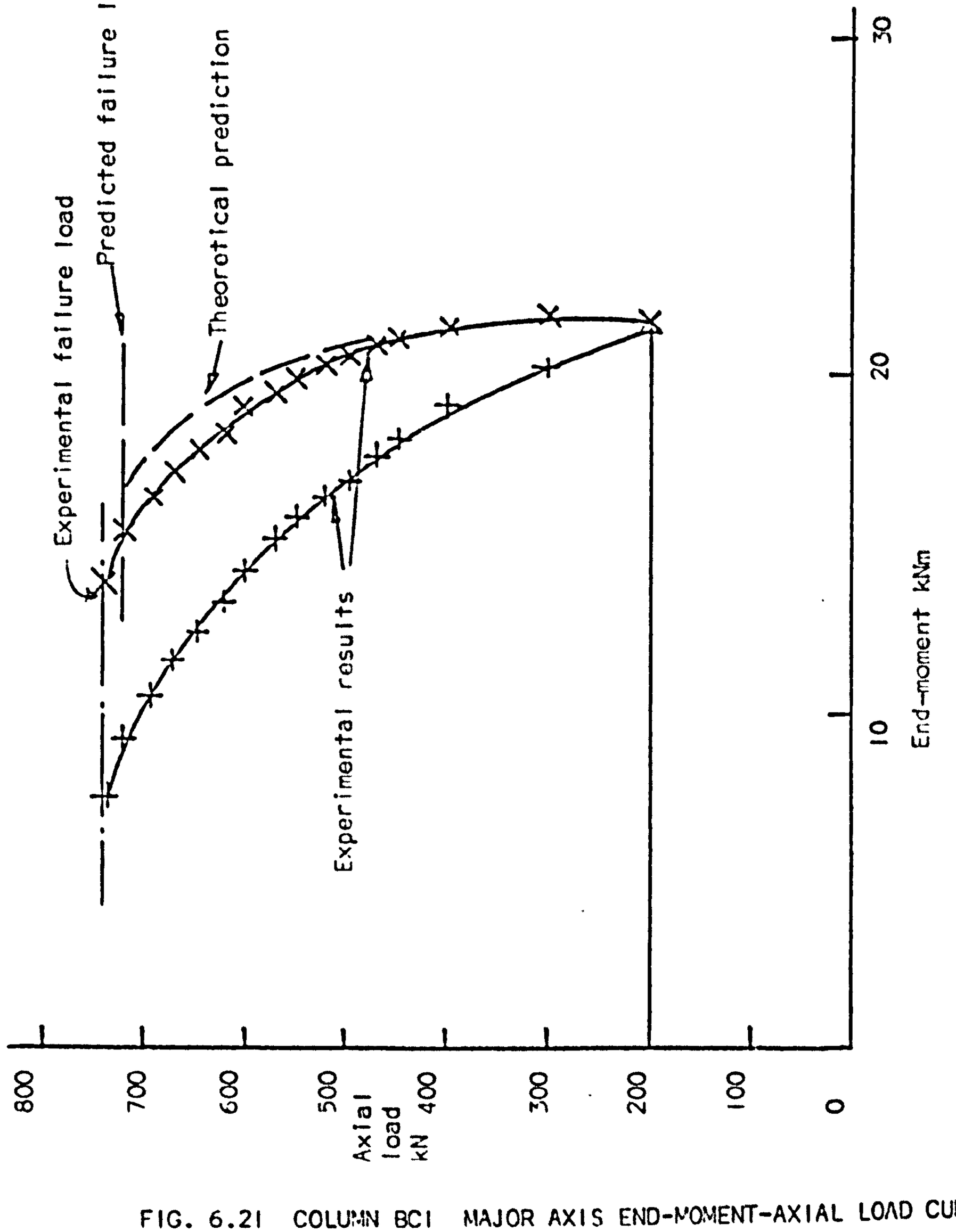

FIG. 6.21 COLUMN BC1 MAJOR AXIS END-MOMENT-AXIAL LOAD CURVES

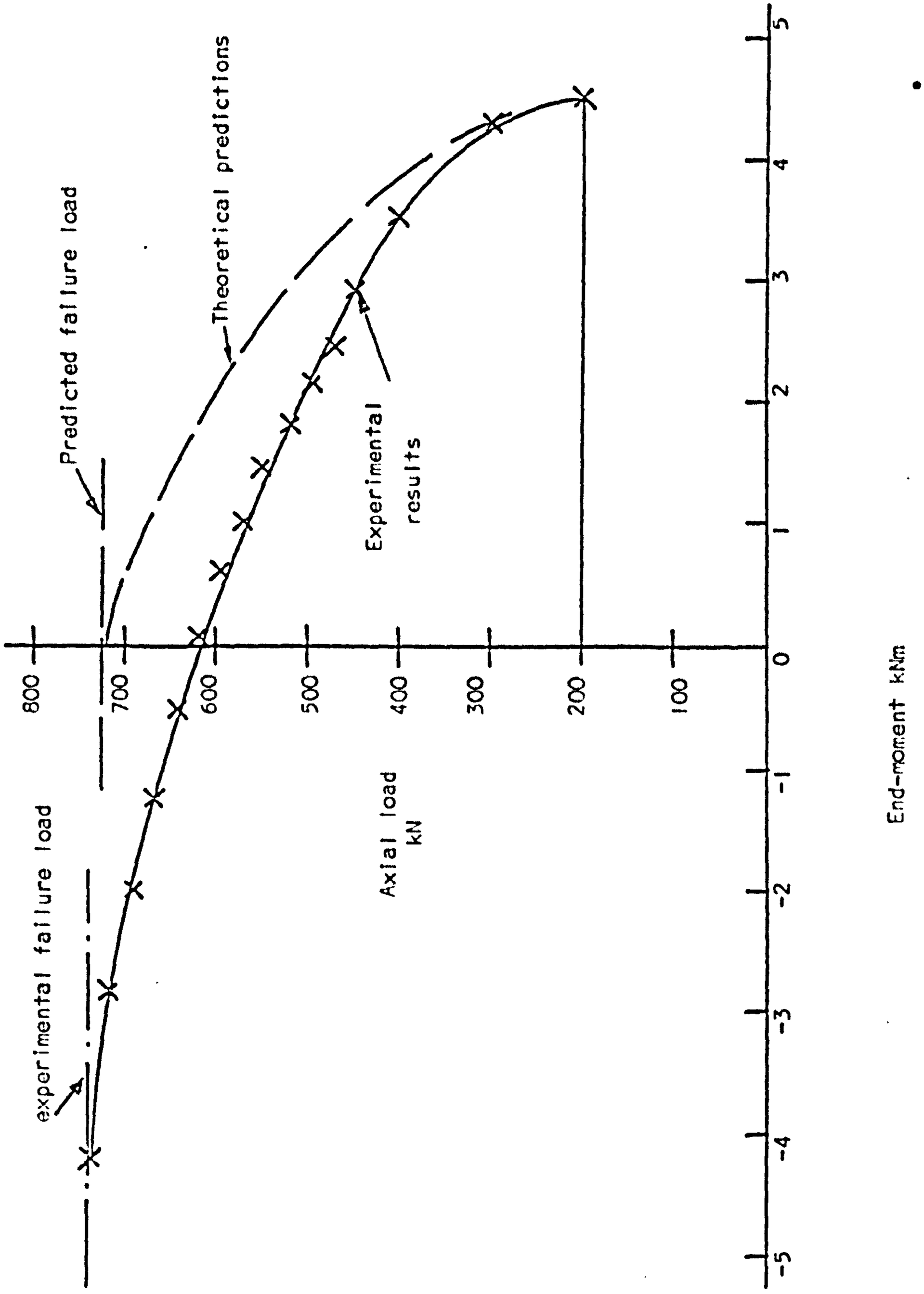

FIG. 6.22 COLUMN BC1 MINOR AXIS END-MOMENT-AXIAL LOAD CURVES

FIG. 6.23 COLUMN BC1 FINAL DEFLECTED SHAPE VIEWED ABOUT MAJOR AXIS

FIG. 6.24 COLUMN BC1 DETAIL OF HINGE

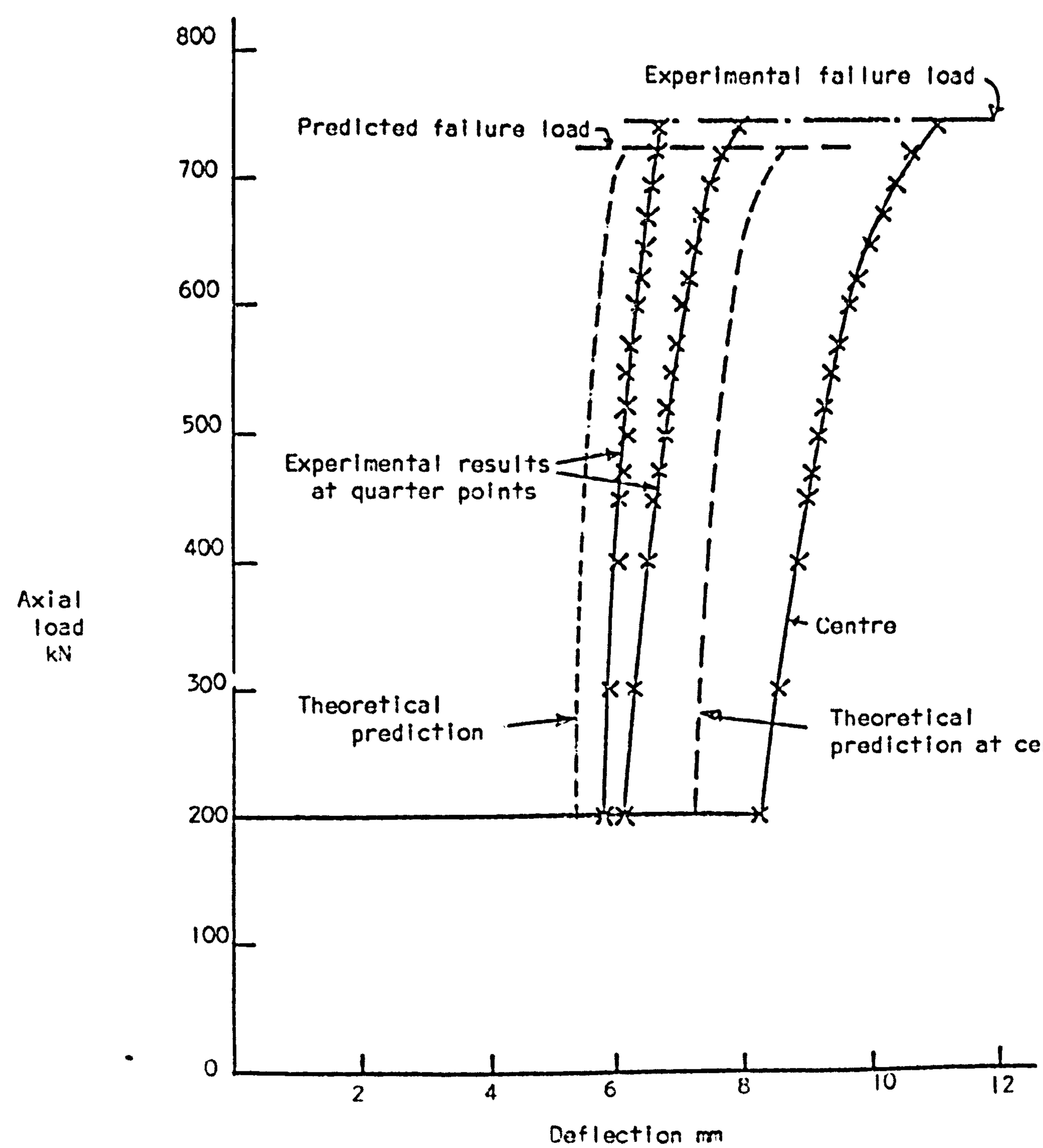

FIG. 6.25 COLUMN BC1 COMPARISON OF MAJOR AXIS DEFLECTIONS

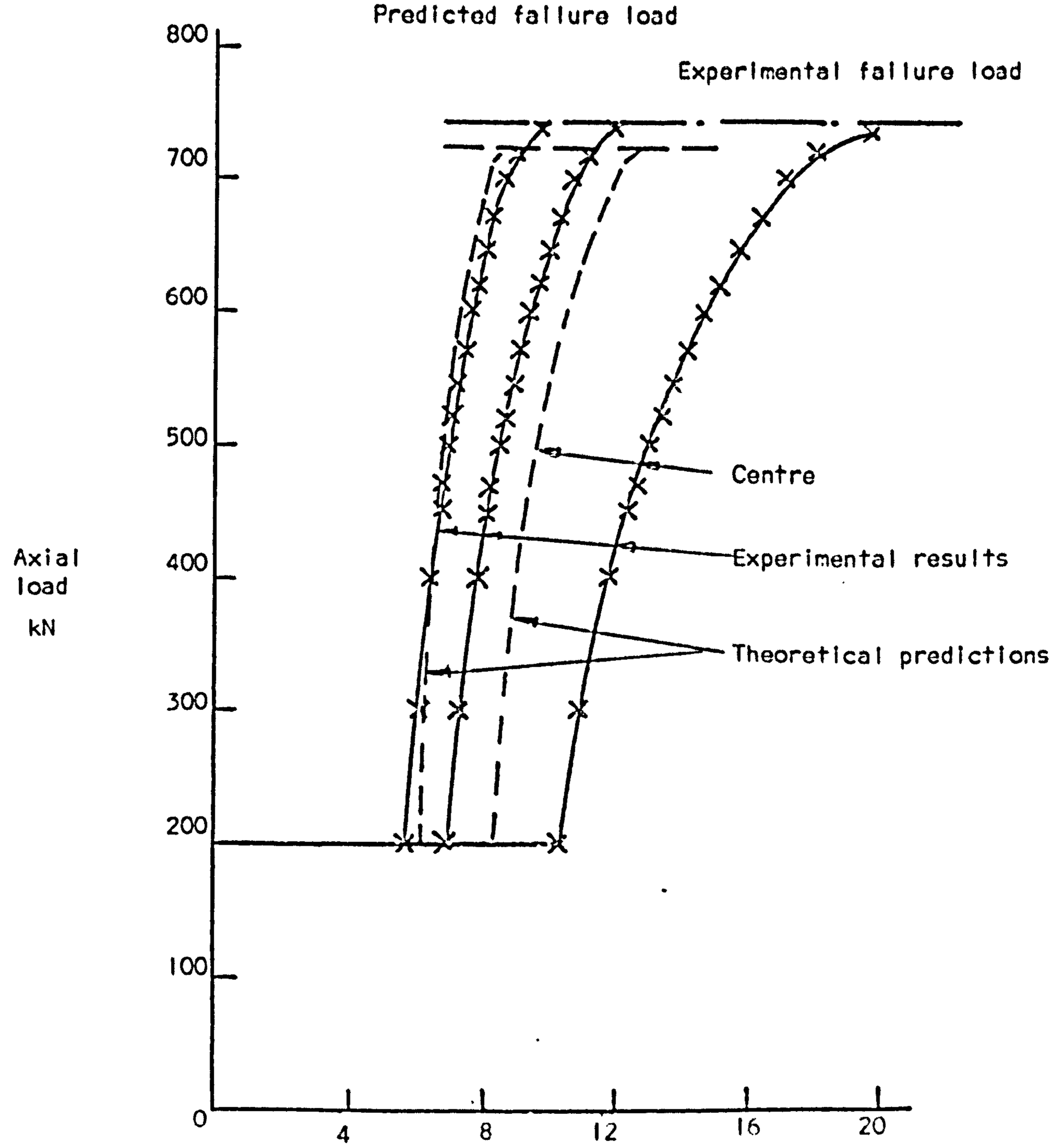

FIG. 6.26 COLUMN BC1 COMPARISON OF MINOR AXIS DEFLECTIONS

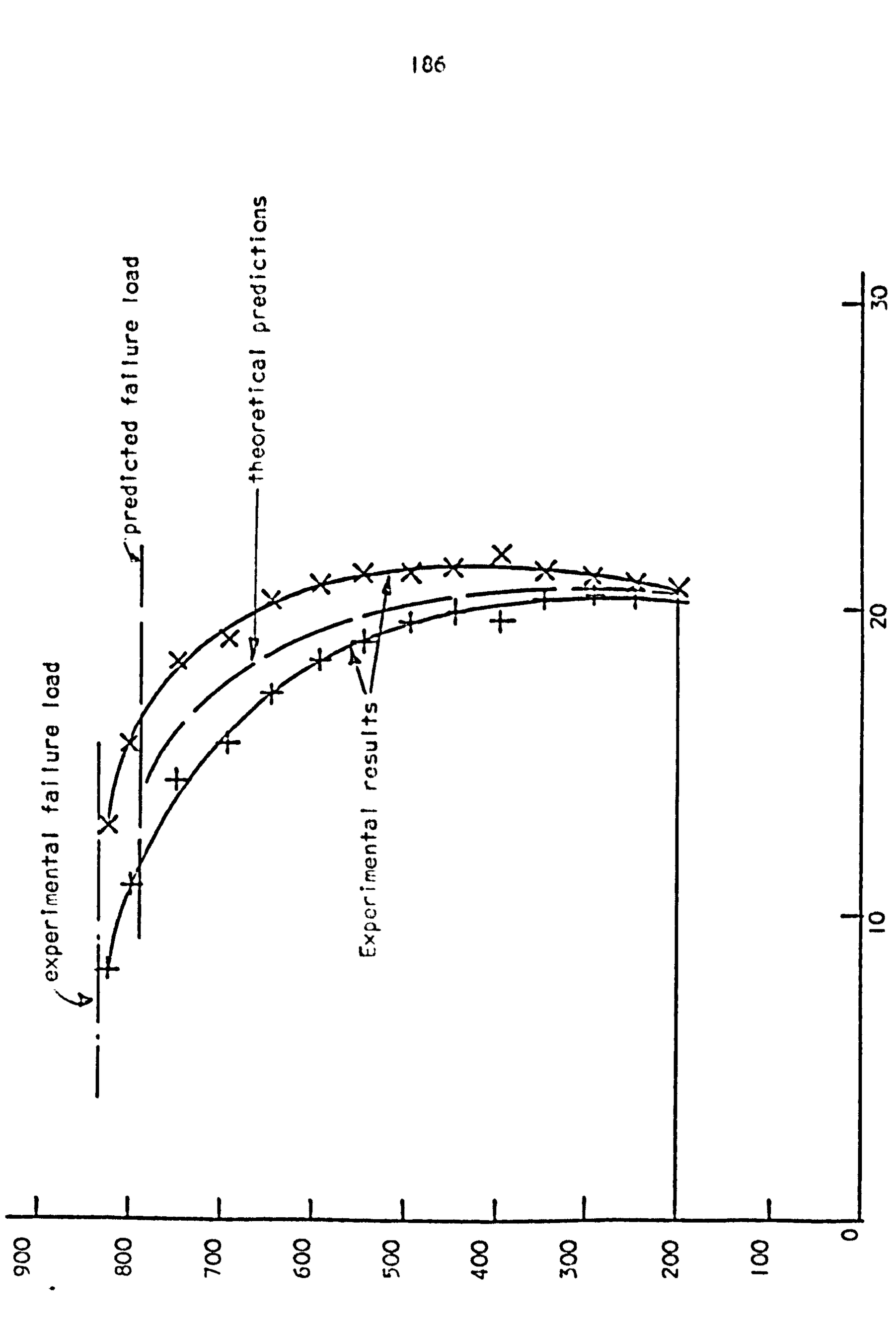

FIG. 6.27 COLUMN BC2 MAJOR AXIS END-MOMENT-AXIAL LOAD CURVES

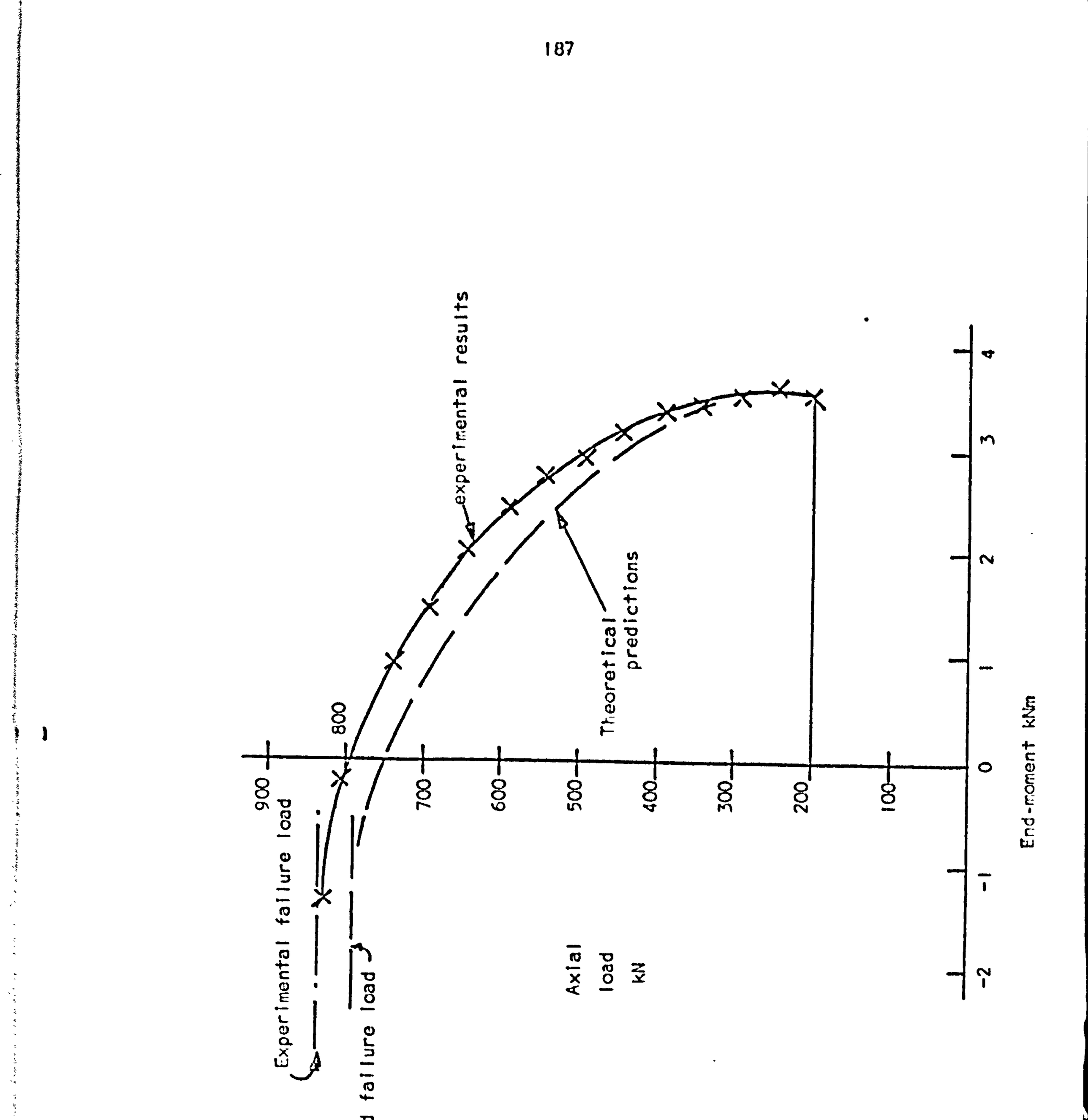

FIG. 6.28 COLUMN BC2 MINOR AXIS END-MOMENT-AXIAL LOAD CURVES

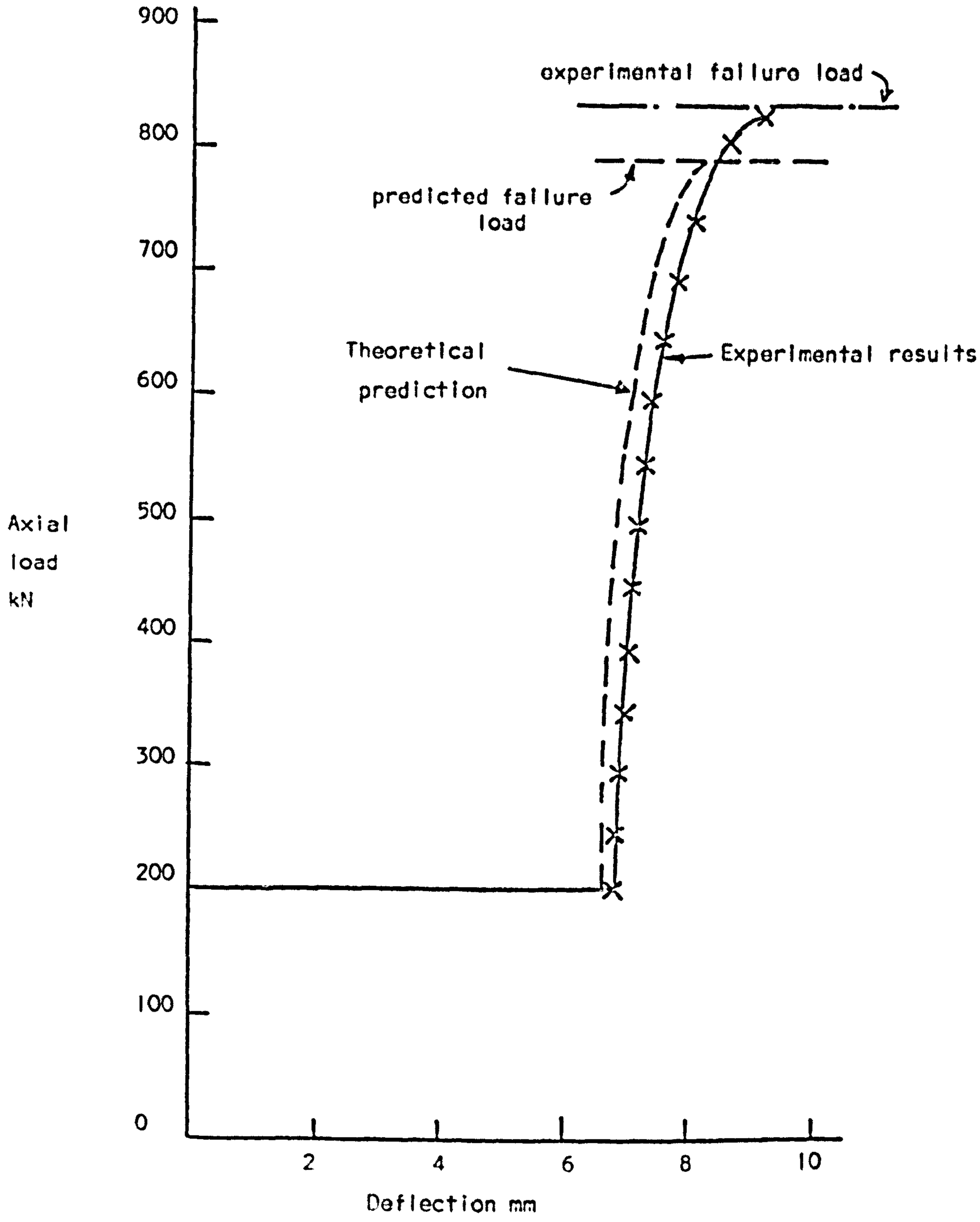

FIG. 6.29 COLUMN BC2 COMPARISON OF MAJOR AXIS DEFLECTIONS AT MID-HEIGHT

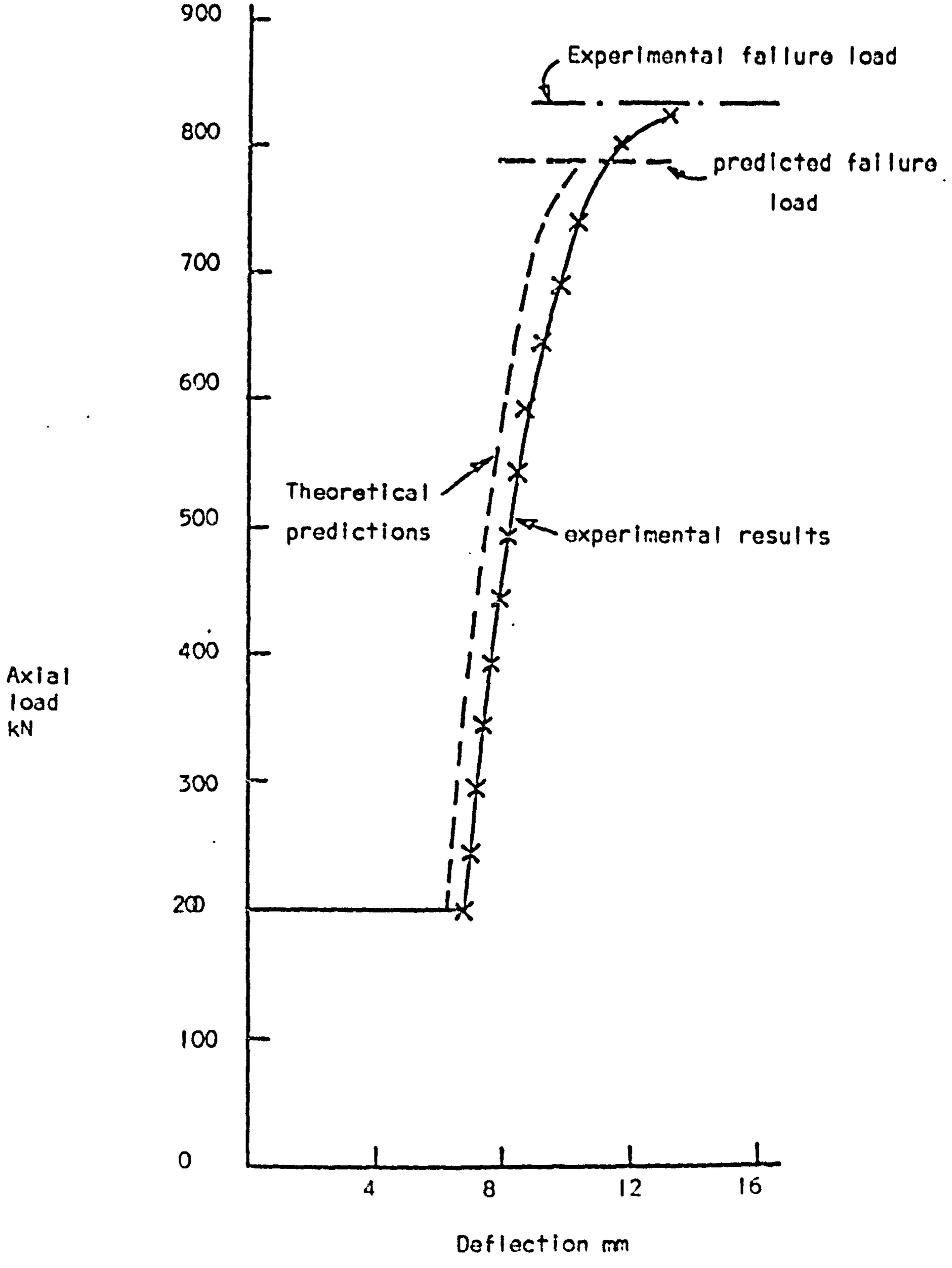

FIG. 6.30 COLUMN BC2 COMPARISON OF MINOR AXIS DEFLECTIONS AT MID-HEIGHT

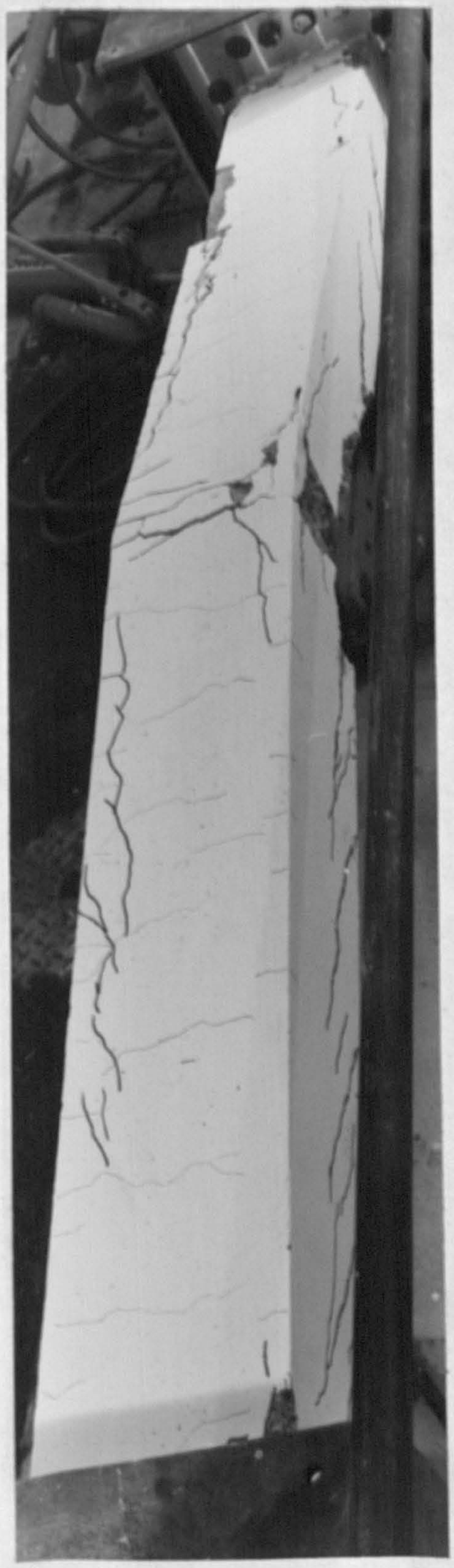

FIG. 6.31 COLUMN BC2 - CRUSHING DUE TO RESTRAINING MOMENTS

FIG. 6.32 COLUMN BC2. GENERAL VIEW OF HINGE AND CRUSHING.

FIG. 6.33 COLUMN BC2 GENERAL VIEW OF FAILURE OF COLUMN

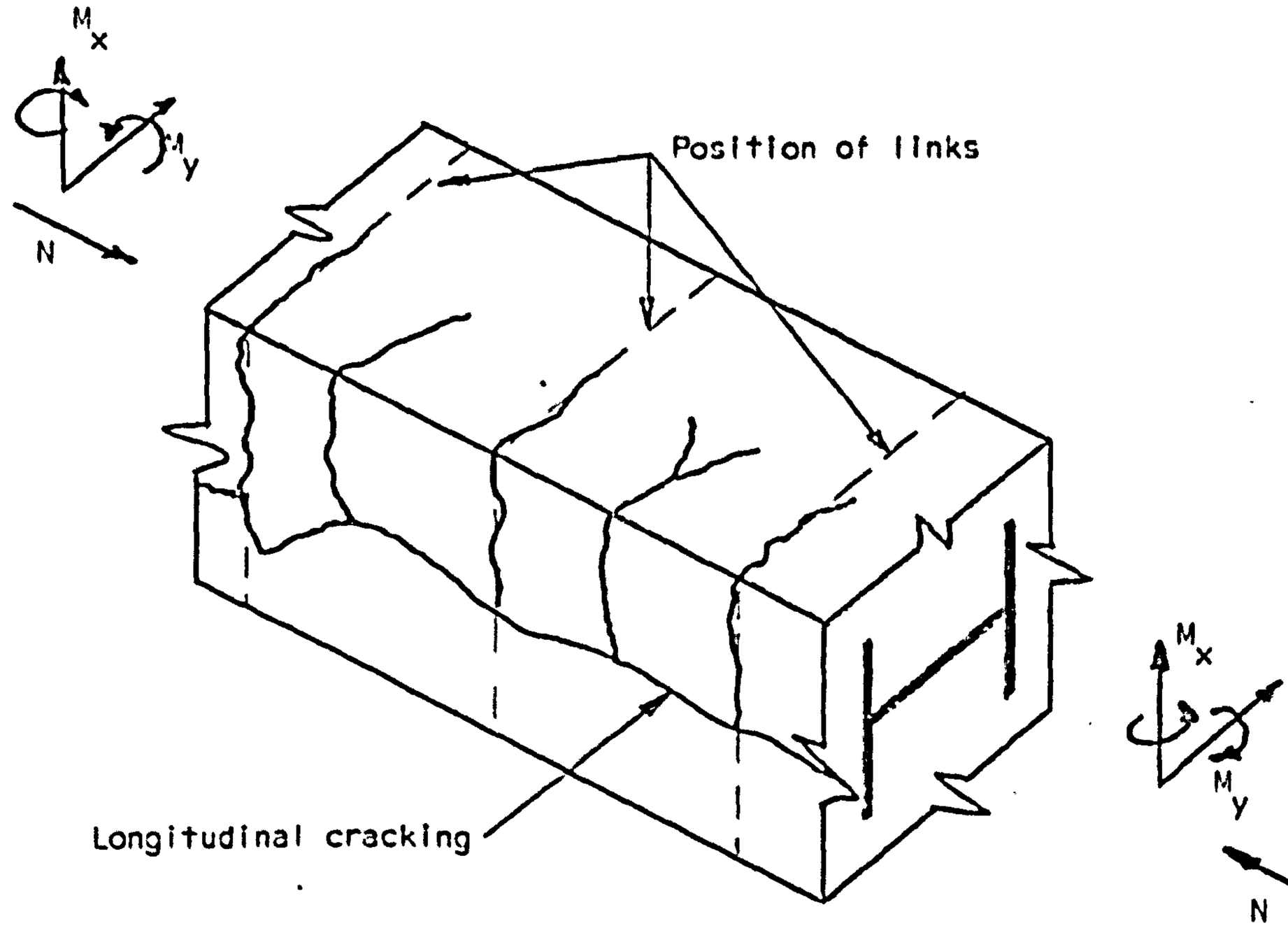

FIG. 6.34 TYPICAL CRACK PATTERN AFTER APPLICATION OF BOTH MAJOR AND MINOR AXIS MOMENTS.

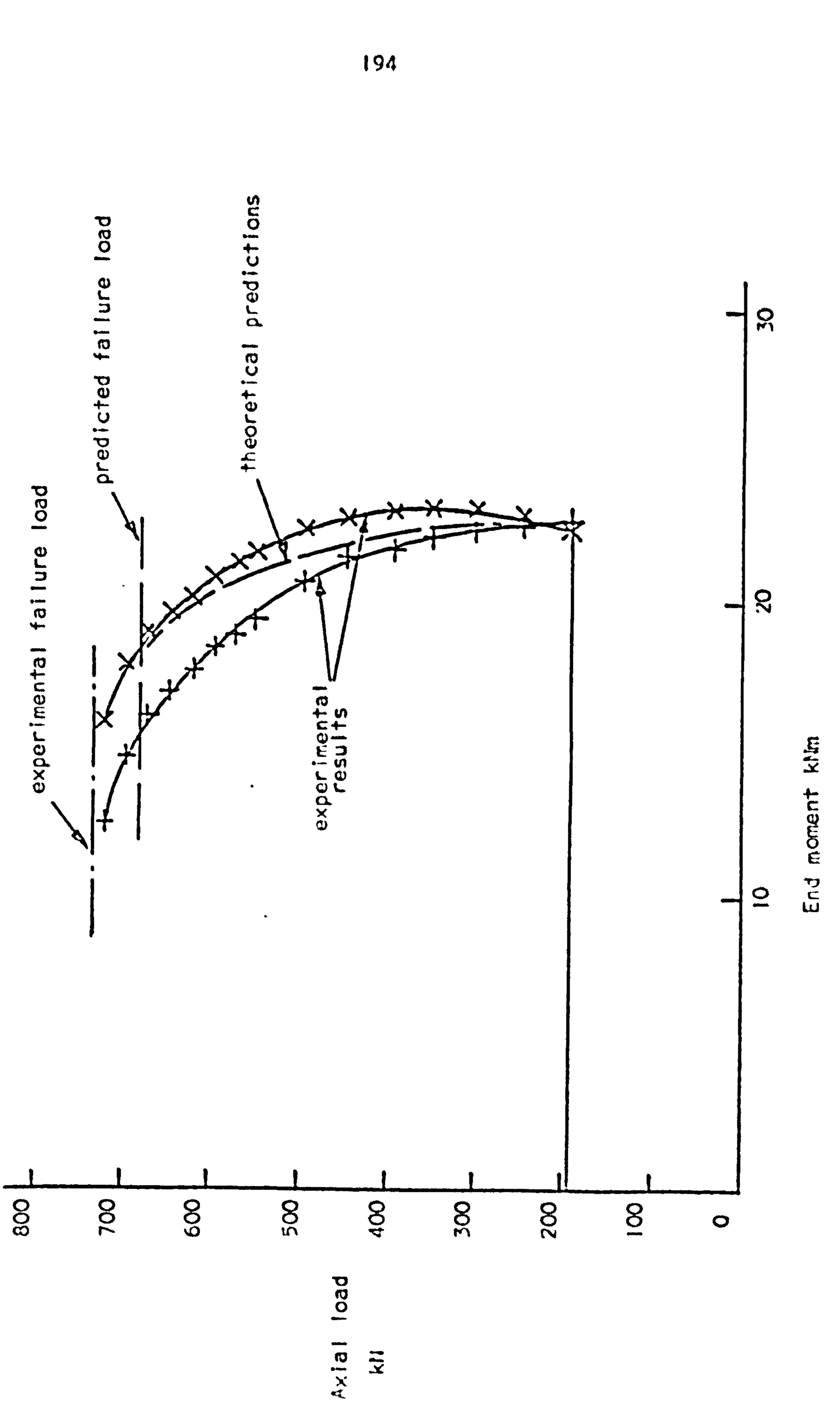

FIG.6.35 COLUMN BC3 MAJOR AXIS END-MOMENT-AXIAL LOAD CURVES

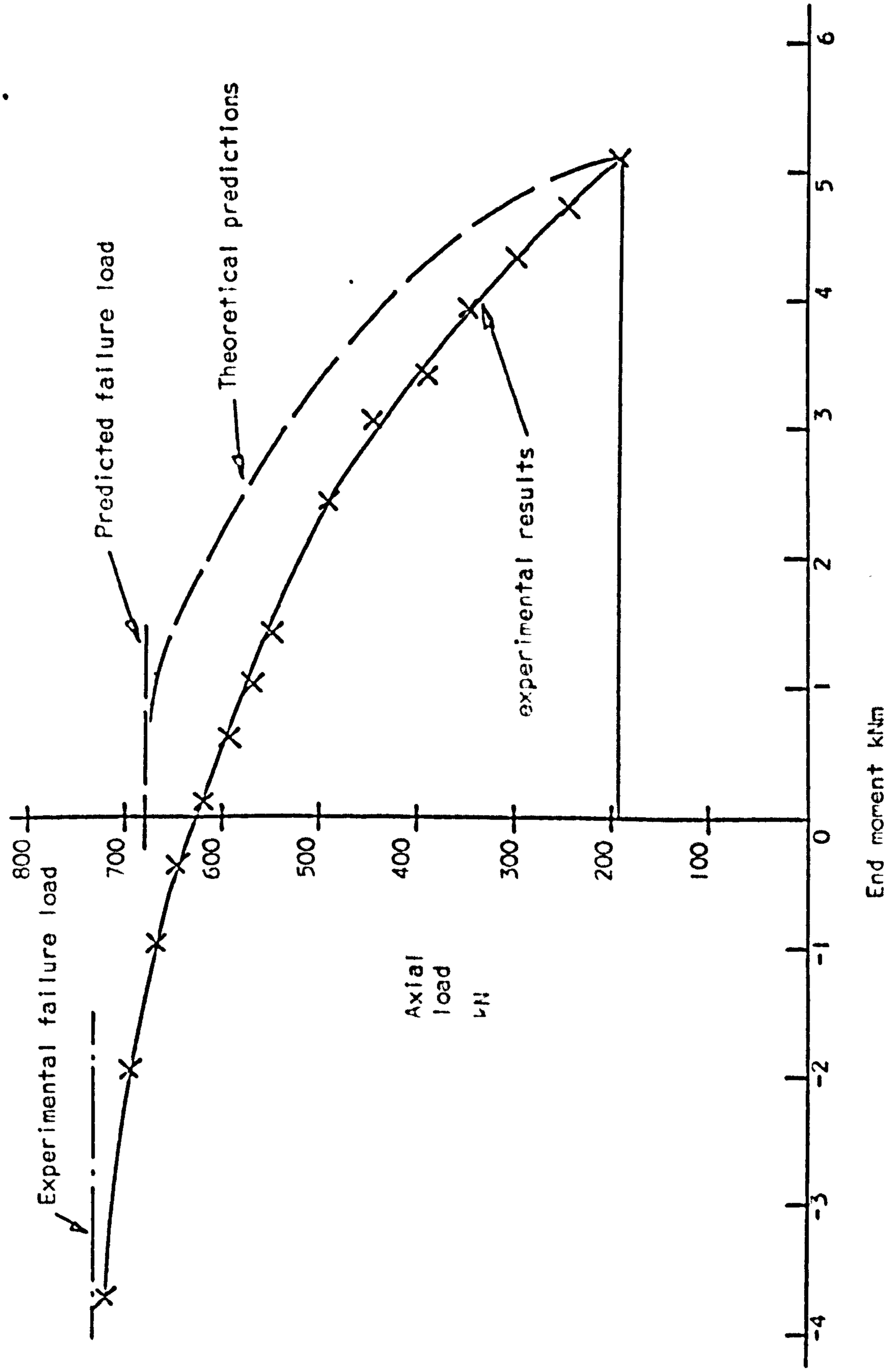

FIG. 6.36 COLUMN BC3 MINOR AXIS END-MOMENT-AXIAL LOAD CURVES

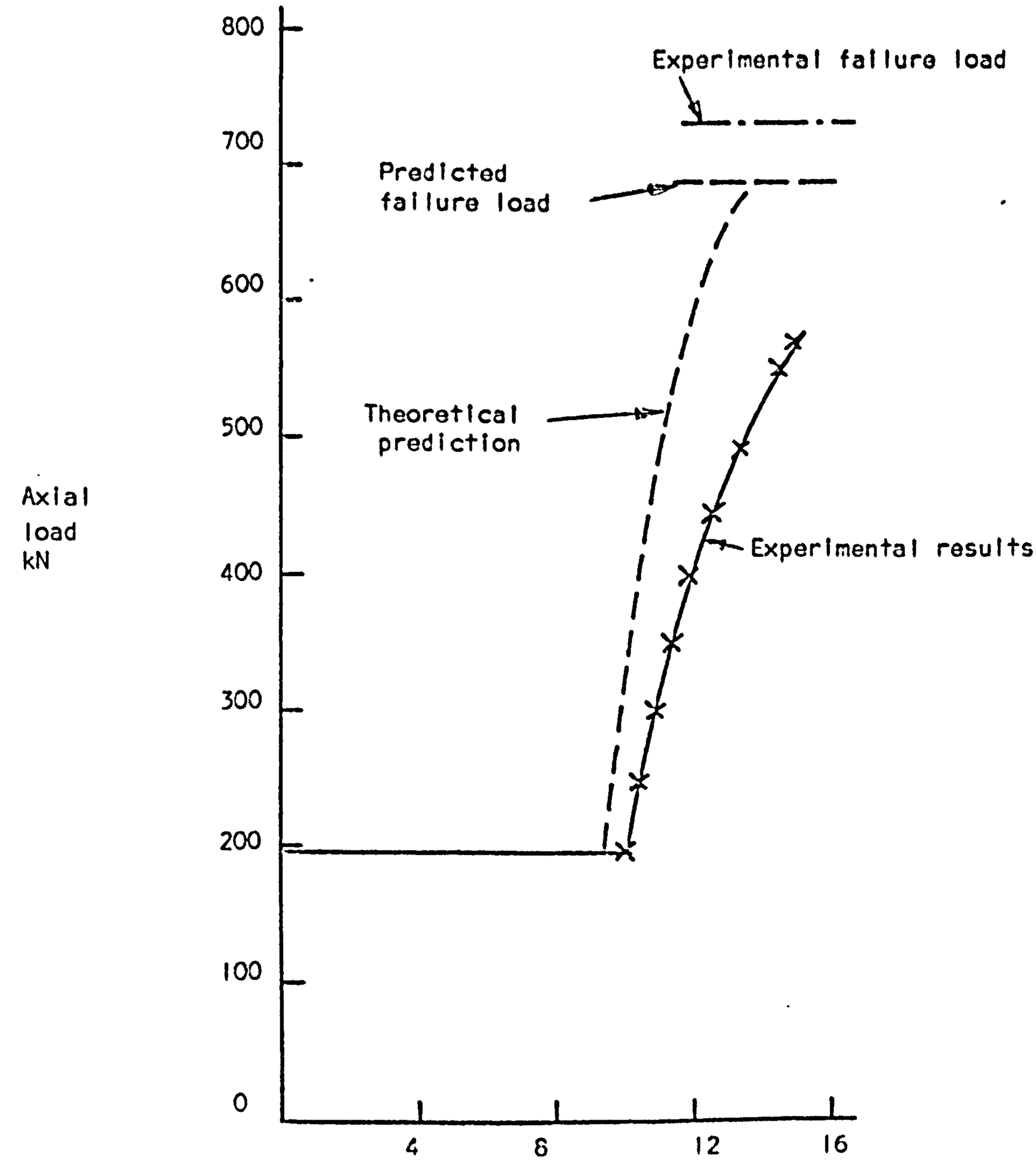

FIG. 6.37 COLUMN BC3 COMPARISON OF MINOR AXIS DEFLECTIONS AT MID-HEIGHT

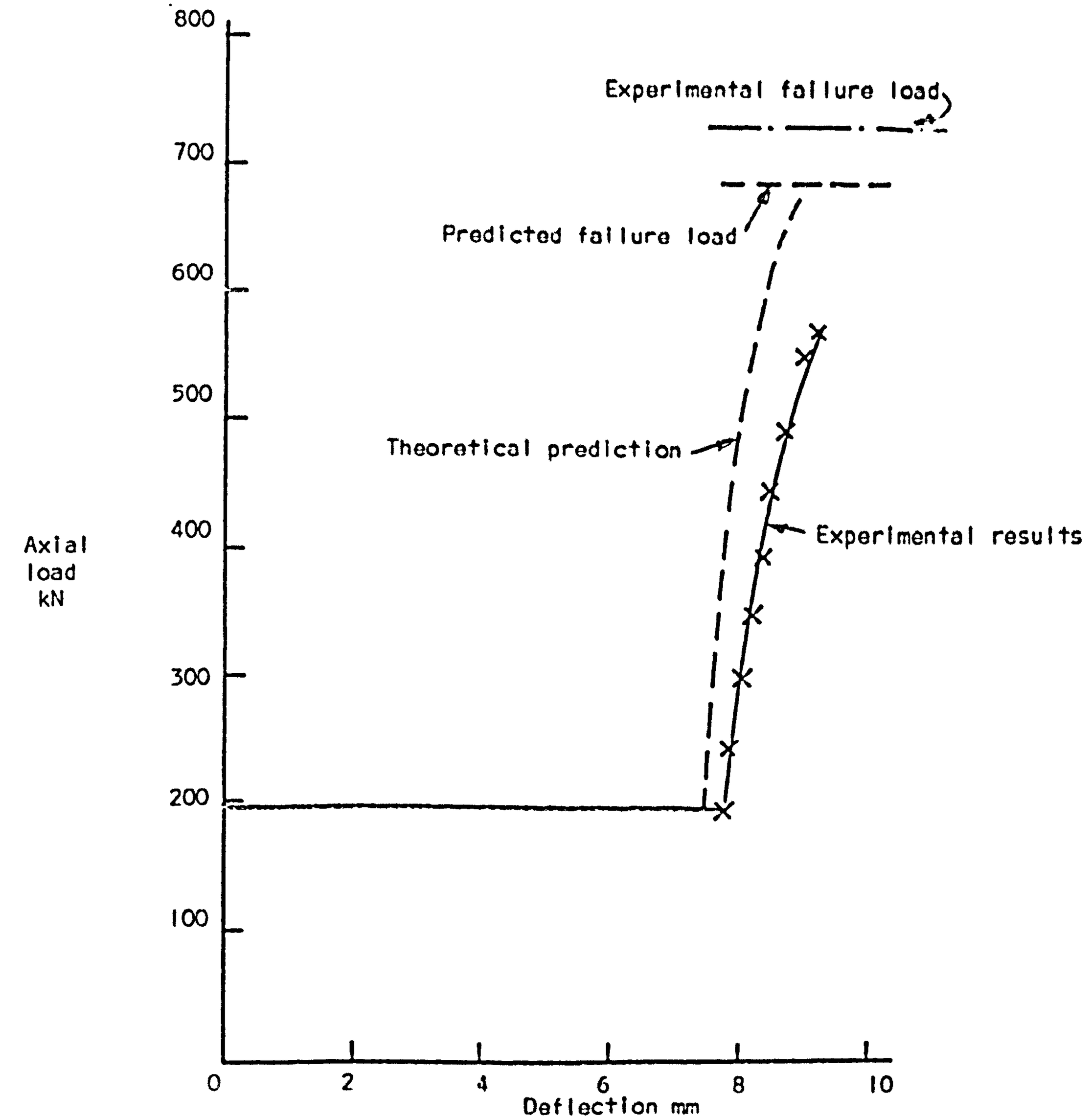

FIG. 6.38 COLUMN BC3 COMPARISON OF MAJOR AXIS DEFLECTIONS AT MID-HEIGHT

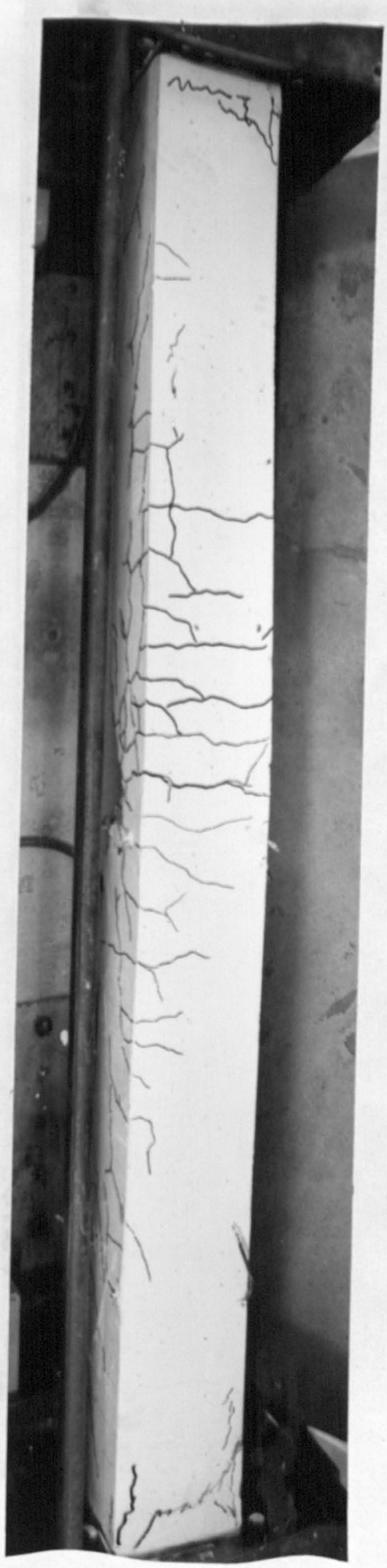

FIG.6.39 COLUMN BC3 VIEW ABOUT MINOR AXIS SHOWING CRUSHING AT ENDS.

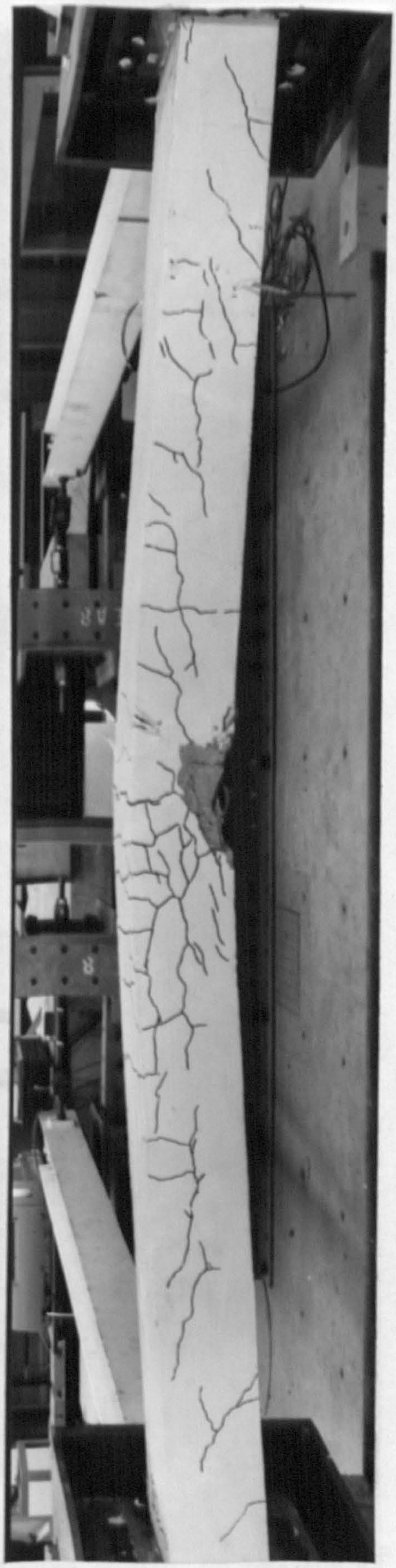

FIG. 6.40 COLUMN BC3 VIEW ABOUT MAJOR AXIS

FIG. 6.41 COLUMN BC3 VIEW ABOUT MAJOR AXIS SHOWING EXTENSIVE CRUSHING

CHAPTER 7. COMPARISON OF THEORETICAL PREDICTIONS AND TEST RESULTS.

7.1 Introduction

The computer program described in Chapter 2 was used to give theoretical predictions of the behaviour of the columns tested. The results of the analyses and details of the comparisons with the test results are given in this Chapter.

7.2 Parameters used in theoretical predictions.

The stress-strain curves used for the steel and the concrete used in the test columns are those given in Chapter 2. The values of yield stress and yield strain for the steel are the average of those obtained from the tension tests and are given in Table 7.1.

The value of maximum concrete stress, σ_u Fig. 2.1, is obtained by multiplying the average stress obtained from the cube tests, Table 5.3, by a factor, K.

Various investigators[54,76] have shown that this factor, K, should consist of two parts, K_1 and K_2 such that

$$K = K_1 \times K_2 \qquad (7.1)$$

where K_1 is a coefficient to relate the 6" cube strength to the strength in uniform compression, which is similar to the cylinder strength, and is equal to about 0.8.

K_2 is a coefficient to allow for variability of concrete strength in a column due partly to migration of water up the column as it is being poured, and partly variations due to poor compaction etc. This factor is usually taken to be equal to about 0.8. Because the columns were cast horizontally in the laboratory and

special care was taken with compaction K_2 has been taken as equal to 1.

For the analysis of the test specimens the value of K was reduced to 0.8/1.05, or 0.76, on the assumption[77] that the strength of a 100 mm cube is 5 per cent higher than that of a 6 in. cube of the same concrete.

The strain at maximum stress is assumed to be 0.0025 and maximum strain is 0.0035.

The concrete was assumed to have a tensile stress strain curve given by

$$\frac{\sigma}{\sigma_u} = C_1 \frac{\epsilon}{\epsilon_u} \qquad (7.2)$$

where

$$\epsilon \geq -0.0001$$

and C_1 is a coefficient as defined in Equation 2.1.

Values of all the main parameters used in the theoretical analyses are given in Table 7.1. Dimensions of the steel cross-section used are given in Table 5.4.

The longitudinal reinforcement was ignored in the analyses, the effect of this is discussed in Section 7.4.

7.3 Discussion of the behaviour of individual tests.

The theoretical predictions of the behaviour of columns RC1 to RC3 and RC5 during testing have been obtained from a computer program, as described in Chapter 2, which ignores out of plane effects. This was because in these tests the loading was only about the one

axis, i.e. that with the restraint. In the biaxial tests, BC1, BC2 and BC3 the biaxial analysis was used. In test RC4 although restrained and loaded about one axis, only, failure was due to instability about the other axis and both biaxial and uniaxial analyses were used.

7.3.1 Column RC1

Fig. 6.2 shows good agreement between the experimental and theoretically predicted deflections at quarter points. The moments at the column ends, Fig. 6.1, agree well with the theory for end 1 the theoretical values being slightly higher. The agreement for end 2 is not as good, the difference in the moments at ends 1 and 2 being due, probably, to variation in the stiffness along the column due to variation in concrete quality. The ultimate loads are given in Table 7.2 and agreement is very good.

7.3.2 Column RC2.

Column RC2 was initially loaded with moments and axial load to a level of 950 kN. The column was then unloaded and reloaded until failure occurred.

Agreement between the experimental and theoretical deflections is good, Fig. 6.5 as it was for column RC1.

The theoretically predicted moments, Fig. 6.4, tend to be slightly lower than those obtained in the test partly due to the fact that the theoretical failure load is 4% lower than the failure load obtained in the test, Table 7.2.

7.3.3 Column RC3

Column RC3 was loaded in such a way as to keep cracking to a minimum. The predicted ultimate load is 18% lower than the failure load in the test and thus deflections and moments Fig. 6.7 and Fig. 6.8 are not in as good agreement as in RC1 and RC2.

This may be partly due to the average cube strength being reduced by two low results from Batch 2, Table 5.3. If these results are ignored in the calculation of the average and the new figure used in the analysis an increase in ultimate strength of up to 8% could be expected. Other reasons for differences between experimental and theoretical results are given in Section 7.4.

7.3.4 Column RC4

This column was analysed using

(a) The uniaxial in plane analysis about the major axis and (b) the biaxial analysis.

To attempt to quantify the effect of the minor axis self weight, imperfections, and eccentricity of loading, estimations of the initial midspan deflection were made. Obviously the use of the uniaxial analysis is equivalent to an initial deflection of zero although the minor axis buckling load is not calculated.

Other central initial deflections used in the analysis were 1.0 mm and 2.5 mm and the results are shown on Fig. 6.11.

The effect of different minor axis initial deflections on the major axis deflections and end moments is not significant Figs.6.12, and 6.13 and compare favourably with those obtained from

the tests except near to failure.

However, the effect on the additional deflection about the minor axis is very marked.

7.3.5 Column RC5

The minor axis deflections, Fig. 6.16, do not agree very well the theoretical predictions which are up to 15% smaller. However at the level of moment tested a small additional moment gives a large increase in deflection.

The theoretical and experimental end-moments, Fig. 6.17, agree extremely well.

The failure load obtained from the computer analysis, Table 7.2, is about 3% less than that obtained in the test.

7.3.6 Columns BC1, BC2, and BC3

Since the three biaxial tests BC1, BC2 and BC3 were of a similar nature the discussion covers all 3 columns unless specifically stated otherwise.

The agreement between deflections, Figs. 6.25, 6.26, 6.29, 6.30. 6.39, and 6.38, obtained from the tests and those from the theoretical predictions is generally reasonable especially major axis deflections. The minor axis deflections in test BC3, Fig. 6.37, are however underestimated by about 4 mm, about 30%.

Agreement between end moments is good, Figs. 6.29, 6.22, 6.27, 6.28, 6.35, 6.36. The difference between the two major axis end-moments from any of the three tests again indicates the variation

in stiffness along the column length due to differences in concrete strength, compaction etc.

The test and theoretical ultimate loads, Table 7.2, are in reasonable agreement.

7.4 General discussion and conclusions of test and computer results.

The deflections and end-moments obtained from the computer analyses and the tests are in broad agreement. The failure loads obtained from the computer analysis are generally conservative, Table 7.2, but in reasonable agreement.

In Chapter 6 the possible sources of error in the test results, measurement errors, misalignment errors and rig defects, were considered. Errors can be introduced into the theoretical results because of the assumptions made for the computer analyses. These assumptions and their possible effect on the results are now considered.

(a) The reinforcement in the cross-section has been ignored in the computer analyses. The area is, however, only about 2% of the cross sectional area of the steel section and the reinforcement is placed within the flanges, Fig. 5.1. The effect of inclusion of the reinforcement in the analysis would be an increase and the failure load of less than 2%.

(b) The self weight of the column has been ignored in the analyses. In tests RC1, RC2, and RC3 this would cause a moment about the minor axis, failure however was a predominantly major axis

failure due to major axis loading followed, after the formation of the hinge, by a minor axis "snap-through". Columns RC1 and RC3 finally failed upwards, i.e. against the self weight.

Column RC4 was an out of plane failure and also failed upwards. This upwards failure was probably due to a small eccentricity of loading and initial imperfections. An attempt has been made to compensate for the effects of self weight, eccentricity of loading, and initial imperfections by the use of an initially deflected shape.

Column RC5 failed predominantly in the plane of loadings, the minor axis, and only deflected appreciably about the major axis very close to failure.

The effects of self weight in the biaxial column tests are much less marked because of loading and restraint in that plane. The self weight moment is of the order of 2% of the ultimate moment of the section.

(c) The residual stresses in the steel section have been ignored. Virdi[54] has shown that neither the AISC pattern[78] nor the Cambridge[75] pattern of residual stresses make much difference to the moment-curvature relationships. The measured residual stresses are not so onerous as the Cambridge pattern, Fig. 5.6, and thus the effect will be very small.

(d) The assumption that the concrete stress reduction factor is 0.75 may be conservative. Basu[48] used 0.8 with 6" concrete cube test results to analyse available tests and found it to give reasonable results. Virdi[48], however, used 0.64 is with 6"

concrete cube test results to analyse his biaxial test results. However, the specimens used by Virdi were cast vertically which may have led to larger variations of strength along the column due to migration of water etc.

(e) The calculation of the stiffness of the beams has been carried out using values from the B.C.S.A. Handbook on Structural Steelwork[79] and hence a small variation in the stiffness values may exist.

It can be seen from the above list of possible causes of errors that the one most likely to affect the results is the value of K, the concrete stress reduction factor.

PARAMETER	COLUMN NUMBER							
	RC1	RC2	RC3	RC4	RC5	BC1	BC2	BC3
	← Uniaxial restraint & loading →					← Biaxial →		
Length mm	2600	2600	2600	5300	5300	2600	2600	2600
Beam stiffness $\frac{EI}{L}$ Major Nmm	4.65×10^9	4.65×10^9	4.65×10^9	4.65×10^9	-	2.2×10^9	2.2×10^9	2.2×10^9
Minor Nmm	-	-	-	-	4.65×10^9	0.42×10^9	0.42×10^9	0.42×10^9
Fixed end moment								
Major End 1 Nmm	212×10^6	197×10^6	275×10^6	497×10^6	-	122×10^6	115×10^6	129×10^6
Major End 2 Nmm		267×10^6						
Minor Nmm	-	-	-	-	550×10^6	30×10^6	23×10^6	35×10^6
Maximum initial def.mm	+1	+0.5	-0.5	maj. +1.5 min. varies	+.25	0	0	0
Maximum concrete stress N/mm^2	27.7	23.0	22.3	32.8	27.6	22.2	21.2	23.1
Steel yield stress N/mm^2	← 288 →					← 277 →		
Steel yield strain	← .0014 →					← .00135 →		

TABLE 7.1 VALUES OF PARAMETERS AND IN ANALYSIS.

TEST NO.	SQUASH LOAD N_{sq} kN	TEST FAILURE LOAD N_f kN	CALCULATED FAILURE LOAD N_c kN	N_f/N_c	N_f/N_{sq}
RC1	1861	1340	1350	0.99	0.72
RC2	1687	1270	1223	1.04	0.75
RC3	1694	1360	1152	1.18	0.80
RC4	2050	850	712	1.19	0.41
RC5	1860	825	803	1.03	0.43
BC1	1216	742	725	1.02	0.61
BC2	1191	834	790	1.06	0.70
BC3	1240	730	685	1.07	0.59
			Mean	1.07	
			Standard deviation	0.065	

TABLE 7.2 COMPARISON OF THEORETICAL AND EXPERIMENTAL FAILURE LOADS

CHAPTER 8. DESIGN METHODS FOR COMPOSITE COLUMNS

8.1 Introduction

Much research effort has been directed towards the problem of the determination of the ultimate load of an isolated pin-ended composite column with axial load and applied end-moments. The closest classification in Horne's chart, Fig. 1.2, is $P_x P_y$ although, since the object of previous investigations has been to produce a design method[50] for isolated columns, in none of these investigations has compatibility with plastically designed beams been checked.

The purpose of this Chapter is to investigate possible design methods for composite columns which form part of a rigid jointed frame. Three main areas are dealt with:

Section 8.2: The use of plastically designed beams and composite columns (P_x or P_y).

Sections 8.3 and 8.4: The use of effective lengths and moment distribution for the design of composite columns restrained by elastic beams (E_x or E_y).

Section 8.5: The use of reduced squash load expressions for the design of stocky composite columns.

These initial studies have been carried out on columns loaded and failing in-plane. However the proposals made in this Chapter can be extended to include biaxially loaded columns ($P_x P_y$; $E_x E_y$; $P_x E_y$; $E_x P_y$) by using the Bresler formula, Equation 1.16.

8.2 The design of columns in frames with plastically designed beams.

If composite columns are to be used within a rigid jointed frame with composite beams that have been designed plastically, then the rotation capacities of neither the beam nor the column should be exceeded. In this section certain cases are analysed to study where problems may arise.

8.2.1 Moment-rotation relationships for hinges in beams.

In the Draft Codes of Practice[81][82] for composite construction, the plastic design of continuous beams is limited to sections which are compact. Climenhaga and Johnson[80] have defined compact composite cross-sections as those with

$$b/t \leq 0.70/\sqrt{\varepsilon_y (3.18 - \sigma_{us}/\sigma_o)}$$

$$d/w \leq (2.44/\sqrt{\varepsilon_y})(1 - 1.4\,\phi) \quad \text{for} \quad 0 \leq \phi \leq 0.28$$

$$d/w \leq 1.48/\sqrt{\varepsilon_y} \quad \text{for} \quad 0.28 < \phi$$

where ε_y is the yield strain of steel in the joist.

ϕ is $A_r \sigma_{yr}/A_s\, \sigma_y$.

A_r is the cross-sectional area of the longitudinal reinforcement

σ_{yr} is the yield stress of the reinforcement

A_s is cross-sectional area of the joist

σ_y is the mean yield stress of the joist

b is the width of the flange of the joist

t is the thickness of the flange

d is the clear depth of the web

w is the thickness of the web

σ_{us} is the ultimate tensile strength of steel,

and σ_o is the yield stress of the joist. They found that a typical moment-rotation relationship for a negative hinge in a compact cross-section was as shown by curve a, Fig. 8.1(a). In compact cross-sections the ultimate moment exceeds that calculated using simple plastic theory, ignoring the concrete in tension, and the available plastic rotations of the hinge always exceeds 0.05 radians. It has been suggested[81] that the maximum rotation available should therefore be taken conservatively, as 0.05 radians for compact beams.

In sagging regions Hope-Gill[88] found that the moment capacity exceeded that calculated using simple plastic theory for rotations up to 0.11 radians, Fig. 8.1(b).

8.2.2 Analysis of simple frame with plastic beams.

The frame given in Figure 8.2, which is loaded to give plastic mechanisms in both beams, and equal single curvature end-moments in the column, is now considered. Equal single curvature end-moments are used because they give the largest end-rotations for given end-moments.

The moment-rotation curves as given in Fig. 8.1(a) for negative hinges and Fig. 8.1(b) for positive hinges are used.

Assuming rigid-plastic beams and referring to Fig. 8.2(b), for compatibility

$$\theta_{h3} = \theta_{h2} + \theta_{h1} + \theta_c$$

and

$$\theta_{h2} = \theta_{h1} + \theta_c$$

where θ_{h1}, θ_{h2}, and θ_{h3} are the rotations of hinges 1, 2 and 3 respectively, θ_c is the column and rotation

thus $\theta_{h3} = 2\theta_{h1} + 2\theta_c$.

For equilibrium

$$\theta_p' < \theta_{h1} < \theta_m'$$
$$\theta_p' < \theta_{H2} < \theta_m'$$
$$\theta_p < \theta_h{}^3 < \theta_m$$

where θ_p and θ_p' are the rotation at which the moment–rotation curves become plastic for positive and negative hinges respectively

and θ_m and θ_m' are the maximum permissible rotations for positive and negative hinges respectively. Hence the following conditions must be satisfied

$$\theta_c < \theta_m' - \theta_p'$$
$$\theta_c < \frac{\theta_m}{2} - \theta_p$$

If θ_p and θ_p' are taken as 0.005 radians then θ_c is controlled by the negative hinge rotation and should be less than 0.045 radians. The positive hinge allows a rotation of up to 0.05 radians.

When the column is designed the optimum section is that which gives just the required moment and axial load capacity at a rotation of less than $\theta_m' - \theta_p'$ if the negative hinge control or $\theta_m/2 - \theta_p$ if the positive hinge controls, e.g. curve 1 Fig. 8.2(c). Curve 2 will also satisfy all conditions

except that it has additional moment capacity. Curve 3 satisfies the load capacity but at an excessive rotation.

Preliminary investigations of the end-moment-end-rotation characteristics of composite columns using a slender column, L/D = 40, Fig. 8.3, show that it is likely that most columns in the practical range reach the maximum end moment (with $\beta = +1$) at end-rotations of less than 0.045 radians, if the axial loads is in excess of about $0.2\ N/N_{sq}$.

8.2.3 Analysis of limited substitute frame with plastic beams

The frame of Fig. 8.2 is, of course, unlikely to occur in practice, so the symmetric frame, Fig. 8.4, is considered with all beams loaded to give plastic mechanisms. The moments acting on the column are obviously zero. If the axial load, N, is increased the column behaves as a pin-ended strut and end-rotations do not become large until close to failure, and are small compared with the maximum permissible hinge rotation. If the column had no initial deflections, eccentricity of loading, etc., no end-rotations would occur until failure, Fig. 3.2.

Often in column design patterned loading, Fig. 8.5, is used to determine the moments and axial loads that the column is to be designed to resist.

It has been shown in Chapter 3, Section 3.6.3 that if the more heavily loaded beams contain a plastic mechanism, Fig. 8.5, then the column can fail by either

Mode 1: a failure of the column, due to a combination of axial load and end-moment, before the development of a plastic hinge in the lightly loaded beam.

Mode 2: a failure due to the formation of a plastic hinge in the lightly loaded beam, Fig. 8.5, and hence zero end-moment on the column and also zero rotational restraint.

For collapse to occur by mode 1 the end-rotation of the lighter loaded beam must be such that it remains elastic: Mode 2 collapse occurs when the rotation of the column is such that a hinge forms adjacent to the column, Fig. 8.5, in the lighter loaded beam.

8.2.4 The inclusion of hinges with elastic plastic-strain-hardening characteristics.

The final case to be considered is that of a column loaded through beams in which all hinges have the same elastic-plastic-strain-hardening rotation characteristics, Fig. 8.6a; any unloading of the hinges is assumed to be elastic.

The beams on both sides of the column are loaded to give plastic mechanisms, Fig. 8.6b, and thus if

$$\theta_{h3} = \theta_{h31} + \theta_{h32}$$

then $\theta_{h31} = \theta_{h32} = \theta_{h1} = \theta_{h2}$.

It is worth noting that this condition can only be satisfied if

$$\theta_{sh} > 2\theta_{p}$$

If the plateau θ_{p} to θ_{sh} is too short then a plastic mechanism cannot occur. When the fixed end of the beam reaches its plastic

moment M_p the central moment is still less that its plastic moment; additional load causes the central moment to increase and also the end-moment to follow the plateau and start to ascend the strain-hardening branch. Cases with hinge moment-rotation characteristics such as this have not been studied.

It can be seen that when the beam is loaded to give a plastic mechanism rotation will continue until $\theta_{h3} = \theta_{sh}$ thus $\theta_{h_2} = \theta_{h_1} = \theta_{sh}/2$.

If axial load is applied to column then a rotation, θ_c, of the column occurs, Fig. 8.bc, and thus the hinge adjacent to joint in beam B starts to unload. To maintain equilibrium, since the beam is carrying its plastic collapse load, the central hinge in the beam must increase its moment capacity and thus commences to move along the strain-hardening branch. In beam 'A' however the hinge adjacent to the column initially only increases in rotation by θ_c until the rotation θ_{h1} becomes equal to θ_{sh} it then moves up the strain-hardening branch and the central hinge starts to unload elastically.

Thus the beams are now exhibiting a rotational stiffness, K, such that

$$K_E \geq K \geq K_{st}$$

where K_E is the elastic rotational stiffness and is

$$\alpha\ EI/L$$

and k_{st} is the strain-hardening rotational stiffness and is

$$\alpha\ E_{SH}\ I/L.$$

Further investigations into this type of behaviour are required especially when plastically designed composite beams are used with slender composite columns or steel columns because this restraint effect due to strain-hardening may compensate for the lack of rotation capacity in the composite beam and thus enable a simple plastic design to be used for any composite frame.

8.2.5 Conclusions.

For symmetric frames Fig. 8.4, with beams designed plastically the following conclusions and suggestions can be made.

(1) That in no-sway frames the effective length of the column should be taken as being equal to its actual length between centrelines of beams.

(2) That columns should be designed for Mode 1 type failure. Thus any out of balance moments should be distributed and the column designed to resist both moments and axial load with an effective length of the column equal to its actual length between centrelines of beams. This method will obviously be conservative for more slender columns where joint rotations are large enough to cause the formation of a hinge in the lightly loaded beam and hence a Mode 2 type failure.

(3) That in most practical frames with plastic beams the rotation capacity of the beams will not be exceeded for the following reasons:

(a) That in general axial load predominates in columns, especially in the lower storeys of a tall building, and thus $N > 0.2\ N_{sq}$ and end-rotations of the column will be small when the ultimate moment-carrying capacity of the column is reached, Fig. 8.3.

(b) That in many cases single-curvature bending with equal end-moments can not occur and thus for a column the end-rotations are smaller for a given end moment than those in Fig. 8.3.

(c) That in the majority of columns, since they will be stocky that is $L/D < 15$, the end-rotation at maximum moment for any given axial load will be small compared to those in Fig. 8.3.

(d) As discussed in Section 8.2.4 the assumption of the elastic-plastic curves for hinge behaviour, Fig. 8.1, is conservative.

(4) It is worth noting that if bare steel sections are to be used instead of composite sections for the columns it is possible that the necessary end-rotation of the column to achieve the required moment will be excessive. This is because steel columns tend to be more slender. The conclusions 3a, 3b and 3d will obviously also apply to steel columns but more research is required before these are used with plastically designed composite beams (see also Section 8.2.4).

8.3 The design of columns in rigid jointed frames with elastic beams.

8.3.1 Introduction

Most design methods for columns within rigid-jointed no-sway frames take some account of the additional strength due to the

restraint offered by the beams. The normal way of doing this is to use either elastic critical loads or elastic effective lengths as one of the basic design parameters.

8.3.2 Proposed design method.

It has been proposed[82] that for the design of composite columns within rigid jointed frames where the beams remain elastic the following design method could be used.

Step 1. Select a suitable cross-section for the column.

Step 2. Calculate the elastic effective length of the column to be designed using charts[83] such as Fig. 8.7.

Step 3. Carry out a moment distribution, ignoring stability effects, to determine the end-moments on the column.

Step 4. Apply the column end-moments calculated from Step 3 to a column of length equal to the effective length calculated in Step 2.

Step 5. Check, using an ultimate load method, that the column of Step 4 is suitable.

To enable the accuracy of the method to be determined a series of initial studies have been carried out, the results of which are discussed here.

8.3.3 Parametric study to check use of effective lengths.

Initially a parametric study was carried out, using the computer program described in Chapter 2, to check the use of effective lengths for concentrically loaded composite columns, constrained to

fail in-plane. Details of the column cross-section, material properties and the frame analysed are given in Fig. 8.8 and Table 8.1.

The stress-strain curve used for the concrete is that given by Equation 2.1 and for steel that given in Fig. 2.1. However to calculate the ratios K_b/K_c a modular ratio, m, of 10 has been assumed hence with E_s taken as 200 kN/m^2, E_c becomes 20 kN/m^2. The stiffness of the beams then remains constant throughout the analysis although the value of Young's Modulus of the concrete in the column is varying. The effect of choice of m is discussed later. Obviously as only the use of effective lengths is checked, the columns have no externally applied end-moments and are constrained to fail in-plane.

Initially a number of pin-ended columns, $K_b/K_c = 0$, of various slenderness ratios, L/D where D is depth of the section in the plane of bending, were analysed to determine the failure load, Table 8.1. The results were used to give the basic column curves, Fig. 8.9, and Fig. 8.10.

The columns were then re-analysed with various end restraints, Table 8.1, to determine the failure loads. The elastic effective length charts Fig. 8.7, were then used with m assumed to be 10 to convert the lengths of the restrained columns to effective lengths. The results of the analyses are plotted against the effective slenderness, L/D, Fig. 8.9 and Fig. 8.10., from which it can be seen they lie very close to the curve obtained from the pin-ended

struts (K_b = 0). None of the results lie beneath the curve, indicating that for these examples the use of effective lengths, with m = 10, is remarkably accurate with the small errors always on the safe side.

Since the value of EI/L for the beam is an independent variable in the analysis we can investigate the effect of the choice of E_c for a column design. The value of E_c in the computer analysis is given by

$$E_c = \frac{d\sigma}{d\varepsilon} = \frac{\sigma_u}{\varepsilon_u}\left\{2.41 - 3.730\,\frac{\varepsilon}{\varepsilon_u} + 1.5\left(\frac{\varepsilon}{\varepsilon_u}\right)^2 - 0.180\left(\frac{\varepsilon}{\varepsilon_u}\right)^3\right\}$$

and because it is dependent on the strain it varies across the cross-section and along the column length. Therefore a value of E_c has to be chosen that will give a reasonable average estimation. The value of E_c = 20 kN/mm^2 has been used because it corresponds to m = 10. If the moment-curvature curves corresponding to this choice of E_c are plotted against the calculated curves, Fig. 8.11 and Fig. 8.12., it can be seen that this is a good choice if the axial loads are greater than 0.2 N_{sq} and the moments less than about 70% of the maximum moment capacity.

Since the columns are under predominantly axial load the use of effective lengths should therefore be accurate.

If E_c is taken as being equal to zero, that is the concrete is assumed to provide no contribution to the stiffness of the composite cross-section, then m = ∞.

Since the beam stiffness of the columns analysed is not altered the ratio K_b/K_c must increase. For the columns analysed with K_b/K_c = 5, when m = 10, the ratio K_b/K_c becomes

approximately 25 with $m = \infty$ and thus the effective length tend to the limit

$$L_E = L/2.$$

These results have been plotted against the new effective lengths, calculated with $K_b/K_c = 25$, as curve 'b' on Fig. 8.9. This shows that even with this extreme situation variation in results of only 5% occur.

Generally in a frame, however, it is the relative values of stiffness that are important and hence in the above case the beam stiffness, assuming that the beam is composite, would also reduce and the ratio $K_c/(K_b + K_c)$ would not vary much.

8.3.4 Study of method with elastic columns

The second part of the study has been carried out to show that the method should only be used for ultimate load design and not for methods which use a limiting stress as the failure criterion. A study of an elastically restrained column, Fig. 8.13, was therefore carried out.

It can be shown[89] that the end-moment, on the column, for a symmetric frame loaded in single curvature is

$$M = \frac{\left(2 - 2c + \frac{8}{s}(c-1) + \frac{4}{s}\frac{\Sigma K}{K_c}(1 - c)\right)}{\left(2 - c - \frac{8}{s} + \frac{4}{s}\frac{\Sigma K}{K_c}^2\right) - c^2} \times M_{OB} \qquad 8.5$$

where M_{OB} is the out of balance fixed end moment

K_c is the column stiffness

ΣK is the total stiffness at a joint and s and c are the stability functions.

Furthermore it can be shown[89] that the mid-height moment, M_{CEN}, is given by

$$M_{CEN} = M \sec \frac{\pi}{2} \sqrt{\frac{N}{N_e}} \qquad 8.6$$

By applying equations 8.5 and 8.6 to the frame at various load levels the theoretical end moments on the column and the moment at the centre of the column can be determined. The results are given in Fig. 8.13 and Fig. 8.14.

If the proposed method is used then the moments predicted, Fig. 8.13, are unconservative, if M_{max} is the criterion of failure. It is also of interest to plot the results of an analysis with the effective length equal to l, which was the basis of the Steel Structures Research Committee's method[10]. This shows the conservatism of such an approach, although it should be noted that when proposed by S.S.R.C., permissible stresses in columns were lower and hence values of N/N_E were very low.

It should be noted also that both the theoretical and the proposed curves tend to $M_{CEN} = \infty$ at the critical load of the frame, $N/N_E = 2.5$. Thus if a column is to be designed which is made of a material which is perfectly elastic then a column is required with an Euler load equal to the critical load of the frame. If however the maximum moments in the column are to be checked then either an analysis including stability effects has to be carried out or a magnification factor which includes the effect of beam restraints used, such as that included in JCR2[57]. Wood[83] has presented the results of a series of analyses and gives limits to the possible variation, the lower limit being

equation 8.6, Fig. 8.15.

It should be noted that if design is to a limiting stress the error in the maximum moment, if equation 8.6 is used, will probably not make much difference to the total stress including axial load stresses etc., at the cross-section under consideration since the error in the stress due to the moment increases as the axial load stress increases.

Similarly if the failure criterion is the attainment of a maximum moment, as CP110[22] then because the moment is only one of the two components, the other being axial load which is accurately determined, the total error in the design loading is small.

8.3.5 The behaviour of an inelastic column.

The behaviour of a column made of a material with an elastic-plastic stress-strain curve is now considered. Until the onset of yield the behaviour of the column is identical to an elastic column; however as yielding occurs the cross-section stiffness, EI_{COL} reduces and hence the end-moments reduce more rapidly, Fig. 8.16 and Fig. 8.17. The effective length determined for the elastic system has obviously now become conservative, that is the actual effective length is now less than that calculated using the original stiffness since $\frac{K_c}{\Sigma K}$ has reduced and is tending to zero. However the load at which the moments change sign, the Euler load for an elastic column, has also reduced, since EI_{col} has reduced due to plasticity.

Thus, if a column is considered at the point of failure, then if the column remains perfectly elastic the distribution of moments is as shown, Fig. 8.17. The distance between the points of contraflexure, at failure, being equal to the elastic effective length. Therefore the column can be designed as a pin-ended column under axial load with a length equal to effective length of the column in the frame.

If however the column is elastic-plastic it has been stated that at failure the effective length is shorter and hence the moment distribution is different, Fig. 8.17. Hence to design this column an elastic-plastic effective length is required which can then be used as the length of the pin-ended column.

If the elastic effective length is used as the length of the column to be designed then the design should be conservative. However, if large beam moments are applied to the column it may not be able to develop the shorter effective length because at some point in the column the moments may exceed, M_p, and thus a material failure occur. To overcome this a conservative distribution of moments, Fig. 8.17, is used in the Draft Bridge Code[82].

8.4 Parametric study of the use of effective lengths and moment distribution.

To check the degree of conservatism and the sensitivity to changes in the modular ratio of the method, when beam loadings are included, a number of analyses were carried out. The column cross-section and frame details are the same as those used for the

effective length analysis.

The frame is loaded by beam loads, which would give a fixed ended beam moment of M_F, and an axial load N. Details of the loadings and other variables are given with the results in Table 8.2.

The results for the two column lengths analysed have been plotted on Fig. 8.18 the effective length ratio for $m = 10$ being $L_E/L = 0.68$. It can be seen that, as expected from the theory, the method is conservative and increasingly so as the applied beam moment increases.

If the two extremes of values of m are investigated then the sensitivity of the method to changes in the value of E_c can be seen.

If $m \to 0$, $E_c \to \infty$ and $K_b/K_c \to 0$. The two effects, the distribution at moments and the instability effects are now considered separately. It can be seen that when instability is considered the column tends to become pin-ended and th s $L/L_E \to 1.0$. However, in relation to the beam, the column has become very stiff and thus tends to attract the total fixed end moment. Hence at $M_F/M_{ULT} = 1.0$ the column will fail with $N = 0$, Fig. 8.19. It is worth noting that with short composite columns an increase in axial load will also give an increase in moment capacity, Curve 'b' Fig. 8.19, because with moment and low axial load tensile cracks form. Increasing axial load causes these cracks to close and thus an increase in load capacity. Curve 'a' is the expected curve for a column made of a material that does not exhibit this characteristic.

The other extreme is with $m = \infty$, that is an under-estimation of E_c. As the area of the steel-core reduces then $K_b/K_c \to \infty$ and $L_E/L \to 0.5$. Thus, in that limit, the effective length has been underestimated and an unconservative estimation of the failure load results. Because the beams are relatively much stiffer than the column

no moment is distributed into the column and as M_F/M_{ULT} increases no account is taken of loss of load capacity due to moment action. Thus the loads become unconservative for short columns, and very unconservative for slender columns. It can be seen from Fig. 8.9 and Fig. 8.10 that the worst estimations will occur with L/D between approximately 30 and 40 since in this region the gradient of the curve has its largest value.

As discussed in Section 8.3.3 it is generally the ratio of stiffness between beams and columns that is important and thus any error in the estimation of E_c, and hence m, would be reflected in the calculation of both K_b and K_c.

It should be noted that to analyse the columns with the calculated effective lengths and end-moments the exact analysis has been used. Thus any method, such as that of Basu and Sommerville[50], which can be used to design pin-ended columns with axial load and applied end moments exactly, or conservatively, is suitable for use in the method of Section 8.3.2.

8.5 The use of "squash load" expressions for the design of elastically restrained composite columns.

8.5.1 Introduction.

The Code of Practice for the Structural Use of Concrete, CP110,[22] allows certain columns, within no-sway frames, to be designed using simplified expressions based on a proportion of the squash load. If the column is short, that is the ratio $L_E/D \leq 12$, where L_E is the elastic effective length of column, and carries axial load only then it need only satisfy the condition that

$$N \leq 0.9\, N_{sq} \qquad 8.7$$

The value of $0.9\, N_{sq}$ is used to make an allowance for construction tolerances. If the column is in a frame with an approximately symmetrical arrangement of beams then the condition that has to be satisfied is that

$$N \leq 0.8\, N_{sq}. \qquad 8.8$$

It should be remembered that partial factors of safety for the materials and loadings have to be included in the expressions when used for the design of columns.

The Draft Bridge Code[82] has adopted a slightly different approach for short axially loaded columns in that equation 8.7 is replaced by

$$N \leq 0.85\, K_{1y} N_{sq} \qquad 8.9$$

where K_{1y} is the ratio of the permissible axial load, from a strut curve, to the squash load.

Since a large proportion of practical columns satisfy these conditions design of columns is simplified by the use of squash load expressions.

The object of this section is therefore to carry out an initial investigation into the use of similar expressions for restrained composite columns.

8.5.2. <u>A re-assessment of the parametric surveys to establish squash load expressions</u>.

The results of the parametric surveys, Tables 8.1 and 8.2 can be used to establish the bounds for a simplified design method.

From Table 8.2 it is noted that all but the most heavily loaded of the short columns can carry over $0.85\ N_{sq}$. From Table 8.1 by linear interpolation, which is conservative, the expected reduction in load capacity if the slenderness is increased from $L/D = 10$ to $L/D = 15$ is for $K_b/K_c = 1$ is about 5%.

The reason that these columns, even with large initial out of balance beam fixed end moments, M_F, carry such high loads is that as the axial load is increased the moment is shed back into the beams, which must therefore be capable of resisting these increased moments without losing stiffness. Wood[58] has recommended that such beams should be designed as elastic continuous beams on props.

8.5.3. Inclusion of biaxial end-moments.

To enable the extension of the method to include biaxially loaded columns it is necessary to initially consider the possible effects of patterned loading.

For an internal column it can be seen from Fig. 8.19 that to have the worst single-curvature moments acting on the column that either loading 'a' for major axis moments or loading 'b' for minor axis moments is required. In both cases, if the frame is symmetric, the applied moment about the other axis is zero. In practice some allowance is usually made to take account of construction tolerances, initial imperfections, etc. This allowance can be in the form of a small moment.

Inspection of Table 8.2 shows that for small applied end moments, $M_F/M_{ULT} < 0.5$, the effect on the failure load of a short column is small, less than 2%. From Table 8.1 it can be seen that $N_{ux} \triangleq N_{uy}$. Thus substituting, in the modified Bresler formula, for major axis single curvature bending with small minor axis moments gives

$$\frac{1}{N_{xy}} = \frac{1}{N_x} + \frac{1}{0.98N_{uy}} - \frac{1}{N_{uy}} \quad .$$

and hence $N_{xy} \triangleq N_x$

Similarly it can be shown that the reduction for minor axis single curvature moments with small major axis moments is small.

8.5.4 Proposed design method.

The design method proposed is that if restrained columns satisfy the following criteria about each axis then they can be designed such that

$$N \leq 0.8\, N_{sq} \qquad 8.10$$

where N is the axial load to be resisted by the column and N_{sq} is the ultimate axial load of the column.

The criteria are

(1) $L/D \leq 15$

(2) $M_F/M_{ULT} \leq 1.5$ about one axis and

≤ 0.5 about the second axis

and (3) $K_b/K_c \geq 1.0$.

Criteria (2) and (3) have to be satisfied at each end of the column. These limits have been derived from Table 8.1 and Table 8.2 and Section 8.5.3 and are based on analyses carried out on columns loaded in symmetric single curvature. Thus since this is the worst possible condition the design method applies to frames in which unequal end-moments exist about one or both axes.

The ratio L/D = 15, is equivalent when $K_b/K_c = 1$, to $L_{eff}/D = 10$ which is slightly more onerous than the CP110 condition. However the design method does allow for heavier out-of-balance beam loadings.

In cases in which the failure is about one axis only then the conditions are that

(1) $L/D \leq 15$

(2) $M_F/M_{ULT} \leq 1.5$

and (3) $K_b/K_c \geq 1.0$

for Equation 8.10 to be used.

L/D	m = 10		MINOR AXIS	MAJOR AXIS
	K_b/K_c	L_{off}/D	N/N_{sq}	N/N_{sq}
10	0	10	0.909	0.909
10	1	6.8	0.971	0.976
10	5	5.5	0.971	0.978
20	0	20	0.667	0.714
20	1	13.6	0.882	0.888
20	5	11.0	0.900	0.900
30	0	30	0.407	0.467
30	1	20.4	0.693	0.742
30	5	16.5	0.786	0.808
40	0	40	0.250	0.294
40	1	27.2	0.480	0.560
40	5	22.0	0.626	0.683

TABLE 8.1 RESULTS OF ANALYSES OF COLUMNS WITH END RESTRAINTS.

L/D	K_b/K_c	M_F/M_{ULT}	THEORETICAL $\frac{N_{TH}}{N_{sq}}$	PROPOSED METHOD					
				m = 10		m = ∞		m = 0	
				$\frac{N_f}{N_{sq}}$	$\frac{N_f}{N_{TH}}$	$\frac{N_f}{N_{sq}}$	$\frac{N_f}{N_{TH}}$	$\frac{N_f}{N_{sq}}$	$\frac{N_f}{N_{TH}}$
40	1	0	0.480	0.470	0.98	0.667	1.39	0.250	0.52
		0.5	0.355	0.315	0.89	0.667	1.88	0.037	0.10
		1.5	0.217	0.093	0.43	0.667	3.07	0	0
		2.5	0.143	0.019	0.13	0.667	4.66	0	0
10	1	0	0.971	0.968	0.997	0.981	1.01	0.909	0.94
		0.5	0.954	0.884	0.93	0.981	1.03	0.720	0.75
		1.5	0.885	0.774	0.87	0.981	1.11	0	0
		2.5	0.792	0.600	0.76	0.981	1.24	0	0

TABLE 8.2 RESULTS OF ANALYSES OF COLUMNS WITH BEAM LOADINGS

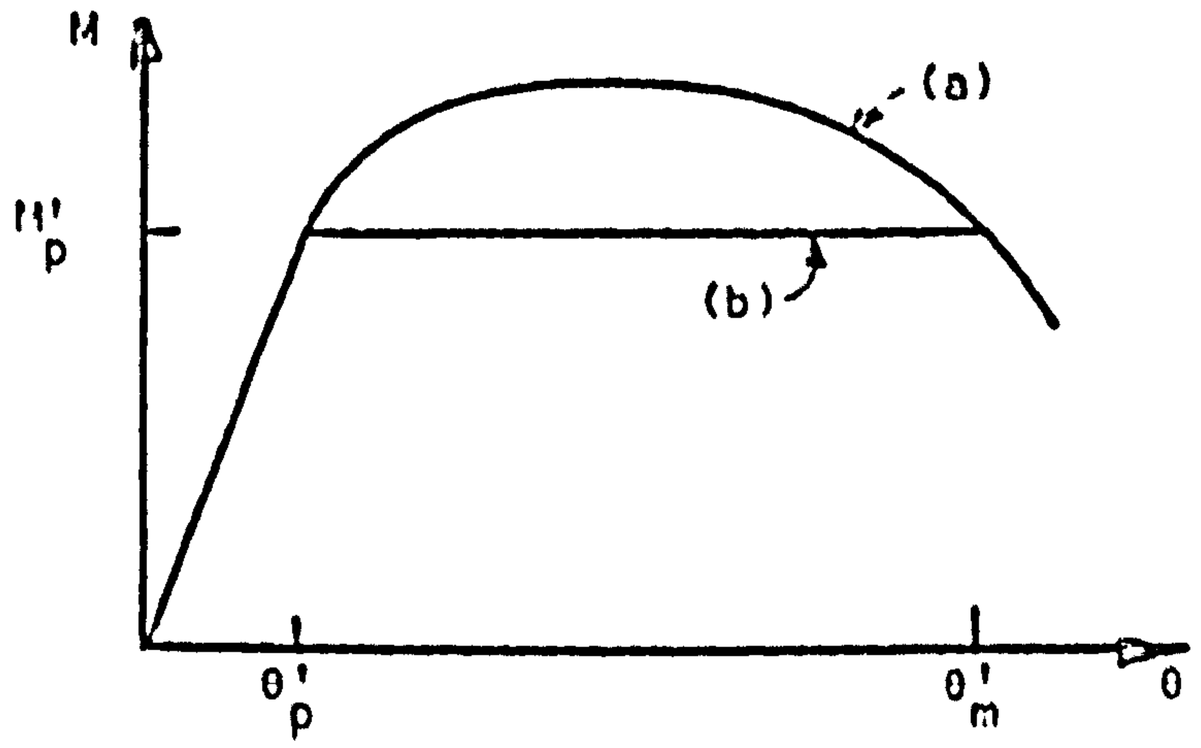

(a) Negative hinges (hogging)

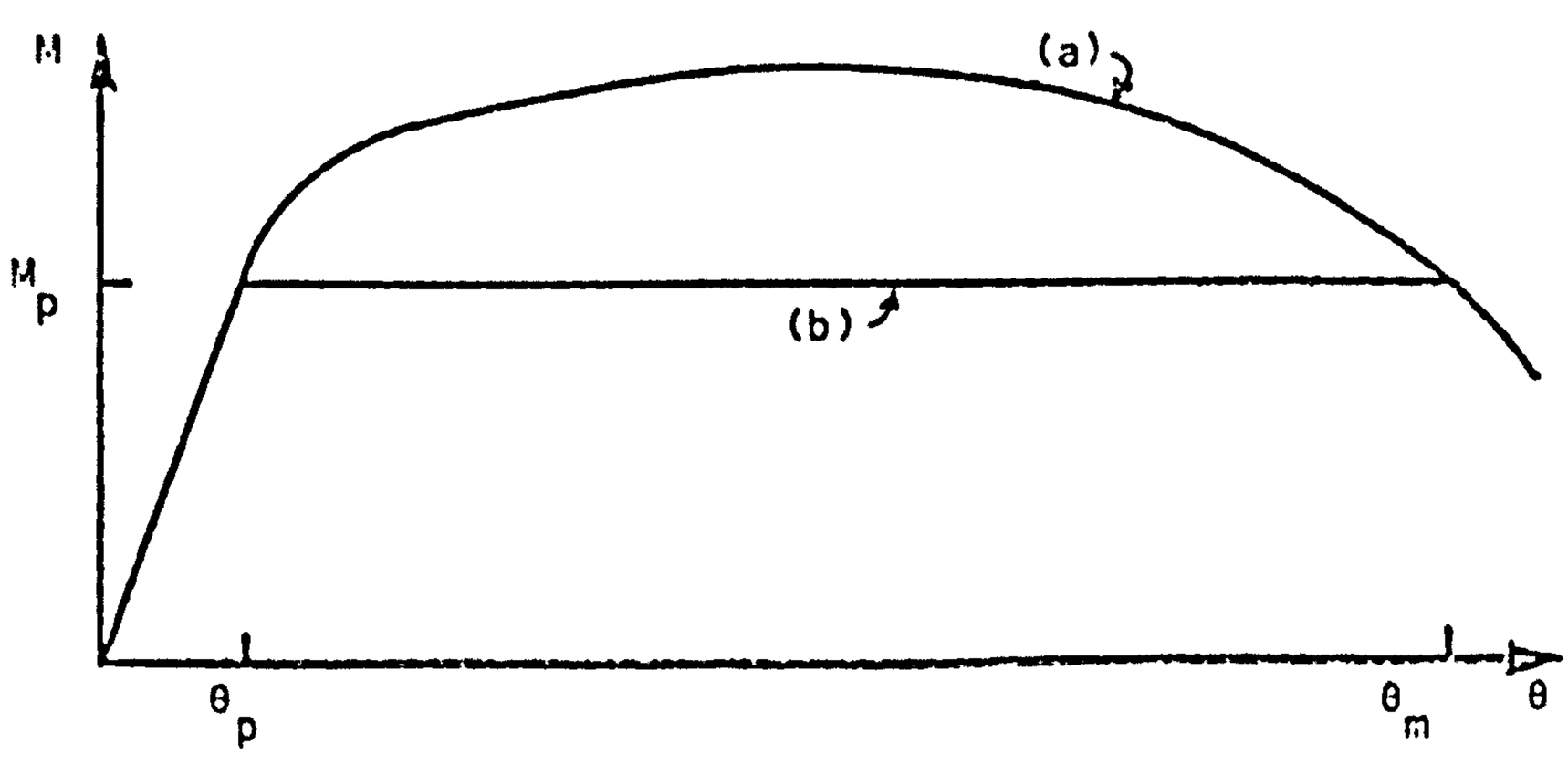

(b) Positive hinges (sagging)

FIG. 8.1 MOMENT-ROTATION CURVES FOR HINGES IN COMPACT COMPOSITE BEAMS

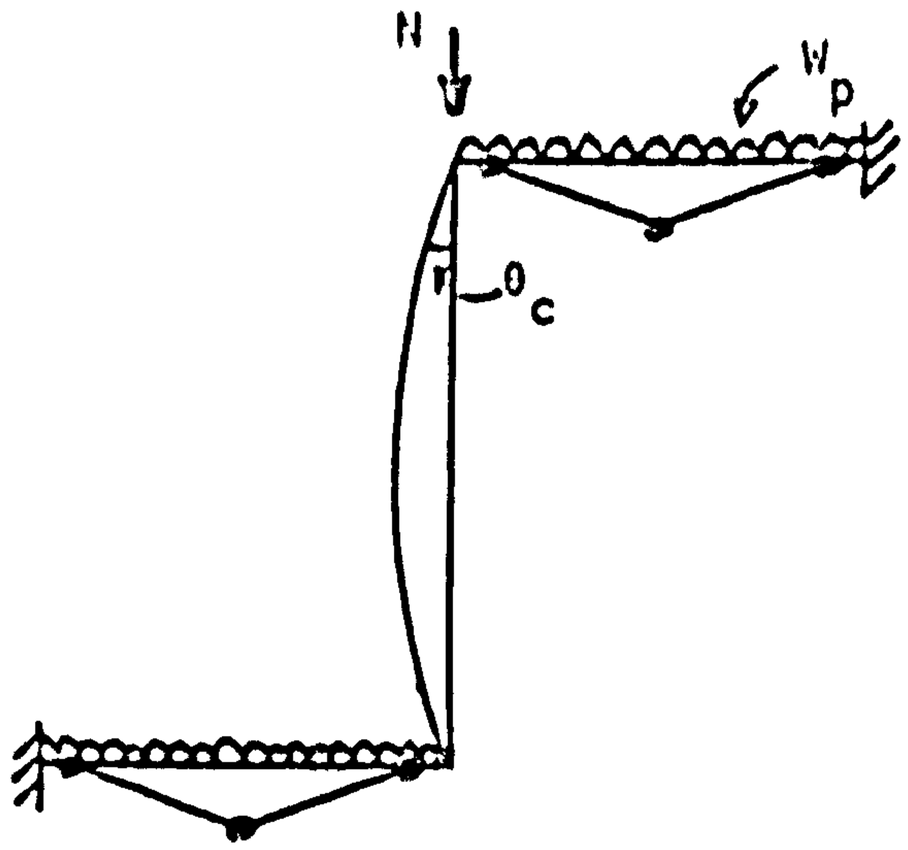

(a) Frame and loading

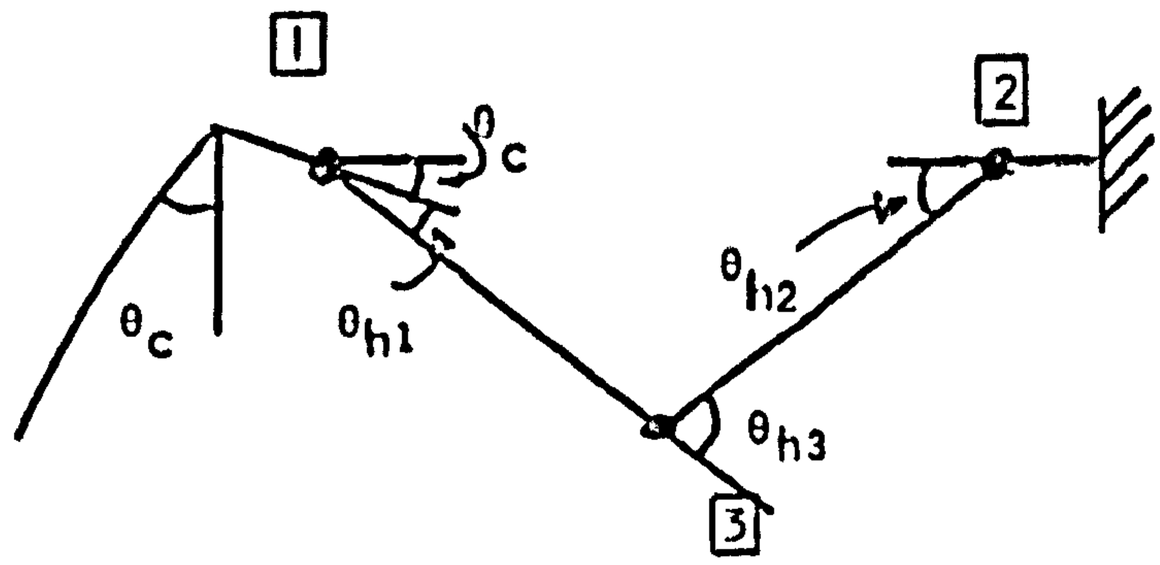

(b) Mechanism in top beam

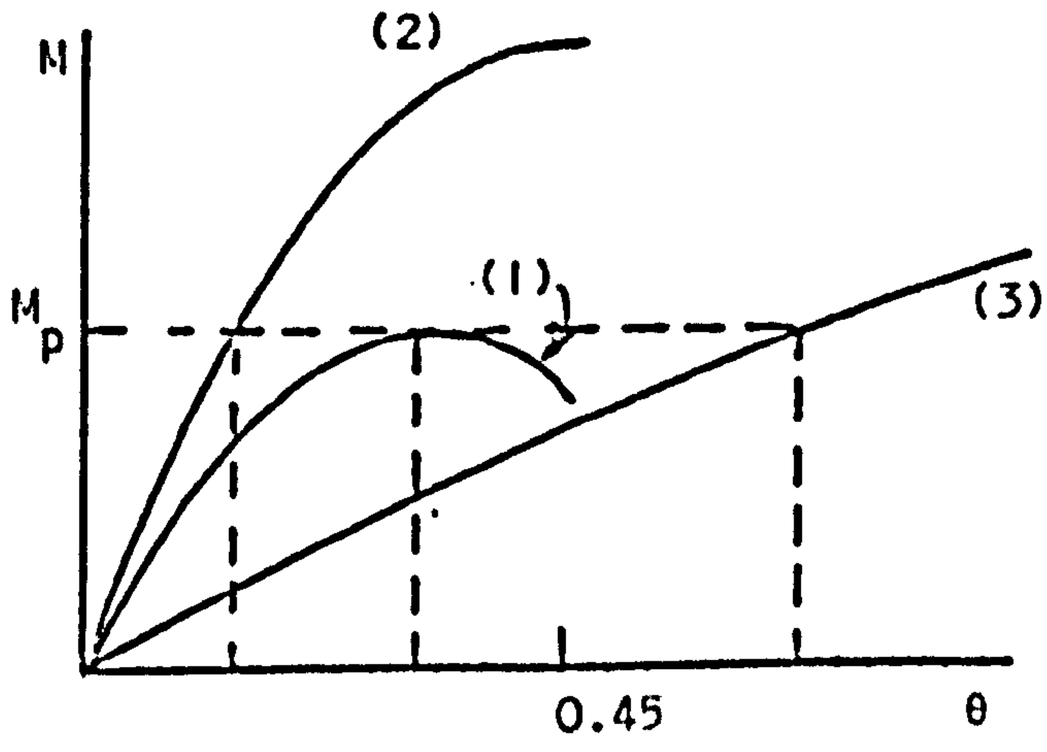

(c) Moment-rotation curves for column

FIG. 8.2 EXAMPLE OF PLASTICALLY DESIGNED FRAME

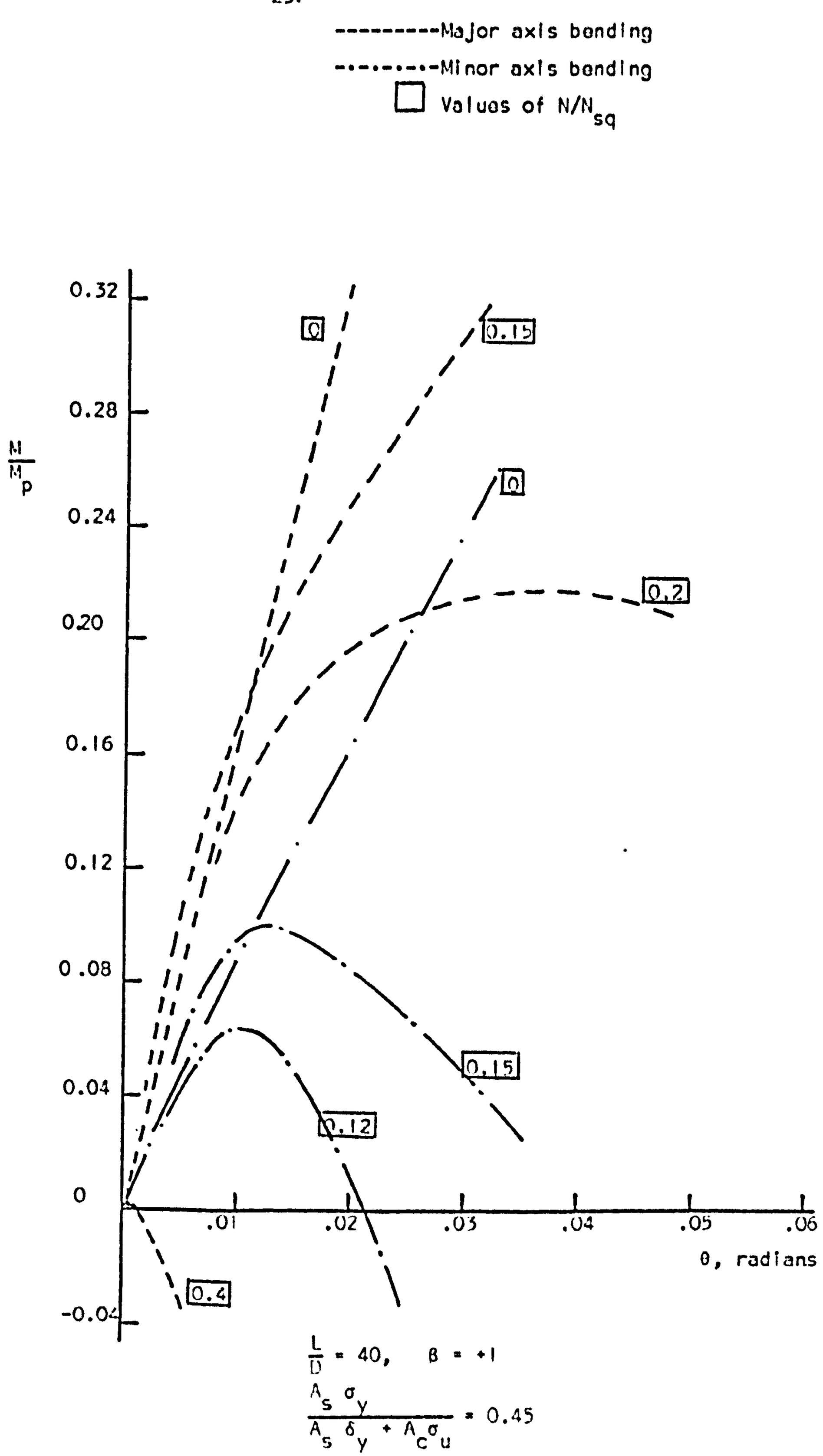

$\frac{L}{D} = 40, \quad \beta = +1$

$\frac{A_s \sigma_y}{A_s \delta_y + A_c \sigma_u} = 0.45$

FIG. 8.3 MOMENT ROTATION CURVES

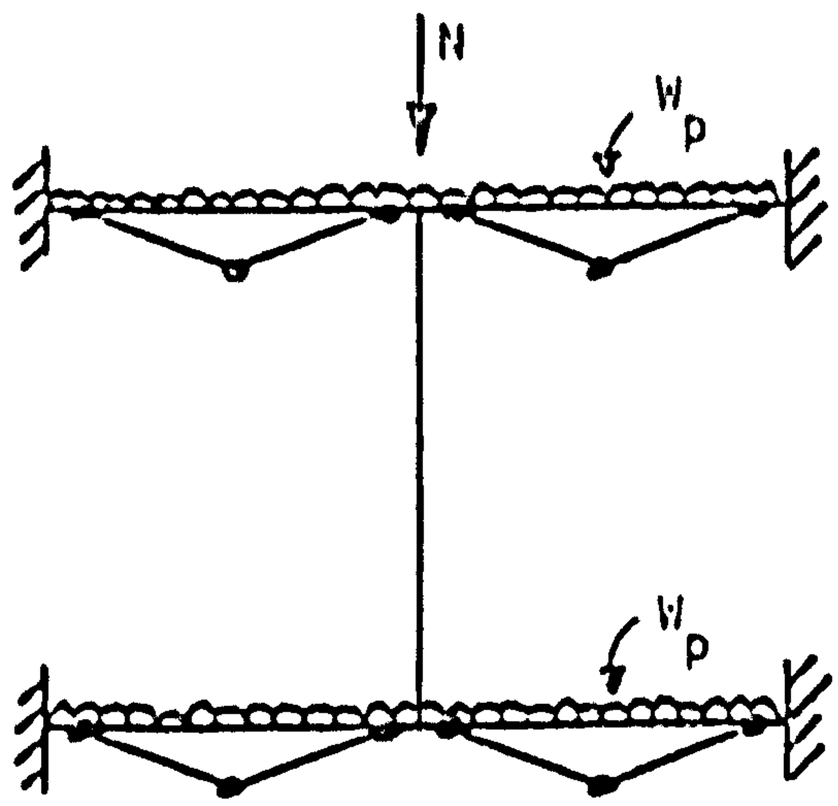

FIG. 8.4 SYMMETRIC FRAME LOADED TO GIVE PLASTIC MECHANISMS IN ALL BEAMS

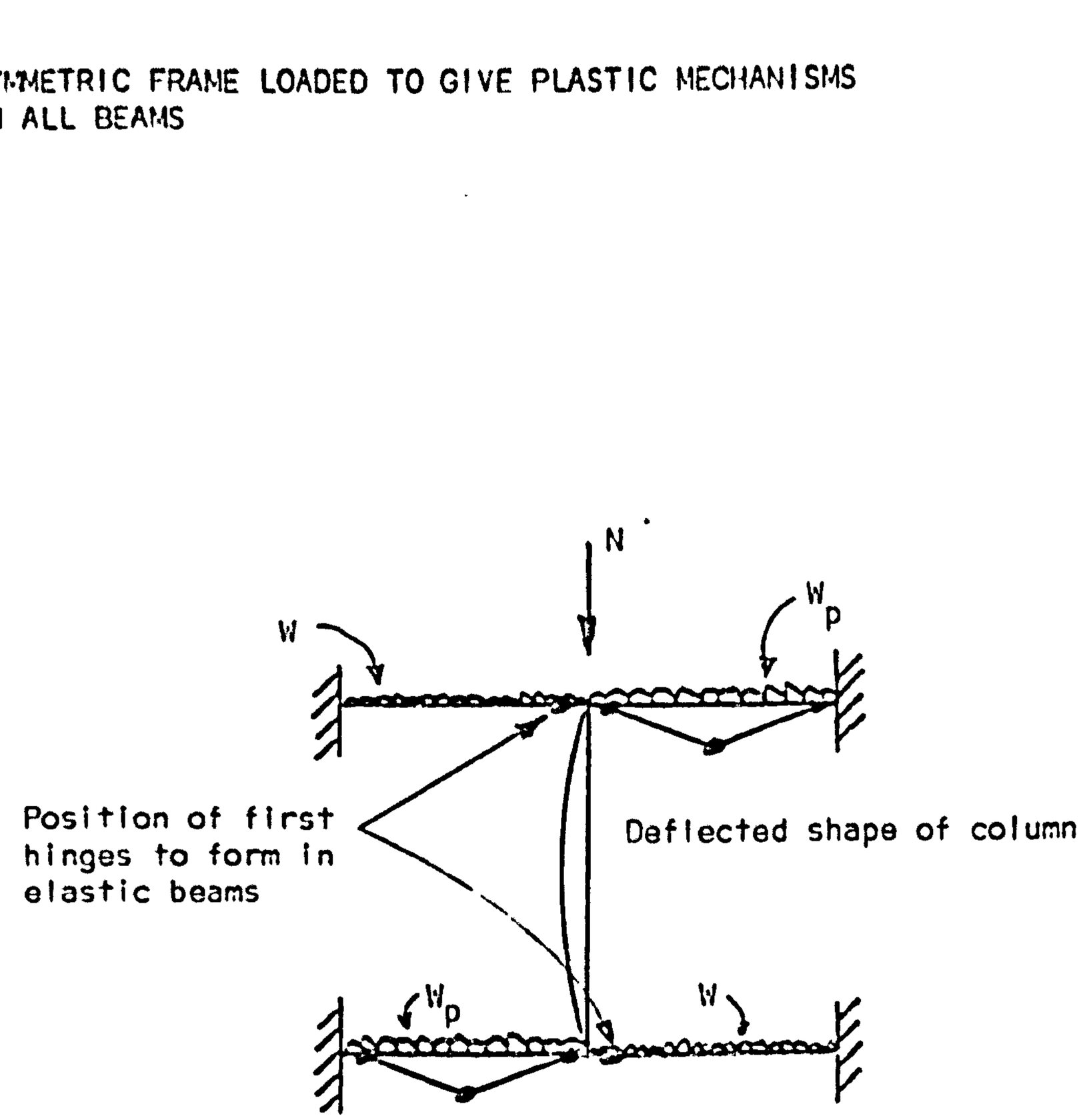

FIG. 8.5 SYMMETRIC FRAME WITH PATTERNED LOADING

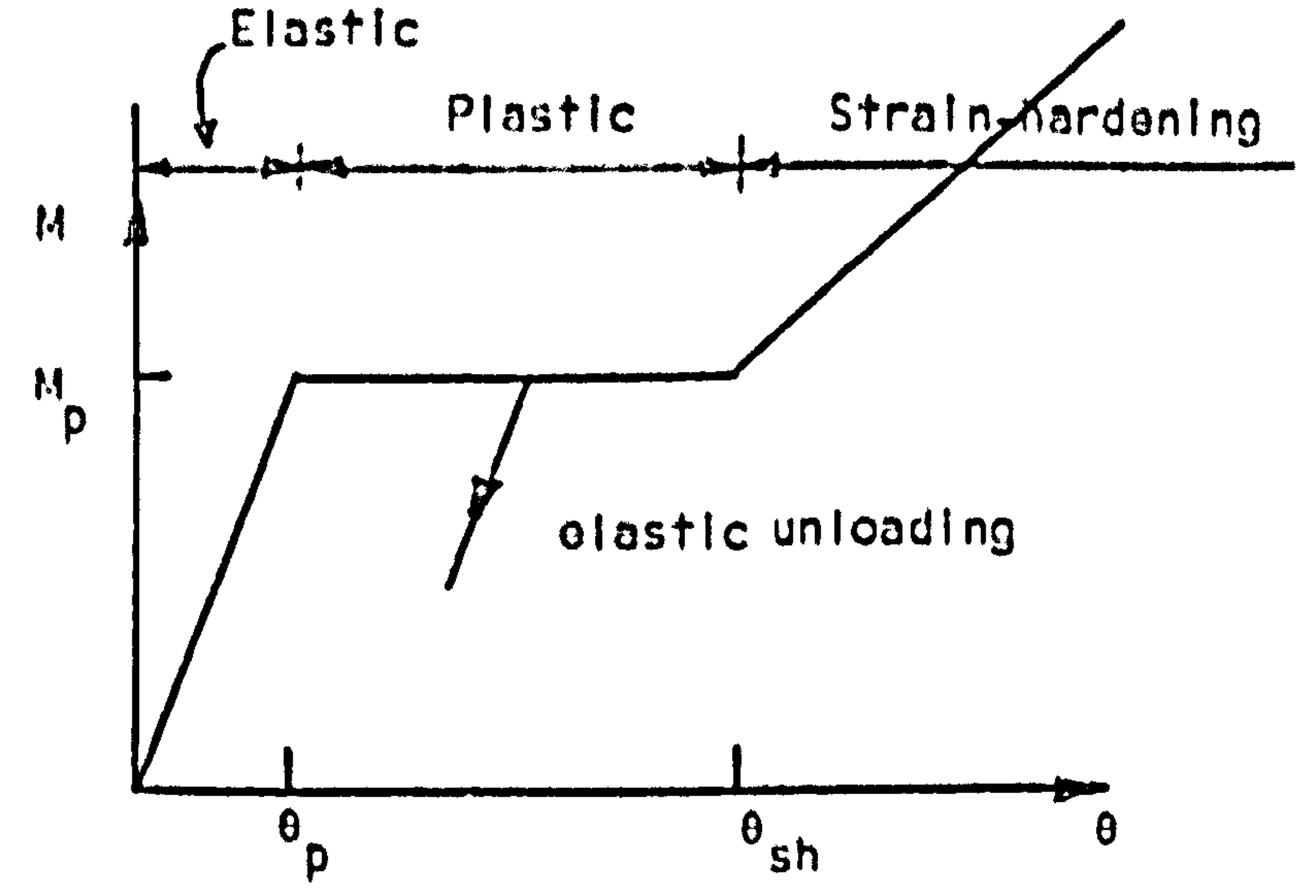

(a) Hinge moment-rotation characteristics

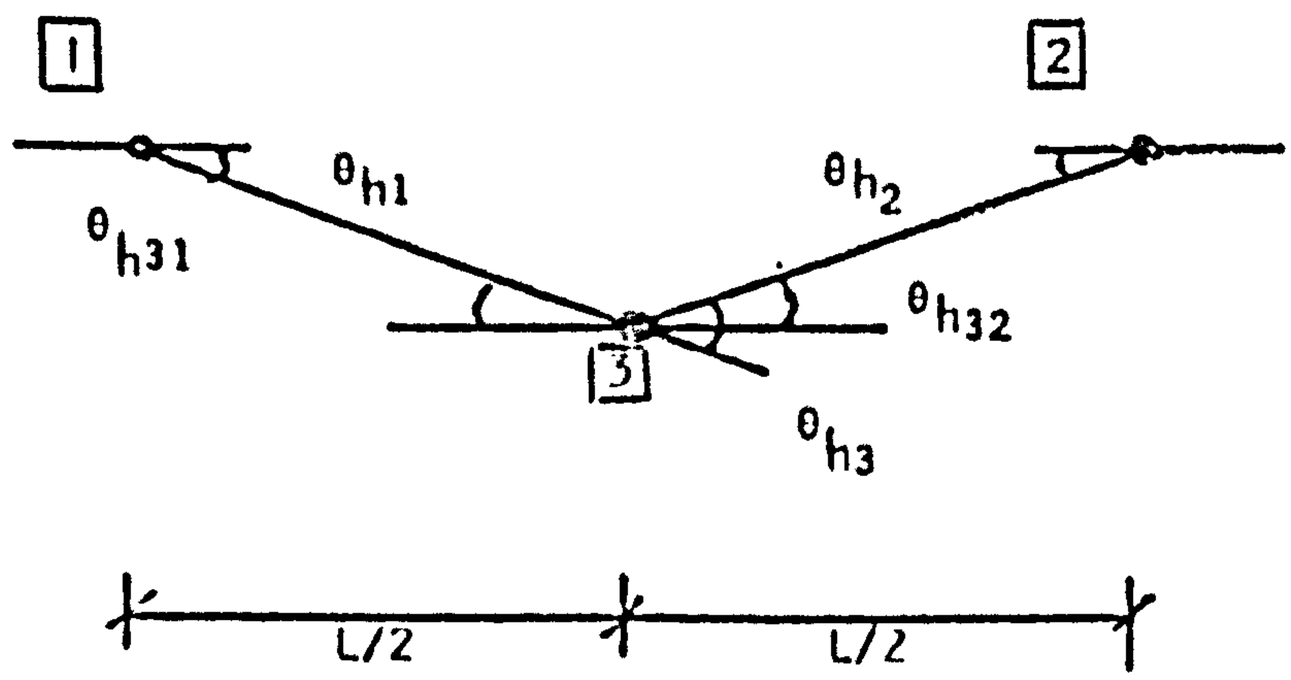

(b) Beam mechanism

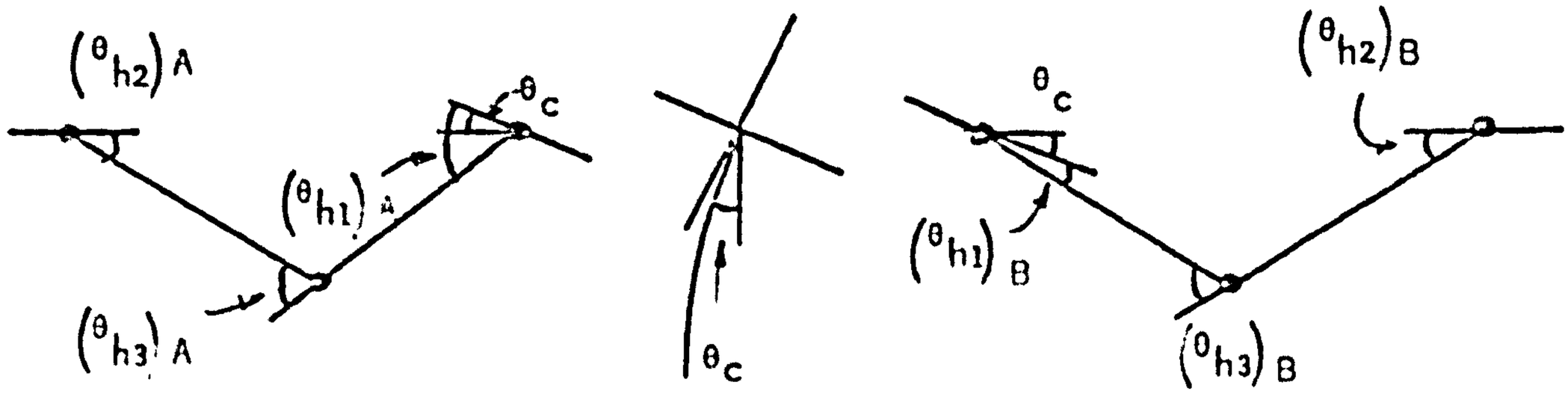

Beam A

Beam B

(c) Beam - column behaviour

FIG. 8.6 BEAMS WITH ELASTIC-PLASTIC-STRAIN-HARDENING RELATIONSHIPS

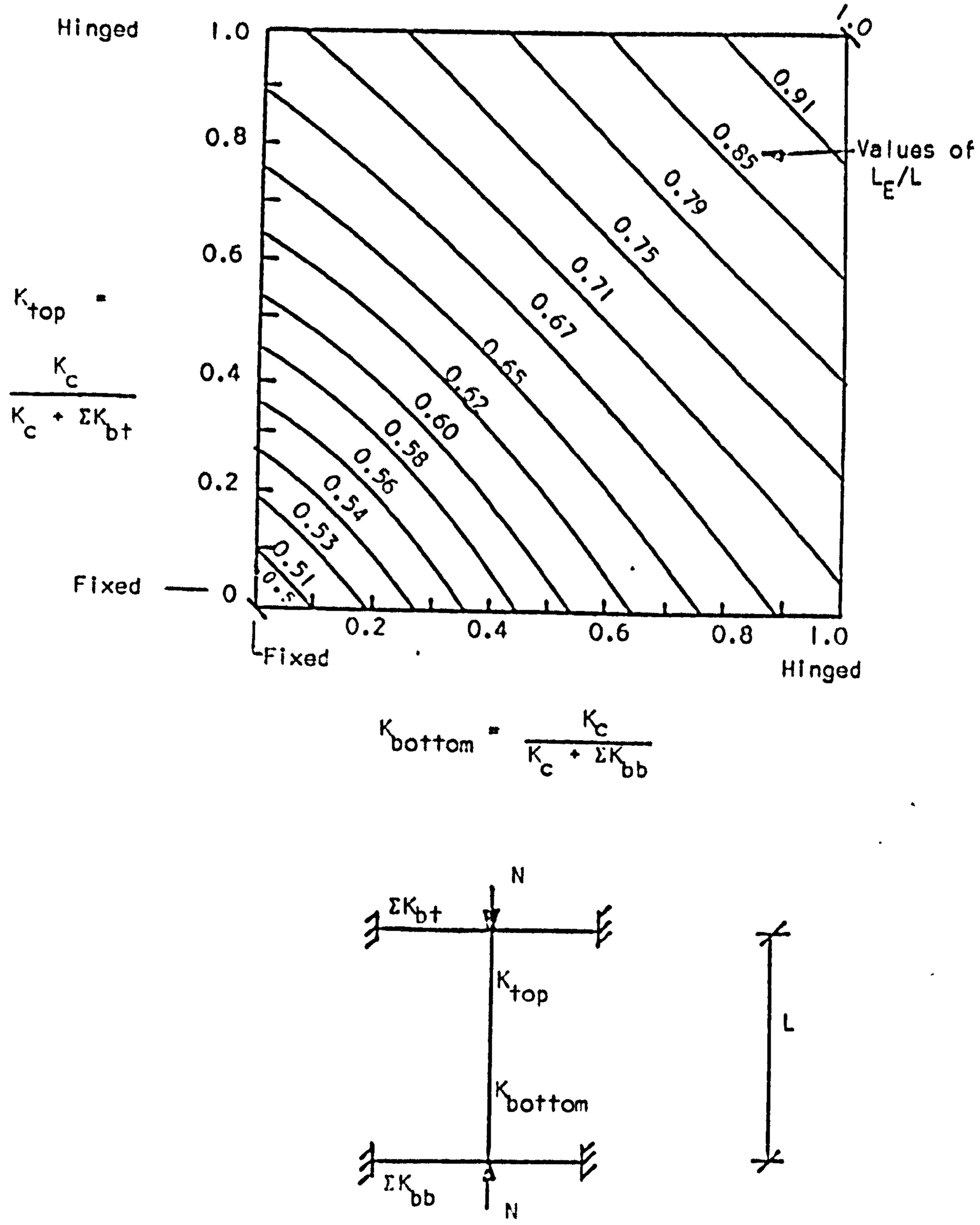

FIG. 8.7 ELASTIC CRITICAL LOADS OF SINGLE COLUMNS RESTRAINED BY BEAMS (NO SWAY ALLOWED)

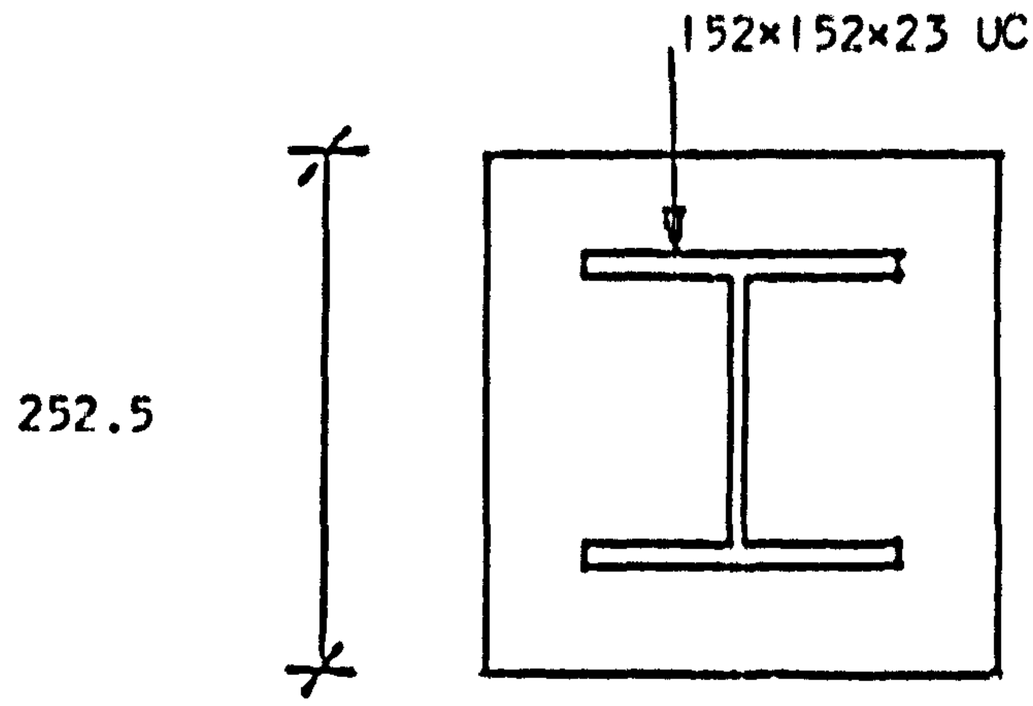

σ_y = 245 N/mm^2
E_s = 200 kN/mm^2
σ_u = 30 N/mm^2

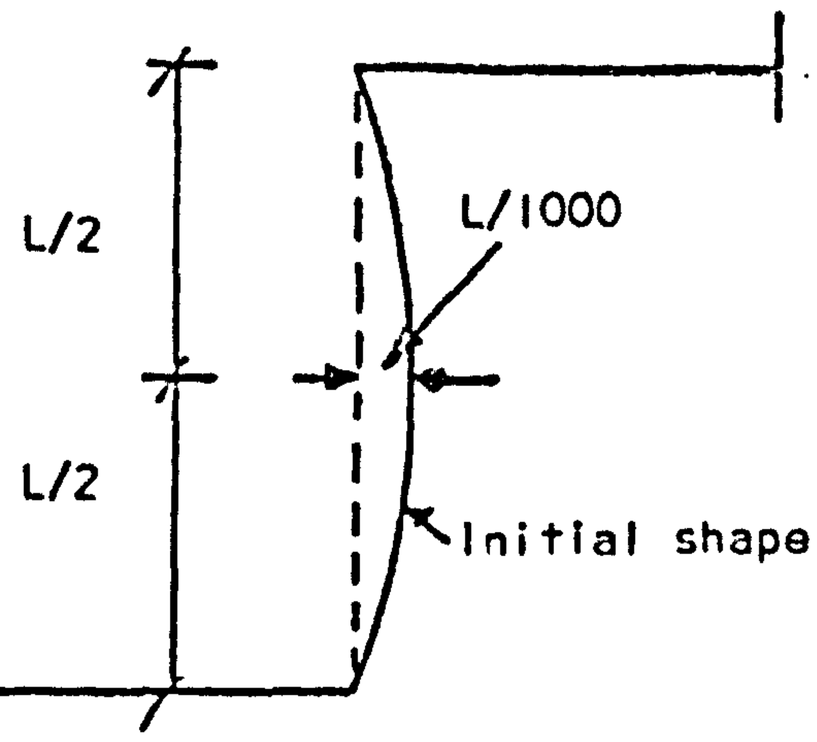

FIG. 8.8 FRAME USED FOR COMPUTER TESTS

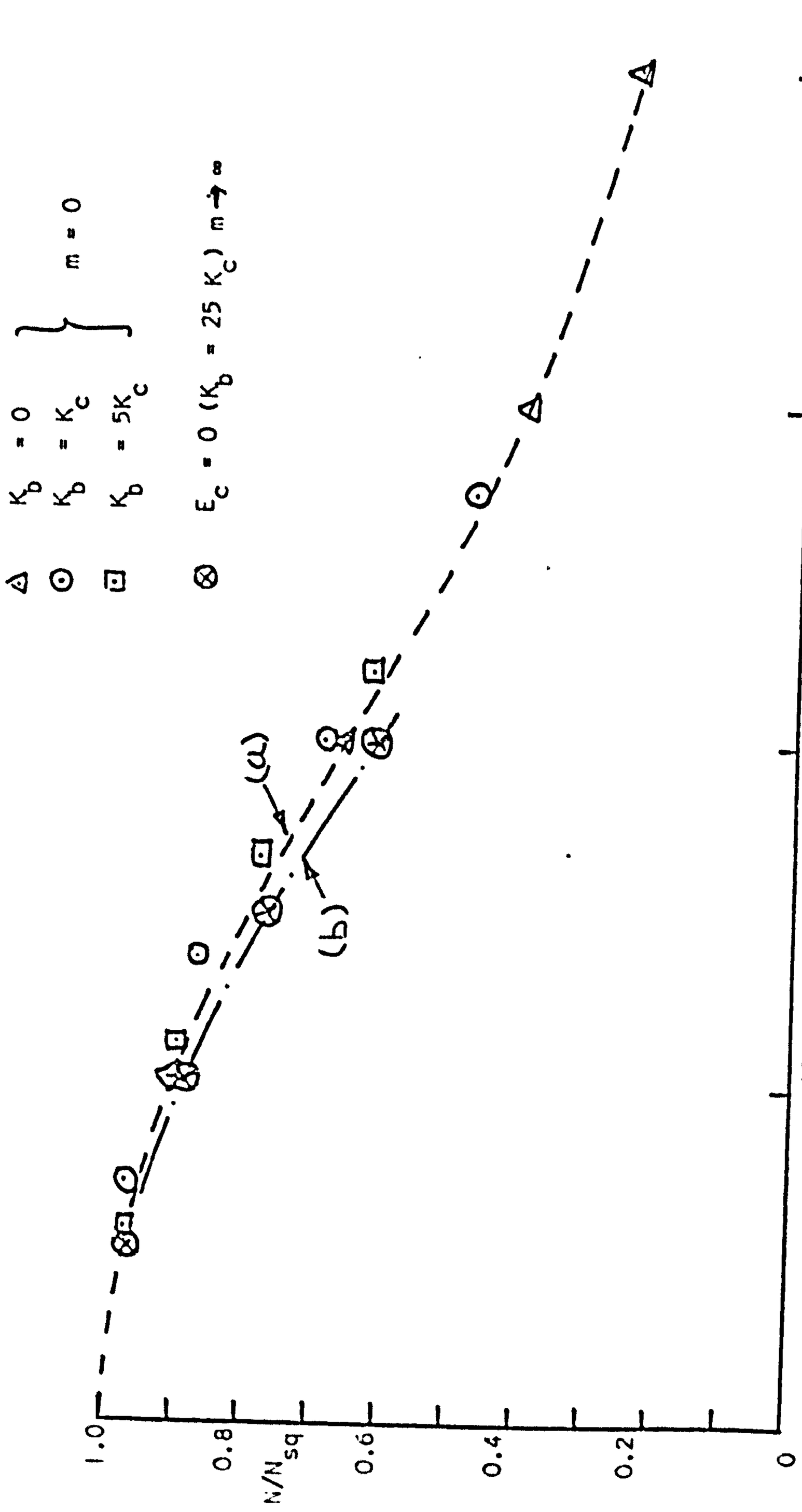

FIG. 8.9 COMPARISON OF MINOR AXIS EFFECTIVE LENGTHS

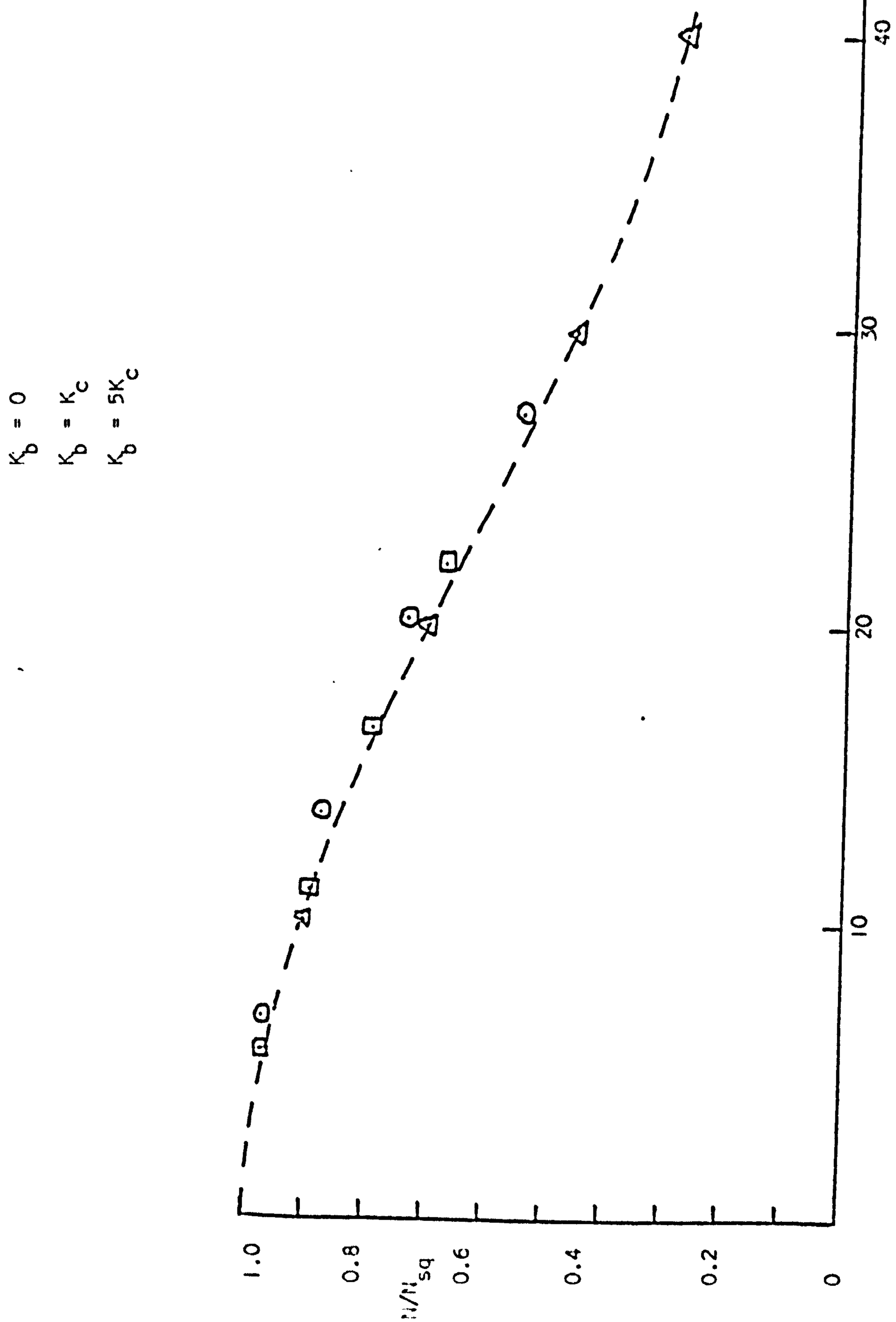

FIG. 8.10 COMPARISON OF MAJOR AXIS EFFECTIVE LENGTHS

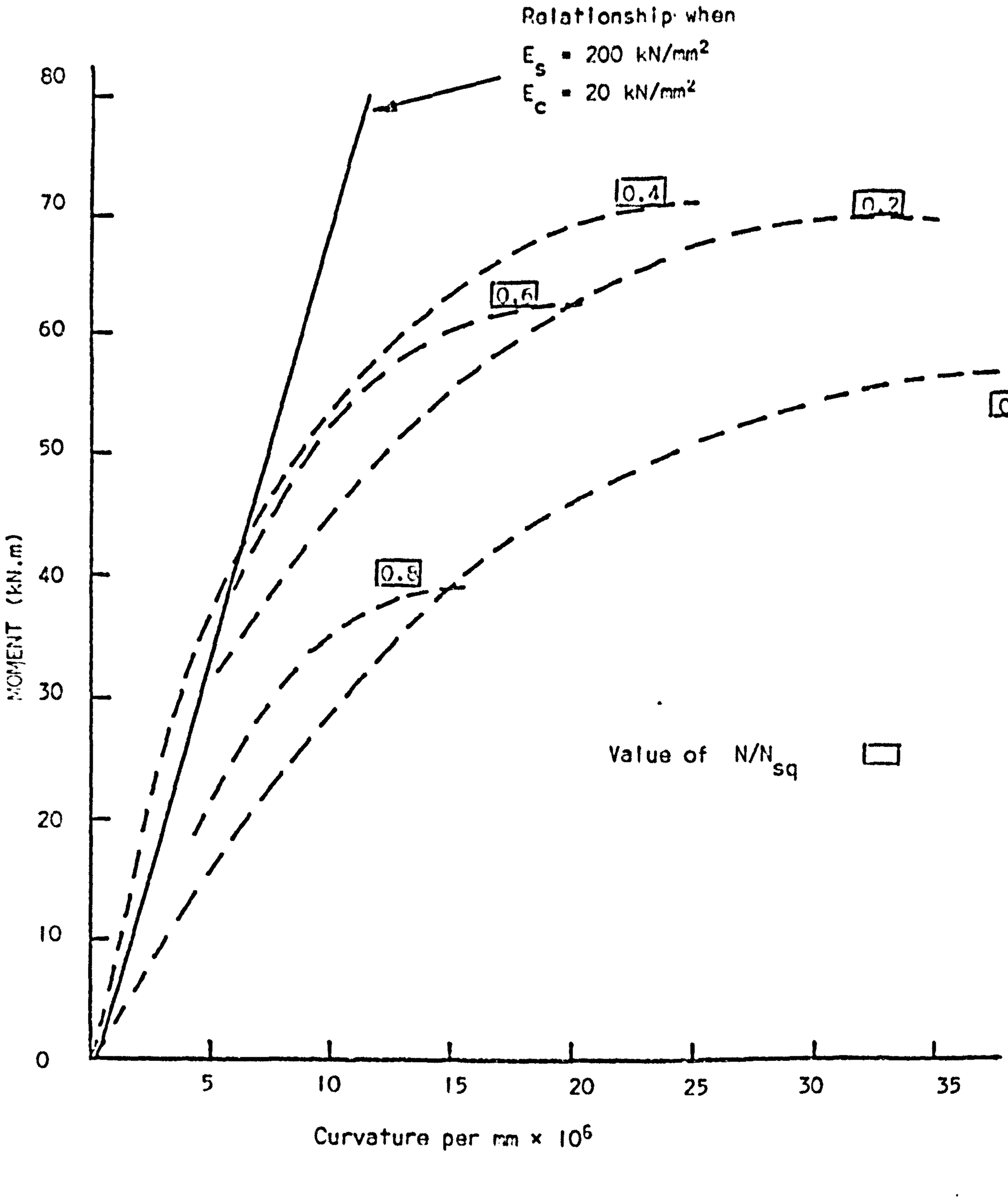

FIG. 8.11 MINOR AXIS MOMENT-CURVATURE RELATIONSHIPS

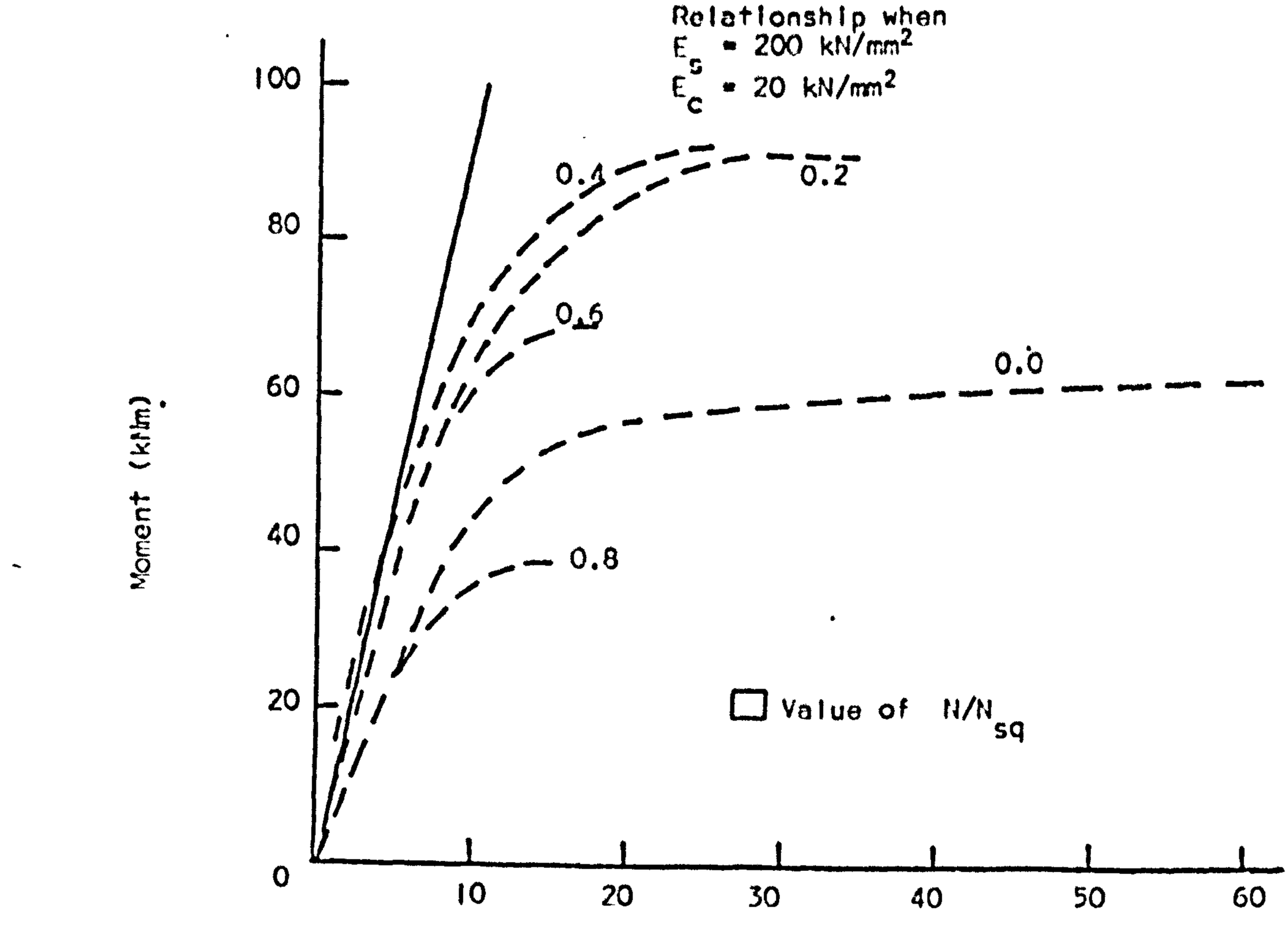

FIG. 8.12 MAJOR AXIS MOMENT-CURVATURE RELATIONS

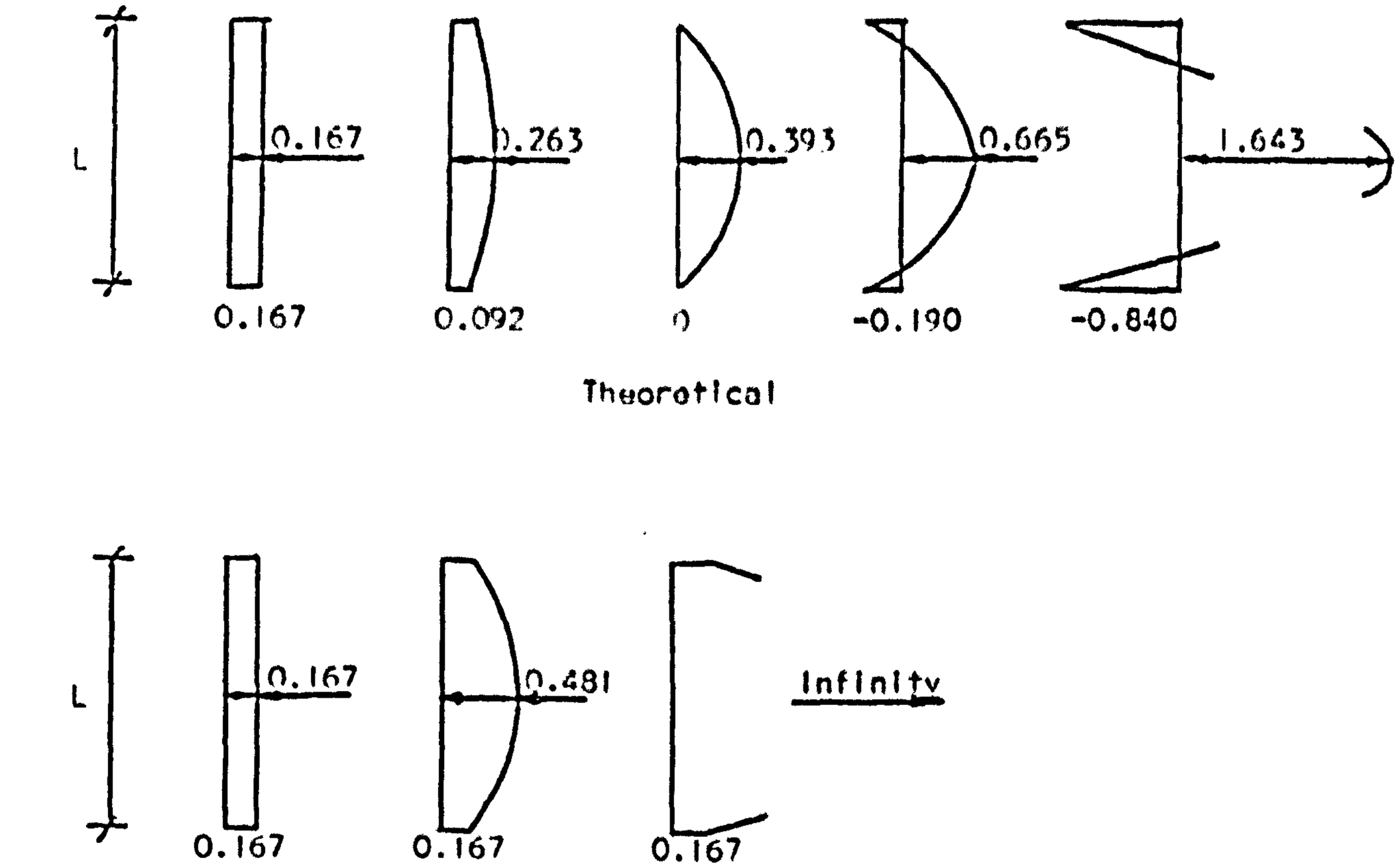

Notes (i) Moments are expressed as proportion of beam fixed end-moments

(ii) N_E is the Euler load of the column

FIG. 8.13 COMPARISON OF METHODS OF ESTIMATING MAXIMUM COLUMN MOMENT

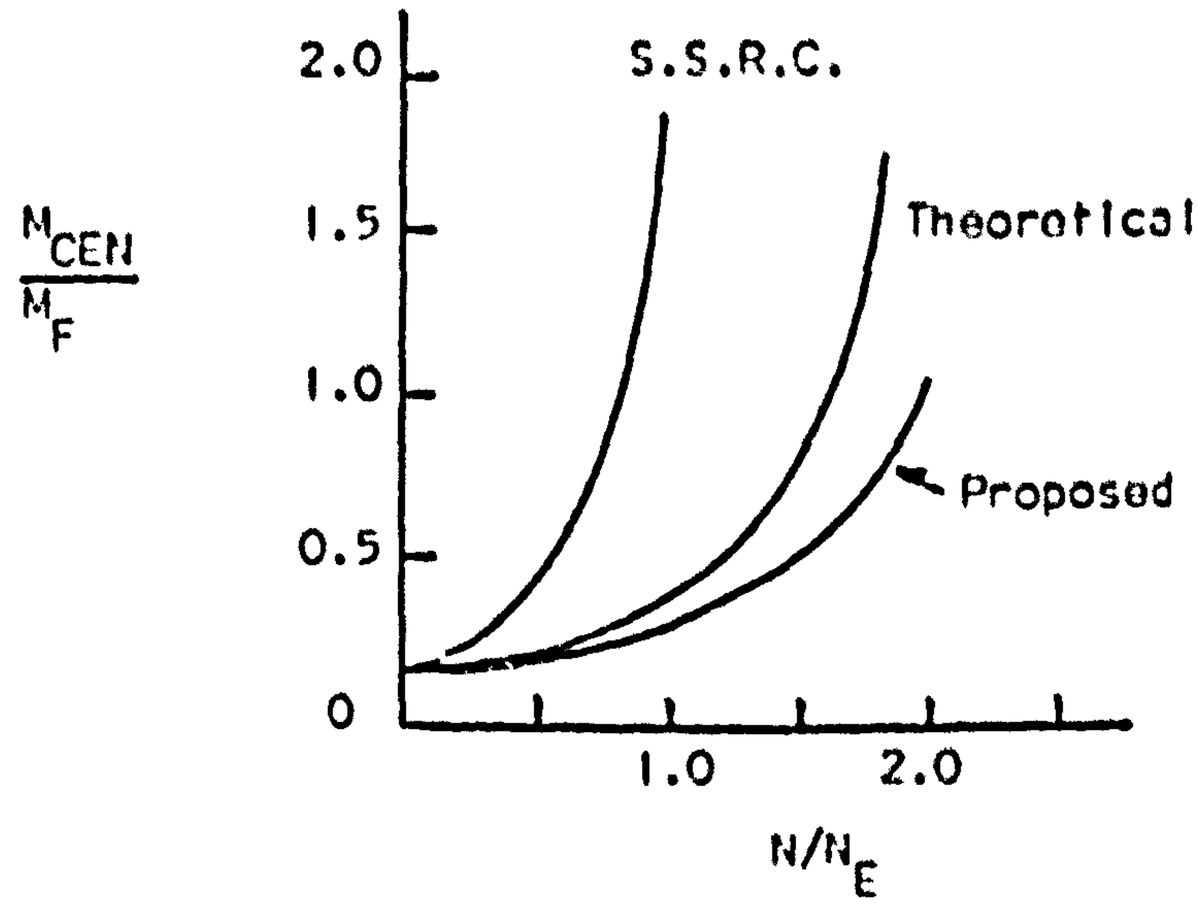

FIG. 8.14 ERRORS IN METHODS OF ESTIMATING MAXIMUM COLUMN MOMENTS

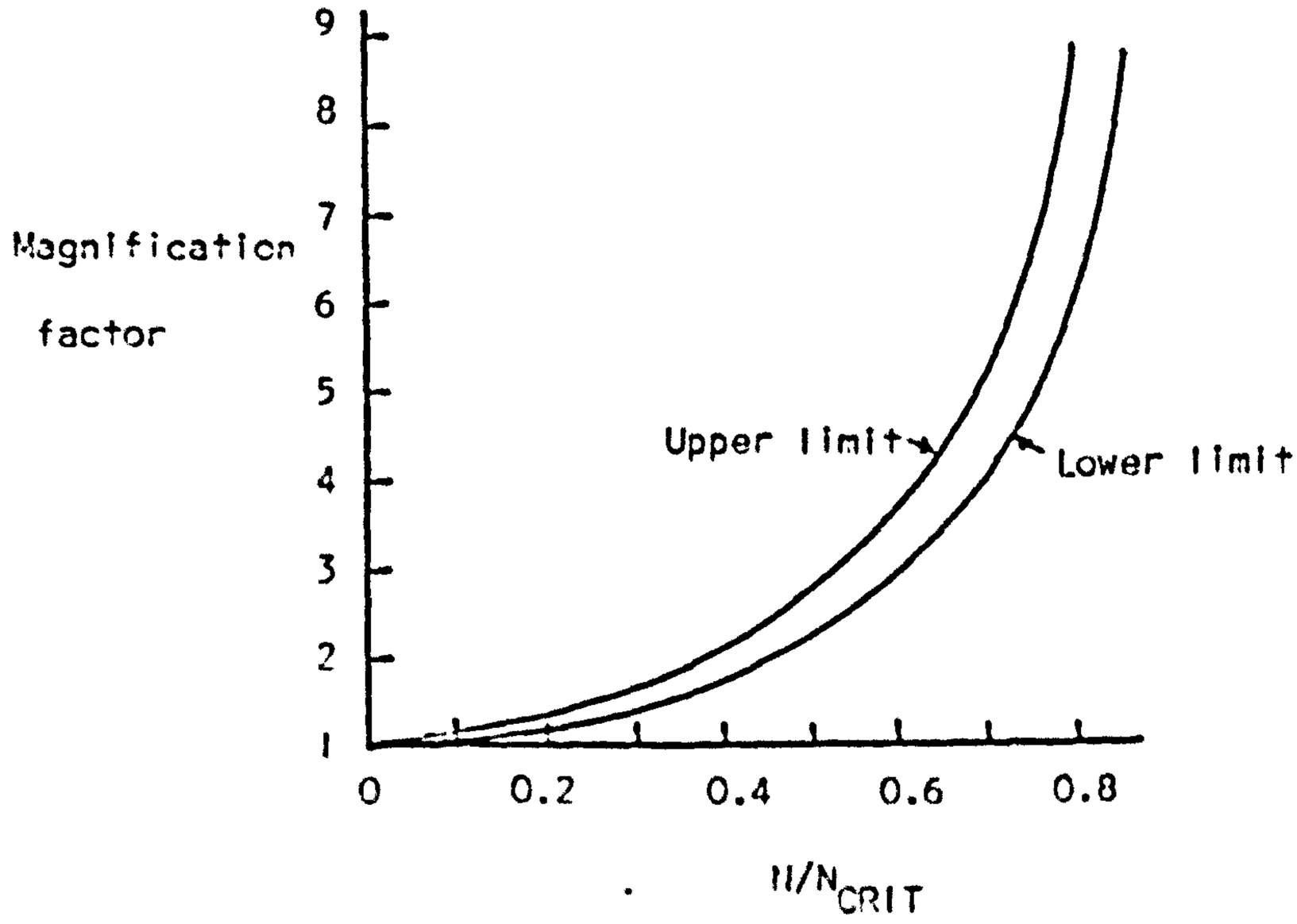

FIG. 8.15 MAGNIFICATION FACTOR FOR MAXIMUM COLUMN MOMENTS

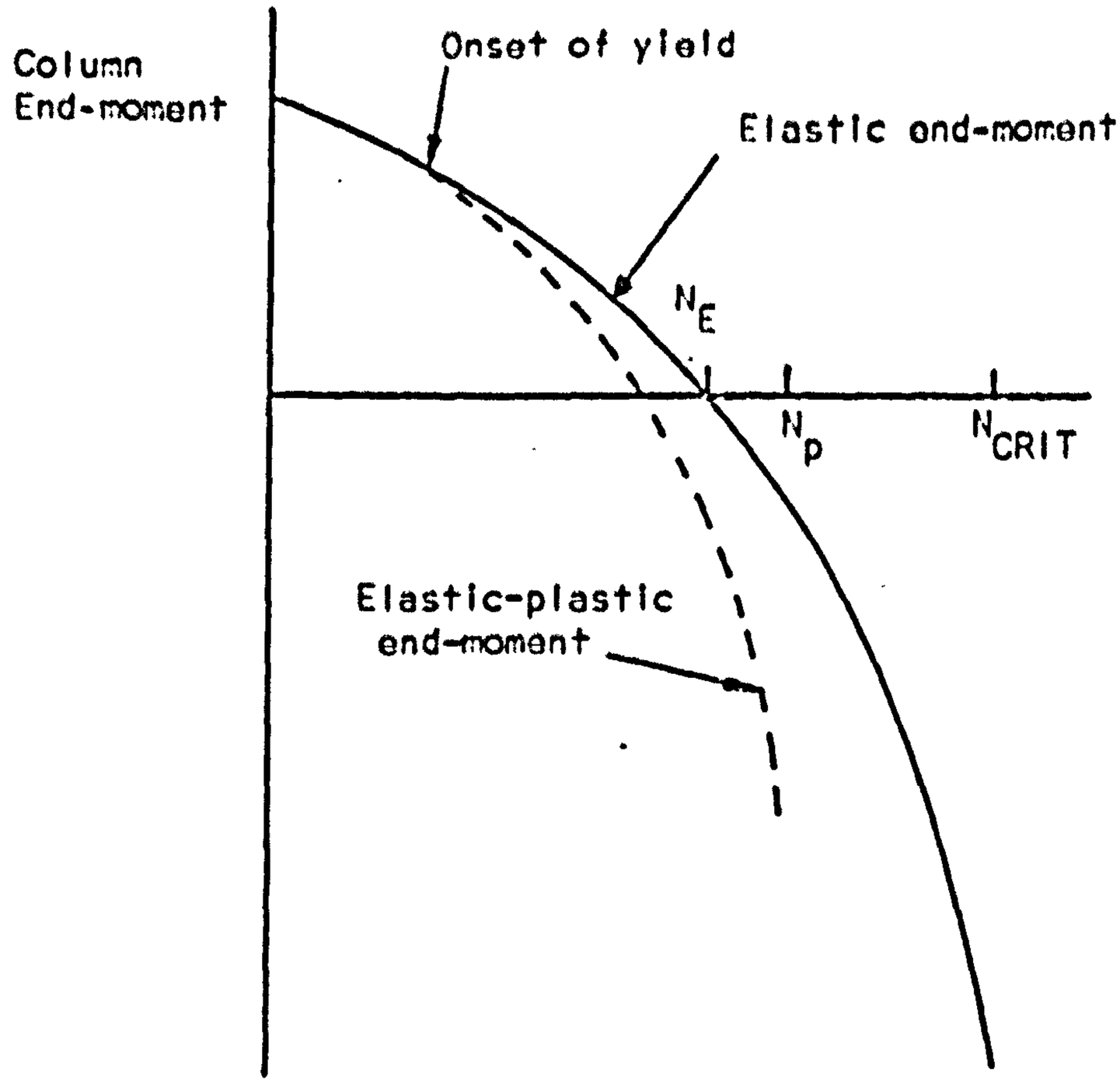

FIG. 8.16 VARIATION OF COLUMN END-MOMENT WITH INCREASE IN AXIAL LOAD.

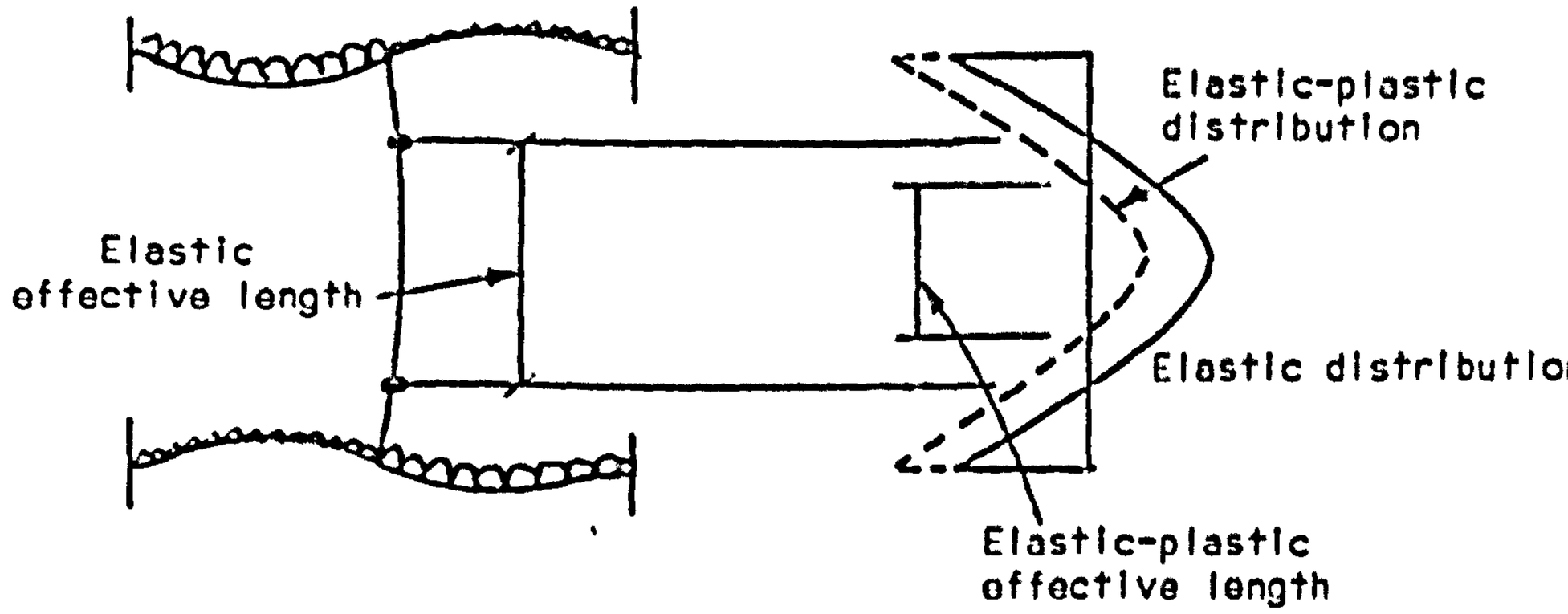

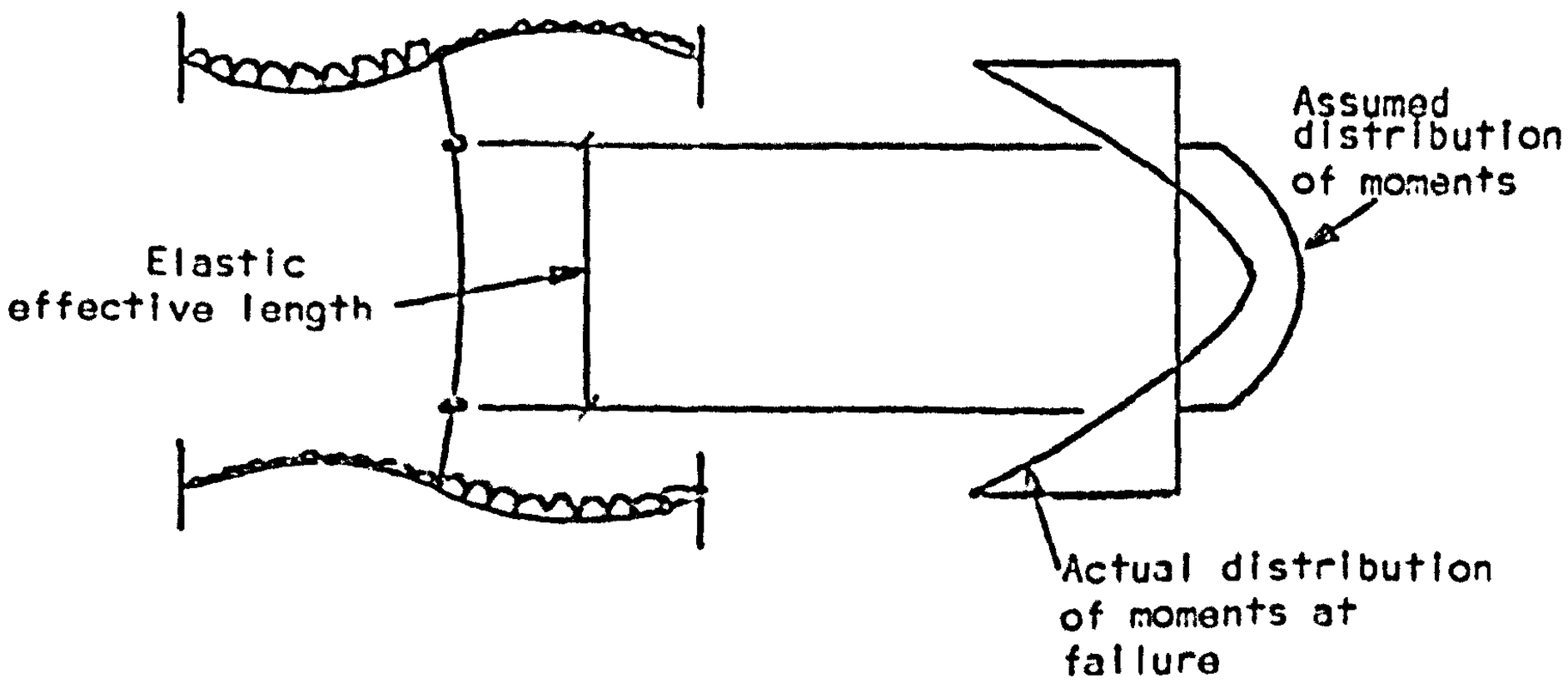

FIG. 8.17 DISTRIBUTION OF MOMENTS AT FAILURE

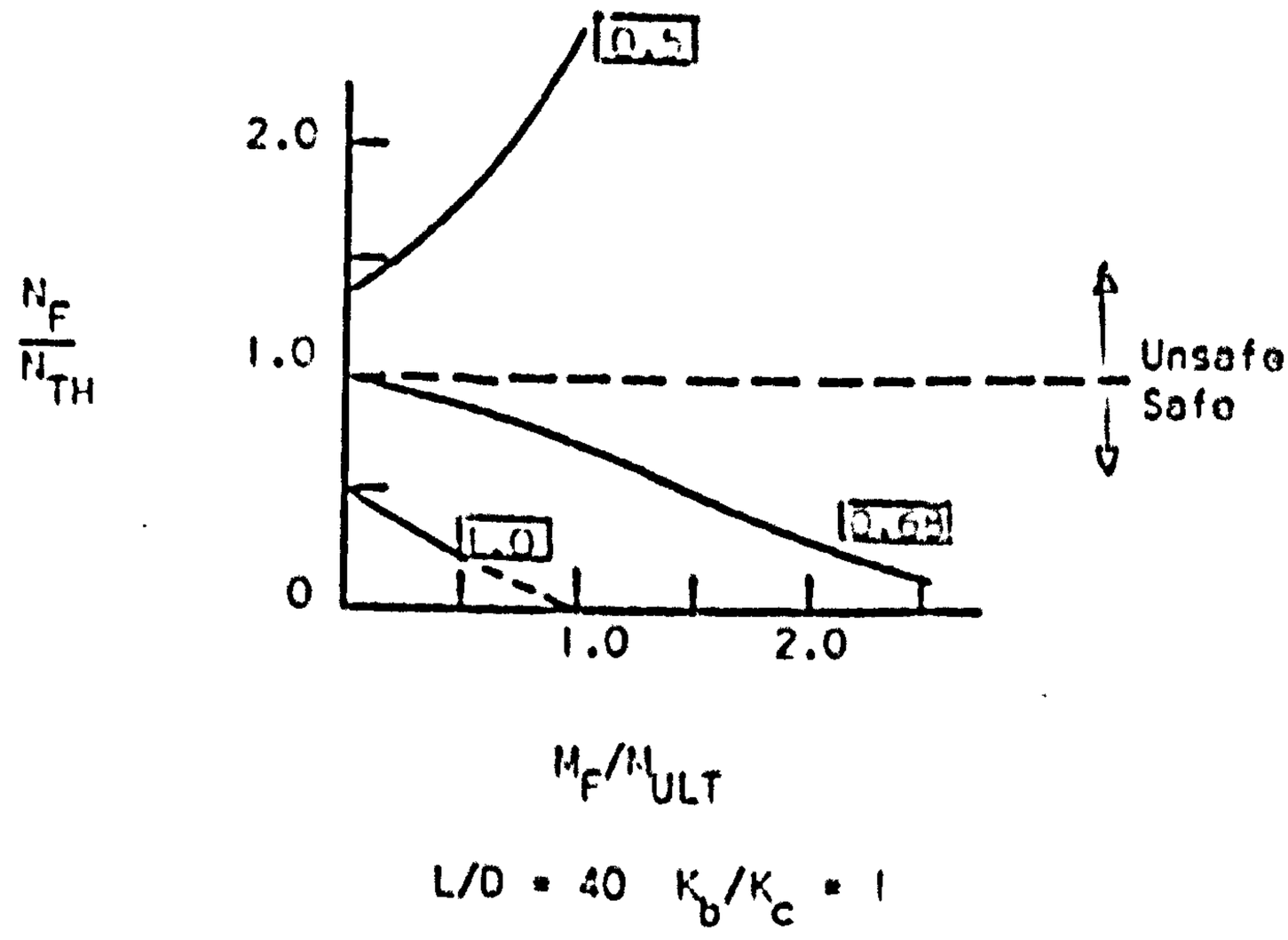

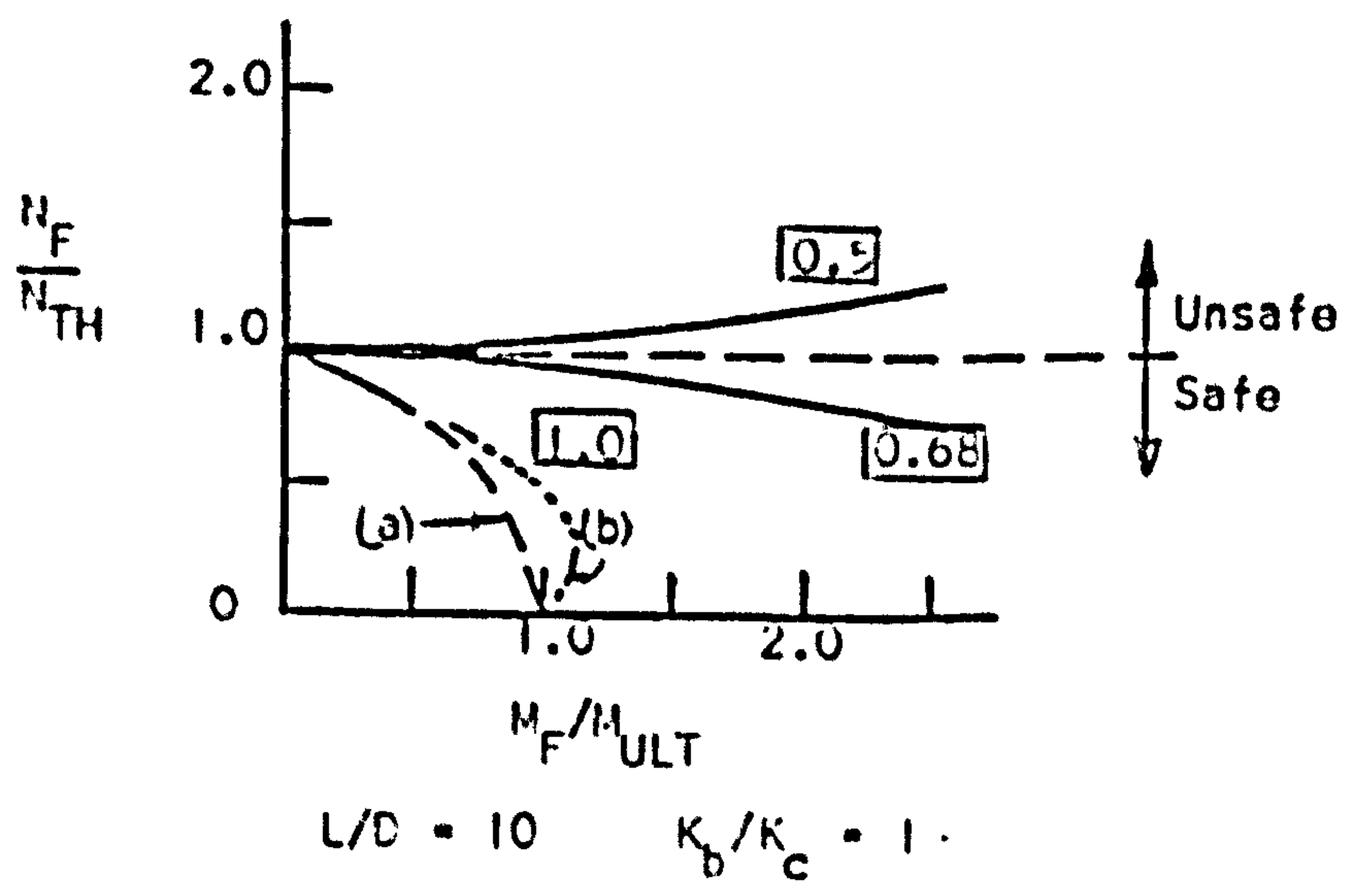

Fig. 8.18 COMPARISON OF LOAD CAPACITY WITH VARIOUS EFFECTIVE LENGTHS

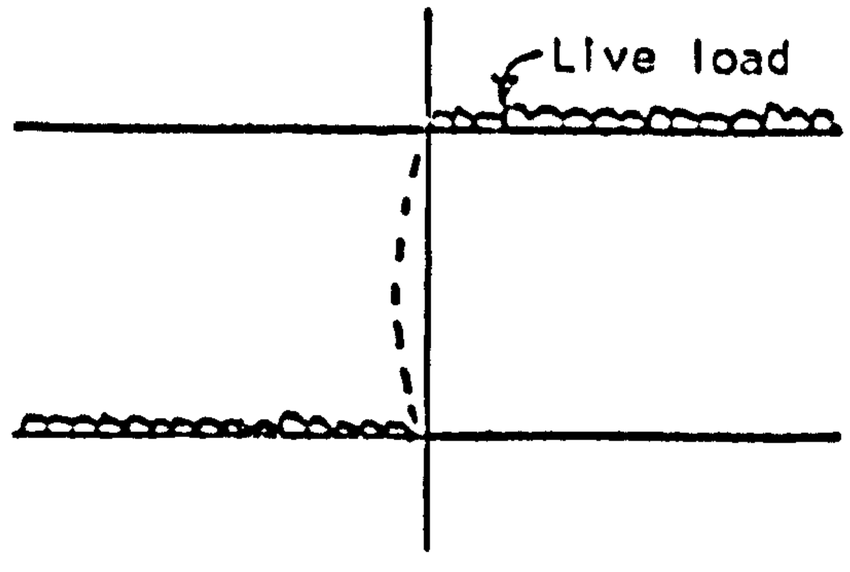

Section AA

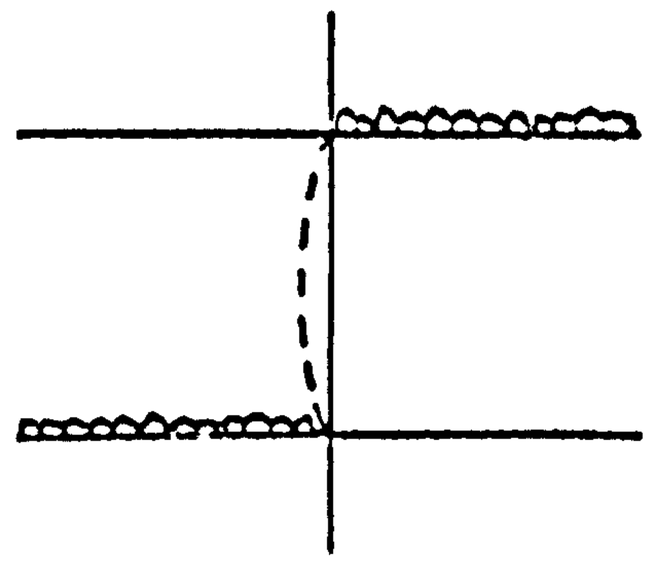

Section BB

Major axis, loading a

Minor axis, loading b

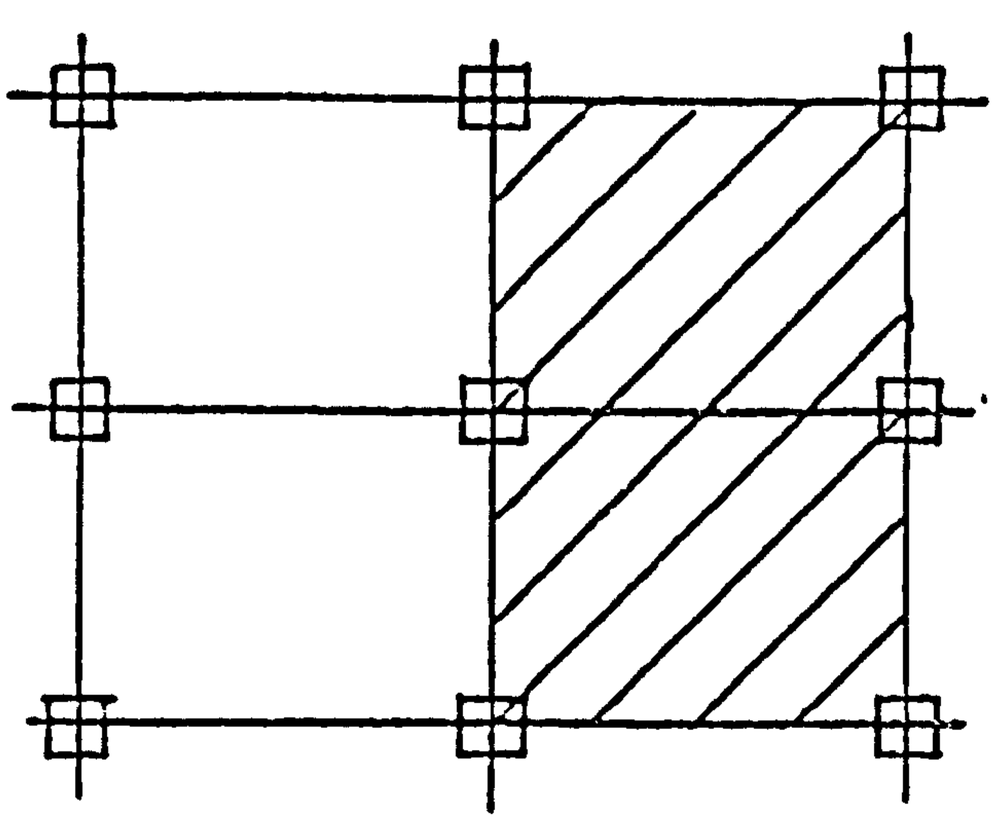

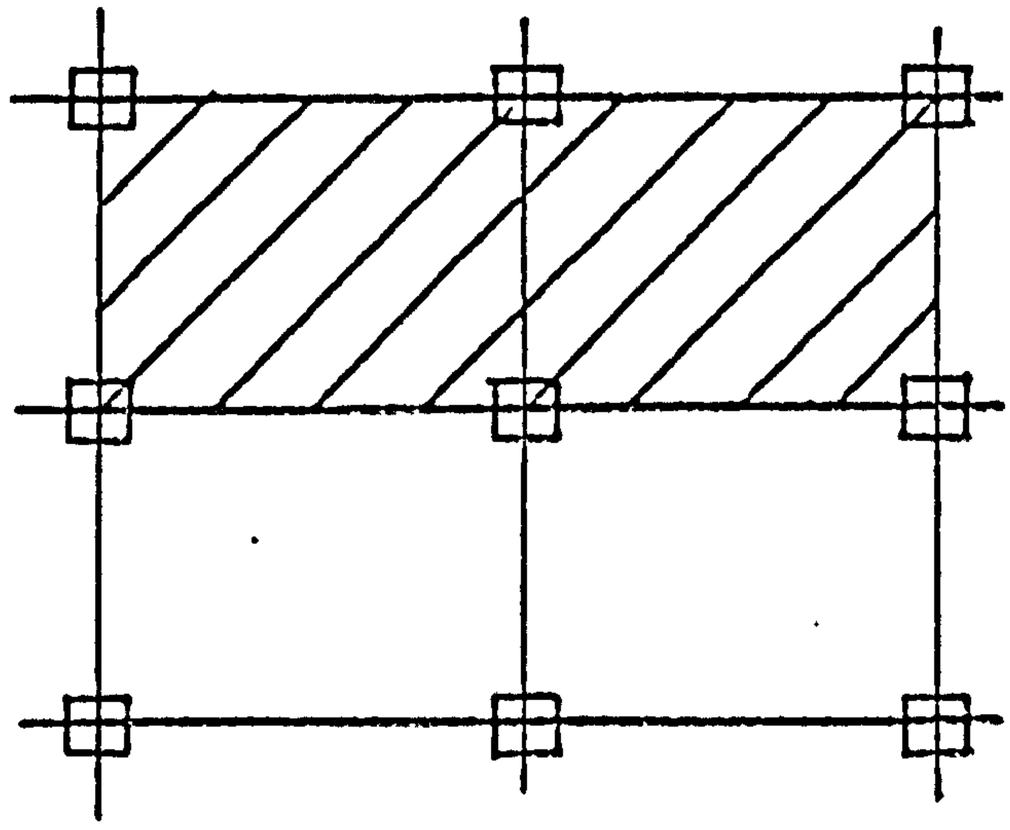

Upper floor plan

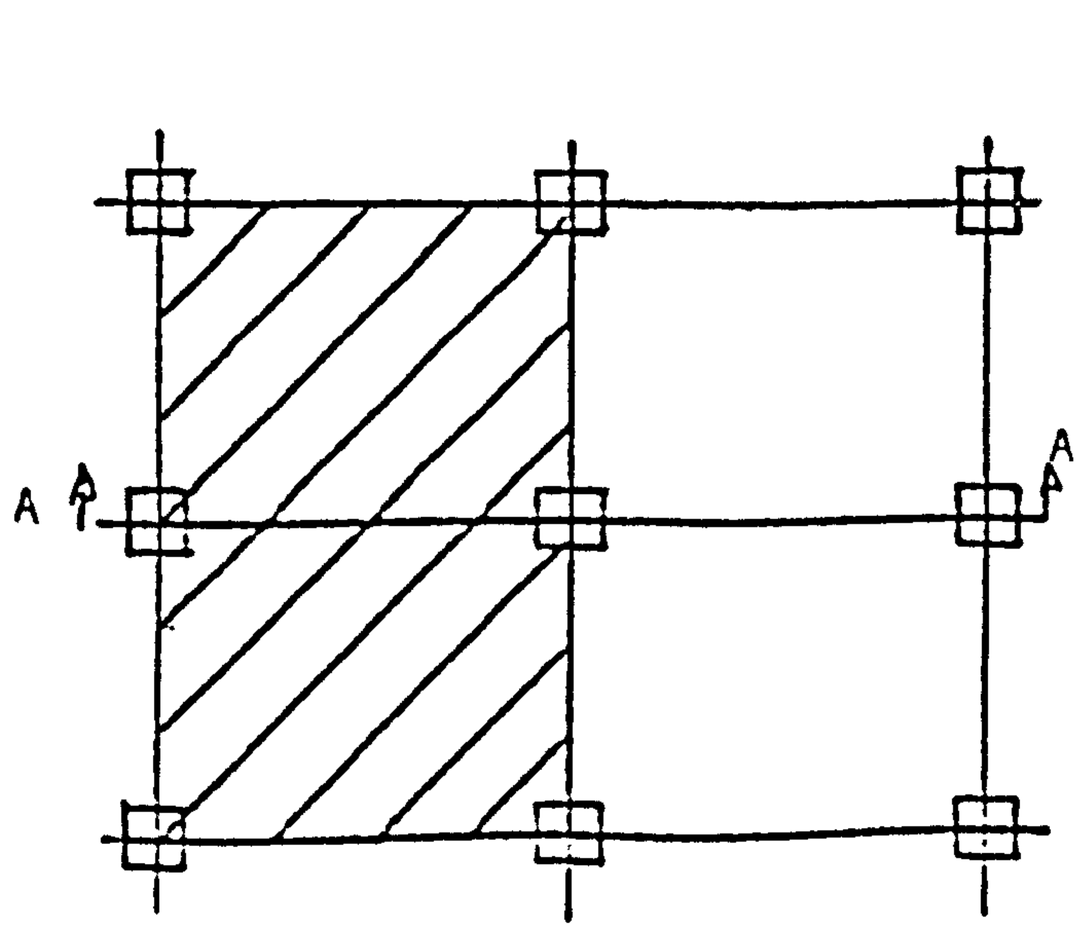

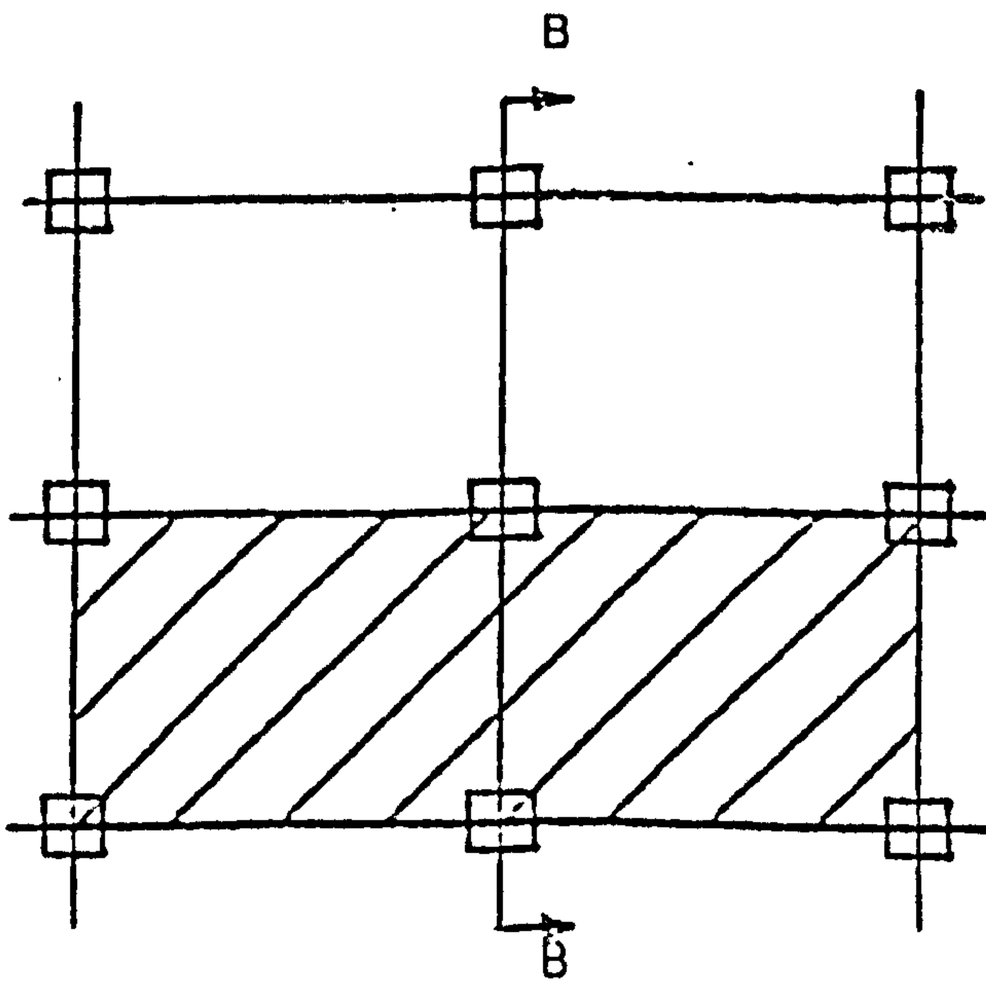

Lower floor plan

FIG. 8.19 ARRANGEMENT OF LIVE LOADS TO GIVE THE WORST COMPONENT OF SINGLE CURVATURE IN INTERNAL COLUMNS.

CHAPTER 9. CONCLUSIONS AND SUGGESTIONS FOR FUTURE WORK.

9.1 Introduction

The object of this Chapter is to summarise the conclusions made in previous Chapters and make suggestions where further work is required. References to the Sections where a fuller account of the conclusions or the behaviour of a column may be found are given.

9.2 Conclusions.

9.2.1 Theoretical analysis

An analysis for biaxially loaded inelastic columns with both rotational and directional restraints at the column ends has been presented. Because the method involves the solution of the flexural differential equations using finite difference expressions an exact solution is obtained as the number of nodes for the finite difference expressions is increased. It is found that in general, however, no more than 16 nodes are required to give results within 4% of the exact solution (Section 2.8).

The main advantages of the analysis are that:

(1) It includes the effects of directional restraint and thus if the restraint is zero a sway solution can be obtained. The value of the restraint can also be set to include the effects of infill panels etc. If the directional restraint is set to infinity then no-sway solutions are obtained (Section 2.3.3).

(2) It can be extended to include additional effects such as axial shortening and torsion.

(3) It only has small error matrices (Section 2.6).

9.2.2. Tests on composite columns.

Eight rotationally restrained no-sway composite columns have been tested to failure using a purpose-built rig. The results from these tests have compared with predictions from the computer analysis and have shown good agreement (Section 7.3 and Table 7.2). The computed predictions of failure loads are, in general, conservative.

One of the three biaxially loaded and restrained columns exhibited premature spalling along the compression zone and further research is required in this area to determine whether this may occur at loads low enough to cause problems at the servicoability limit state (Section 6.4).

The more slender of the columns tested, RC4 and RC5, failed initially by instability followed by the formation of a hinge. (Section 6.3 Fig. 6.15). The remainder of the columns exhibited extensive crushing of the concrete and the formation of hinges followed by an instability failure (Chapter 6). A number of the columns tested exhibited moment reversal (e.g. Fig. 6.28).

The results of the tests on composite columns and other tests on pin-ended tapered steel columns[86] have shown the suitability of the test rig for a variety of column types, end conditions and loadings.

9.2.3 Design methods for composite columns in rigid jointed frames.

Preliminary studies of composite columns within rigid jointed frameworks have led to the following proposals:-

(1) That composite columns in frames with plastically designed composite beams will generally not exceed the permissible beam rotation capacity of the axial load is greater than 20% of the squash load of the column (Section 8.2.5).

(2) That failure of short columns in frames with plastically designed beams and patterned loading may occur before the column end-rotation is large enough to have activated the first plastic hinge in the lightly loaded beam (Section 8.2.5) and until further investigations have been carried out the column should be designed to carry the full out of balance moment.

(3) That the use of steel columns with plastically designed composite beams should include a check on the required end-rotation of the column to mobilise the necessary moment capacity since it is likely that this rotation will often exceed the maximum end-rotation of the beam, (Section 8.2.5).

(4) That in frames with elastic beams the use of elastic effective lengths and moment distribution to calculate the end moments on the column to be designed is conservative, (Section 8.4).

(5) That having calculated the end moments and the effective length of the column to be designed the method of Basu and Somerville[50] can be used to design the column, (Section 8.4).

(6) If the column is stocky, $L/D \leq 15$, restrained by beams at either end such that $K_b/K_c \geq 1$ and has out of balance beam fixed end-moments which do not exceed 1.5 times the ultimate moment

of the column at either end then the cross-section can be designed such that $N \leq 0.8\, N_{sq}$ (Section 8.5). If the column is loaded about the second axis by out of balance fixed end-moments of less than 0.5 times the ultimate moment and satisfies the conditions above it can also be designed as above.

9.3 Suggestions for future work.

The first extension to the computer program should be the inclusion of the moment-rotation relationships for composite beams. The behaviour of the composite limited substitute frame with joints assumed fully rigid can then be investigated and thus the design of composite columns with plastic beams developed further. The effect of choice of the value of effective elastic restraint from a composite beam, when the beams are designed elastically, on the behaviour of the column can also be investigated further.

The program could also be used to carry out investigations into the behaviour of steel columns with plastically designed composite beams.

As more research is carried out on the behaviour of real joints the moment-rotation characteristics of these joints could be included in the analysis to allow the investigation of the behaviour of frames with real joints to be carried out.

Shear restraint characteristics to include the effects of walls etc., can also be included so that sway frames can be investigated and rules formulated for when such frames can be treated as no-sway frames for design.

Further tests are required on biaxially restrained composite columns, especially with the non-linear type of restraint provided by composite beams.

For the design of no-sway rigid-jointed frames Wood[58] has suggested that P_xE_y design is likely to lead to the most economical solution. Because composite columns tend to have less variation of the ratio of major to minor axis flexural rigidity and also tend to be stockier a P_xP_y solution may be the optimum. However the studies of restraint carried out in Chapter 8, Table 8.1, do show that a small amount of restraint can be beneficial and can also lead to simple design methods (Section 8.4).

More research is obviously now required to determine the more economical approach and its limitations, if any.

REFERENCES

1. Euler, L., De curvis elastis, Lausanne and Geneva, 1744.

2. Euler, L., Sur la force de colonnes, Mémoires de l'Académie de Berlin, 1759.

3. Considére, A., Resistance des pieces comprimées, Congres International de procedés de construction, 1889.

4. Engesser, F., Schelzerische Bavzeitung, Vol. 26, p.24, 1895.

5. V. Kármán, T., Die Knickfestigkeit gerader Stäbe, Physikallsche Zeitschrift, Vol. 9, p. 136, 1908.

6. V. Kármán, T., Untersuchungen über Knickfestigkeit, Mittellungen über Forschungsarbeiten auf dem Gebiete des Ingenieurwesens, No. 81, Berlin, 1910.

7. Westergaard, H.M., and Osgood, W.R., Strength of steel columns, Trans. A.S.M.E., Vols. 49-50, APM-50-9, p. 65, 1928.

8. Chwalla, E., Die Stabilität zentrisch und exzentrish gedrückter Stäbe aus Baustahl, Sitzungsberichte der Akademie de Wissenschaften in Wien, Abt. IIa, p.469, 1928.

9. Jezek. K., Die Tragfahigkeit des exzentrisch beanspruchten und des querbelasteten Druckstabes aus einen ideal plastischen Material, Sitzungsberichte de Akademie der Wissenschaften in Wien, Abt. IIa, Vol. 143, 1934.

10. Baker, J.F., and Holder P.D., The behaviour of a pillar forming part of a continuous member in a building frame. Final Report Steel Structures Research Committee, DSIR, HMSO, 1936.

11. Baker, J.F., Horne, M.R., and Heyman, J., The steel skeleton, Vol. II; CUP, 1956.

12. Horne, M.R., The stanchion problem in frame structures designed according to ultimate carrying capacity, Proc. Instn. Civ. Engrs., Part III, Vol. 5, 1956 .

13. Horne, M.R., Safe loads on I section columns in structures designed by plastic theory, Proc. Instn. Civ. Engrs., September 1964, pp. 137-150.

14. Horne, M.R., The plastic design of columns B.C.S.A., Publication 23, 1964.

15. Galambos, T.V., and Ketter, R.L., Columns under combined bending and thrust, Trans. A.S.C.E., Vol. 126, 1961.

16. Newmark, N.M., Numerical procedure for computing deflections, moments and buckling loads, Trans. A.S.C.E., Vol. 108, 1943.

17. Ketter, R.L., Further studies of the strength of beam-columns, Trans. A.S.C.E., Vol. 127, Pt. II, 1962.

18. Rossow, E.C., Barney, G.B., and Lee, S.L., Eccentrically loaded steel columns with initial curvature, Proc. A.S.C.E., J. Struct. Div., Vol. 93, April 1967.

19. Cranston, W.B., Determining the relation between moment, axial load and curvature for structural members, Technical Report TRA 395, Cement and Concrete Association, London,June 1966.

20. Cranston, W.B., A computer method for the analysis of restrained columns, Technical Report TRA 402, Cement and Concrete Association, London, April 1967.

21. Cranston, W.B., Analysis and design of reinforced concrete columns, Research Report 20, Cement and Concrete Association, London, 1972.

22. British Standards Institution, CP110: Part 1: 1972, The structural use of concrete, London, 1972.

23. Harstead, G.A., Birnstiel, C., and Leu, K-C., Inelastic H-columns under biaxial loading, Proc. A.S.C.E., J. Struct. Div., Vol. 94, October 1968.

24. Vinnakota, S., and Aoshima, Y., Inelastic behaviour of rotationally restrained columns under biaxial bending, The Structural Engineer, Vol. 52, July 1974.

25. Birnstiel, C., Leu, K-C., Tesaro, J.A., and Tomasetti, R.L., Experiments on H-columns under biaxial bending, New York University, January 1967.

26. Gent, A.R., and Milner, H.R., The ultimate load capacity of elastically restrained H-columns under biaxial bending, Proc. I.C.E., Vol. 41, December 1968.

27. Young, B.W., Axially loaded steel columns, Camb. Univ. Eng. Dept., Tech. Rep. CUED/C-struct/TR11, 1971.

28. Young, B.W., In-plane failure of steel columns subjected to uniaxial applied end-moments, Camb. Univ. Eng. Dept., Tech. Rep. CUED/C-struct/TR12, 1971.

29. Young, B.W., Residual stresses in hot rolled sections, Camb. Univ. Eng. Dept., Tech. Rep. CUED/C-struct/TR8, 1971.

30. Johnston, B.G., and Cheyney, L., Steel columns of rolled wide-flange section, A.I.S.C. Progress Report No. 2, November 1942.

31. Van Kuren, R.C., and Galambos, T.V., Beam-column experiments, Proc. A.S.C.E., J. Struct. Div. Vol. 90, ST2, April 1964.

32. Campus, F., and Massonet, C., Recherche sue le flambement de colonnes en acier A37 à profil en double té sollicitees obliquement, Bull de C.E.R.E.S. Liege, 1955.

33. Young, B.W., Design of unbraced steel columns subjected to biaxial applied end-moment, Camb. Univ. Eng. Dept., Tech. Rep. CUED/C-Struct/TR13, 1971.

34. Young, B.W., Restrained Column design, Camb. Univ. Eng. Dept., Tech. Rep. CUED/C-Struct/TR13, 1971.

35. Gent, A.R., Elastic-plastic column stability and the design of no-sway frames, Proc. I.C.E., Vol. 34, June 1966, pp.129-151.

36. Bondale, D.S., The effect of concrete encasement on eccentrically loaded steel columns, Ph.D. Thesis, University of London, 1962.

37. Talbot, A.N., and Lord, A.R., Tests of columns: An Investigation of the value of concrete as reinforcement for structural steel columns, University of Illinois Eng. Expt. Stn. Bull. No. 56, March 1912.

38. Mensch, L.J., Composite columns, Journal A.C.I., Vol. 2, No. 3, November 1930, pp.263-280.

39. Emperger, F., Discussion on Reference 33, Proc. A.C.I., Vol. 27, 1930-31, pp. 1311-1318.

40. Burr, W.H., Composite columns of concrete and steel, Proc. I.C.E., Vol. 188, 1912, pp. 114-126.

41. Faber, O., Steel reinforced with concrete, Concrete and Construction Engg., Vol. 19, No. 12, December 1924, pp. 755-763.

42. Stang, A., Wittemore, H.L., and Parsons, D.E., Some tests of steel columns encased in concrete, Journal of Research of the National Bureau of Standards, Vol., 16, No. 3, Research paper No. 873, March 1936, pp. 265-287.

43. British Standards Institution, BS449: 1948, The use of structural steel in building, London, 1948.

44. Faber, O., Savings to be effected by the more rational design of cased stanchions as a result of recent full size tests, The Structural Engineer, Vol. 34, No. 3, March 1956.

45. Rizk, A.A., The effect of concrete encasement on the behaviour of steel framed buildings, Ph.D. Thesis, University of Leeds, September 1957.

46. Stevens, R.F., Encased steel stanchions and BS449, Engineering, Vol. 188, No. 4879, October 1959.

47. British Standards Institution, BS449: 1959, The use of structural steel in building, London, 1959.

48. Basu, A.K., Computation of failure loads of composite columns, Proc. I.C.E., Vol. 36, No. 6980, March 1967.

49. Basu, A.K., and Hill, W.F., A more exact computation of failure loads of composite columns, Proc. I.C.E., Vol. 40, No. 7074, May 1968.

50. Basu, A.K., and Somerville, W., Derivation of formulae for the design of rectangular composite columns, Proc. I.C.E., Supplementary Volume No. 7206S, December 1969.

51. Roderick, J.W., and Rogers, D.F., Load carrying capacity of composite columns, J.A.S.C.E., Vol. 95, No. ST2, February 1969, pp. 209-228.

52. Sharples, B.P.M., Composite columns, Ph.D. Thesis, University of Cambridge, 1970.

53. Virdi, K.S., and Dowling, P.J., The ultimate strength of composite columns in biaxial bending, Proc. I.C.E., Vol. 55, March 1973, pp. 251-272.

54. Virdi, K.S., Inelastic column behaviour, Ph.D. Thesis, University of London, 1973.

55. Virdi, K.S., and Dowling, P.J., The ultimate strength of biaxially restrained columns, CESLIC Report CC12, Imperial College, London, March 1975.

56. Milner, H.R., The elastic-plastic stability of stanchions bent about two axes, Ph.D. Thesis, University of London, 1966.

57. Joint Committees Second Report on fully-rigid multi-storey welded steel frames. The Institution of Structural Engineers and Institute of Welding, 1971.

58. Wood, R.H. A new approach to column design. Department of the Environment, 1973.

59. Smith, R.F. and Roberts, E.H. Test of a fully continuous multi-storey frame of high yield steel. Journal of the Institution of Structural Engineers, Vol. 49, No. 10, pp.203-212, 1971.

60. Wood, R.H., Needham, F.H. and Smith, R.F. Test of a multi-storey rigid steel frame. Journal of the Institution of Structural Engineers, Vol. 46, No. 4, pp.107-119, April 1968.

61. British Standards Institution CP114 : 1957, The structural use of reinforced concrete in buildings, London, 1963.

62. Bresler, B. Design criteria for reinforced concrete columns under axial load and biaxial bending. ACI Journal, Proceedings Vol. 57, No. 5, pp. 481-490, Nov. 1960.

63. Building Code requirements for reinforced concrete (ACI-318-71), American Concrete Institute, Detroit, Michigan, February 1971.

64. Macgregor, J.G., Breen, J.E. and Pfrang, E.O. Design of slender columns, ACI Journal, Proceedings, Vol. 67, pp.6-28, Jan. 1970.

65. Taylor, J.C. TP95A Simple design of cased struts. B/20 British Standards Institution, 1974.

66. Barnard, P.R., and Johnson, R.P., Ultimate strength of composite beams, Proc. I.C.E., Vol. 32, No. 6836, Oct. 1965.

67. Warner R.F., Biaxial moment thrust curvature relations, Proc. A.S.C.E., J. Struct. Div., Vol. 95, May 1969.

68. Procter A.N., Tests on stability of concrete encased I-beams, Part One, The Consulting Engineer, February 1967.

69. Hutchings, R., The elasto-plastic behaviour of columns under biaxial loading. Ph.D. Thesis, Manchester University 1973.

70. Wood, R.H., Studies in composite construction, Part II. The interaction of floors and beams in multi-storey buildings, H.M.S.O., 1955.

71. Taylor, D.A., An experimental study of continuous columns, Proc. I.C.E., Vol. 53, June 1972.

72. British Standards Institution, TP.69, Draft specification for cased struts, B/20/5, 1973.

73. British Standards Institution, B.S.18, Methods for tensile testing of metals, London, 1962.

74. Sankey A.P. The measurement of residual stresses. Report on research project, University of Warwick, 1974.

75. Young B.W., Residual stresses in hot rolled sections. Cambridge University Engineering Department. Technical Report No. CUED/C-Struct/TR.8 (1971).

76. Ferguson P.M., and Breen J.E., Investigation of the long concrete column in a frame subject to lateral loads. Symposium on Reinforced Concrete Columns A.C.I., Publication SP-13. 1965.

77. Neville A.M., Properties of concrete, Pitman, 1963.

78. Huber, A.W., and Beedle, L.S., Residual stress and the compressive strength of steel. The Welding Journal, Vol. 33, No. 12, December 1954.

79. Handbook on structural steelwork B.C.S.A. & Constrado. 1971.

80. Climenhaga J.J., and Johnson R.P., Local buckling in continuous composite beams, The Structural Engineer, Vol. 50, September 1972.

81. Johnson R.P. and Smith D.G.E., Cross-section slenderness ratios, TP 208, B/20/5 Sub-committee, British Standards Institution, January 1976.

82. The design of composite bridges, Part 5, Draft British Standard Specification, 1975.

83. Wood R.H., Effective lengths of columns in multi-storey buildings Parts 1, 2 and 3. The Structural Engineer, July, August, and September, 1974.

84. Wood R.H., The stability of tall buildings. Proc. I.C.E. September 1958.

85. Horne M.R., and Merchant W., The stability of frames, Pergamon, 1965.

86. Salter J.B., Column behaviour and deflection control in steel frames, Ph.D. Thesis, University of Warwick, 1976.

87. Vitkovitch, P. (Ed.), Field analysis, London, van Nostrand, 1966.

88. Hope-Gill M.C., The ultimate strength of continuous composite beams, Ph.D. Thesis, University of Cambridge, 1974.

89. Wood R.H., Lawton W.T., and Goodwin E., Rapid design of multi-storey rigid-jointed steel frames, Note A58, Building Research Station, DSIR, 1957.

Appendix A1

The Newton-Raphson technique for the determination of roots of non-linear simultaneous equations.

A1.1 Method for two equations.

Consider two equations in two unknowns

$$f(x, y) = 0$$
$$g(x, y) = 0 \qquad \text{(A1.1)}$$

and let x_o, y_o be initial approximate solutions. The method seeks to obtain corrections Δ_x and Δ_y on x_o and y_o so that the corrected values will be

$$x = x_o + \Delta_x$$
$$y = y_o + \Delta_y \qquad \text{(A1.2)}$$

for which

$$f(x_o + \Delta_x, y_o + \Delta_y) = 0$$
$$g(x_o + \Delta_x, y_o + \Delta_y) = 0 \qquad \text{(A1.3)}$$

Expansion of equations A1.3 by Taylor's theorem gives

$$f(x_o + \Delta_x, y_o + \Delta_y) = f(x_o, y_o) + f'_x(x_o, y_o)\,\Delta_x + f'_y(x_o, y_o)\Delta_y + \ldots = 0$$
$$g(x_o + \Delta_x, y_o + \Delta_y) = g(x_o, y_o) + g'_x(x_o, y_o)\Delta_x + g'_y(x_o, y_o)\Delta_y + \ldots = 0 \qquad \text{(A1.4)}$$

where f'_x, f'_y, g'_x, g'_y are notation for partial derivations.

Ignoring all terms higher than first order and rearranging A4 gives

$$f'_x(x_o,y_o)\Delta_x + f'_y(x_o,y_o)\Delta_y = -f(x_o,y_o)$$

$$g'_x(x_o,y_o)\Delta_x + g'_y(x_o,y_o)\Delta_y = -g(x_o,y_o) \qquad \text{(A1.5)}$$

which can be solves simultaneously to give Δ_x and Δ_y. The process is then repeated using

$$x_1 = x_o + \Delta_x \qquad \text{(A1.6)}$$

$$y_1 = y_o + \Delta_y$$

and evaluating the functions and their partial derivatives at x, y. The process is repeated until the desired degree of accuracy is obtained.

A1.2 Extension to 'n' equations and use in structural problems

In most structural applications the differentiation is carried out numerically by incrementing each independent variable in turn.

e.g. $f'_x(x_o,y_o)\Delta_x$

$$= \left(\frac{f(x_o + \delta_x, y_o) - f(x_o,y_o)}{\delta_x}\right)\Delta_x \qquad \text{(A1.7)}$$

and similarly for $f'_y(x_o, y_o)\Delta_y$ etc.

Substituting these differentials into A5 and rearranging gives

$$\begin{bmatrix} \dfrac{f(x_o + \delta_x, y_o) - f(x_o, y_o)}{\delta_x} & \dfrac{f(x_o,y_o + \delta_y) - f(x_o,} \\ \dfrac{g(x_o + \delta_x, y_o) - g(x_o,y_o)}{\delta_x} & \dfrac{g(x_o,y_o + \delta_y) - g(x_o,y_o)}{\delta_y} \end{bmatrix}$$

$$\begin{bmatrix} -f(x_o, y_o) \\ -y(x_o, y_o) \end{bmatrix} = \begin{bmatrix} \Delta_x \\ \Delta_y \end{bmatrix} - \qquad \text{(A1.8)}$$

thus $\underline{[\Delta] = - [E]^{-1} [f]}$ (A1.9)

where E is the matrix of errors. Extension to solution of equations of higher degree is accomplished by the use of Taylor's Theorem and results in equations similar to A1.9 where the order of E is the same as the number of variables.

Appendix A2 Column analysis by integration of the shear equation.

A2.1. Theory. A saving could be made in computation time in the moment curvature relationships if these can be entered with known curvatures, ϕ_x and ϕ_y and axial load, N, as the error matrix reduces from 3×3 to a single term. The following method is an attempt to do this whilst retaining the advantage of equilibrium on each iteration.

Consider the column in Fig. A2-1 then

$$M_1 = M_1 - S_1 x + Nv \tag{A2.1}$$

and hence

$$\frac{dM_1}{dx} = -M_1 + N\frac{dv}{dx} \tag{A2.2}$$

As $M_1 = -(EI)_1\left(\frac{d^2v}{dx^2}\right)_1$

If $(EI)_1$ is variable, due to plasticity, cracking, etc.,

$$\text{then } \frac{dM_1}{dx}\left(1 + \frac{d^2v}{dx^2}\frac{dEI}{dM}\right) = -EI\frac{d^3v}{dx^3} \tag{A2.3}$$

Equation A2.3 can now be forward solved using central differences. If we consider a node in the analysis, Fig. A2-2, where v_o, v_1, v_2 and v_3 are known then the curvature at node 2 can be calculated, and from the moment curvature relationships the value of EI. $\frac{dM_1}{dx}$ is calculated from equation A2.2 and $\frac{dEI}{dM}$ is found using backward differences on nodes 2 and 1.

Equation A2.3 can now be solved for $\frac{d^3v}{d_x^3}$ and hence, by the use of central differences v_4 found.

The extension to the biaxial case involves the solution of the flexural equations about both axes. The moment-thrust-curvature relations are then entered with two curvatures ϕ_x and ϕ_y.

A2.2 Starting analysis

Consider the top end of a column, Fig. A2-3. If M_1 is known then from the moment curvature relationships the curvature can be found and $\frac{dEI}{dM}$ estimated. As the shear will be known $\frac{dM}{dx}$ can be calculated from equation A2.2. Solution of equation A2.3 gives $\frac{d^3v}{dx^3}$ and by use of finite differences operating on nodes 0, 1, 2 and 3 the deflection at node 3 can be found.

A2.3 Comments on analysis.

The analysis has been programmed and various tests carried out. During each test external moments calculated during the analysis have been compared with the internal moments obtained from the moment-curvature relationships. Agreement has not always been good and this seems to be due to the calculation of the function $\frac{dEI}{dM}$. Discontinuities occur in the values due to elements being uncracked at one load level and then cracking, Fig. A2-4, and similarly with yielding elements.

This method of analysis has thus been discontinued but it is felt that the method is potentially powerful enough to warrant further investigation.

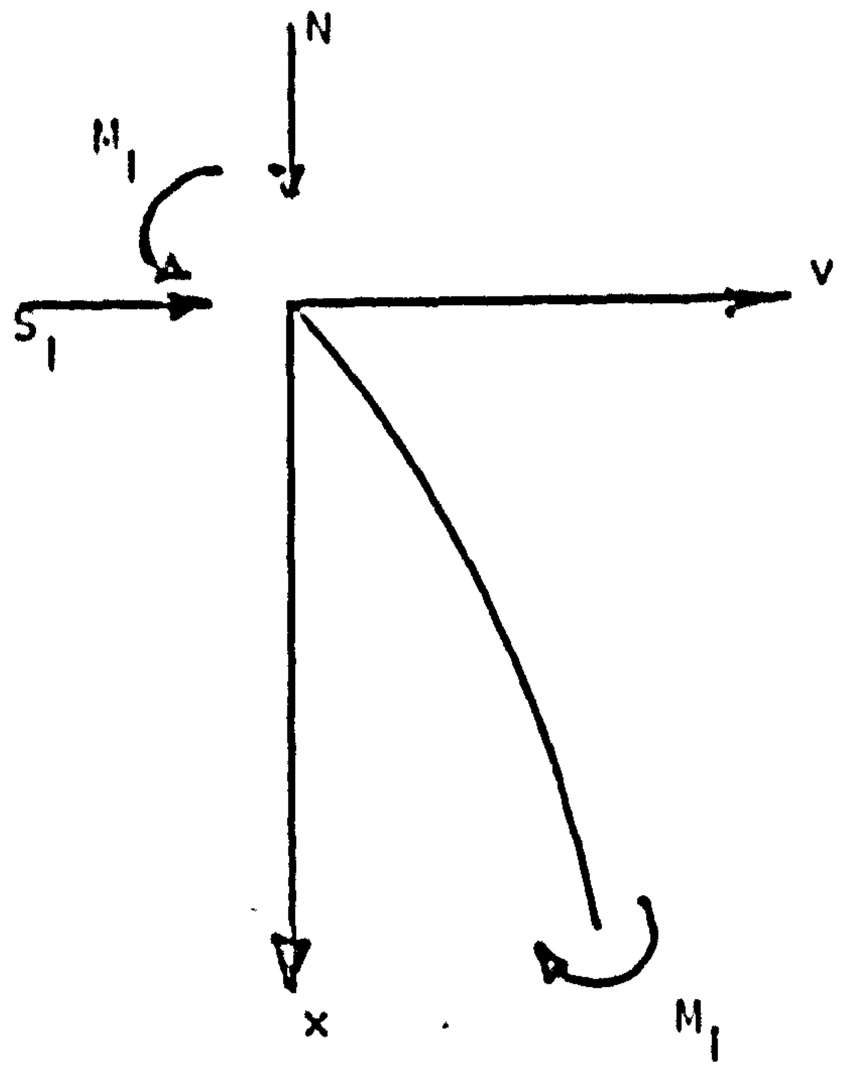

FIG. A2.1 FORCES ON A COLUMN

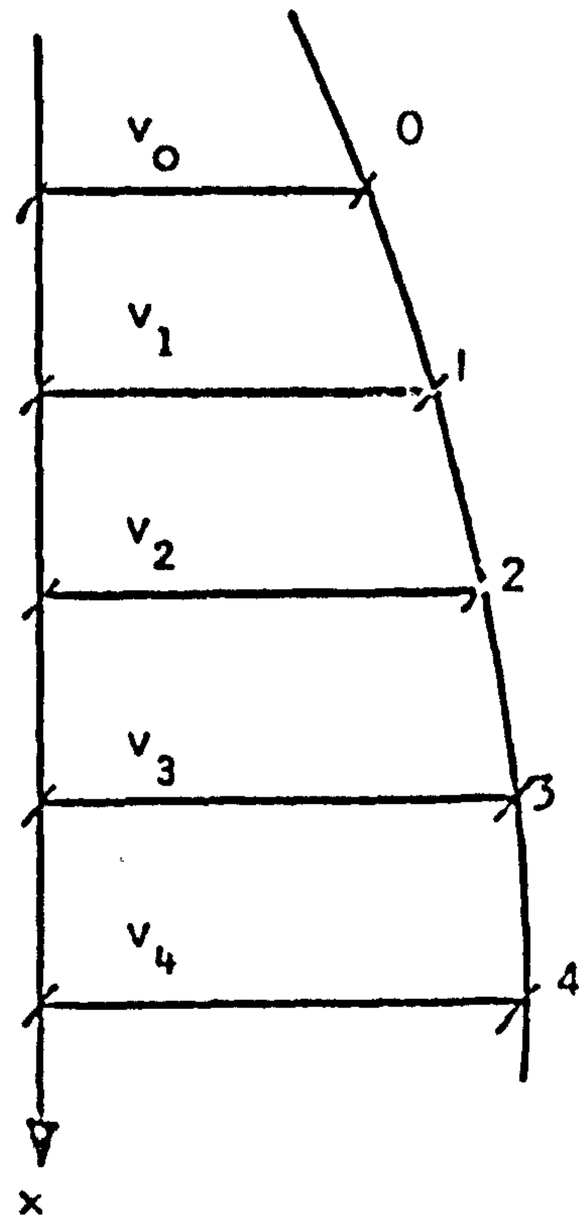

FIG. A2.2 NODES ALONG THE COLUMN

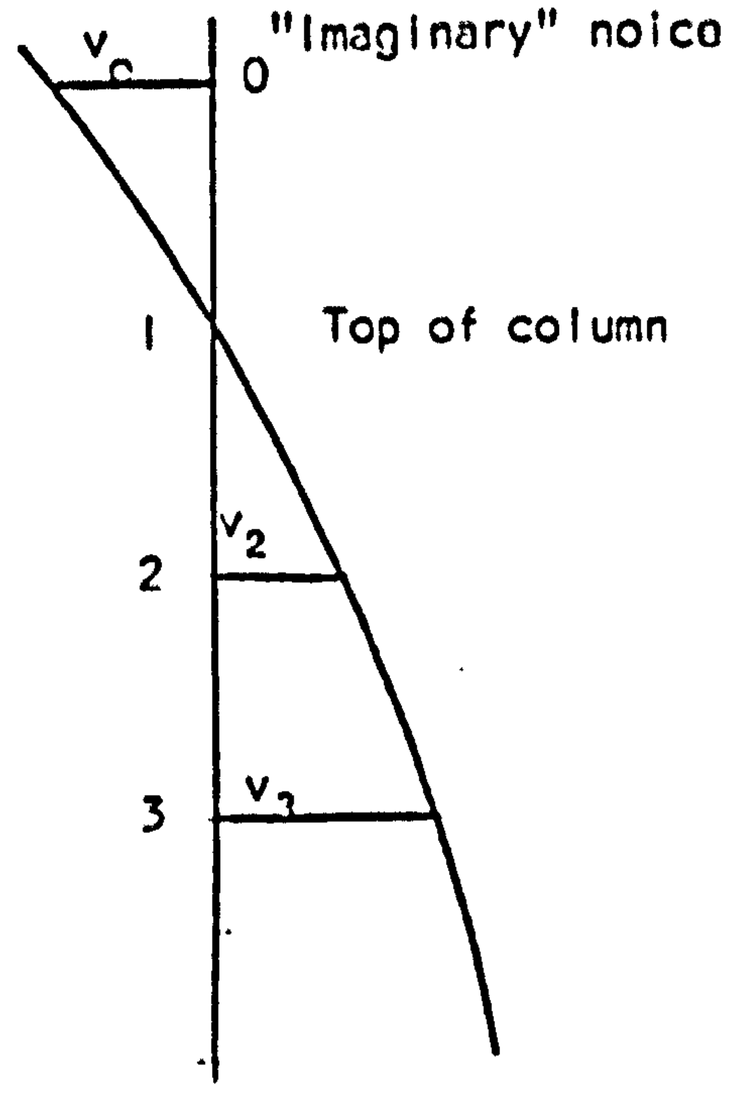

FIG. A2.3 NODES NEAR TOP OF COLUMN

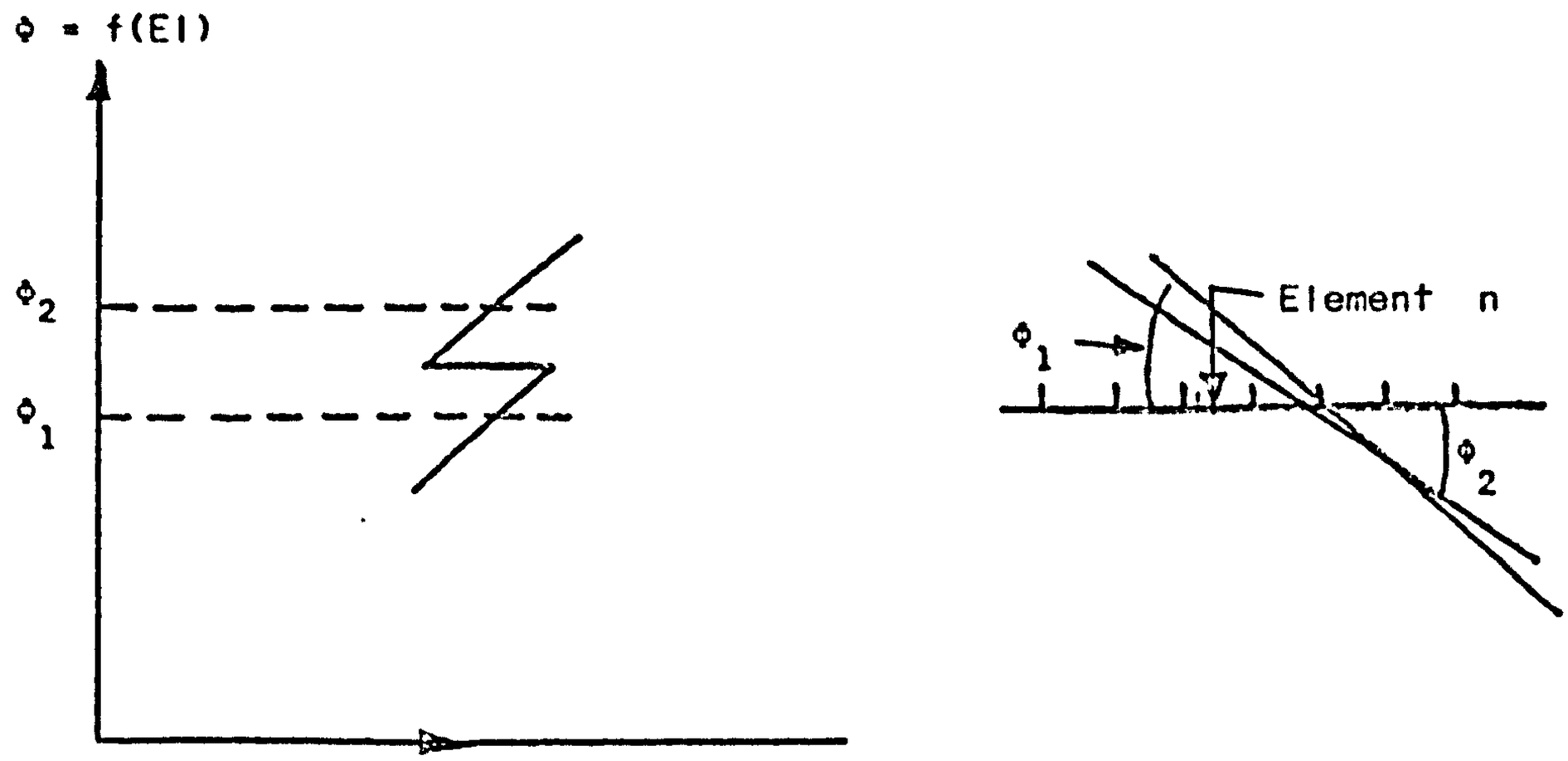

If $\phi = \phi_1$ average strain on element $n < \Sigma_{cr}$

$\phi = \phi_2$ average strain on element $n > \Sigma_{cr}$

where Σ_{cr} = cracking strain

FIG. A2.4 DISCONTINUITIES IN M - ϕ RELATIONSHIPS.

Appendix A3 . Use of over relaxation to analyse columns.

A3.1 Theory. Young[27] has used a method of analysis based on the successive over-relaxation of deflection residuals. This method has been extended to biaxially loaded composite columns.

Considering Fig. A3-1 the equilibrium equation is

$$M_1 = M_e = Nw_o - S_1 x_1 + M \tag{A3.1}$$

where M_1 = internal moment at node 1

and M_e = external moment at node 1.

M_1 is also linked by the curvature relationship

$$M_1 = -\phi K \tag{A3.2}$$

where K is a function of the flexural stiffness EI.

If the deflected shape is estimated then for the correct shape

$$\phi K + Nv_e - S_1 x_1 + M_1 = 0 \tag{A3.3}$$

Substituting in the finite difference expression for ϕ using node numbering as Fig. A3.2.

$$\left[v_1 + v_3 - 2v_o \right] \frac{K}{\ell^2} + Nv_o - S_1 x_1 + M_1 = 0 \tag{A3.4}$$

where ℓ is the element length.

If the incorrect deflected shape has been chosen then equation A3.4 is obviously not equal to zero. Equation A3.4 can be written as

$$v_1 + v_3 - G_o v_o + H_o = 0$$

where $G_o = 2 + \frac{N\ell^2\phi}{M_1}$

and $H_o = \frac{\ell^2\phi}{M_1} \left[Sx_i - M_1 \right]$

The extrapolated Liebemann Method[87] then gives that the correction to be applied to a node is given by

$$\delta v_o^{n+1} = v_o^{n+1} - v_o^n = \frac{\alpha}{\sigma_o}\left(v_1^{n+1} + v_3^n - \sigma_o v_o^n + H_o\right) \qquad (A3.5)$$

where α is a factor used to tune the computer and varies between 1 and 2, and n is the number of the iteration.

A3.2 Comments on the analysis.

The analysis has been programmed and various tests carried out using it. The main advantage of the method is that, as with the integration of the shear equation method, that it enters the moment curvature relationships with two curvatures and axial load.

The disadvantages are that it is slow to converge and that if used in a restrained analysis method it would have to be used as an internal iteration. Each iteration is of course not in equilibrium and this is of no use for the preparation of charts etc.

This method of analysis has been discontinued and is probably not suitable for highly non-linear problems such as composite column analysis.

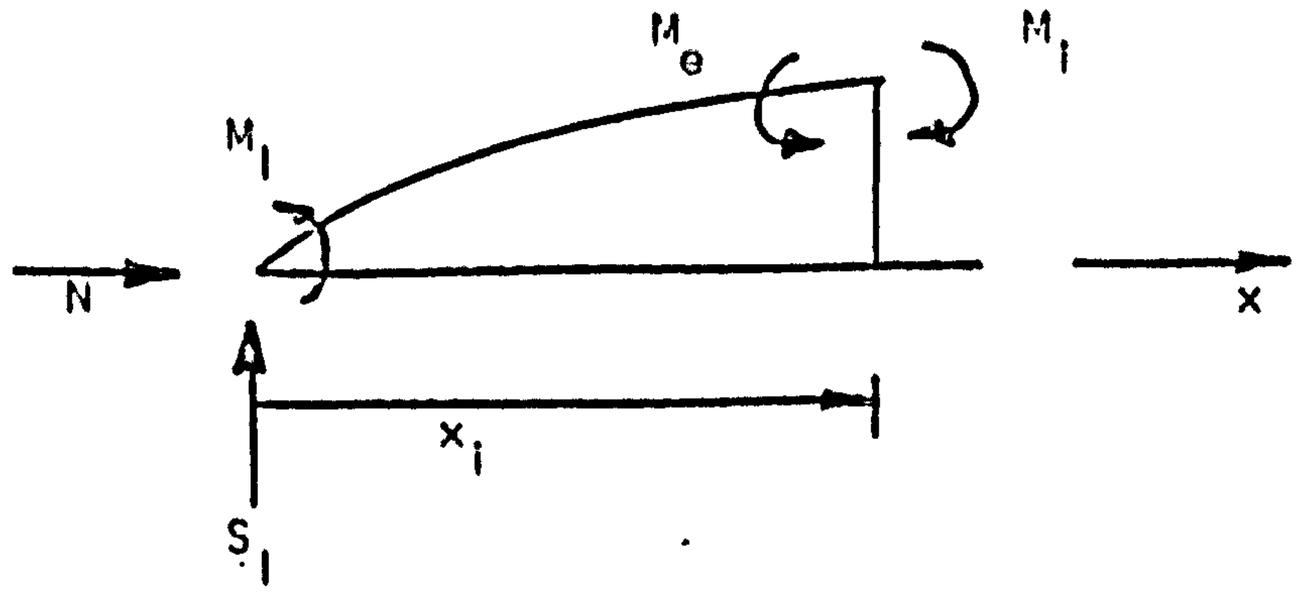

FIG. A3.1 FORCES ON A COLUMN

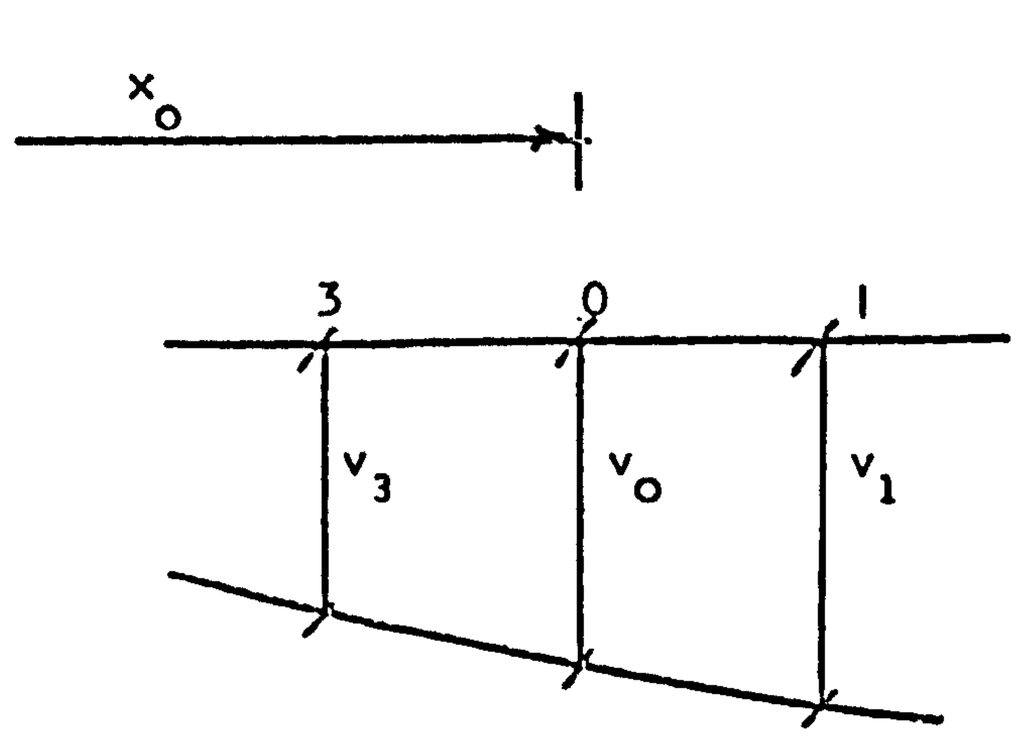

FIG. A3.2 DEFLECTIONS AND NODE NUMBERING

Appendix A4. Derivation of finite difference expressions using Taylor's series.

The Taylor series expansion around the point $x = a$, Fig. A3.1 is

$$f(x) = f(a) + (x - a)\, f^{1}(a) + (x - a)^2\, f^{11}(a)/2! + \ldots.$$

Evaluating the series for the points $x = x_1$ and $x = x_{-1}$ gives

$$f_1 = f_o + \ell f_o^{\,1} + \frac{\ell^2}{2!} f_o^{\,11} + \frac{\ell^3}{3!} f_o^{\,111} + \frac{\ell^4}{4!} f_o^{\,1V} + \ldots. \qquad \text{(A4.1)}$$

$$f_I = f_o - \ell f_o^{\,1} + \frac{\ell^2}{2!} f_o^{\,11} - \frac{\ell^3}{3!} f_o^{\,111} + \frac{\ell^4}{4!} f_o^{\,1V} - \ldots. \qquad \text{(A4.2)}$$

Subtracting A3.2 from A3.1 and re-arranging gives

$$f_o^{\,1} = \frac{f_1 - f_{-1}}{2\ell} - \frac{\ell^2}{3!} f_o^{\,111} - \frac{\ell^4}{5!} f_o^{\,V} - \ldots. \qquad \text{(A4.3)}$$

the expression $\dfrac{f_1 - f_{-1}}{2\ell}$ is used in the analysis as the finite difference representation for $f_o^{\,1}$ the terms, in equation A3.3, $\frac{-\ell^2}{3!} f_o^{\,111} - \frac{\ell^4}{5!} f_o^{\,1V} \ldots.$ are the error terms.

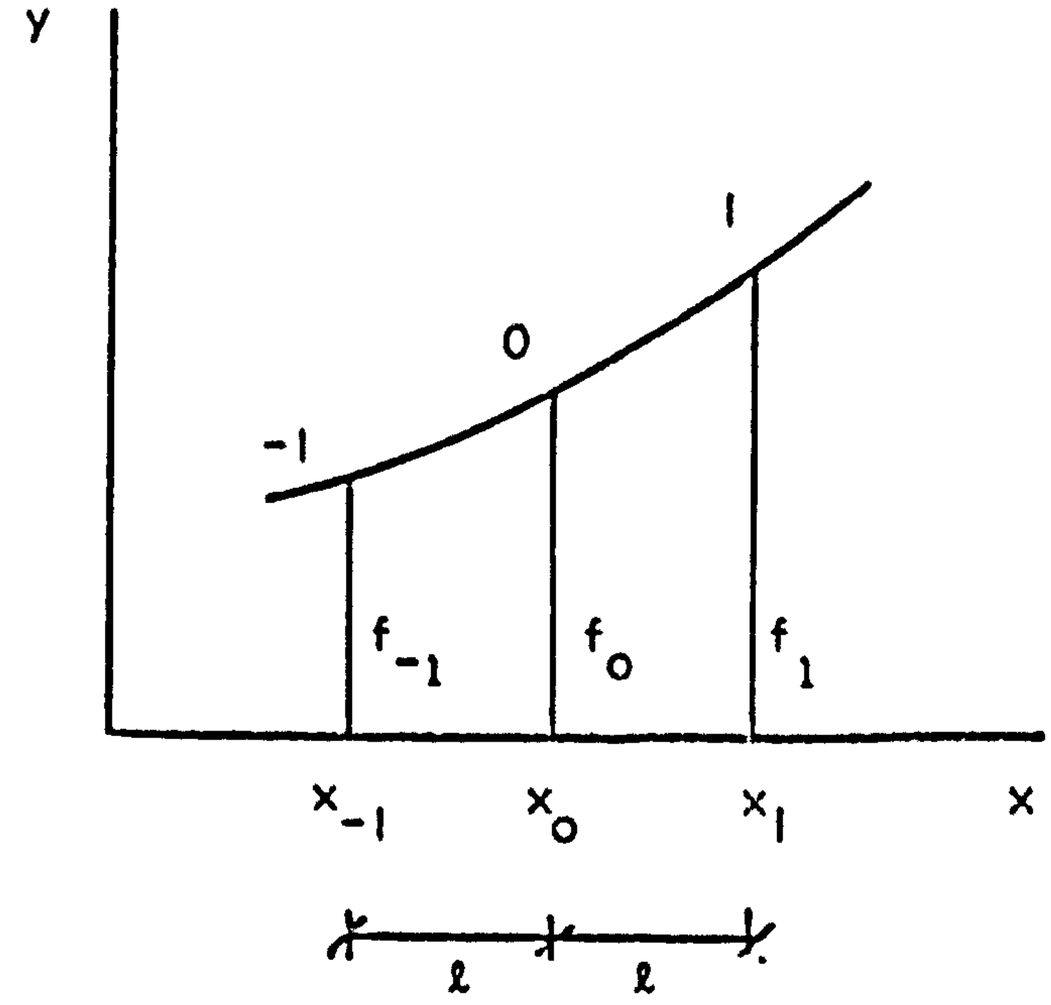

FIG. A4.1 DEFINITION OF NODES AND DEFLECTIONS

Appendix A5 The stub stanchion effect.

Consider the column and beam loading arrangement of Fig. A5.1. If the fixed end moments due to the beam loading are M_{FA} and M_{FB} then

$$\theta_A = \frac{L}{6EI}\left[2M_A - 3M_{FA}\right] \qquad (A5.1)$$

for symmetric beam loads where

$$M_{FB} = -M_{FA}.$$

EI is the flexural rigidity

L is the span of the beam

and M_A is the moment at end A.

From statics it is found that

$$M_E = M_A + P(\ell_s + d_b)\theta_A$$

hence $$\theta_A = \frac{\left[2M_E - 3M_{FA}\right]L}{6EI + 2PL(\ell_s + d_b)} \qquad (A5.2)$$

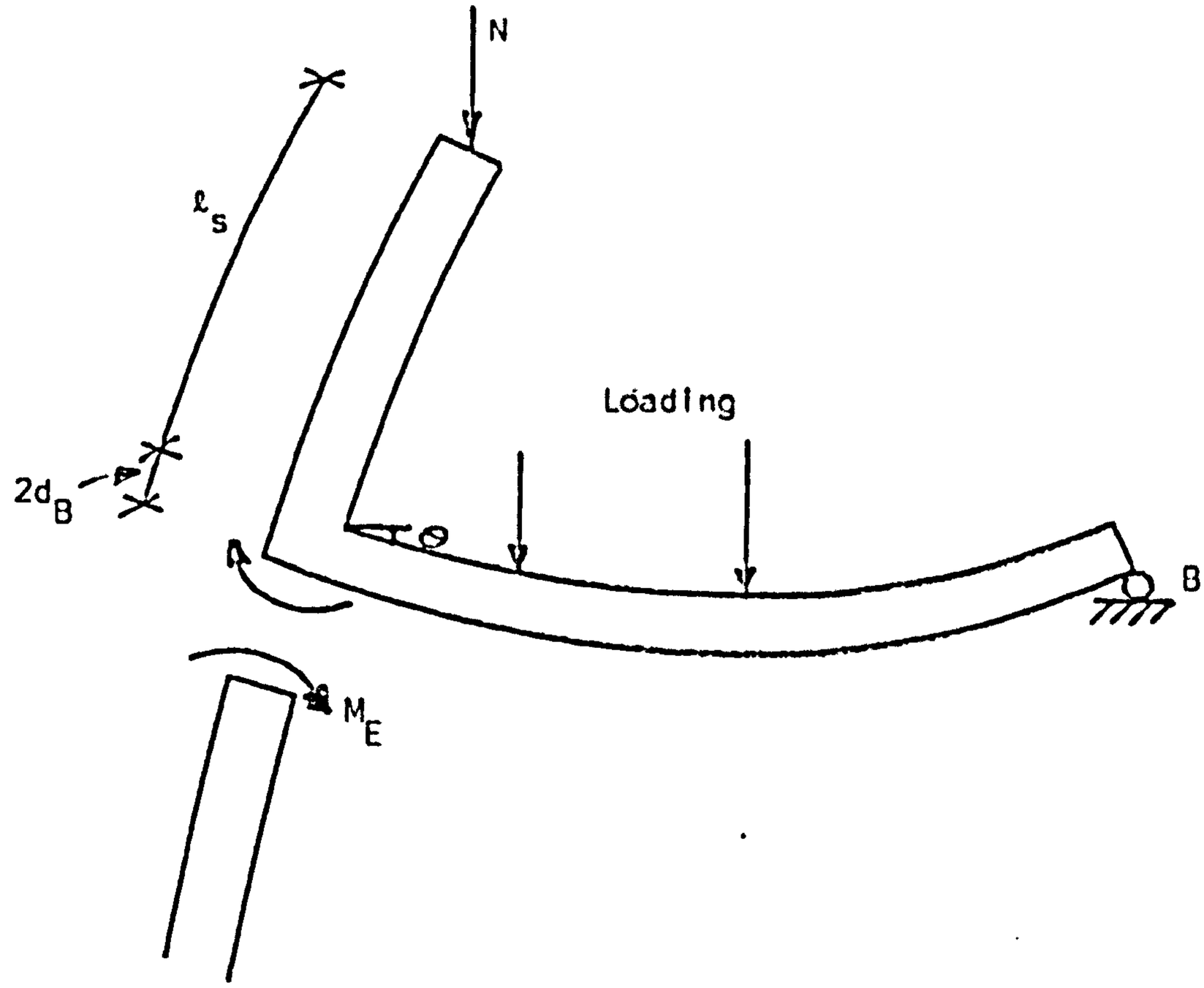

FIG. A5.1 FORCES ON COLUMN-BEAM JOINT